



N° d'ordre : / 2019

Autorisation de soutenance N°/2019

THÈSE DE DOCTORAT

Présentée pour l'obtention du grade de DOCTORAT 3^{ème} Cycle

Filière : Automatique

Option : Diagnostics Industriel

Par : M. Bachir NAIL

Thème

Contribution to Fault Tolerant Control and Fault Detection Based on Advanced Control Approaches

Soutenue publiquement, le 13 /06/2019, devant le jury composé de :

Nom et Prénom	Grade	Etablissement de rattachement	Désignation
Mr Larbi BOUKEZZI	Professeur	Université de Djelfa	Président
Mr Abdellah KOUZOU	Professeur	Université de Djelfa	Directeur de thèse
Mr Ahmed HAFAIFA	Professeur	Université de Djelfa	Co Directeur de thèse
Mr Said DRID	Professeur	Université de Batna	Examineur
Mr Achour BETKA	Professeur	Université de Biskra	Examineur
Mr Slami SAADI	MCA	Université de Djelfa	Examineur
Mr Vicenç PUIG	Professeur	Université de Barcelone	Invité

Dedication

إهداء

أهدي ثمرة جهدي
إلى أمي الحبيبة
إلى روح أبي الغالي
إلى كل أفراد عائلتي

وإلى كل رفاقي الأعزاء في الجامعة وخارجها

نايل البشير

Acknowledgements

Acknowledgements

First of all, I would like to thank my supervisor and Ph.D. director: Prof. **KOUZOU Abdellah**. And I would like to thank my co-supervisor and Ph.D. co-director: Prof. **HAFIFA Ahmed**. This work would not have been possible without their support. I thank them so much for providing me a wonderful environment for working, learning, and expressing my creativity, for believing in me and for giving me ideas, suggestions, helps, and words of encouragement whenever I needed them. They have been, and will always be, examples of good workers, good colleagues, good researchers, and good persons. Thank you.

I would like to thank Prof. **Vicenç Puig Cayuela**, for his humility, advice, help, guidance and corrections, also thank him for his help to me to do short-term internships in the control system lab in UPC University, Terrassa, Barcelona, Spain.

I would like to thank Mr **Larbi BOUKEZZI**, Professor at The University of Djelfa, for the honor he gives me by accepting the presidency of the jury of this thesis. My thanks also go to Mr **Said DRID**, Professor at The University of Batna, Mr **Achour BETKA**, Professor at The University of Biskra and Mr **Slami SAADI**, Professor at The University of Djelfa, Mr **Vicenç Puig Cayuela**, Professor at The Polytechnic University of Catalonia, and who kindly did me the honor to examine this work and to be members of the jury.

List of scientific publications carried out in this thesis

Journal-article

1. **Bachir Nail**, Abdellah Kouzou, and Ahmed Hafaifa. Robust Block Roots Assignment in Linear Discrete-Time Sliding Mode Control for a Class of Multivariable System: Gas Turbine Power Plant Application. Transactions of the Institute of Measurement and Control, Vol. 41, no. 5 (March 2019): 1216-1232, [Link](#).
2. **Bachir Nail**, Abdellah Kouzou, Ahmed Hafaifa, Nadji Hadroug, and Vicenç Puig. A Robust fault diagnosis and forecasting approach based on Kalman filter and Interval Type-2 Fuzzy Logic for efficiency improvement of centrifugal gas compressor system. Diagnostyka, Vol. 20, no. 2 (May 2019): 57-75, [Link](#).
3. **Bachir Nail**, Abdellah Kouzou, and Ahmed Hafaifa, Parametric identification and stabilization of turbo-compressor plant based on matrix fraction description using experimental data, Journal of Engineering Science and Technology, Vol. 13, no. 6 (June 2018): 1-20, [Link](#).
4. Bekhiti, Belkacem, Abdelhakim Dahimene, **Bachir Nail**, and Kamel Hariche. On λ -Matrices and Their Applications in MIMO Control Systems Design. International Journal of Modelling, Identification and Control, Vol. 29, no. 4 (2018): 281-294, [Link](#).
5. Bekhiti, Belkacem, Abdelhakim Dahimene, **Bachir Nail**, and Kamel Hariche. On The Order Reduction of MIMO Large Scale Systems Using Block-Roots of Matrix Polynomials. International Journal of Computer Aided Engineering and Technology, Forthcoming articles (2018), [Link](#).
6. Bekhiti, Belkacem, Abdelhakim Dahimene, Kamel Hariche, and **Bachir Nail**. Intelligent Block Spectral Factors Relocation in a Quadrotor Unmanned Aerial Vehicle. International Journal of Systems, Control and Communications, Vol. 8, no. 4 (2017): 303-334, [Link](#).
7. Bekhiti Belkacem, Abdelhakim Dahimene, **Bachir Nail**, and Kamel Hariche, On the theory of λ -matrices based MIMO control system design, Control and Cybernetics, Vol. 44 no. 4 (2016): 421-443, [Link](#).

Conference-paper

1. **Bachir Nail**, Abdellah Kouzou, Ahmed Hafaifa, and Vicenç Puig. Optimal Static State-Feedback Controller Design for MIMO LTI Systems Based on Constraints Block Roots and Interior-Point Algorithm: Application to Gas Compressor System. In 2018 International Conference on Applied Smart Systems (ICASS), 1-6. Medea, Algeria: IEEE, 2018. [Link](#).

-
2. **Bachir Nail**, Abdellah Kouzou, Ahmed Hafaifa, Parametric state feedback stabilization using block poles: Application to centrifugal gas compressor power plant, The International Multi-Conference on Systems, Signals and Devices 2018 "ssd18" Hammamet on 19-22 March 2018, Tunisia, [Link](#).
 3. **Bachir Nail**, Abdellah Kouzou, Ahmed Hafaifa, Ahmed Chaibet, Power plant system identification based on extended least square kronecker operator, International Scientific Conference on Engineering, Technologies and Systems TECHSYS 2017, Technical University- Sofia, Plovdiv branch 18-20 May 2017, Plovdiv, Bulgaria, [Link](#).
 4. **Bachir Nail**, Abdellah Kouzou, Ahmed Hafaifa, Bekhiti Belkacem, Parametric Output Feedback Stabilization In MIMO Systems: Application to Gas Turbine Power Plant, 8th International Conference on Modelling, Identification and Control (ICMIC), IEEE Xplore , Pages: 971-976 ,15-17 Nov. 2016, Algiers, Algeria, [Link](#).
 5. Nadji Hadrouge, Ahmed Hafaifa, Abdellah Kouzou, **Bachir Nail**, Active fault tolerant control based on a fuzzy system applied to a turbocharger, 8th International Conference on Modelling, Identification and Control (ICMIC) ,IEEE Xplore , Pages: 560- 565, 15-17 Nov. 2016, Algiers, Algeria, [Link](#).
 6. Bekhiti Belkacem, Abdelhakim Dahimene, **Bachir Nail**, and Kamel Hariche, Robust block roots relocation via MIMO compensator design, 8th International Conference on Modelling, Identification and Control (ICMIC), IEEE Xplore , Pages: 971-976 ,15-17 Nov. 2016, Algiers, Algeria, [Link](#).
 7. **Bachir Nail**, Abdellah Kouzou, Ahmed Hafaifa, Block Pole Assignment Stabilization In Large Scale Systems Application to Gas Turbine Power Plant, The 2nd International Conference on Technological Advances in Electrical Engineering (ICTAEE'16), 24-26 Oct. 2016, Skikda, Algeria, [Link1](#), [Link2](#)..
 8. Bekhiti Belkacem, Abdelhakim Dahimene, **Bachir Nail**, On Block roots of matrix polynomials based MIMO control system design, 4th International Conference on Electrical Engineering (ICEE), Boumerdes, IEEE Xplore, Pages: 1-6, 2015, [Link](#).

Book-chapter

1. **Bachir Nail**, Abdellah Kouzou, Ahmed Hafaifa, Digital Stabilizing and Control for Two-Wheeled Robot. New Developments and Advances in Robot Control, Studies in Systems, Decision and Control 175, 2019, [Link](#).
2. **Bachir Nail**, Nadji Hadroug, Ahmed Hafaifa, Abdellah Kouzou, Faults detection and localization of centrifugal gas compressor system using fuzzy logic and hybrid Kernel-SVM Methods. Diagnosis, Fault Detection & Tolerant Control, Decision and Control, 2019, Accepted.

Workshop

1. Summer University DOCTORIALES 2017, this scientific event, organized by the Ministry of Higher Education and Scientific Research, in collaboration with "The Science Edit for the Developing World", University A. MIRA - Bejaia, from 1 to 6 August 2017, [Link1](#),[Link2](#).

2. Modifying quickest flow problems to obtain realistic evacuation paths, MODCLIM (Modeling Clinic for Industrial Mathematics) workshop, University of Koblenz-Landau, Germany (from the 17th to the 21st of May, 2016), [Link1](#),[Link2](#).
3. Workshop in Modeling Clinic for Industrial Mathematics/ European Study Group With Industry ESGI 112 7th Sep - 11th Sep 2015 Lappeentanta University of Technology, Finland, [Link1](#),[Link2](#).



Short-internship

1. Short internship from 12/04/2019 to 23/04/2019 under the supervisor of Prof. Vicenç Puig, in Advanced Control Systems (SAC) Lab. Universitat Politècnica de Catalunya (UPC), Rambla de Sant Nebridi, Terrassa, Barcelona, Spain.
2. Short internship from 27/04/2018 to 11/05/2018 under the supervisor of Prof. Vicenç Puig, in Advanced Control Systems (SAC) Lab. Universitat Politècnica de Catalunya (UPC), Rambla de Sant Nebridi, Terrassa, Barcelona, Spain.
3. Short internship from 17/12/2017 to 30/12/2017 , in the national petroleum society **SONATRCH**. Regional direction In-Amenas, Production Division, Exploration Activity-Production.

My Accounts in scientific organizations

- My home page in university: <http://www.univ-djelfa.dz/labo/laadi/b.nail>
- My google scholar account: <https://scholar.google.com/citations?user=ZghKJNgAAAAJ&hl=fr>
- My researchgate account: https://www.researchgate.net/profile/Bachir_Nail
- My Scopus iD account: <https://www.scopus.com/authid/detail.uri?authorId=57159550100>
- My ORCID iD account: <https://orcid.org/0000-0002-2542-8391>
- My ResearcherID account: <http://www.researcherid.com/rid/M-3613-2016>
- My Publons account: <https://publons.com/a/1531504>
- My Kudos account: https://www.growkudos.com/profile/bachir_nail

Table of Contents

 Dedication	ii
Acknowledgements	iv
List of scientific publications	vi
Journal-article	vi
Conference-paper	vi
Book-chapter	vii
Workshop	vii
Short-internship	viii
My Accounts in scientific organizations	viii
Table of Contents 	ix
List of Tables	xiv
List of Figures	xv
List of Algorithms	xviii
Nomenclature	xix
General Introduction	1
I Introduction	1
II Motivation and Problem Statement	2
III Thesis Objectives	3
IV Thesis Outline	3
Chapter 1	3
Chapter 2	4
Chapter 3	4
Chapter 4	4
First part	4
Second part	4
Chapter 5	4
V References	5
1 Background in Fault Detection and Fault Tolerant Control	9

1	Introduction	9
2	Background in Fault Detection strategies	9
2.1	Basic principle of diagnosis	9
2.2	Diagnostic assistance approach	10
2.3	Different stages of industrial diagnosis	10
	Fault Identification	11
	Making Decision	11
2.4	Classification of diagnostic methods based on models	12
3	Background in Fault Tolerant Control	12
3.1	Hardware Redundancy Techniques	12
3.2	Passive Fault Tolerant Control Techniques	13
3.3	Active Fault Tolerant Control Techniques	13
4	Conclusion	17
5	References	17
2	Multivariable Robust Static State-Feedback Controller design	19
1	Introduction	19
2	Preliminaries and Problem Statement	19
	Problem statement	21
3	Main results	21
3.1	The calculation of robust sliding matrix gain G	23
3.2	The computation of matrix gain K via robust block roots assignment	24
	3.2.1 A polynomial matrix	24
	3.2.2 The concept of block roots (solvents)	25
	3.2.3 The right solvent	25
	How To choose the closed-loop block roots (Regulator Block Roots)	26
	The condition of complete set roots	26
	The extracting from a complete set of right block roots	27
	The state feedback design	27
4	The proposed algorithm steps	28
5	Experimental application on gas turbine GEMS5001P system	28
	5.1 Parametric model of the studied Gas turbine system	28
	5.2 Comments and Interpretations on the obtained results	32
	5.3 The Effects of the block roots on the performance of the proposed controller	32
6	Conclusion	33
7	References	34
3	Multivariable Optimal Static Output-feedback Controller design	36
1	Introduction	36
2	Preliminaries	37
	2.1 Block Canonical Forms Transformation of controllability	37
	2.2 Block Canonical Forms Transformation of observability	38
3	Constraints optimization problem	38

4	Problem statement	39
5	Main results	40
5.1	The selection of the heart matrix $A_h(\theta)$	42
	Optimization procedure	42
6	The proposed algorithm steps	45
7	Experimental application and results	45
7.1	Implementation of Proposed optimal SOF controller	47
7.2	Comparative study and discussion results	48
	Frequency domain, singular values, stability and robustness analysis	51
7.3	The proposed controller algorithm presents some limitations with suggested solutions	52
8	Conclusion	52
9	References	52
4	Faults-detection approaches based on Interval Type-2 Fuzzy Logic and Interval Observer: A comparative study	55
1	Introduction	55
2	Centrifugal gas compressor BCL 505 system	56
	Faults detection and remaining time forecasting approach Based on Interval Type-2 Fuzzy logic	58
3	Outputs estimation based on Kalman filter	58
4	Preliminary concepts about Interval Type-2 Fuzzy Logic	59
5	The proposed FDI setup for a centrifugal gas compressor plant	60
5.1	Fault detection and isolation (FDI)	61
5.2	Forecasting the remaining time	65
6	Economic study	66
6.1	Reparation costs	66
6.2	Benefits	67
	Fault detection based on interval observer using block roots assignment and grey wolf optimizer	68
7	Preliminaries	68
7.1	Interval Relations	68
7.2	Nonnegative Linear Invariant-Time (LTI) Systems	68
	7.2.1 Case of LTI Continuous-time systems	68
	7.2.2 Case of LTI Discrete-time systems	69
7.3	Survey on matrix polynomials	69
7.4	The concept of Block roots	71
	7.4.1 The left Block roots	71
	7.4.2 The choice form of the desired Block roots	71
7.5	Problem statement	72
	Design of observer matrix gain L	73
8	Main results	73
9	Constrained nonlinear optimization	74
10	The proposed algorithm steps	75

11	Experimental application and results	76
12	Interval observer-based fault detection	80
13	Conclusion	81
14	References	82
5	A robust fractional-order $PI^\lambda D^\mu$ controller design based on pseudo block-roots assignment	85
1	Introduction	85
2	Preliminaries	85
2.1	Canonical Block Controller Form Transformation	85
2.2	Matrix Fraction Descriptions (MFDs)	86
2.3	Characteristics of matrix polynomials with integer order	87
2.4	Fundamentals of fractional-order calculus	87
3	Problem statement	88
4	Main results	90
4.1	Case 1	91
4.2	Case 2	93
4.3	Case 3	94
4.4	The choice of the desired Pseudo-Block-Roots	96
4.5	Controller parameters tuning under model uncertainty using grey wolf optimizer	98
	Optimization procedure	99
5	The proposed algorithm steps	101
6	Experimental application and results	101
7	Passive FTC Investigation	107
8	Conclusion	109
9	References	109
	General Conclusion	112
X	Introduction	112
	First	112
	Second	112
	Third	113
	Part one	113
	Part two	113
	Fifth	113
XI	Contributions	114
XII	Further studies	114
A	GE MS5001P Gas Turbine System and Robustness-Sensitivity Theories	115
I	GE MS5001P Gas Turbine dynamical model	115
II	The robustness stability and sensitivity performance analysis	116
II.1	The sensitivity of eigenvalues (robust performance)	116
II.1.1	The relative change	117
II.1.2	The robust stability	117

III	References	118
B	BCL 505 Centrifugal Gas Compressor System with Supplementary Data	119
I	BCL 505 Centrifugal Gas Compressor dynamical model and Hassi R'Mel gas field	119
II	References	122
C	Supplementary Data of fractional-order $PI^\lambda D^\mu$ controller application results	124
Abstracts		130
	Arabic	131
	English	132
	French	133

List of Tables

TABLE	Page
2.1 The norms (1,2,inf) of the sliding matrix G associated to each methods	30
2.5 Comparative study	30
2.2 Time specifications (Settling time t_s and maximum peak M_p)	31
2.3 Robust stability (Eigenvalues sensitivity $s(\lambda_i)$)	31
2.4 Robust performance (Relative change r in the eigenvalues λ_i under perturbation)	31
3.1 Comparison the ($\ \cdot\ _\infty$, ROC and BTs) characteristics of each SOF matrix gain K methods	48
3.2 Comparison the time specifications of dynamic system response in each methods	49
3.3 Robust stability (Eigenvalues sensitivity $s(\lambda)$)	49
3.4 Robust performance (Relative change r in the eigenvalues λ under perturbation)	50
3.5 Stability measures	50
4.1 The threshold faults detection	63
4.2 Faults identification and classification	65
4.3 Comparative study and performance analysis	81
5.1 The matrices gains of the proposed controller according to each cases	96
A.1 General performance of gas turbine GE MS5001P	117
B.1 General performance of centrifugal gas compressor BCL 505	121

List of Figures

FIGURE	Page
1.1 General structure of a diagnostic system	10
1.2 Different stages of industrial diagnosis	11
1.3 Classification of diagnostic methods	12
1.4 Different steps of fault tolerant control	13
1.5 Different steps of fault tolerant control	14
1.6 Different steps of fault tolerant control	15
1.7 General structure of a diagnostic system	16
2.1 Phase portrait under Sliding mode control effect	20
2.2 Schematic of SSF controller gain stabilization.	21
2.3 Comparison between the Sign, Sat and Tanh functions	23
2.4 Schematic bloc diagram of gas turbine (GE MS5001P) with inputs/outputs model identification	29
3.1 Schematic of SOF controller gain stabilization.	40
3.2 Diagram of the desired dynamic matrix \bar{A}	42
3.3 Flowchart of the Grey Wolf Optimizer	44
3.4 The studied centrifugal gas compressor system BCL 505 installed in the natural gas compression station	46
3.5 Schematic block diagram of the studied centrifugal gas compressor system driven by two shaft gas turbines.	46
3.6 GWO evolution during the tuning optimization process	50
3.7 The change of objective function f in terms of GWO iteration	50
3.8 Bode diagram of the CLS	50
3.9 Nyquist diagram of the CLS	50
3.10 Robust stability of CLS.	51
3.11 worst-case gain of uncertain CLS	51
3.12 Zeros-Poles map of Uncertain CLS	51
3.13 Singular values of CLS	51
4.1 Schematic diagram of of the proposed FDI approach.	56
4.2 Centrifugal gas compressor BCL 505 body, with real view in vertical joint plane	57
4.3 Observed and experimental discharge pressure, and the error between them	58
4.4 Observed and experimental discharge temperature, and the error between them	58
4.5 The structure of the type-2 Fuzzy Logic System.	59

4.6	Real-time faults detection diagnosis configuration for centrifugal gas compressor.	60
4.7	The discharge pressure $P2$ with and without faults	62
4.8	The discharge temperature $T2$ with and without faults	62
4.9	The detection faults of ($P2$) with respect to a threshold	62
4.10	The detection faults of ($T2$) with respect to a threshold	62
4.11	Type-2 fuzzy sets of discharge pressure $P2$ expert model faults detection	63
4.12	Type-2 fuzzy sets of discharge temperature $T2$ expert model faults detection	63
4.13	The fault evaluation of ($P2$) gas compressor system examined	64
4.14	The fault evaluation of ($T2$) gas compressor system examined	64
4.15	The status of scratch on the blades of the impeller1 and after reparation.	64
4.16	The status of light streaks at the spacers level and after reparation.	65
4.17	The status of O-ring joints defective.	65
4.18	Forecasting time level danger of ($P2$)	66
4.19	Forecasting time level danger of ($T2$)	66
4.20	The diagnosis approach impact on the financial cost	67
4.21	The evolution of the grey wolf population values during the tuning optimization process	77
4.22	The change of objective function f in terms of GWO iteration	77
4.23	Interval estimation of state x_1	78
4.24	Interval estimation of state x_2	78
4.25	Interval estimation of state x_3	78
4.26	Interval estimation of state x_4	78
4.27	Interval error estimation of state x_1	78
4.28	Interval error estimation of state x_2	78
4.29	Interval error estimation of state x_3	79
4.30	Interval error estimation of state x_4	79
4.31	Forecasting time level danger of $P2$	79
4.32	Interval estimation of output $P2$	79
4.33	Interval error estimation of output $P2$	79
4.34	Interval error estimation of output $T2$	79
4.35	The adaptive interval threshold generated by interval observer of output $P2$ in presence of faults	81
4.36	The adaptive interval threshold generated by interval observer of output $T2$ in presence of faults	81
5.1	Closed loop system of the system $G(s)$ and the controller $C(s)$	89
5.2	Stability region for the fractional-order LTI systems with allowable region	97
5.3	Flowchart of the Grey Wolf Optimizer.	100
5.4	Schematic block diagram of the studied centrifugal gas compressor system driven by two shaft gas turbines.	102
5.5	The evolution of the grey wolf population values during the tuning optimization process	105
5.6	The change of objective function J in terms of GWO iteration	105
5.7	Output signal of reference and real discharge pressure	105
5.8	Output signal of reference and real discharge temperature	105
5.9	The error between the reference and real outputs signals	105
5.10	CLS pseudo-roots position in complex σ -plane	105

5.11	Nyquist diagram of the CLS	106
5.12	Bode diagram of the CLS	106
5.13	Output signal of reference and real discharge pressure under $-90\% \leq \Delta\theta \leq +90\%$ of nominal system uncertainty	106
5.14	Output signal of reference and real discharge temperature under $-90\% \leq \Delta\theta \leq +90\%$ of nominal system uncertainty	106
5.15	The error between the reference and real outputs signals under $-90\% \leq \Delta\theta \leq +90\%$ of nominal system uncertainty	106
5.16	CLS pseudo-roots position in complex σ -plane under $-90\% \leq \Delta\theta \leq +90\%$ of nominal system uncertainty	106
5.17	Schematic design of Robust FO- $PI^\lambda D^\mu$ Passive FTC system.	107
5.18	Output discharge pressure signals of no faulty (reference) and faulty system under embedded PID controller and with PFTC approach	108
5.19	Error between faulty system under embedded PID controller and under proposed PFTC approach	108
5.20	Output temperature pressure signals of no faulty (reference) and faulty system under embedded PID controller and with passive FTC approach	108
5.21	Error between faulty system under embedded PID controller and under proposed PFTC approach	108
5.22	External additive disturbance	109
5.23	External multiplicative disturbance	109
A.1	Axial compressor of GE Gas turbine 5001P	116
A.2	Turbine of GE Gas turbine 5001P	116
B.1	Combustion chambers of GE Gas turbine 5002C	119
B.2	HP and LP of centrifugal gas compressor	119
B.3	HP and LP rotor	120
B.4	Multiplier of rotor speed	120
B.5	Stator of GE Gas turbine 5002C	120
B.6	Rotor of of GE Gas turbine 5002C	120
C.1	High performance Xenon PC used for optimization computing	129

List of Algorithms

1	Robust static state-feedback controller algorithm	28
2	Optimal static output-feedback controller algorithm	45
3	Robust interval observer algorithm	75
4	Robust fractional-order $PI^\lambda D^\mu$ controller algorithm	101
5	Kalman observer algorithm	122

Nomenclature

Number Sets

\mathbb{C}	Complex Numbers
\mathbb{R}	Real Numbers
\mathbb{Z}	Integer Numbers

Greeks

λ	Eigenvalues
λ^*	Complex conjugate eigenvalues
\otimes	Kronecker product
$\bar{\sigma}$	Biggest singular values
σ	Singular values
Θ	Compact set
$\theta/\hat{\theta}$	Matrix parameters/Estimated matrix parameters
$\underline{\sigma}$	Smallest singular values

Acronyms

ACS	Acquisition Control System
AIC	Akaike Information Criterion
ARIMA	Auto-regressive Integrated Moving Average
BCL 505	Barrel type body, Closed disc counter wheel, Free vortex diffuser, 500 mm Wheels diameter, 5 Number of the wheels
EKF	Extended Kalman Filter
ESRIV	Extended Simplified Refined Instrumental Variable
FD	Fault Detection
FDD	Fault Detection and Diagnosis

FDI	Fault Detection and Isolation
FL	Fuzzy Logic Type-1
FL-2	Fuzzy Logic Type-2
FO-PI ^{λ} D ^{μ}	Fractional Order Proportional Integrator Derivative
FPE	Final Prediction Error
FTC	Fault Tolerant Control
GA	Genetic Algorithm
GCV	Gas Control Valve
GE	General Electric
GWO	Grey Wolf Optimizer
HP	Hight Pressure
IPM	Interior Point Method
IV	Instrumental Variable
LMFD	Left Matrix Fraction Description
LNG	Liquefied Natural Gas
LP	Low Pressure
LSL	Lower Specification Limit
MFDs	Matrix Fraction Descriptions
MIMO	Multi Input Multi Output
PFTC	Passive Fault Tolerant Control
PLC	Programmable Logic Controller
PSO	Practical Swarm Optimization
RMFD	Right Matrix Fraction Description
RMSE	Root Mean Square Error
SISO	Single Input Single Output
SOF	Static Output Feedback
SPC	Statistical Process Control
SQC	Statistical Quality Control

SRIV	Simplified Refined Instrumental Variable
SS	State Space
SSF	Static State Feedback
USL	Upper Specification Limit
VAF	Variance Accounting For

Other Symbols

E_{P2}	Error discharge pressure
E_{T2}	Error discharge temperature
$\hat{}$	Indicates estimated values
S	Quasi sylvester matrix equation
\mathcal{X}	Quasi matrix polynomial
\bar{e}/\underline{e}	Upper and Lower error
\bar{x}/\underline{x}	Upper and Lower state
\bar{y}/\underline{y}	Upper and Lower output
\mathbf{m}	Average value
s	Standard deviation
$d(.)$	Faults vector
e	Error signal
$F1, F2$ and $F3$	Faults
I	Identity matrix
J	Cost function
k	Discrete time
N	Length data
O	Zero matrix
$P1$	Aspiration Pressure
$P2/\hat{P}2$	Discharge pressure/Observed discharge pressure
$P_{k k-1}/P_{k k}$	Covariance/Updated covariance
Q_k	Process noise covariance matrix

R	Block roots
r	Residual signal
R_k	Measurement noise covariance
t	Continuous time
$T1$	Aspiration Temperature
$T2/\hat{T}2$	Discharge temperature/Observed discharge temperature
u	Control signal
V_r/V_L	Right and Left Block Vandermonde matrix
x	State vector
X/\hat{X}	State/Estimated state
y	Output signal
Y/\hat{Y}	Output signal/Filtered output signal
Y_{op}	Optimal output signal
z^{-1}	Delay operator
\tilde{Y}_k	Measurement residual
K_k	Optimal Kalman gain
S_k	Innovation covariance
$u^*[k]/y^*[k]$	Pre-filtered input/output signals respectively
A,B,C and D	State space matrices
col{.}	Transforms a matrix into a column vector

General Introduction

I Introduction

Fault tolerant control has become one of the major concerns in the design of complex automated systems [1, 2]. Because of the complexity of the processes and the increase of hardware or software technological elements that are often integrated into the control loops of these systems. Indeed, many methods and techniques based on dynamic models have been developed for the detection of anomalies, the treatment of these anomalies and the decision making concerning the reconfiguration of the system or its objectives [3–6]. These topics are often addressed in the FTC (Fault Tolerant Control) literature and have been the subject of much work by the scientific community [7, 8]. Historically, previous work in this area has been driven by aeronautical and space applications [9, 10].

The frequency domain techniques have been the principal tools of analysis, modeling and design of linear dynamic systems, since the early days of control and system theory. However, the dynamic systems that can be presented by a scalar m^{th} order linear differential equations with constant coefficients, $\sum_{i=0}^n a_i y^{(n-i)} = \sum_{i=0}^m b_i u^{(m-i)}$, ($n > m$) [14] are amenable to this type of analysis see [12, 13]. These systems are mono variable have a single input and a single output (SISO). In this case, they are modeled by a transfer function, i.e. A ratio of two scalar polynomials. The dynamic properties of the SISO systems (stability, time response, etc...) depend to large extent on the roots of the denominator or in other words on the solution of the underlying homogeneous differential equation [15]. The denominator of such system is a scalar polynomial and its spectral characteristics depend on the location of its roots (poles) in the complex plane, hence the factorization (roots finding) of scalar polynomials is an important tool of analysis and design for linear dynamic systems (Dahime et al. 2009).

For the multivariable systems with multi input and multi output (MIMO), the dynamics can be presented by high-degree coupled vector differential equations i.e. l^{th} degree m^{th} order vector linear differential equations with constant matrix coefficients $\sum_{i=0}^l A_i y^{(l-i)} = \sum_{i=0}^m B_i u^{(l-i)}$, [16, 17], and can be considered as an extension to the scalar case resulting in matrix transfer functions. When one studies high order multivariable systems, the dimension of the matrices involved becomes prohibitive. Therefore, there is a reappreciation nowadays of matrix transfer function (which become rational matrices) descriptions on distinguished two cases left and right descriptions [15–17]. In this context, the properties of the studied dynamic system are to a large extent determined by the latent roots and /or the spectral factors of a matrix polynomial. Therefore, Many research papers have been published in the past and recent years about the matrix polynomial theory and their applications in systems and control theory. References [18–24] are a few samples of this trend. The modern standard linear system theory is well covered in [14, 25, 26]. The Polynomial matrix approach to linear multivariable system

analysis and design became popular since 1970's [27–30].

II Motivation and Problem Statement

In the modelling of the dynamic systems or power plants, several descriptions can be used to represent them. Two commonly used model descriptions for linear time-invariant multivariable systems are the state space description (SSD) and the transfer function matrix description (TFMD) or matrix fraction description (MFD) [32]. In this thesis a linear multi-variable time-invariant system described by the following state space equations have been considered:

$$\begin{cases} \dot{x}(k+1) = Ax(k) + Bu(k) \\ y(k) = Cx(k) \end{cases} \quad (1)$$

Where A is system or state matrix, B is control or input matrix, C is observer or output matrix and D is coupling or transmission matrix. The behavior of these such systems can be studied via the eigenstructure, the eigenvalues and the eigenvectors, of the system matrix A , respectively. The eigenvalues and eigenvectors are the major indicators which can directly and explicitly determine the system performance and robustness than other indicators because are present the heart of the dynamic system. Hence their assignment (placement) eigenvalues and eigenvectors, should improve the feedback system performance and robustness distinctly and effectively. Eigenstructure assignment (placement) (EA) is the process or technique that applying a negative feedback to a linear, time-invariant system with the objective of forcing the eigenvalues and eigenvectors to become as close as possible to a desired eigenstructure [32].

Many research works have been done on EA and more specially on airspace and flight control systems such as [33–44].

The system (I.1) can be also described by a m -inputs p -outputs transfer function $G(s)$ in matrix fractions description as follows:

$$G(s) = N_R(s)D_R(s)^{-1}, G(s) = D_L(s)^{-1}N_L(s) \quad (2)$$

Where $N_R(s)$, $N_L(s)$, $D_R(s)$, and $D_L(s)$ are matrix polynomials of degree equal or less to l , and of order m or p . l being the controllability and/or the observability index. These matrix polynomials are polynomials which their coefficients are matrices of right dimensions [32].

The feedback static or dynamic gain matrix permitting the assignment of the desired set of roots (eigenvalues, poles) is not unique, this is due, in the case of block roots placement method, to the fact that different block roots can be constructed from the same set of eigenvalues. i.e. block roots can be placed in the right and the left matrix polynomial, can be also placed in several forms (controller, observer, diagonal, general, etc.) of block roots which contain the same eigenvalues, the degree of freedom offered by the choice of the block roots could be exploited to satisfy some desired closed loop system performances (the system response characteristics, robustness, tracking, decoupling, regulation, etc...). This can be done by choosing the structure of the roots to be placed which gives the best and optimal feedback gain matrix that achieved the desired objectives. In the static state feedback case, the problem assumes that all states considered are measurable. Unfortunately, and this is impractical for many systems. For this reason, a static output feedback matrix gain, or dynamic compensator are studied in this thesis. Many research papers have considered using block roots of matrix polynomials for solving some linear algebra problems or control system problems such as [45–52].

In this thesis, we are going to investigate the effect of the bloc roots of matrix polynomial on the performance specifications of some famous controllers laws, and trying to proposing a mathematical algorithms that we can

integrating the block roots in its design, such as sliding mode control theory [16]. The selection of the optimal and the robust block roots of matrix polynomial in some times can be considered as problem, should be solved. Also the matrix fraction description of the studied dynamic system presented in (2) with integer-order, if we consider this description has a no integer-order, how we can design a controller law for this important case of system, how can assign the set of block roots for this kind of matrix polynomials of fractional order (no integer-order), have they the same specification such as the matrix polynomials with integer order ?. All of this problems can be solved based on, proposed algorithms and approaches using some mathematical tools, with the extension of some famous definitions and theorems.

III Thesis Objectives

The objectives of this thesis are the following:

- Propose an approach for the design of robust state-feedback controllers in presence of uncertain system parameters based on block roots assignments.
- Propose an approach for the design of robust output-feedback controllers in presence of uncertain system parameters based on matrix fraction description proprieties.
- Using the metaheuristics optimization algorithms to select the best block roots that can guarantee some desired performances despite the uncertainties.
- Design a robust interval observer for faults detection based on block roots of matrix polynomials.
- Design a robust faults detection approach based on fuzzy logic expert system.
- Trying to extend the matrix polynomials and the bloc roots concepts from the integer-order to the fractional-order.

IV Thesis Outline

The thesis is organized in five chapters:

Chapter 1 The first chapter presents a background about the three mean points used in this thesis:

1. A background about the matrix polynomial and their applications and uses in multivariable control system design, where a historical overview on the right and the left matrix fraction description (MFD), The Block Roots concept, the Vandermonde matrix, and its applications in modelling, estimation and observation domain.
2. A background about Fault Tolerant Control (FTC), and their classification into three categories: Hardware Redundancy Techniques (HRT), Passive Fault Tolerant Control (PFTC), and Active Fault Tolerant control (AFTC).
3. A background about Fault Detection and Diagnosis (FDD) and their classifications.

Chapter 2 The second chapter proposed a state feedback controller designed based on combination of the block roots of matrix polynomial and sliding mode algorithm, where the proposed controller is addressed to the multivariable LTI systems, in this design all the system states assumed to be available and measured in the output, an investigation on a gas turbine system (GE MS5001P) is carried out, which is used in electrical power generation plants, where the dynamic model of this gas turbine is obtained based on experimental data obtained on site, the obtained results of this implementation show the stability robustness of this proposed algorithm. Sometimes is difficult and expensive to have the measurement of the whole state vector, because of technical reasons (unmeasurable or un-accessible variables) or economic aspect (price of sensors). For this reason, several control algorithms have been developed that use only output information to control the system. The next part of this thesis treats this drawback.

Chapter 3 The third part presents an optimal static output-feedback (SOF) controller algorithm for multivariable LTI systems is designed. The key idea is to exploit the canonical Block Transformations (BTs) matrices of the block controllability and observability respectively. The objective is to define the unknown closed-loop system (CLS) dynamics that is completely characterized in terms of the block matrix called the heart matrix A_h . The optimal A_h block matrix, that guarantees the stability of the CLS, is computed using Genetic Algorithms (GAs), considering the best selection CLS specifications. To illustrate the performance of the proposed SOF controller, highlight some important characteristics, and to prove its efficiency, a centrifugal gas compressor system is introduced as case study. Based on this application, a comparative study is carried out, using several optimization techniques (Particle Swarm Optimization (PSO) and Interior-Point Method (IPM)) and a recent H_∞ controller approach, to demonstrate the feasibility of our proposed design methodology.

Chapter 4 The fourth chapter divided into two parts:

First part presents a Robust Faults detection Based on Interval Type II Fuzzy logic, where the expert system is designed based on Type-2 Fuzzy logic, and the Kalman observer is used to filtered the noised output signals, where the main aim is to improve the whole studied system energy efficiency taking into account the economic aspect, the present work is achieved by an important task which is the prediction of the remaining time of the system under study to reach the danger and/or the failure stage based on the ARIMA model, where the objective within the industrial application is to set of the maintenance schedules in time and precisely. The obtained results prove the performance of the proposed faults diagnosis and detection.

Second part propose a optimal interval observer, its design is based on block roots of matrix polynomial and grey wolf optimizer addressed to the multivariable uncertain systems, the choice flexibility of the block roots is play a key role for the design of the observer matrix gain L , the obtained results of application of this proposed interval observer in fault detection proves its validity and superiority comparing with the first approach.

Chapter 5 The fifth part presents a Multivariable Optimal Fractional-order $PI^\mu D^\lambda$ Controller Design Subject to Robust FTC The multivariable fractional-order $PI^\mu D^\lambda$ Controller is designed based on optimal pseudo block roots which are chosen using Grey Wolf Optimizer (GWO), the main idea is to assign a set of desired pseudo block roots to the close loop system (CLS), and solving the obtained quasi diophantine equation and the pseudo Sylvester matrix, using linear system equations solver tool, in order to obtained the matrices gains of the $PI^\mu D^\lambda$ Controller K_p , K_i and K_d respectively, the tuning of the fractional integrator and derivative parameters λ and μ

respectively is done based on GWO, the proposed controller is subjected to passive FTC applied on centrifugal gas compressor system, the obtained results show the best performance and stability of this controller despite in the presence of the uncertainties and the injected disturbance on the whole of the studied dynamical system.

V References

- [1] R. Isermann, *Fault-Diagnosis Systems: An Introduction from Fault Detection to Fault Tolerance*. Berlin, Heidelberg: Springer Berlin Heidelberg, 2006.
- [2] Blanke M, Kinnaert M, Lunze J, Staroswiecki M *Diagnosis and fault-tolerant control*. Springer, Berlin, 2006.
- [3] T. Jain, J. J. Yamé, and D. Sauter, *Active Fault-Tolerant Control Systems*, vol. 128. Cham: Springer International Publishing, 2018.
- [4] C. Hajjiev and F. Caliskan, *Fault Diagnosis and Reconfiguration in Flight Control Systems*, vol. 2. Boston, MA: Springer US, 2003.
- [5] Farrell, J. A., Berger, T. and B. D. Appleby. Using learning techniques to accommodate unanticipated faults, *IEEE Control Systems Magazine*, Vol. 13, pp. 40-49, 1993.
- [6] Napolitano, M. R., Molinaro, G., Innocenti, M. Seanor, B. and Martinelli, D. A complete hardware package for a fault-tolerant control system using on-line learning neural networks, In *proceedings of the American Control Conference*, San Diego, CA, pp. 2615-2619, 1999.
- [7] D. Rotondo, *Advances in gain-scheduling and fault tolerant control techniques*. Thesis, Cham: Springer, 2018.
- [8] J. Lunze and J. H. Richter, *Reconfigurable Fault-tolerant Control: A Tutorial Introduction*, *European Journal of Control*, vol. 14, no. 5, pp. 359-386, Jan. 2008.
- [9] S. Ijaz, L. Yan, M. T. Hamayun, and C. Shi, Active fault tolerant control scheme for aircraft with dissimilar redundant actuation system subject to hydraulic failure, *Journal of the Franklin Institute*, vol. 356, no. 3, pp. 1302-1332, Feb. 2019.
- [10] D. Rotondo, F. Nejjari, A. Torren, and V. Puig. Fault tolerant control design for polytopic uncertain LPV systems: application to a quadrotor. In *Proceedings of the 2nd International Conference on Control and Fault-Tolerant Systems (SYSTOL)*, pages 643-648, 2013.
- [11] L. Wang and L. Wang, *Reconfigurable Flight Control Design for Combat Flying Wing with Multiple Control Surfaces*, *Chinese Journal of Aeronautics*, vol. 25, no. 4, pp. 493-499, Aug. 2012.
- [12] Distefano, J.J., Stubberud, A. R., Williams, I.J. *Theory and Problems of Feedback and Control Systems*, Mc. Graw Hill, 1967.
- [13] Gohberg, I., Lancaster P., and Rodman, L. *Matrix polynomials*, Academic Press, 1982.
- [14] Katsuhiko Ogata, *Modern Control Engineering*, Prentice Hal, Edition 5, 2010.

- [15] M. Yaici and K. Hariche, On eigenstructure assignment using block poles placement, *European Journal of Control*, vol. 20, no. 5, pp. 217-226, Sep. 2014.
- [16] B. Nail, A. Kouzou, and A. Hafaifa, Robust block roots assignment in linear discrete-time sliding mode control for a class of multivariable system: gas turbine power plant application, *Transactions of the Institute of Measurement and Control*, Vol. 41 no. 5, pp. 1216-1232, 2019.
- [17] B. Nail, A. Kouzou, A. Hafaifa, and V. Puig, Optimal Static State-Feedback Controller Design for MIMO LTI Systems Based on Constraints Block Roots and Interior-Point Algorithm: Application to Gas Compressor System, in *2018 International Conference on Applied Smart Systems (ICASS)*, Medea, Algeria, 2018, pp. 1-6.
- [18] S. Ahn, Stability of a matrix polynomial in discrete systems, *IEEE Transactions on Automatic Control*, vol. 27, no. 5, pp. 1122-1124, Oct. 1982.
- [19] P. Resende and E. Kaszkurewicz, A sufficient condition for the stability of matrix polynomials, *IEEE Transactions on Automatic Control*, vol. 34, no. 5, pp. 539-541, May 1989.
- [20] W. C. Karl and G. C. Verghese, A sufficient condition for the stability of interval matrix polynomials, *IEEE Transactions on Automatic Control*, vol. 38, no. 7, pp. 1139-1143, Jul. 1993.
- [21] J. Lavaei and A. G. Aghdam, A Necessary and Sufficient Condition for Robust Stability of LTI Discrete-Time Systems using Sum-of-Squares Matrix Polynomials, in *Proceedings of the 45th IEEE Conference on Decision and Control*, San Diego, CA, USA, 2006, pp. 2924-2930.
- [22] L.-S. Shieh and S. Sacheti, A matrix in the block Schwarz form and the stability of matrix polynomials, *International Journal of Control*, vol. 27, no. 2, pp. 245-259, Feb. 1978.
- [23] M. Solak, Divisors of polynomial matrices: Theory and applications, *IEEE Transactions on Automatic Control*, vol. 32, no. 10, pp. 916-920, Oct. 1987.
- [24] C. D. Athalye, D. Pal, and H. K. Pillai, ℓ_∞ -stability analysis of discrete autonomous systems described by Laurent polynomial matrix operators, *Systems & Control Letters*, vol. 93, pp. 13-20, Jul. 2016.
- [25] Kailath, T., *Linear Systems*, Prentice Hall, Englewood Cliffs, 1980.
- [26] Chen, C.T., *Linear System Theory and Design*, Holt Rinehart and Winston, New York, 1984.
- [27] Rosenbrock, H.H., Distinctive problems of process control, *Chem. Eng. Prog.*, Vol. 58, pp. 43-50, 1962.
- [28] Callier F.M. and Desoer, C.A., *Multivariable Feedback Systems*, Springer-Verlag, New York, 1982.
- [29] Falb P.L. and Wolovich, W.A., Decoupling in the Design and Synthesis of Multivariable Control Systems, *IEEE Trans. Auto. Control*, Vol. AC-129 pp. 651-659, 1967.
- [30] Kucera, V., *Discrete Linear Control: The Polynomial Equation Approach*, John Wiley and Sons, Chichester, 1979.
- [31] B. Bekhiti, *Multivariate Control System Design Using the Theory of Matrix Polynomials*. Thesis, univ Boumerdes, 2018.

- [32] M. Yaici, MIMO Systems Compensator Design. Thesis, univ Boumerdes, 2014.
- [33] R. Muñoz-Mansilla, J. M. Díaz, J. Aranda, and D. Chaos, Robust control for high-speed crafts using QFT and eigenstructure assignment, *IET Control Theory & Applications*, vol. 4, no. 7, pp. 1265-1276, Jul. 2010.
- [34] X. Yang, B. Chen, and Y. Chen, An eigenstructure-based 2D DOA estimation method using dual-size spatial invariance array, *Science China Information Sciences*, vol. 54, no. 1, pp. 163-171, Jan. 2011.
- [35] H. Wu, Eigenstructure assignment-based robust stability conditions for uncertain systems with multiple time-varying delays, *Automatica*, vol. 33, no. 1, pp. 97-102, Jan. 1997.
- [36] B. Zhou and G. Duan, An explicit solution to polynomial matrix right coprime factorization with application in eigenstructure assignment, *Journal of Control Theory and Applications*, vol. 4, no. 2, pp. 147-154, May 2006.
- [37] C. Yang, J. Liu, and Y. Liu, Solutions of the generalized Sylvester matrix equation and the application in eigenstructure assignment, *Asian Journal of Control*, vol. 14, no. 6, pp. 1669-1675, Nov. 2012.
- [38] H. Ouyang, D. Richiedei, A. Trevisani, and G. Zanardo, Eigenstructure assignment in undamped vibrating systems: A convex-constrained modification method based on receptances, *Mechanical Systems and Signal Processing*, vol. 27, pp. 397-409, Feb. 2012.
- [39] D.-K. Gu, D.-W. Zhang, and G.-R. Duan, Parametric Control to a Type of Descriptor Quasi-linear Systems via Output Feedback, *IEEE Access*, pp. 39911-39922, 2019.
- [40] A. Wu and T. Iwasaki, Pattern Formation Via Eigenstructure Assignment: General Theory and Multi-Agent Application, *IEEE Transactions on Automatic Control*, vol. 63, no. 7, pp. 1959-1972, Jul. 2018.
- [41] J. A. Vazquez Trejo, M. Adam Medina, G. Ortiz Torres, J. Reyes Reyes, and G. V. Guerrero Ramirez, Robust Control System Design using Eigenstructure Assignment with Uncertain Parameters for a Double-Pipe Heat Exchanger, *IEEE Latin America Transactions*, vol. 16, no. 3, pp. 851-858, Mar. 2018.
- [42] Guang-RenDuan, Circulation algorithm for partial eigenstructure assignment via state feedback, *European Journal of Control*, In Press, Feb. 2019.
- [43] C. Wang, L. Guo, and J. Qiao, Event-triggered adaptive fault-tolerant control for nonlinear systems fusing static and dynamic information, *Journal of the Franklin Institute*, vol. 356, no. 1, pp. 248-267, Jan. 2019.
- [44] Active aeroelastic output feedback control with partial measurements by the method of receptances, *Aerospace Science and Technology*, vol. 86, no. 1, pp. 47-63, Mar. 2019.
- [45] Ignacio Ojeda, Kronecker Square Roots and the Block Vec Matrix, *The American Mathematical Monthly*, vol. 122, no. 1, pp. 60, 2015.
- [46] B. Bekhiti, A. Dahimene, B. Nail, et al, Block-structure relocation via state and state derivative feedback: eigenspace of matrix polynomials characterization. *Journal of Control and Systems Engineering*, vol. 4, no. 1, 95-111, 2016.
- [47] J. Leyva-Ramos, A new method for block partial fraction expansion of matrix fraction descriptions, *IEEE Trans. Autom. Cont.*, Vol. AC-36, No.12, pp. 1482-1485, 1991.

- [48] V. R. Dehkordi and B. Boulet, "Robust controller order redeuction", *Int. J. Cont.*, Vol. 84, No. 5, pp. 985-997, 2011.
- [49] B. Bekhiti, A. Dahimene, B. Nail, K. Hariche, and A. Hamadouche, On Block roots of matrix polynomials based MIMO control system design, in 2015 4th International Conference on Electrical Engineering (ICEE), Boumerdes, Algeria, 2015, pp. 1-6.
- [50] B. Nail, A. Kouzou, A. Hafaifa, and V. Puig, Optimal Static State-Feedback Controller Design for MIMO LTI Systems Based on Constraints Block Roots and Interior-Point Algorithm: Application to Gas Compressor System, in 2018 International Conference on Applied Smart Systems (ICASS), Medea, Algeria, 2018, pp. 1-6.
- [51] B. Bekhiti, A. Dahimene, B. Nail, and K. Hariche, On λ -matrices and their applications in MIMO control systems design, *International Journal of Modelling, Identification and Control*, vol. 29, no. 4, pp. 281-294, 2018.
- [52] Nail B., Kouzou A., Hafaifa A. (2019) Digital Stabilizing and Control for Two-Wheeled Robot. In: Derbel N., Ghommam J., Zhu Q. (eds) *New Developments and Advances in Robot Control. Studies in Systems, Decision and Control*, vol 175. Springer, Singapore, 2019, pp. 237-253.

Background in Fault Detection and Fault Tolerant Control

1 Introduction

The increase in productivity, quality and availability of industrial systems are major issues, mainly related to the safety and reliability of these industrial facilities (safety of people, the environment and equipment). Recently, several modern methods have been designed to control the dependability of industrial systems, aim to increase production rates while reducing maintenance time, these methods focus on the achievement of an effective diagnosis to these systems. impaired by faults or malfunctions [1]. Fault tolerant control (FTC) is the name given to all those techniques that are capable of maintaining the overall system stability and acceptable performance in the presence of faults. In other words, a closed-loop system which can tolerate component malfunctions, while maintaining desirable performance and stability properties is said to be a fault tolerant control system (FTCS) [1]. In this chapter, the main concepts of fault tolerant control and fault detection are presented, as well as the different methods and approaches used in this field. The disadvantages and advantages of each method presented will be highlighted.

2 Background in Fault Detection strategies

2.1 Basic principle of diagnosis

The increase in monitoring can be achieved by improving the diagnostics of the functional units but also by implementing a maintenance strategy adapted to the installation studied.

A diagnostic system must therefore be able to perform the following three essential steps: fault detection, fault location and fault identification. The implementation of such an approach need to generate indicators of faults or symptoms, then to correctly interpret these symptoms to determine the origin of the fault, that is to say the element with abnormal operation and finally to make a decision for a return to normal operation of the installation . The development of a structure such as that presented Figure. 1.1 requires the exploitation of all the knowledge available on the installation [2–4].

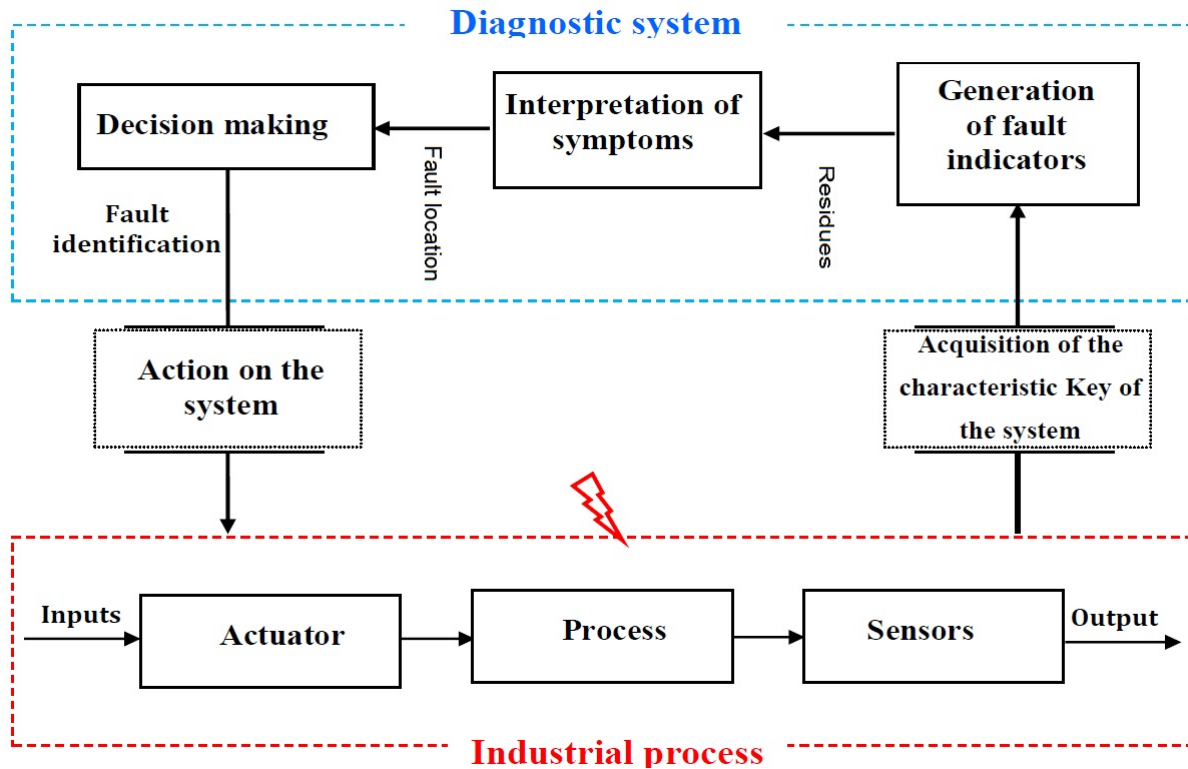


Figure 1.1: General structure of a diagnostic system

2.2 Diagnostic assistance approach

The different arrangements to be made beforehand in order to carry out an active diagnostic assistance approach [2, 3, 5–8]:

- Study of the technical and economic interest of the implementation of the diagnostic system taking into account the experience feedback on the costs of failures,
- Study of the technical reliability of the diagnostic assistance system to ensure that techniques and technologies are available and operational for the problem to be solved,
- Creation of a project team with all stakeholder to define and write the detailed specification book,
- Validation of the specifications by the managers of the company for the launch of the realization and its implementation,
- Training and information of stakeholder for effective use of the diagnostic support system,
- Realization and implementation of the on-site diagnostic assistance system,
- Establishment of feedback to evaluate the economic and social impacts of the diagnostic support system [3, 9, 10].

2.3 Different stages of industrial diagnosis

The different phases of industrial surveillance essential to the design, realization and use of diagnostic assistance techniques are illustrated in Figure. 1.2. These different stages of the industrial diagnosis are summarized as

follows [12, 13].: **Acquisition of data, Generation of fault indicators, Detection of faults and localization a fault.**

The purpose of the localization is to locate a detected fault occurring on the actuators, on the sensors, on the command or the controlled system, indicating which organ or component is affected by:

Fault Identification : The determination of the size and temporal behavior of a fault.

Making Decision : This involves deciding on the steps to follow to keep the desired performance of the system under control [2, 3].

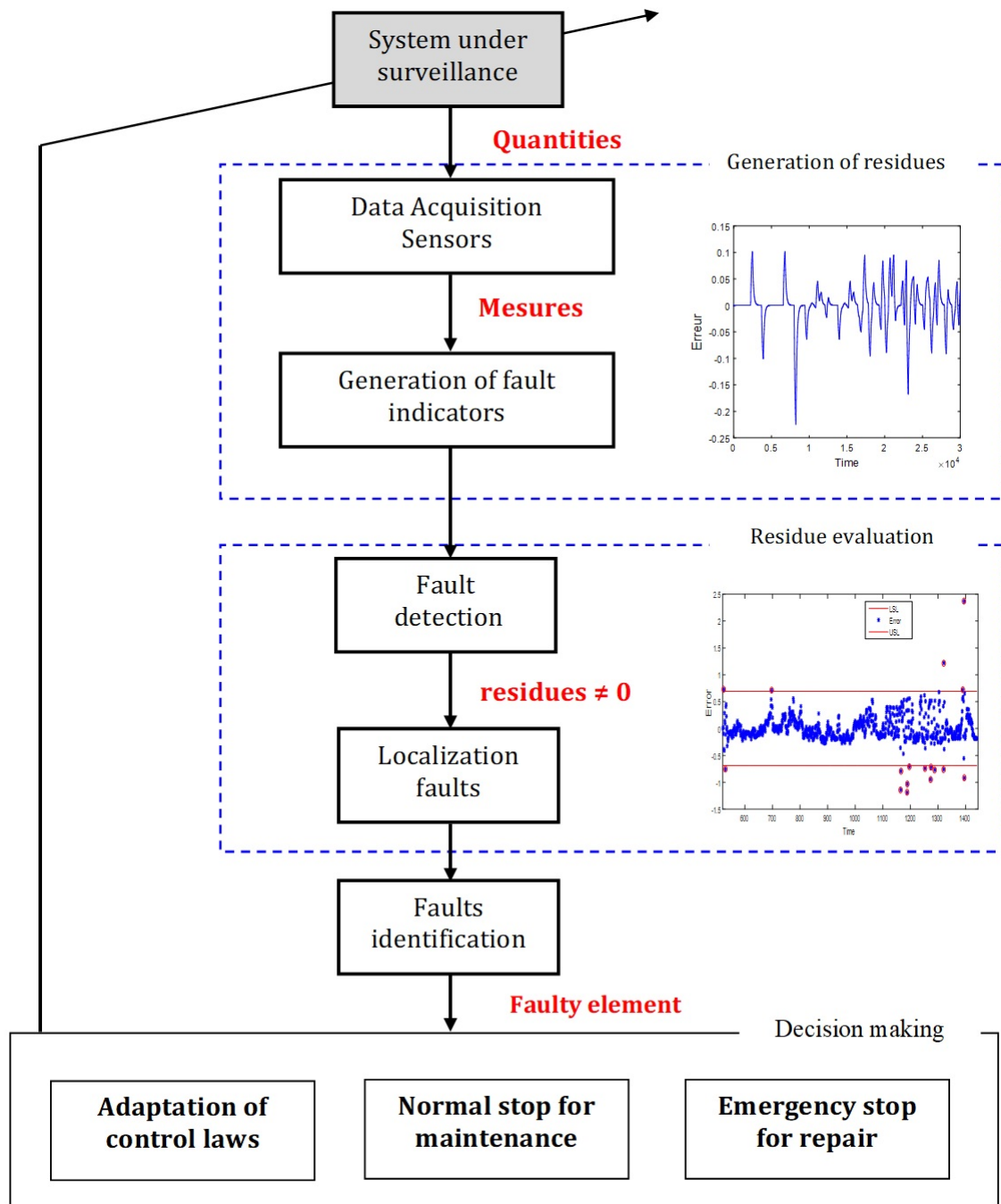


Figure 1.2: Different stages of industrial diagnosis

2.4 Classification of diagnostic methods based on models

In this part, we will represent a classification of diagnostic techniques, divided into two main families: Quantitative techniques, based on a characterization of the signals input / output systems or techniques and techniques using the concept of artificial intelligence, called qualitative diagnosis, as shown in Figure. 1.3.

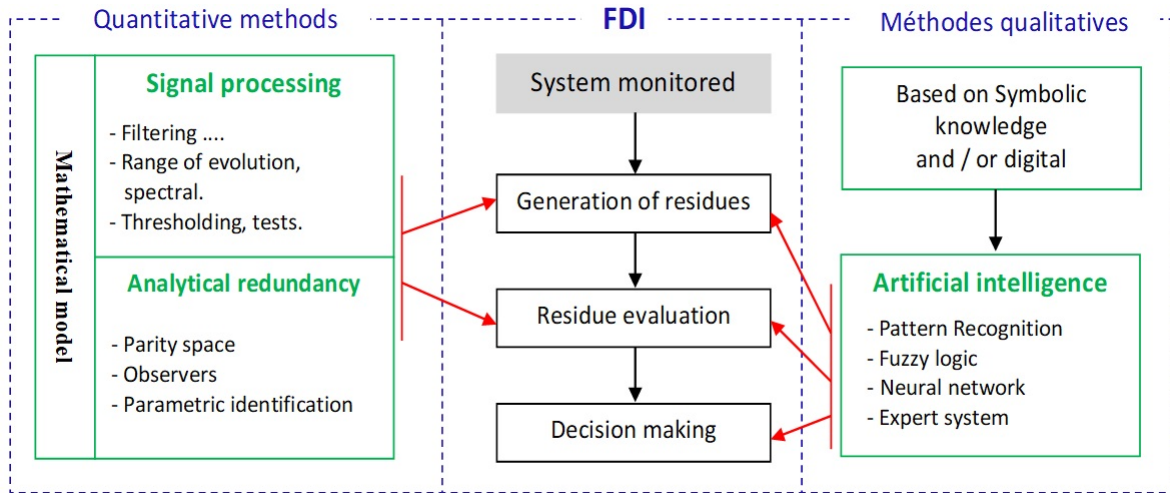


Figure 1.3: Classification of diagnostic methods

3 Background in Fault Tolerant Control

A fault tolerant system has the ability to maintain nominal goals despite the occurrence of a fault and to accommodate it automatically. In particular, it makes it possible to guarantee system stability and / or acceptable performance in the presence of faults [9, 19, 20]. Despite the fact that a standard control scheme ensures the desired stability and performance of the system in the nominal case, it is very limited and can guide the system towards uncontrolled behavior or even instability. in the presence of a fault. To overcome such shortcomings, particular control laws, taking into account the effect of the fault, have been developed with the precise aim of protecting the desired performances. The FTC problem has begun to draw more and more attention in a wider range of industrial and academic communities, due to the increased safety and reliability demands beyond what a conventional control system can offer. FTC applications include aerospace, nuclear power, automotive, manufacturing and other process industries.

The current FTC methods can be classified into three categories:

- Hardware redundancy techniques
- Analytical redundancy techniques: passive fault tolerant control (PFTC)
- Analytical redundancy techniques: active fault tolerant control (AFTC).

3.1 Hardware Redundancy Techniques

In principle, the tolerance to control system failures can be improved if two or more sensors/actuators, each separately capable of satisfactory control, are implemented in parallel. This approach is referred to as hardware redundancy. A voting scheme is used for the redundancy management, comparing control signals to detect and

overcome failures. With two identical channels, a comparator can determine whether or not the control signals are identical; hence, it can detect a failure but cannot identify which component has failed. Using three identical channels, the control signal with the middle value can be selected (or voted), assuring that a single failed channel never controls the plant. A two-channel system is considered fail-safe because the presence of a failure can be determined, but it is left to additional logic to select the unfailed channel for control. The three-channel system is fail-operational, as the task can be completed following a single failure. Systems with four identical control channels can tolerate two failures and still yield nominal performance. Problems encountered in implementing hardware redundancy include: selection logic, reliability of voting, increased hardware and maintenance costs.

3.2 Passive Fault Tolerant Control Techniques

The passive FTC techniques synthesize a controller so that the closed-loop system is stable, or has some desired performance, for some combinations of failure elements defined a priori. This is done by using the results in the robust control area, considering faults as if they were uncertainties or system perturbations. In particular, the term passive indicates that no actions are required by the FTCS after the prescribed faults have occurred during the system's operation.

This approach has the advantage of needing neither fault diagnosis schemes nor controller reconfiguration, but it has limited fault tolerant capabilities and the price to pay for its simplicity is a loss of performance with respect to the nominal case. Also, in passive FTC no time delay exists between the fault occurrence and the corresponding action. For these reasons, the design of passive FTCS has attracted a lot of attention from the academic community [4]. A good historical overview about development and research of passive FTC techniques can be found in [5]. Some of the passive FTC approaches found in the literature are: reliable linear quadratic (LQ), H_∞ robust control and passive FTC using LMIs.

- Reliable Linear Quadratic (*LQ*) Approach
- H_∞ Robust Control
- Passive FTC Using Linear Matrix Inequalities (LMIs)

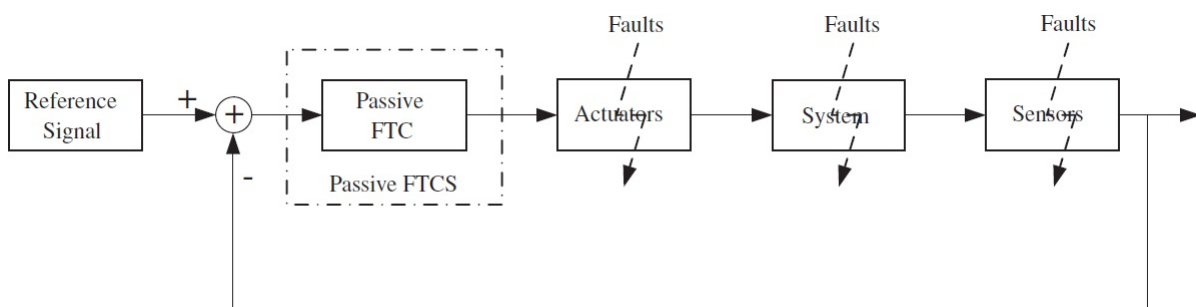


Figure 1.4: Different steps of fault tolerant control

3.3 Active Fault Tolerant Control Techniques

As pointed out in [2], an active FTC system can be typically divided into four subsystems:

- a reconfigurable controller

- a fault diagnosis scheme
- a controller reconfiguration mechanism
- a command/reference governor

The inclusion of both a fault diagnoser and a reconfigurable controller within the overall control system scheme is the main feature distinguishing active FTC from passive FTC. Key issues in active FTC consist in how to design:

- a controller that can be reconfigured
- a fault diagnosis scheme with high sensitivity to faults and robustness against model uncertainties, variations of the operating conditions, and external disturbances
- a reconfiguration mechanism that allows recovering the pre-fault system performance as much as possible, in presence of uncertainties and time delays in the fault diagnosis, as well as constraints on the control inputs and the allowed system states

Based on the online information of the post-fault system, the reconfigurable controller should be designed to maintain stability, desired dynamic performance and steady-state performance. In addition, in order to ensure that the closed-loop system can track a desired trajectory under fault occurrence, a reconfigurable feedforward controller often needs to be synthesized. Also, a command/reference governor that adjusts the reference trajectory automatically should be added to avoid potential actuator saturation and to take into consideration the degraded performance after fault occurrence.

Some of the existing active FTC techniques that can be found in the literature are the following: linear quadratic (LQ), pseudo-inverse method (PIM), intelligent control (IC), gain-scheduling (GS), model following (MF), adaptive control (AC), multiple model (MM), integrated diagnostic and control (IDC), eigenstructure assignment (EA), feedback linearization (FL)/dynamic inversion (DI), model predictive control (MPC), quantitative feedback theory (QFT) and variable structure control (VSC)/sliding mode control (SMC).

Anyway, even if each individual control design method has been developed separately, in practice a combination of several of these methods may be more appropriate to achieve the best performance.

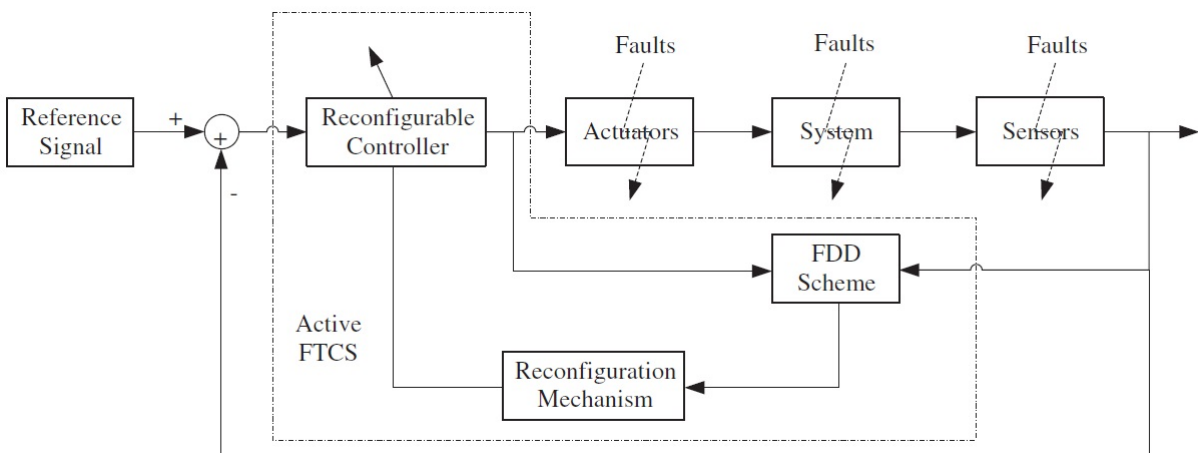


Figure 1.5: Different steps of fault tolerant control

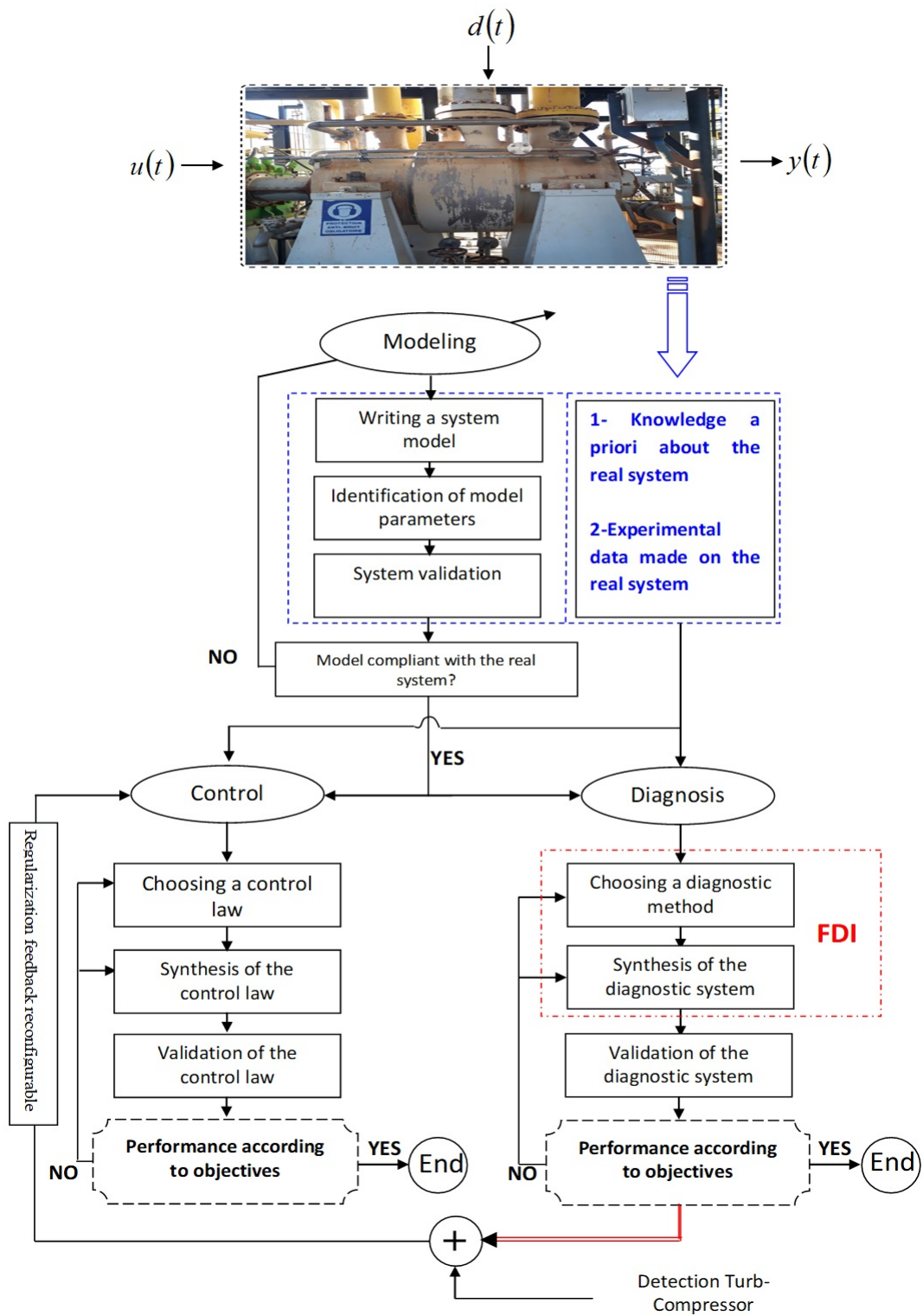


Figure 1.6: Different steps of fault tolerant control

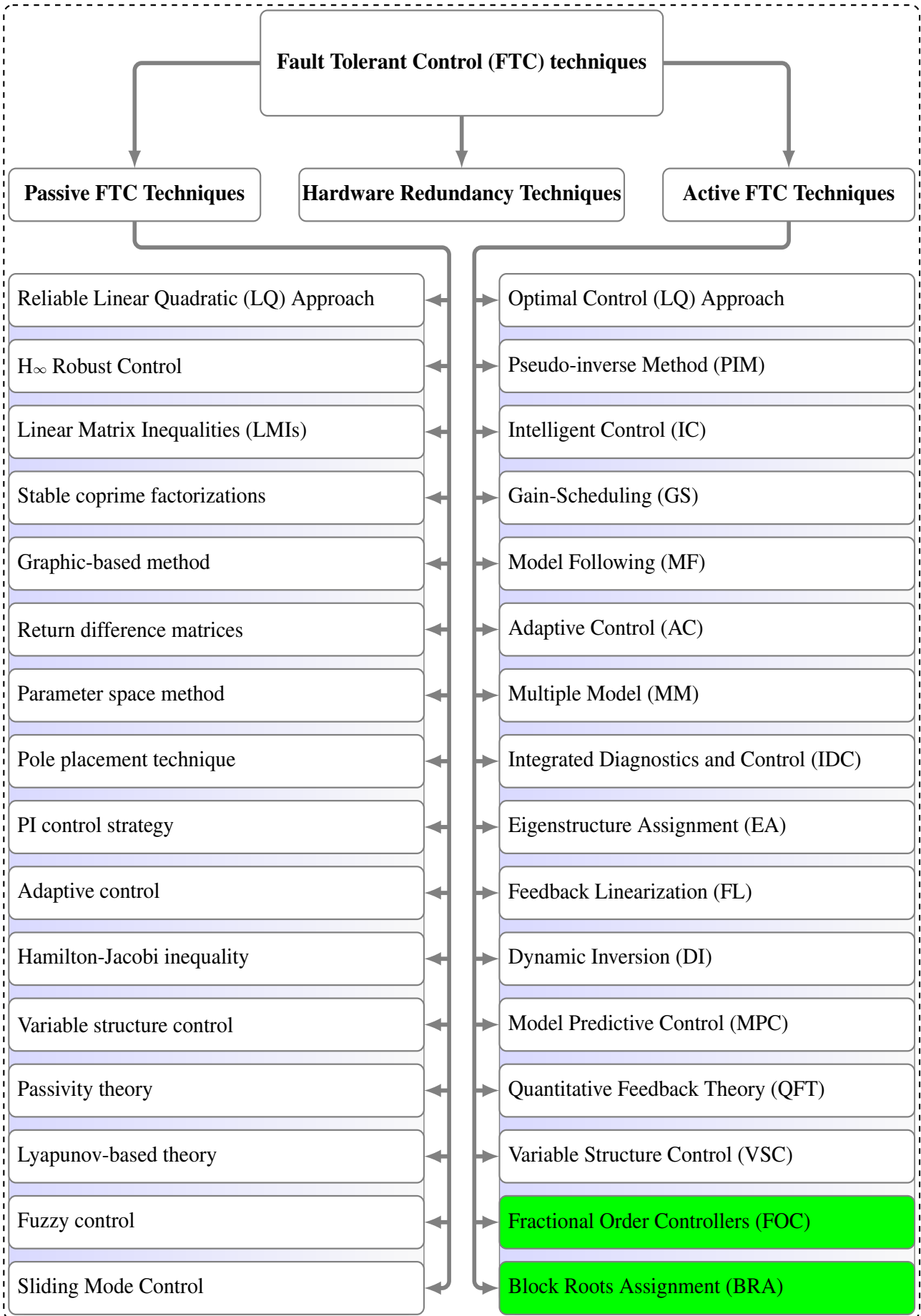


Figure 1.7: General structure of a diagnostic system

4 Conclusion

In this chapter we have presented different methods for the realization of FDI structures using observers. The diagnosis of failures and degradation is an essential element in the industry where each company chooses one or more diagnostic methods according to its maintenance policy and according to the field of applications. It is done in three stages. The first step is the detection of faults that solves the problems of thresholding of the residues, the second step corresponds to the location step for obtaining optimal structures of fault signatures. And finally, the identification stage that defines the default type that appears in this situation. As a result of this work, we became interested in model-based diagnostic methods obtained by artificial intelligence techniques for the treatment of gas turbine system vibration problems. The next chapter aims to make the vibration detection and localization step more robust.

5 References

- [1] D. Rotondo, *Advances in gain-scheduling and fault tolerant control techniques*. Thesis, Cham: Springer, 2018.
- [2] N. Hadrouge, *Commande neuro floue tolérante aux défauts d'une turbine à gaz : Contribution à la détection de vibrations*. Thesis, univ djelfa, 2017.
- [3] Frank P. M. and Ding X., Survey of robust residual generation and evaluation methods in observer-based fault detection systems. *Journal of Process Control*, 1997, vol. 7, no. 6, pp. 403-424.
- [4] Frank P.M, Alcorta-Garcia.E et Köppen-Seliger, Modelling for fault detection and isolation versus modelling for control. *Mathematical and Computer Modelling of Dynamical Systems*, 2001, vol. 7, no. 1, pp. 1-46.
- [5] Ahmed Boubenia, Ahmed Hafaiifa, Abdellah Kouzou, Kamal Mohammedi and Mohamed Becherif, Carbon dioxide capture and utilization in gas turbine plants via the integration of power to gas. *Petroleum Elsevier*, 2017, vol. 3, pp. 127-137.
- [6] Ailer P., Santa I., Szederkenyi G. and Hangos K.M., Nonlinear model-building of a low-power gas turbine, *Periodica Polytechnica Series on Transportation Engineering*, 2001, vol. 32, pp. 117-135.
- [7] Gertler Janos J., Analytical redundancy methods in failure detection and isolation in complex plants. *Control Theory and Advanced Technology*, 1993, vol. 9, no. 1, pp. 259-285.
- [8] Karim Salahshoor, Mojtaba Kordestani, Design of an active fault tolerant control system for a simulated industrial steam turbine. *Applied Mathematical Modelling*, 2014, vol. 38, no. 5-6, pp. 1753-1774.
- [9] Abdelhafid Benyounes, Ahmed Hafaiifa and Mouloud Guemana, Fuzzy logic addresses turbine vibration on Algerian gas line. *Oil & Gas Journal*, 2016, vol. 114, no. 1, pp. 22-28
- [10] Alfredo Ursúa, Pablo Sanchis, Static-dynamic modelling of the electrical behaviour of a commercial advanced alkaline water electrolyser. *International Journal of Hydrogen Energy*, 2012, vol. 37, no. 24, pp. 18598-18614.

- [11] Ahmed Hafaifa, Guemana Mouloud, and Belhadef Rachid, Fuzzy Modeling and Control of Centrifugal Compressor Used in Gas Pipelines Systems. *Multiphysics Modelling and Simulation for Systems Design and Monitoring*, Book Chapter, Applied Condition Monitoring, 2015, vol. 2, pp.379-389.
- [12] Jyh-Shing Roger Jang, CT Sun, Functional equivalence between radial basis function networks and fuzzy inference systems. *IEEE Transactions on Neural Networks*, 1993, vol. 4, no. 1, pp. 156-159.
- [13] J. Jiang and X. Yu, Fault-tolerant control systems: A comparative study between active and passive approaches, *Annual Reviews in Control*, vol. 36, no. 1, pp. 60-72, Apr. 2012.

Multivariable Robust Static State-Feedback Controller design

1 Introduction

The loss of monitoring in the stability of some important industrial processes causes a dramatic accidents that can lead to many severe problems and damages, such as human accident, loss of production, damage of equipments and assets...etc.

The main contribution of the present work is to developed a stability control algorithm which is based on state feedback matrix static gains, where the availability and the measurability of the states in the outputs should to be ensured, the design of the proposed controller is based on matrix fraction description and the block roots of matrix polynomials, in this chapter, the proposed and the developed stability control technique is applied on a gas turbine system which presents a very complex industrial systems. This system is an internal combustion engine which uses the gaseous energy of air, convert the chemical energy of the fuel into mechanical energy, indeed, gas turbines are also called combustion turbines, and it is one of the most important parts of modern industry using this type of machinery, different comparison study is introduced in this chapter to prove the domination of the proposed controller.

2 Preliminaries and Problem Statement

Let consider the following linear single-input continuous-time dynamic model of spring-mass-damper system, which is described by dynamic state as:

$$\begin{pmatrix} \dot{x}_1 \\ \dot{x}_2 \end{pmatrix} = \begin{pmatrix} 0 & 1 \\ \alpha & \beta \end{pmatrix} \begin{pmatrix} x_1 \\ x_2 \end{pmatrix} + \begin{pmatrix} 0 \\ 1 \end{pmatrix} u \quad (2.1)$$

Define a line in the state space, shown in Figure. 2.1, as follows:

$$s(t) = x_2(t) + \lambda x_1(t), \quad \lambda > 0 \quad (2.2)$$

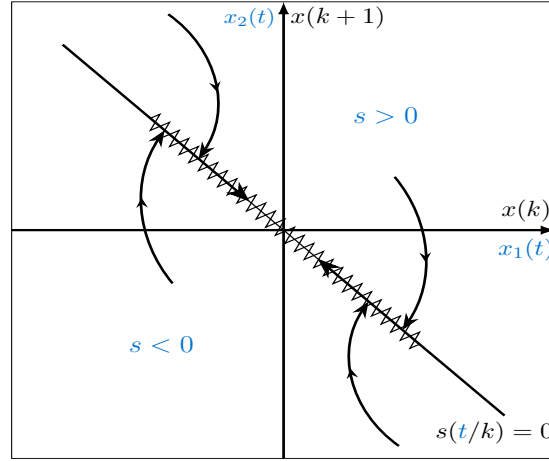


Figure 2.1: Phase portrait under Sliding mode control effect

When $s = 0$, the line passes through the origin of the state space, and this line will be called the **sliding line**. The first objective is to ensure that the system will reach this line from any initial conditions in a finite time and will remain on this line after reaching it. The condition to achieve this objective is called **reaching** or **attractive condition** Slotine and Coet see [1] and is described as

$$\dot{s} = -\delta \text{sgn}(s), \quad \delta > 0 \quad (2.3)$$

where the **sign** function $\text{sgn}(s)$ is defined as follows:

$$\text{sgn}(s) = \begin{cases} +1 & \text{if } s > 0 \\ -1 & \text{if } s < 0 \end{cases} \quad (2.4)$$

When $s > 0$, \dot{s} is a negative constant δ , and s will decrease linearly to $s = 0$ in a finite time. Similarly, when $s < 0$, \dot{s} is a positive constant δ , and s will increase linearly to $s = 0$ in a finite time. The condition (2.3) is also written as

$$s\dot{s} < 0 \quad (2.5)$$

When the system remains on the sliding line, $\dot{s} = 0$. The corresponding input u is called the **equivalent control**, u_{eq} , and is obtained by differentiating (2.2) and using state equations (2.1):

$$\dot{s} = \alpha x_1 + (\beta + \lambda) x_2 + u \quad (2.6)$$

For $\dot{s} = 0$,

$$u_{eq} = -\alpha x_1(t) - (\beta + \lambda) x_2(t) \quad (2.7)$$

Therefore, to satisfy the reaching condition (2.3), the control law is

$$u(t) \triangleq u_{eq}(t) - \delta \text{sgn}(s) \quad (2.8)$$

On the sliding line, $u(t) = u_{eq}$ and state equations (2.1) become

$$\begin{pmatrix} \dot{x}_1 \\ \dot{x}_2 \end{pmatrix} = \begin{pmatrix} 0 & 1 \\ 0 & -\lambda \end{pmatrix} \begin{pmatrix} x_1 \\ x_2 \end{pmatrix} \quad (2.9)$$

The eigenvalues of this system are 0 and $-\lambda$. The zero eigenvalue reflects the fact that the system is constrained to remain on the $s = 0$ line. Hence, the effective dynamics on the sliding line is represented by $-\lambda$, which is in the

left half of the complex plane when $\lambda > 0$. Here, the effective dynamics can also be derived from (2.2) by using the first state equation and $s = 0$:

$$\dot{x}_1 + \lambda x_1 = 0 \quad (2.10)$$

In summary, the sliding mode control input has two parts: linear and nonlinear. The nonlinear part, sgn function, ensures the reaching condition. After the system has reached the sliding line, the control law is linear full state feedback seen (2.7).

Problem statement Generalized this full state feedback sliding mode controller to the class of discrete-time multi-inputs/multi-outputs (MIMO) systems using the concept of the matrix polynomials, and obtaining the robust matrix G which achieves the global stability in closed loop system as shown in Figure. 2.2, and this based on block roots assignments and tangent hyperbolic function. The next section presents the proposed algorithm steps which solve this problem with detail.

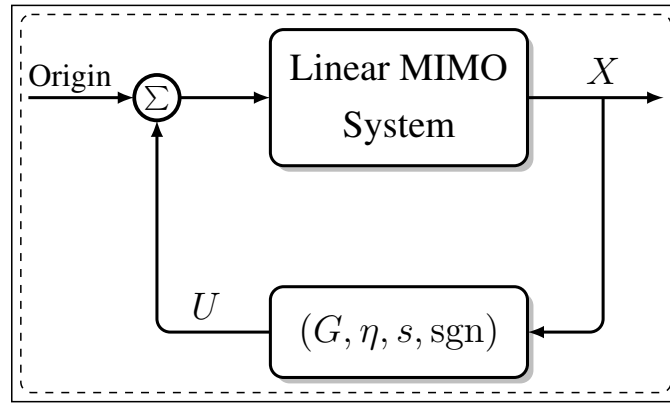


Figure 2.2: Schematic of SSF controller gain stabilization.

3 Main results

The MIMO linear invariant discrete-time system can be described in dynamic state equation as follows:

$$x(k+1) = Ax(k) + Bu(k) \quad (2.11)$$

Where $A \in \mathbb{R}^{n \times n}$, $B \in \mathbb{R}^{n \times m}$

For m inputs, there are m new planes in the state space obtained by this definition:

$$s_i(k) = g_i^T x(k) \quad , \quad i = 1 \ 2 \ \dots \ m \quad (2.12)$$

These new planes pass through the origin of the state space, by deriving (2.12) with respect to k and substituting into (2.11) we obtain

$$s_i(k+1) = g_i^T x(k+1) = g_i^T Ax(k) + g_i^T Bu(k) \quad (2.13)$$

(2.13) can be rewritten in a matrix form as follows:

$$s(k+1) = GAx(k) + GBu(k) \quad (2.14)$$

Where, $s(k) = [s_1(k) \ s_2(k) \ \dots \ s_m(k)]^T$, and $G = [g_1 \ g_2 \ \dots \ g_m]^T$, from (2.12), it is also noted that

$$s(k) = Gx(k) \quad (2.15)$$

To ensure that the state variable $x(k)$ slides toward the surface, the two conditions have to be satisfied, $s(k) = 0$ and $\implies s(k+1) = 0$, this is the case where the intersection of the all m sliding plans, crosses the origin of the state space, therefore from (2.14) the equivalent control $u_{eq}(k)$ can be written as follows:

$$u_{eq}(k) = -(GB)^{-1}GAx(k) \quad (2.16)$$

The matrix GB has been assumed to be nonsingular.

In order to reduce the undesirable chattering phenomenon, the hyperbolic tangent function (Tanh) was proposed in several previous works as shown in Figure. 2.3, [2–5]. Indeed, it presents a robust compensator which provides and switches the control action smoothly and ensures avoiding the chattering phenomenon. This robust compensator is continuously differentiable with respect to the both variables, the time variable k , and the surface control variable $s(k)$ which guarantees the asymptotic stability. In comparison with the conventional bang-bang signum (Sign) and saturation (Sat) functions, it can be said that the superiority of the robust compensator based on hyperbolic tangent function in ensuring a smooth control input and the stability convergence of the closed-loop system can be achieved [5], consequently, the discontinuous (switching) control u_d can be expressed as follows:

$$u_d = \beta \tanh(s(k)) \quad (2.17)$$

Where, the whitening sliding gain matrix β is chosen as a diagonal positive matrix, and a much better reaching law condition for each plane is given by [6] and described in Figure. 2.1 It takes the following form:

$$|s(k+1)| < |s(k)| \quad (2.18)$$

A suitable control law u satisfying the reaching condition law as presented in (2.18), will guarantee to all the state trajectories to be remaining within a domain of decreasing or at the worst case within a domain of non increasing radius. The inequality presented in (2.18) can be decomposed into two inequalities as follows:

$$[s(k+1) - s(k)] \tanh(s(k)) < 0 \quad (2.19)$$

and

$$[s(k+1) + s(k)] \tanh(s(k)) \geq 0 \quad (2.20)$$

The sliding control law which satisfies all conditions takes the following form:

$$u = u_{eq} + u_d \quad (2.21)$$

Finally, the control law is selected as follows:

$$u(k) = u_{eq}(k) + \beta \tanh(s(k)) \quad (2.22)$$

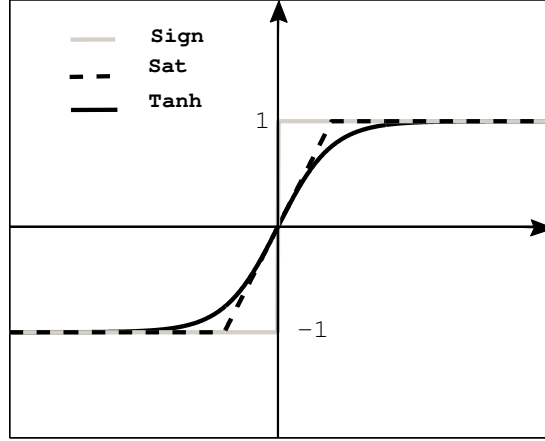


Figure 2.3: Comparison between the Sign, Sat and Tanh functions

3.1 The calculation of robust sliding matrix gain G

The similarity transformation proposed in this paper is defined as follows:

$$p(k) = Fx(k) \quad (2.23)$$

Where,

$$F = \begin{pmatrix} N_r & \vdots & B \end{pmatrix} \quad (2.24)$$

N_r : Right kernel (null space) of matrix B^T , such that

$$B^T N_r = 0 \quad (2.25)$$

The state variable is obtained as follows:

$$x(k) = F^{-1}p(k)$$

Based on (2.11) and (2.23) the following system is obtained:

$$p(k+1) = A_s p(k) + B_s u(k) \quad (2.26)$$

Where, $A_s = FAF^{-1}$ and $B_s = FB$.

The singular value decomposition (SVD) of a matrix $B^T \in \mathbb{R}^{m \times n}$ may be written as

$$B^T = U \Sigma V^T \quad (2.27)$$

The right null space N_r of a matrix A is the columns of V corresponding to singular values equal to zero. From [7] and [8], the columns of the $n \times (n-m)$ matrix N_r are composed of basis vectors of the right null space of B^T .

Because of the special structure of the matrix F , the first $(n-m)$ rows of B_s turn out to be zeros. Hence, the new state vector $p(k)$ is decomposed as follows:

$$p(k) = \begin{pmatrix} p_1(k) \\ p_2(k) \end{pmatrix} \quad (2.28)$$

Where $p_1(k)$ and $p_2(k)$ are $(n - m)$ and m dimensional vectors, respectively, partitioning the dynamic state (2.26)

$$\begin{pmatrix} p_1(k+1) \\ p_2(k+1) \end{pmatrix} = \begin{pmatrix} A_{s11} & A_{s12} \\ A_{s21} & A_{s22} \end{pmatrix} \begin{pmatrix} p_1(k) \\ p_2(k) \end{pmatrix} + \begin{pmatrix} 0 \\ B_{sr} \end{pmatrix} u(k) \quad (2.29)$$

The sliding planes can take the following forms

$$s(k) = p_2(k) + Kp_1(k) \quad (2.30)$$

Where $K \in \mathbb{R}^{m \times (n-m)}$ is gain matrix

$$s(k) = \begin{pmatrix} K & I_m \end{pmatrix} \begin{pmatrix} p_1(k) \\ p_2(k) \end{pmatrix} \quad (2.31)$$

$$s(k) = \begin{pmatrix} K & I_m \end{pmatrix} Fx(k)$$

Equating (2.15) with (2.31), the sliding matrix G is obtained such as

$$G = [K \quad I_m]F \quad (2.32)$$

(2.32) indicates that the determination of the sliding matrix G elements depends on the calculation of the matrix K elements. The stability of the dynamic system can be ensured on the intersection of the all sliding plans, when the condition of $s(k) = 0$. Consequently, the following expression is obtained:

$$p_2(k) = -Kp_1(k) \quad (2.33)$$

(2.25) yields,

$$\begin{cases} p_1(k+1) = A_{s11}p_1(k) + A_{s12}p_2(k) \\ p_2(k+1) = A_{s21}p_1(k) + A_{s22}p_2(k) + B_{sr}u(k) \end{cases} \quad (2.34)$$

From the first dynamic state of (2.34), $p_2(k)$ is considered as the input, whereas (2.33) presents the state feedback law, [8] demonstrated that (A_{s11}, A_{s12}) are controllable if (A, B) are controllable.

The design of the matrix gain K can be achieved based on the use of the MFD theory by assigning robust block roots, that allow to ensure the stability of the eigenvalues of the new matrix $(A_{s11} - KA_{s12})$ (their values are kept within the unit circle). To prove the effectiveness of the proposed control, a comparison with classical and advanced algorithms, such as pole placement [9], Discrete-time linear quadratic regulator [10], Eigen-structure assignment [11], and State and State Derivative Feedback [12] is presented in this paper.

From (2.11) and (2.16), the system dynamics on the intersection of sliding planes is given by

$$x(k+1) = (A - B(GB)^{-1}GA)x(k) \quad (2.35)$$

3.2 The computation of matrix gain K via robust block roots assignment

3.2.1 A polynomial matrix

Given a set of complex matrices $\{A_0, A_1, \dots, A_l\}$ of dimension $\mathbb{R}^{m \times m}$, the set of the following matrix is the matrices coefficients of the λ polynomial matrix of degree l and order m .

$$A(\lambda) = A_0\lambda^l + A_1\lambda^{l-1} + \dots + A_{l-1}\lambda + A_l \quad (2.36)$$

Consider the system described by the following Discrete-time dynamic state equation

$$p_1(k+1) = A_{s11}p_1(k) + A_{s12}p_2(k) \quad (2.37)$$

where, $A_{s11} \in \mathbb{R}^{(n-m) \times (n-m)}$ and $A_{s12} \in \mathbb{R}^{(n-m) \times m}$ the transformation of the system into the block controllable form needed to checking both essential conditions

- The number $(n - m)/m = l$ is an integer.
- The matrix W_c is of full rank $(n - m)$.

Remark 1. If l is not an integer, the dimensions of the system (2.11) and first dynamic (2.34) do not verify the previous condition then, according to [13], the system can be extended by adding a set of low (non-dominant) stable eigenvalues on the diagonal entries of the state matrix A so that the condition is fulfilled.

Block controllability matrix

$$W_c = \begin{pmatrix} A_{s12} & A_{s11}A_{s12} & \dots & A_{s11}^{l-1}A_{s12} \end{pmatrix} \quad (2.38)$$

Then, the transformation matrix T_c [14] is given as follows:

$$T_c = \begin{pmatrix} T_{cl} \\ T_{cl}A_{s11} \\ \vdots \\ T_{cl}A_{s11}^{l-2} \\ T_{cl}A_{s11}^{l-1} \end{pmatrix}, \quad T_{cl} = (O_m \quad O_m \quad \dots \quad I_m)W_c^{-1} \quad (2.39)$$

The new dynamic system state equation becomes:

$$p_1(k+1) = A_c p_1(k) + B_c p_2(k) \quad (2.40)$$

with, $A_c = T_c A_{s11} T_c^{-1}$, $B_c = T_c A_{s12}$

$$A_c = \begin{pmatrix} O_m & I_m & \dots & O_m \\ O_m & O_m & \dots & O_m \\ \vdots & \vdots & \dots & \vdots \\ O_m & O_m & \dots & I_m \\ -A_l & -A_{l-1} & \dots & -A_1 \end{pmatrix}, \quad B_c = \begin{pmatrix} O_m \\ O_m \\ \vdots \\ O_m \\ I_m \end{pmatrix}$$

3.2.2 The concept of block roots (solvents)

The l block roots $R \in \mathbb{R}^{m \times m}$ are the solvents of the λ polynomial matrix $A(\lambda)$, there exist two types of roots right and left, in this algorithm just focusing for assigning a right block roots.

3.2.3 The right solvent

Given the polynomial matrix of order m and degree l defined by:

$$D_R(z) = I_m z^l + A_1 z^{l-1} + \dots + A_l \quad (2.41)$$

A right solvent defined by $R \in \mathbb{R}^{m \times m}$ matrices satisfying:

$$D_R(R) = A_0 R^l + A_1 R^{l-1} + \dots + A_{l-1} R + A_l = 0_m \quad (2.42)$$

How To choose the closed-loop block roots (Regulator Block Roots) The characteristic polynomial matrix of the feedback gain matrix is obliged to equal a wanted polynomial matrix $D_d(\lambda)$, which may be extracted from a set of desired block roots $R \in \mathbb{R}^{m \times m}$, these right block roots are to be selected from class of stable eigenvalues chosen in the dominant zone and without consuming the dynamics of the system in the same time, there are many forms will be selected (controller/observer and diagonal/general forms), the diagonally form is restricted in this research.

$$R = \left(\overbrace{\left[\begin{array}{c|c|c} \lambda_1 & 0 & 0 \\ \hline 0 & \ddots & 0 \\ \hline 0 & 0 & \lambda_m \end{array} \right]}^{R_1}, \dots, \overbrace{\left[\begin{array}{c|c|c} \lambda_{n-2m} & 0 & 0 \\ \hline 0 & \ddots & 0 \\ \hline 0 & 0 & \lambda_{n-m} \end{array} \right]}^{R_l} \right) \quad (2.43)$$

The condition of complete set roots Consider the set of solvents $\{R_1, R_2, \dots, R_l\}$ extracted from the eigenvalues $(\lambda_1, \lambda_2, \dots, \lambda_n)$ of a matrix A_c , where $\{R_1, R_2, \dots, R_l\}$ is a complete set of roots if and only if:

$$\begin{cases} \sigma(R_i) \cup \sigma(R_j) = \sigma(A_c) \\ \sigma(R_i) \cap \sigma(R_j) = \emptyset \\ \det(V_r(R_1, R_2, \dots, R_l)) \neq 0 \end{cases} \quad (2.44)$$

Where, σ Denotes the spectrum of the matrix and V_r is the Right Block Vandermonde matrix corresponding to $\{R_1, R_2, \dots, R_l\}$ given as:

$$V_r(R_1, R_2, \dots, R_l) = \begin{pmatrix} I_m & I_m & \cdots & I_m \\ R_1 & R_2 & \cdots & R_l \\ \vdots & \vdots & \ddots & \vdots \\ R_1^{l-1} & R_2^{l-1} & \cdots & R_l^{l-1} \end{pmatrix} \quad (2.45)$$

The conditions for the existence of the complete set of roots have been proved by [15].

Remark 2. A right block vandermonde matrix extracted from a complete set of roots of a polynomial matrix is assumed and must to be nonsingular.

Remark 3. Based on the characteristics of the matrices diagonalization [7], and by using the definition presented by [7], if the matrix of the desired block roots $\text{diag}([\lambda_1 \ \cdots \ \lambda_m])$ is diagonalizable or a diagonal matrix, there exists an invertible matrix P_r which can transform it into an equivalent matrix R which is also diagonalizable or a diagonal matrix and it maintains its same previous eigenvalues. The transformation equation is given as follows:

$$R \triangleq P_r \text{diag}([\lambda_1, \ \cdots, \ \lambda_m]) P_r^{-1} \quad (2.46)$$

The invertible matrix P_r is chosen initially randomly until the optimal eigenvectors are obtained.

Firstly, this transformation is used to select the best eigenvectors, which means that to obtain the desired optimal block roots R , the optimal eigenvalues and the optimal eigenvectors are chosen separately. Secondly, to avoid falling into cases of ill-conditioned and singularity problems, especially in the right block Vandermonde matrix V_r , when $V_r V_r^{-1} \neq I_{(n-m)}$ which is corresponding to the case presented in this work.

The extracting from a complete set of right block roots Let us consider a complete set of right block roots $\{R_1, R_2, \dots, R_l\}$ for the polynomial matrix $D(\lambda)$, if R_j is a right block roots of $D(\lambda)$:

$$R_j^l + D_1 R_j^{l-1} + \dots + D_{l-1} R_j + D_l = O_m \quad (2.47)$$

$$D_1 R_j^{l-1} + \dots + D_{l-1} R_j + D_l = -R_j^l \quad (2.48)$$

Replacing j from 1 to l , the following is obtained:

$$[D_{dl}, D_{d(l-1)}, \dots, D_{d1}] = -[R_1^l, R_2^l, \dots, R_l^l] V_r^{-1} \quad (2.49)$$

Where V_r is the right block Vandermonde matrix.

The state feedback design Consider the linear discrete-time dynamic system described by the previous first state dynamic (2.34).

by applying of the state feedback $p_2 = -K p_1(k)$ on the dynamic state equation, where $K \in \mathbb{R}^{m \times (n-m)}$ gain matrix, after the transformation to the block controllable form, the following is obtained:

$$p_2(k) = -K_c p_1(k) \quad (2.50)$$

$$K = K_c T_c = [K_{cl}, K_{c(l-1)}, \dots, K_{c1}] T_c \quad (2.51)$$

$$\text{where, } K_{ci} \in \mathbb{R}^{m \times m} \quad i = 1 \ 2 \ 3 \ \dots \ l$$

Then, the dynamic state feedback equation is shown below

$$p_2(k+1) = (A_c - B_c K_c) p_1(k) \quad (2.52)$$

Where

$$(A_c - B_c K_c) = \begin{pmatrix} O_m & \dots & O_m \\ O_m & \dots & O_m \\ \vdots & \dots & \vdots \\ O_m & \dots & I_m \\ -(A_l + K_{cl}) & \dots & -(A_1 + K_{c1}) \end{pmatrix}$$

The polynomial matrix of the dynamic system under the feedback gain matrix control is

$$D(\lambda) = I_m \lambda^l + (A_1 + K_{c1}) \lambda^{l-1} + \dots + (A_l + K_{cl}) \quad (2.53)$$

From a set of desired eigenvalues (Regulator eigenvalues) constructed a set of right block roots (Regulator block roots), then the obtained characteristic polynomial matrix is extracted, by putting

$$D_d(\lambda) = D(\lambda)$$

Getting the coefficients $K_{ci} = D_{di} - A_i$ as follows:

$$K_{ci} = (D_{di} - A_i) \quad i = 1 \ 2 \ 3 \ \dots \ l \quad (2.54)$$

Finally, the robust gain matrix K is obtained by the following formula

$$K = K_c T_c \quad (2.55)$$

4 The proposed algorithm steps

Summarizing all the important steps of the proposed controller

Algorithm 1 Robust static state-feedback controller algorithm

- Step 1 Checking the ratio $(n - m)/m = l$ must be an integer.
- Step 2 Checking the rank of block controllability matrix W_c of system (2.11) which must equal to n (full rank).
- Step 3 Calculating the transformation sliding matrix F via Right kernel (null space) matrix N_r , based on the SVD decomposition, equations (2.24), (2.25) and (2.27).
- Step 4 Decomposing the new transformation system $p(k + 1)$ into two variables states $p_1(k + 1)$, $p_2(k + 1)$ and constructing the matrices A_{s11} and A_{s12} , as in (2.26) and (2.27).
- Step 5 Obtaining the formula of the sliding matrix G in terms of matrix gain K , see (2.33).
- Step 6 Computation of matrix gain K using Block roots (solvents) based on the theory of MFD, as follows:
- Step 7 Checking the block controllability W_c should be full rank $(n - m)$, see (2.38).
- Step 8 Transforming the system into block controllable form, see (2.38), (2.39) and (2.40).
- Step 9 Choosing the desired l set right block roots, as stable and diagonally, see (2.43).
- Step 10 Calculating the right block Vandermonde matrix V_r , as in equation (2.45), and which must be nonsingular.
- Step 11 The gain matrix K obtained from (2.50) to (2.55).
- Step 12 Finally, The sliding matrix G calculated via (2.32).
-

5 Experimental application on gas turbine GEMS5001P system

5.1 Parametric model of the studied Gas turbine system

The studied model of the GEMS5001P gas turbine in this chapter is A MIMO system obtained based on parametric system identification based on real data acquired within the normal mode operation rang on site[25], the studied system has two main outputs: the rotor speed and the exhaust temperature that are affected and interacted directly by three main inputs: the gas control valve (GCV), the axial temperature compressor discharge (TCD), and the axial pressure compressor discharge (PCD). A schematic diagram is presented in Figure. 2.4, which clarifies the inputs/outputs and the main components and sections (axial compressor, combustion chambers and turbine) and the electricity alternator as load, [25].

The studied system is presented in linear discrete-time state space block observable canonical form and takes the following form:

$$\begin{cases} x(k + 1) = Ax(k) + Bu(k) \\ y(k) = Cx(k) + Du(k) \end{cases} \quad (2.56)$$

where the system has order $n = 12$ with three inputs ($m = 3$) and two outputs ($p = 2$) and their matrices are presented in (A.1), (Appendix A).

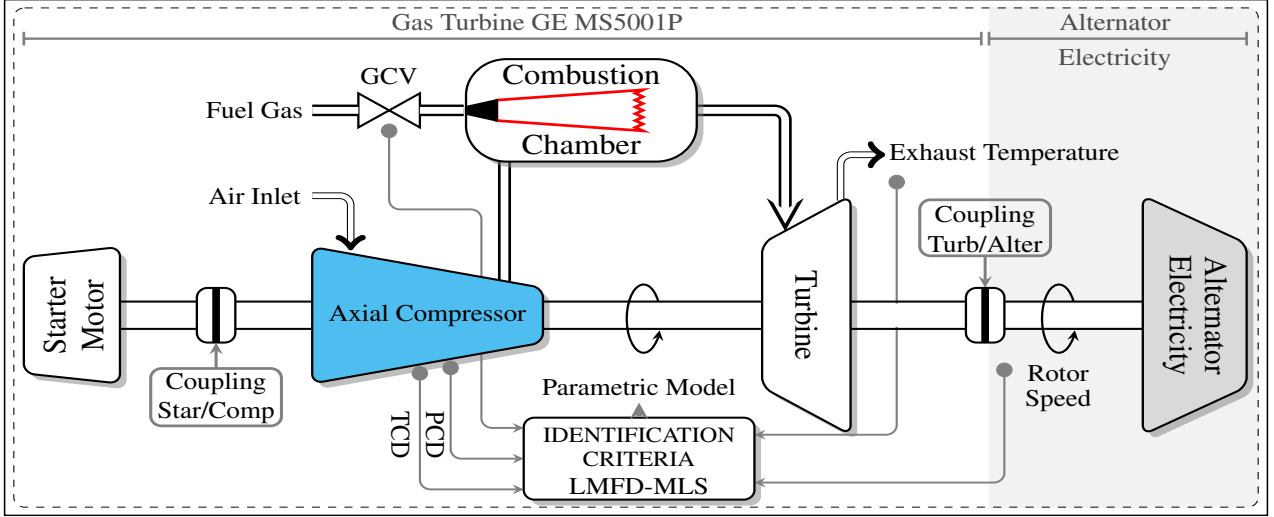


Figure 2.4: Schematic bloc diagram of gas turbine (GE MS5001P) with inputs/outputs model identification

In order to achieve the main purpose of the present paper the proposed algorithm is applied on the studied system flowing the steps aforementioned as follows:

- ✓ The ratio $v = n/m$ equals to $12/3 = 4$, it is an integer.
- ✓ The block controllability matrix is satisfied as $\text{rank}(W_c) = 12$ (full rank).
- ✓ The transformation sliding matrix F of dimension $\mathbb{R}^{12 \times 12}$ is calculated following (2.35), (2.36) and (2.37).
- ✓ The decomposition matrices $A_{s11} \in \mathbb{R}^{9 \times 9}$ and $A_{s12} \in \mathbb{R}^{9 \times 3}$ are calculated via (2.40) and (2.41).
- ✓ The block controllability of the decomposition matrices is satisfied (A_{s11}, A_{s12}), $\text{rank}(W_c) = 9$ (full rank).
- ✓ The transformation of the system into bloc controllable form based on the matrix transformation $T_c \in \mathbb{R}^{9 \times 9}$, following (2.50), (2.51) and (2.52).
- ✓ The desired $l = (n - m)/m = 9/3 = 3$ right block roots (solvents) in controllable form can be constructed using 9 eigenvalues that are chosen to be diagonally assigned as follows:

$$R_1 = P_{r1} \cdot \text{diag}[\mathbf{0.5 \ 0.4 \ 0.3}] \cdot P_{r1}^{-1}, \quad R_2 = P_{r2} \cdot \text{diag}[\mathbf{-0.6 \ 0.2 \ -0.1}] \cdot P_{r2}^{-1}$$

$$\text{and } R_3 = P_{r3} \cdot \text{diag}[\mathbf{0.8 \ 0.55 \ 0.7}] \cdot P_{r3}^{-1}$$

The invertible matrices P_{r1} , P_{r2} and P_{r3} are chosen randomly in order to assign the eigenvectors of the block roots that are chosen as follows:

$$P_{r1} = \begin{pmatrix} 0.2177 & 0.5043 & 0.5931 \\ 0.2971 & 0.1651 & 0.3030 \\ 0.4913 & 0.2502 & 0.1482 \end{pmatrix}, \quad P_{r2} = \begin{pmatrix} 0.8809 & 0.7506 & 0.8055 \\ 0.2668 & 0.2651 & 0.6859 \\ 0.8386 & 0.5681 & 0.2995 \end{pmatrix}, \quad P_{r3} = \begin{pmatrix} 0.9350 & 0.3383 & 0.9632 \\ 0.5007 & 0.8265 & 0.6156 \\ 0.5409 & 0.5479 & 0.9454 \end{pmatrix}$$

Finally,

$$R_1 = \begin{pmatrix} 0.3810 & -0.2617 & 0.2110 \\ -0.0351 & 0.3026 & 0.1349 \\ -0.0643 & 0.0200 & 0.5164 \end{pmatrix}, \quad R_2 = \begin{pmatrix} 5.8922 & -4.7139 & -5.3206 \\ 1.9502 & -1.6402 & -1.7179 \\ 5.1790 & -4.0508 & -4.7520 \end{pmatrix}, \quad R_3 = \begin{pmatrix} 0.9415 & 0.0051 & -0.2494 \\ 0.1968 & 0.5282 & -0.0887 \\ 0.1766 & -0.0923 & 0.5802 \end{pmatrix}$$

✓ The right block Vandermonde matrix $V_r \in \mathbb{R}^{9 \times 9}$, which is nonsingular is calculated following (2.54).

✓ The whitening sliding gain matrix β has been set to a unit matrix.

✓ The corresponding feedback gain matrix K is calculated based on (2.49) to (2.54) as follows:

$$K = \begin{pmatrix} -89.4924 & 111.0282 & -300.6983 & 95.7004 & -161.6562 & 272.3846 & 37.6439 & -34.0074 & 127.2957 \\ 00.7212 & -001.0538 & 004.9563 & 03.7175 & -002.4314 & 004.5086 & -05.9833 & 06.4046 & -011.3184 \\ 15.0275 & -019.3187 & 055.9466 & -11.7331 & 025.2013 & -049.8754 & -09.1118 & 05.2496 & -016.6305 \end{pmatrix}$$

✓ Based on equation (26) the resulting sliding matrix gain G is obtained:

$$G = \begin{pmatrix} -0.1088 & -0.9578 & 1.7735 & -0.0089 & -0.5286 & 1.2487 & -2.0173 & 0.0117 & 0.5507 & 0.4132 & 0.0215 & -0.3337 \\ 0.0017 & 0.0062 & -0.0117 & -0.0007 & 0.0047 & -0.0090 & 0.0126 & 0.0001 & -0.0036 & -0.0047 & -0.0007 & 0.0074 \\ 0.0192 & 0.1538 & -0.2859 & 0.0005 & 0.0861 & -0.1986 & 0.3207 & -0.0016 & -0.0879 & -0.0579 & -0.0037 & 0.0638 \end{pmatrix}$$

In order to select the robust sliding matrix gain G , and to prove the effectiveness and the advantage of proposed algorithm, a comparative study with classical and recent controllers algorithms, such as the classical pole placement with assigning stable eigenvalues, the discrete-time linear quadratic regulator based on minimizing criteria of trajectory and energy control, the eigenstructure assignment based on eigenvalues and eigenvectors placement separately, and finally the state and the state derivative feedback method based on the theory of polynomials matrix using the kronecker product.

Table 2.1: The norms (1,2,inf) of the sliding matrix G associated to each methods

K	$\ G\ _1$	$\ G\ _2$	$\ G\ _{inf}$
Pole placement	36.2398	44.3571	82.0297
DLQR	22.2743	30.4674	78.2330
Eigen-S Assignment	38.1816	46.5546	95.1315
S-D-Feedback	66.3356	78.5478	115.0456
Proposed Method	23.5060	32.5326	79.7440

Table 2.5: Comparative study

		Pole placement	DLQR	Eigen-S Assignment	S-D-Feedback	Proposed Method
Norm		Suitable	Excellent	Unsuitable	Unsuitable	More suitable
	Time specifications	Unsuitable	Unsuitable	Suitable	More suitable	Excellent
Robust stability	$s(\lambda_i)$	Unsuitable	Unsuitable	More suitable	Suitable	Excellent
	M_1	Unsuitable	Unsuitable	Suitable	Suitable	Excellent
	M_2	Unsuitable	Suitable	Suitable	Suitable	Excellent
	M_3	Unsuitable	Unsuitable	Suitable	Suitable	Excellent
Robust performance	$r(\lambda_i)$	Unsuitable	More suitable	More suitable	More suitable	Excellent

The obtained results from the calculation of the gain matrix K based on the application of all the steps aforementioned of the proposed algorithm have been compared with the other methods such as pole placement, DLQR, E-S assignment and S-D feedback and are presented in Table 2.1 to Table 2.5 This comparison has been performed based on the obtained results under similar conditions such as the initial states values, desired poles, and the same percent of the injected disturbances.

Table 2.2: Time specifications (Settling time t_s and maximum peak M_p)

K	x_1	x_2	x_3	x_4	x_5	x_6	x_7	x_8	x_9	x_{10}	x_{11}	x_{12}
Pole placement	t_s	60	62	62	62	62	60	61	60	60	59	66
	M_p	73.4124	143.6067	275.8774	480.0302	63.8776	245.0559	743.8175	632.2685	1.3667×10^3	189.4790	45.4683
DLQR	t_s	40	37	51	50	51	33	39	32	35	28	32
	M_p	32.3220	61.5960	35.9795	82.4200	36.4478	72.6120	41.6670	95.2383	31.4945	18.3202	31.8723
Eigen-S Assignment	t_s	39	38	45	42	39	30	34	35	21	30	40
	M_p	28.4440	56.3750	30.9560	75.5260	32.654	45.6870	88.3983	25.3345	77.5180	15.1580	21.533
S-D-Feedback	t_s	40	39	30	38	42	40	32	32	30	15	35
	M_p	27.4520	50.8980	28.7795	68.3250	31.4576	40.7770	84.1483	22.3925	67.5150	10.5201	19.5625
Proposed Method	t_s	37	37	28	37	36	31	31	29	23	29	28
	M_p	15.7367	30.4302	8.6442	25.3969	11.3107	26.7737	11.7880	32.1579	21.0985	4.8510	14.2140

Table 2.3: Robust stability (Eigenvalues sensitivity $s(\lambda_i)$)

K	$s(\lambda_1)$	$s(\lambda_2)$	$s(\lambda_3)$	$s(\lambda_4)$	$s(\lambda_5)$	$s(\lambda_6)$	$s(\lambda_7)$	$s(\lambda_8)$	$s(\lambda_9)$	$s(\lambda_{10})$	$s(\lambda_{11})$	$s(\lambda_{12})$
Pole placement	213.0689	213.0689	129.6670	95.5432	524.5128	524.5128	238.5749	238.5749	468.5414	1.2891×10^3	3.3986×10^3	1.7970×10^3
DLQR	31.9535	262.7456	262.7456	1.8277×10^3	1.8277×10^3	54.6149	54.6149	226.1670	226.1670	131.6216	91.3962	257.1033
Eigen-S Assignment	28.1816	201.5546	118.1315	92.1314	403.6781	70.1324	60.1132	205.2677	198.0733	122.1607	85.1675	200.0324
S-D-Feedback	27.3356	197.5478	115.0456	90.4378	450.6071	70.8843	59.1353	207.2858	198.0397	120.0826	80.0051	198.1568
Proposed Method	12.7286	91.0052	91.0052	28.4540	28.4540	83.3787	83.3787	126.9331	126.9331	398.3625	249.5613	11.8031

Table 2.4: Robust performance (Relative change r in the eigenvalues λ_i under perturbation)

K	Stability Measures														
	$r(\lambda_1)$	$r(\lambda_2)$	$r(\lambda_3)$	$r(\lambda_4)$	$r(\lambda_5)$	$r(\lambda_6)$	$r(\lambda_7)$	$r(\lambda_8)$	$r(\lambda_9)$	$r(\lambda_{10})$	$r(\lambda_{11})$	$r(\lambda_{12})$	M_1	M_2	M_3
Pole placement	1.3032	1.3032	1.6573	0.8501	1.3177	1.6066	2.1953	1.9951	0.9318	1.6810	2.7652	1.7502	0.2725×10^{-5}	0.1337×10^{-5}	0.1438×10^{-5}
DLQR	8.1193×10^{-4}	0.0185	0.0185	0.1157	0.1157	0.091	0.091	0.0933	0.0933	9.8883×10^{-4}	0.0149	0.1588	0.8220×10^{-4}	0.3989×10^{-3}	0.4289×10^{-4}
E-S Assignment	8.0182×10^{-4}	0.0113	0.0172	0.1004	0.1240	0.0821	0.0852	0.0134	0.0537	7.8484×10^{-4}	0.0124	0.1736	0.2316×10^{-3}	0.1124×10^{-3}	0.1208×10^{-3}
S-D-Feedback	7.953×10^{-4}	0.0105	0.0984	0.0592	0.0695	0.0699	0.0133	0.0665	0.0455	7.1431×10^{-4}	0.4035	0.1530	0.2659×10^{-3}	0.1290×10^{-3}	0.1387×10^{-3}
Proposed Method	7.5237×10^{-4}	0.0031	0.0031	0.0019	0.0019	0.0100	0.0100	0.0065	0.0065	8.2511×10^{-4}	0.3331	0.0551	0.2300×10^{-2}	0.1116×10^{-2}	0.1200×10^{-2}

5.2 Comments and Interpretations on the obtained results

- In Table 2.1, the amplitude of the gain matrix G has been calculated for the different norms of order 1, 2 and infinity with the four aforementioned methods and the proposed method. It is obvious from these results that the proposed method and the DLQR method give the G norm with minimum values in comparison with the other methods. But the DLQR method has less characteristics specifications. It can be said that the obtained G matrix under the proposed method allows to ensure a high performance with minimal energy control.
- Table 2.2 presents the time specification (Settling time and Maximum peak M_p) for each states, it is clear that the proposed method gives the minimal settling times t_s and maximal peak M_p respectively in comparison with the other methods, this result can be explained by the effect of the diagonally assignment of the robust block roots constructed from speed eigenvalues/eigenvectors.
- The results of the eigenvalues sensitivity after the injection of some perturbations ΔA into the dynamic matrix A are presented in Table 2.3. It is obvious that the proposed method is more robust against the changes in the internal dynamics in comparison with the other methods.
- The checking of the relative change in the eigenvalues r_i is presented in Table 2.4. These results indicate that there is a small change in regard to the results of the proposed method, on the other hand there are significant changes within the results obtained based on the other algorithms, it can be said that these significant changes may cause instability problem.
- Through the definition of the stability measures and based on the results presented in Table 5 and shown in Figure 16, it is clear that the best algorithm which ensures the maximum values in the three measures of M_{s1} , M_{s2} and M_{s3} and more particularly the measures of M_{s1} and M_{s3} , is the proposed algorithm. Consequently, the proposed algorithm can fulfill the requirement of the best stability quality measures.
- Following the results presented in Table 2.5, which summarizes all the results of the presented comparison study. It can be concluded that the proposed algorithm can ensure the best robustness stability and the best sensitivity performance analysis in comparison with the other algorithms presented in this paper.

5.3 The Effects of the block roots on the performance of the proposed controller

- The block roots R_i are matrices that contain **the latent eigenvalues and the latent eigenvectors** that can be assigned in the same time, and this important property cannot be achieved under other algorithms.
- A transfer-function matrix of invariant-time multivariable system can be formulated in block terms after some manipulations [16–19] is given as follows:

$$Y(\lambda) = \left(\sum_{i=1}^l CX_i(\lambda I_m - R_i)^{-1} Y_i B \right) U(\lambda) \quad (2.57)$$

Where, λ : is a complex variable, (X_i, Y_i, R_i) characterize the whole state space dynamic system, X_i : is the right block vector corresponding to the block root R_i and Y_i : is the left block vector corresponding to the block root R_i . It is noted that the block root is the **basic component** of the the left and the right block vectors as explained in details in [16–19], so it can be said that the block roots R_i affects completely the system due the capture of the system dynamics along the operational range. It is important to clarify that this feature is not existing within the other algorithms.

- The block spectral decomposition of the matrix A_c [14] and [20] can be expressed as follows:

$$A_c = \sum_{i=1}^l X_{ci} R_i Y_{ci} \quad (2.58)$$

After some transformations the block partial fraction expansions, expressed in terms of projectors contribution can be presented as follows:

$$e^{At} = \sum_{i=1}^l X_i e^{R_i t} Y_i \quad (2.59)$$

Based on (2.58), it is clear that the pair (X_i, Y_i) presenting the right and the left block vectors affect directly **the shape** of the response. On the other side, the block roots R_i alters **the stability** where they affect directly **the stability convergence** of the controller, the **transient response**, the **steady state** and the **decay response** at the same time.

- The block roots R_i assignment provides a large degree of freedom in the design of feedback gain matrix K , where they can be placed in the **left** or in the **right** of MFD system and can be chosen under flexible forms such as **diagonal form, controllable form and observable form** in order to achieve the best performance.
- The MFD system is transformed automatically into partial subsystems (blocks) which facilitates handling and controlling them instead of the control the fully system.

6 Conclusion

In this chapter, a new robust discrete-time sliding mode controller have been introduced, based on the assignment of block roots for a class of MIMO linear systems. The block roots (solvents) that are extracted from the dominant eigenvalues are assigned diagonally, where the block roots placed in the right block controllable form (right block vandermonde matrix) of the new transformed decomposed system via matrix gain K . To validate the proposed algorithm, the GE MS500P gas turbine is investigated in this chapter due to its importance in many industries, especially in electrical power generation. This proposed algorithm is applied to the best chosen real model of the gas turbine system, which is obtained from experimental data obtained on-site, using parametric identification based on LMFD MIMO least squares. In order to prove the robustness stability of the proposed algorithm, the stability measures have been performed to show its effectiveness and validity. Furthermore, a comparison study among the classical and recent algorithms is presented, where the obtained results prove clearly the high performances, robustness and effectiveness of the proposed algorithm, the effect of the assigning block roots are very clear in the obtained results, and the very important the direct impact to improving the power generation in this gas turbine (GE MS5001P). On the other side, the presented controller algorithm can be consider as a promising solution for solving many problems of stability in several industrial applications. However, the limitation of this proposed algorithm is associated to two problems:

- The ratio n/m must be integer, if not there are many propositions in literatures (ex: extending the original system), so this problem is solved.
- The block controllability matrix must have a full rank, if this condition is not satisfied the proposed algorithm is not valid. However, in some model systems the model order reduction can solve this problem.

Further interesting researches can focus on the optimal block roots selection which allows to reduce the norm (amplitude) of the sliding matrix G with less control energy control as possible. In the next chapter, a multivariable optimal static output-feedback controller design is proposed based only on the availability of the outputs.

7 References

- [1] J.-J. E. Slotine and J. A. Coetsee, Adaptive sliding controller synthesis for non-linear systems, *International Journal of Control*, vol. 43, no. 6, pp. 1631-1651, Jun. 1986.
- [2] X. Cheng, G. Tang, P. Wang, and L. Liu, Predictive Sliding Mode Control for Attitude Tracking of Hypersonic Vehicles Using Fuzzy Disturbance Observer, *Mathematical Problems in Engineering*, vol. 2015, pp. 1-13, 2015.
- [3] M. Furat and I. Eker, Chattering-eliminated adaptive sliding mode control: an experimental comparison study, *Turkish Journal of Electrical Engineering & Computer Sciences*, vol. 24, no. 1, pp. 605-620.
- [4] P. Lesniewski and A. Bartoszewicz, Discrete time sliding mode inventory management-Hyperbolic tangent reaching law based approach, in *2014 19th International Conference on Methods and Models in Automation and Robotics (MMAR)*, Miedzyzdroje, 2014, pp. 276-281.
- [5] Gangbing Song and R. Mukherjee, A comparative study of conventional nonsmooth time-invariant and smooth time-varying robust compensators, *IEEE Transactions on Control Systems Technology*, vol. 6, no. 4, pp. 571-576, Jul. 1998.
- [6] S. Sarpturk, Y. Istefanopulos, and O. Kaynak, On the stability of discrete-time sliding mode control systems, *IEEE Transactions on Automatic Control*, vol. 32, no. 10, pp. 930-932, Oct. 1987.
- [7] G. Strang, *Introduction to Linear Algebra*. 5th ed. Wellesley, 2016, MA: Wellesley-Cambridge.
- [8] V. I. Utkin, K. D. Yang, Methods for construction of discontinuity planes in multidimensional variable structure systems, *Avtomat. i Telemekh.*, 1978, no. 10, 72-77; *Autom. Remote Control*, 39:10 (1979), 1466-1470
- [9] B. Moore, On the flexibility offered by state feedback in multivariable systems beyond closed loop eigenvalue assignment, *IEEE Transactions on Automatic Control*, vol. 21, no. 5, pp. 689-692, Oct. 1976.
- [10] K. Ogata, *Discrete-time Control Systems*. 1995, 2nd ed. Englewood Cliffs, NJ: Prentice Hall.
- [11] A. N. Andry, E. Y. Shapiro, and J. c. Chung, Eigenstructure Assignment for Linear Systems, *IEEE Transactions on Aerospace and Electronic Systems*, vol. AES-19, no. 5, pp. 711-729, Sep. 1983.
- [12] B. Bekhiti, A. Dahimene, B. Nail, et al, Block-structure relocation via state and state derivative feedback: eigenspace of matrix polynomials characterization. *Journal of Control and Systems Engineering*, vol. 4, no. 1, 95-111, 2016.
- [13] Leang Shieh, Yih Tsay, and R. Yates, State-feedback decomposition of multivariable systems via block-pole placement, *IEEE Transactions on Automatic Control*, vol. 28, no. 8, pp. 850-852, Aug. 1983.

-
- [14] M. Yaici and K. Hariche, On eigenstructure assignment using block poles placement, *European Journal of Control*, vol. 20, no. 5, pp. 217-226, Sep. 2014.
- [15] P. Lancaster and M. Timenetski, *The Theory of Matrices: With Applications*. 2nd ed. Orlando, 1985, FL: Academic Press.
- [16] B. Bekhiti, A. Dahimene, B. Nail, K. Hariche, and A. Hamadouche, On Block roots of matrix polynomials based MIMO control system design, in *2015 4th International Conference on Electrical Engineering (ICEE)*, Boumerdes, Algeria, 2015, pp. 1-6.
- [17] B. Nail, A. Kouzou, A. Hafaifa, and V. Puig, Optimal Static State-Feedback Controller Design for MIMO LTI Systems Based on Constraints Block Roots and Interior-Point Algorithm: Application to Gas Compressor System, in *2018 International Conference on Applied Smart Systems (ICASS)*, Medea, Algeria, 2018, pp. 1-6.
- [18] B. Bekhiti, A. Dahimene, B. Nail, and K. Hariche, On λ -matrices and their applications in MIMO control systems design, *International Journal of Modelling, Identification and Control*, vol. 29, no. 4, pp. 281-294, 2018.
- [19] Nail B., Kouzou A., Hafaifa A. (2019) Digital Stabilizing and Control for Two-Wheeled Robot. In: Derbel N., Ghommam J., Zhu Q. (eds) *New Developments and Advances in Robot Control*. Studies in Systems, Decision and Control, vol 175. Springer, Singapore, 2019, pp. 237-253.
- [20] L. S. Shieh, Y. T. Tsay, and N. P. Coleman, Algorithms for solvents and spectral factors of matrix polynomials, *International Journal of Systems Science*, vol. 12, no. 11, pp. 1303-1316, Jan. 1981.
- [21] C.-C. Tsui, A new robust stability measure for state feedback systems, *Systems & Control Letters*, vol. 23, no. 5, pp. 365-369, Nov. 1994.
- [22] C.-C. Tsui, *Robust Control System Design: Advanced State Space Techniques*, (2004) Second edition, *Marcel Dekker*.
- [23] B. Moaveni and A. K. Sedigh, Input-output pairing analysis for uncertain multivariable processes, *Journal of Process Control*, vol. 18, no. 6, pp. 527-532, Jul. 2008.
- [24] W.I. Rowen, Simplified mathematical representations of heavy duty gas turbines, *ASME Journal of Engineering for Gas Turbines and Power*, vol. 105, no. 4, pp. 865-869, 1982.
- [25] B. Nail, A. Kouzou, and A. Hafaifa, Robust block roots assignment in linear discrete-time sliding mode control for a class of multivariable system: gas turbine power plant application, *Transactions of the Institute of Measurement and Control*, vol. 41, no. 5, pp. 1216-1232, Mar. 2019.

Multivariable Optimal Static Output-feedback Controller design

1 Introduction

The hypothesis of being able to know the complete state of real processes in modern control engineering is not always realistic. Sometimes is difficult and expensive to have the measurement of the whole state vector, because of technical reasons (unmeasurable or unaccessible variables) or economic aspect (price of sensors). For this reason, several control algorithms have been developed that use only output information to control the system. The design of this kind of controllers, that only use the static output feedback (SOF) information, has long been an active and challenging area but difficult from theoretical point of view. Moreover, it is considered one of the basic problems in control theory, falling in the NP-hard category.

In this chapter, the optimal SOF controller algorithm has been proposed for multivariable LTI systems. The main idea is to calculate the block transformations matrices of the model system in both the observable and the controllable forms using similarity block canonical forms transformation [2–6]. This transformation is the key idea of the proposed approach, where the multiplication of both transformation matrices in the left and the right, allow to restrict the control range of the desired dynamics from the dimension space of the plant to the dimension space of the SOF matrix gain K . In this way, the desired eigenvalues of the closed-loop system (CLS) are under the control of the heart matrix A_h , which belong to the same dimension space of the SOF matrix gain. The selection of the A_h matrix which achieves the stability of the CLS with optimal SOF matrix gain K is obtained by using a constrained Grey Wolf Optimizer (GWO) [18], that takes in consideration the minimization of the norm of the SOF matrix gain K and maintain the stability in the CLS with proper eigenvalues in the optimal desired region of convergence (ROC).

The proposed SOF control technique is applied for a centrifugal gas compressor system. The studied system is installed in hassi r'mel gas field (in the south of Algeria), which is used in one of the important natural gas compression station. The dynamic model of this system is obtained based on experimental data using parametric system identification [2, 8, 20]. Two comparative studies have been conducted by the obtained results in order to prove the efficiency of our proposal. The first one with the aim of choosing the best optimization algorithm,

where the three optimization algorithms, the Genetic Algorithm (GA) [7], the Particle Swarm Optimization (PSO) [9], and the Interior Point Method (IPM) [10], are compared with GWO [18], The second one with the goal of evaluating the performance of the optimal proposed SOF controller when is compared with a SOF controller which has been published in recent years [11, 12].

2 Preliminaries

Let we consider the following proper linear MIMO discrete-time system described by a state space representation:

$$\begin{cases} x(k+1) = Ax(k) + Bu(k) \\ y(k) = Cx(k) + Du(k) \end{cases} \quad (3.1)$$

with, $x \in \mathbb{R}^n$, $A \in \mathbb{R}^{n \times n}$, $B \in \mathbb{R}^{n \times m}$, $C \in \mathbb{R}^{p \times n}$.

2.1 Block Canonical Forms Transformation of controllability

The block controllability matrix of the system (3.1) is given as follows [2–6]:

$$\Omega_c = (B, AB, A^2B, \dots, A^{l-1}B) \quad (3.2)$$

Definition 3.1. The multivariable system described in (3.1) is block controllable of index l , and can be transformed into a block controller form if the following conditions are satisfied [2–6]:

- The ratio $n/m = l$ is an integer
- The matrix Ω_c has a full rank

If both conditions are satisfied, then the change of coordinates $x_c(k) = T_c x(k)$ transforms the system into the following block controller form

$$\begin{cases} x_c(k+1) = A_c x_c(k) + B_c u(k) \\ y(k) = C_c x_c(k) + D_c u(k) \end{cases} \quad (3.3)$$

The block transformation matrix of controllability T_c is given as follows:

$$\begin{cases} T_c = \begin{pmatrix} T_{c1} \\ T_{c1}A \\ \vdots \\ T_{c1}A^{l-1} \end{pmatrix}, & T_{c1} = (O_m \quad O_m \quad \cdots \quad I_m) \Omega_c^{-1} \end{cases} \quad (3.4)$$

The system is given in the block canonical controllable form as follows:

$$\begin{cases} A_c = T_c A T_c^{-1} = \begin{pmatrix} O_m & I_m & \cdots & O_m \\ O_m & O_m & \cdots & O_m \\ \vdots & \vdots & \cdots & O_m \\ O_m & O_m & \cdots & I_m \\ -A_l & -A_{l-1} & \cdots & -A_1 \end{pmatrix} \\ B_c = T_c B = (O_m \quad O_m \quad \cdots \quad I_m)^T \\ C_c = C T_c^{-1} = (C_l \quad C_{l-1} \quad \cdots \quad C_1) \end{cases} \quad (3.5)$$

with, $x_c \in \mathbb{R}^n$, $A_i \in \mathbb{R}^{m \times m}$, $C_i \in \mathbb{R}^{p \times m}$, $i = \overline{1, l}$, I_m and O_m are $m \times m$ identity and null matrices respectively, and the superscript T denotes the transpose.

2.2 Block Canonical Forms Transformation of observability

The block observability matrix of the system (3.1) is given as follows [2–6]:

$$\Omega_o = \left(C^T, A^T C^T, \dots, (A^T)^{l-1} C^T \right)^T \quad (3.6)$$

Definition 3.2. The multivariable system described in (3.1) is block observable of index l , and can be transformed into a block observer form if the following conditions are satisfied [2–6]:

- The matrix Ω_o has full rank.
- The ratio $n/p = l$ is an integer.

Based on the previous conditions, we can convert the state equation into block observer form using the following similarity transformation $x_o = T_o x$

$$\begin{cases} x_o(k+1) = A_o x_o(k) + B_o u(k) \\ y(k) = C_o x_o(k) + D_o u(k) \end{cases} \quad (3.7)$$

The block transformation matrix of observability T_o is given as follows:

$$\left\{ T_o = \begin{pmatrix} T_{ol} & AT_{ol} & \dots & A^{l-1}T_{ol} \end{pmatrix}, \quad T_{ol} = \Omega_o^{-1} \begin{pmatrix} O_m & O_m & \dots & I_m \end{pmatrix}^T \right. \quad (3.8)$$

The system is given in the block canonical observable form as follows:

$$\left\{ \begin{aligned} A_o = T_o^{-1} A T_o &= \begin{pmatrix} O_p & \dots & O_p & -A_l \\ I_p & \dots & O_p & -A_{l-1} \\ \vdots & \vdots & \vdots & \vdots \\ O_p & \dots & O_p & -A_2 \\ O_p & \dots & I_p & -A_1 \end{pmatrix} \\ B_o = T_o^{-1} B &= \begin{pmatrix} B_l \\ B_{l-1} \\ \vdots \\ B_1 \end{pmatrix}, C_o = C T_o = \begin{pmatrix} O_p \\ O_p \\ \vdots \\ I_p \end{pmatrix}^T \end{aligned} \right. \quad (3.9)$$

3 Constraints optimization problem

The following metaheuristics optimization algorithms: GA, PSO, IPA, and GWO are used to solve a convex multidimensional optimization problems with constraints, to finds the minimum of a problem specified by

$$\text{Find } \mathbf{z} \text{ which minimizes the objective function } f(\mathbf{z}) \quad (3.10)$$

subject to certain set of constraints:

$$\left\{ \begin{aligned} g_i(\mathbf{z}) &\leq 0, & \mathbf{i} &= \overline{1, \dots, \mathbf{n}} \\ h_j(\mathbf{z}) &= 0, & \mathbf{j} &= \overline{1, \dots, \mathbf{m}} \\ lb &\leq \mathbf{z}_k \leq ub, & \mathbf{k} &= \overline{1, \dots, \mathbf{p}} \end{aligned} \right. \quad (3.11)$$

where, \mathbf{z} is the solution vector with p variables $\mathbf{z} = [\mathbf{z}_1, \mathbf{z}_2, \dots, \mathbf{z}_p]$, $g_i(\mathbf{z})$ and $h_j(\mathbf{z})$ represent the inequality constraints and equality constraints respectively, \mathbf{n} is the number of inequality constraints, \mathbf{m} the number of equality constraints and lb and ub are the lower and upper bounds for each variable respectively.

There are several ways for dealing with optimization problems with constraints. It is possible, for reasons of robustness and ease of implementation, to transform a constrained problem into a series of problems without constraint. This transformation is done by adding penalties to the objective function [7].

The objective function $f(\mathbf{z})$ of the problem is then replaced by the following function to be minimized[7]:

$$\Psi(\mathbf{z}, \alpha_i, b_j) = f(\mathbf{z}) \pm \left(\alpha_i \sum_{i=1}^{\mathbf{n}} g_i(\mathbf{z}) + b_j \sum_{j=1}^{\mathbf{m}} h_j(\mathbf{z}) \right) \quad (3.12)$$

where, $\Psi(\mathbf{z}, \alpha_i, b_j)$ is the new fitness function to be optimized, α_i and b_j are called penalty parameters, they take positive values.

4 Problem statement

Consider the following Linear discrete-time uncertain system described by a state space representation:

$$\begin{cases} x(k+1) = A(\theta)x(k) + B(\theta)u(k) \\ y(k) = C(\theta)x(k) \end{cases} \quad (3.13)$$

where, θ is the vector of the uncertain parameters with the bounded values by an compact set Θ as

$$\Theta = \left\{ \theta \in \mathbb{R}^{n\theta} \mid \underline{\theta}_i \leq \theta_i \leq \bar{\theta}_i, \quad i = 1, \dots, n \right\}$$

$$\begin{aligned} \underline{A}(\theta) &\leq A(\theta) \leq \bar{A}(\theta) \\ \underline{B}(\theta) &\leq B(\theta) \leq \bar{B}(\theta) \\ \underline{C}(\theta) &\leq C(\theta) \leq \bar{C}(\theta) \end{aligned} \quad (3.14)$$

where $\underline{\bullet}$ and $\bar{\bullet}$ denote the lower and the upper bound of each matrix, respectively. Note that the inequalities in (3.14) should be understood as element-wise inequalities. Therefore, the uncertainties in matrices $A(\theta)$, $B(\theta)$ and $C(\theta)$ can be decomposed as $A(\theta) = A_n + \Delta A(\theta)$, $B(\theta) = B_n + \Delta B(\theta)$ and $C(\theta) = C_n + \Delta C(\theta)$, where A_n , B_n and C_n are the matrices of the system (3.13), and the nominal part of the system matrices $A(\theta)$, $B(\theta)$ and $C(\theta)$, respectively.

where $x(k) \in \mathbb{R}^n$, $u(k) \in \mathbb{R}^m$ and $y(k) \in \mathbb{R}^p$ are the state, the input and the output vectors.

After applying the static output feedback control $u(k) = -K y(k)$ and using a zero set-point, as shown in Figure. 3.1.

The system represented in (3.13) can be rewritten in the following form:

$$\begin{cases} x(k+1) = A(\theta)x(k) - B(\theta)K y(k) \\ y(k) = C(\theta)x(k) \end{cases} \quad (3.15)$$

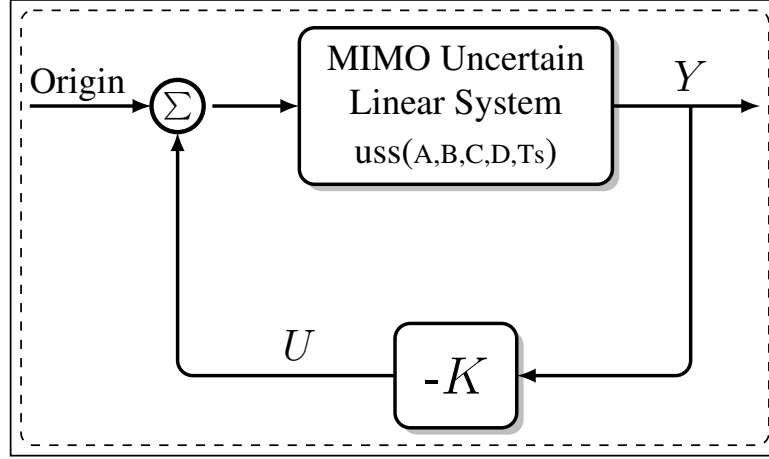


Figure 3.1: Schematic of SOF controller gain stabilization.

The closed-loop system (3.15) can be further expressed as:

$$\begin{cases} x(k+1) = \overline{A}(\theta)x(k) \\ y(k) = C(\theta)x(k) \end{cases} \quad (3.16)$$

where, $\overline{A}(\theta)$ is the desired closed-loop matrix ($A(\theta) - B(\theta)KC(\theta)$)

The problem is how to find the output static feedback matrix K that guarantees stability of the closed-loop system. In this paper, an algorithm is been proposed that combines the block transformation and the Grey Wolf Optimizer.

5 Main results

Generally the SOF controller is affected by both control and observer $B(\theta)$ and $C(\theta)$ matrices respectively from the right and left. This provides an opportunity to exploit the both block transformations BTs of the controllability and the observability that is a new idea in the proposed SOF controller design approach.

From (3.16) the desired closed-loop system matrix given as follows:

$$A(\theta) - B(\theta)KC(\theta) = \overline{A}(\theta) \quad (3.17)$$

and

$$B(\theta)KC(\theta) = A(\theta) - \overline{A}(\theta) \quad (3.18)$$

both sides of the equality from the left and the right by the block transformation matrices $T_c(\theta)$ and $T_o(\theta)$ respectively

$$T_c(\theta)B(\theta)KC(\theta)T_o(\theta) = T_c(\theta)(A(\theta) - \overline{A}(\theta))T_o(\theta) \quad (3.19)$$

From the above definition 1 and definition 2 of T_c , T_o , B_c , C_o we obtain

$$B_c(\theta)KC_o(\theta) = \begin{pmatrix} O_m \\ \vdots \\ I_m \end{pmatrix} (O_p \cdots K) \quad (3.20)$$

and

$$\begin{pmatrix} O_m \\ \vdots \\ I_m \end{pmatrix} (O_p \cdots K) = \left(\begin{array}{ccc|c} O_m & \cdots & & O_m \\ \vdots & \ddots & & \vdots \\ O_m & \cdots & & K \end{array} \right) \quad (3.21)$$

Hence

$$\left(\begin{array}{ccc|c} O_m & \cdots & & O_m \\ \vdots & \ddots & & \vdots \\ O_m & \cdots & & K \end{array} \right) = T_c(\theta)(A(\theta) - \bar{A}(\theta))T_o(\theta) \quad (3.22)$$

By fixing $T_c(\theta)(A(\theta) - \bar{A}(\theta))T_o(\theta) = \Delta(\theta)_{co}$, the static output feedback matrix gain K can be obtained as follows:

$$K = \Delta(\theta)_{co}(n - m + 1 : n, n - p + 1 : n) \quad (3.23)$$

The condition regarding the structure of $\bar{A}(\theta)$ so that the system achieve a desired closed-loop performance be determined as follows:

$$A(\theta)_{co} = T_c(\theta)A(\theta)T_o(\theta) = \left(\begin{array}{cc|c} \Gamma_1(\theta) & \Gamma_2(\theta) & \\ \hline \Gamma_3(\theta) & \Gamma_4(\theta) & \end{array} \right) \quad (3.24)$$

where

$$\begin{aligned} \Gamma_1(\theta) &= A(\theta)_{co}(\overline{1 : (n - m)}, \overline{1 : (n - p)}) \\ \Gamma_2(\theta) &= A(\theta)_{co}(\overline{1 : (n - m)}, \overline{(n - p + 1) : n}) \\ \Gamma_3(\theta) &= A(\theta)_{co}(\overline{(n - m + 1) : n}, \overline{1 : (n - p)}) \\ \Gamma_4(\theta) &= A(\theta)_{co}(\overline{(n - m + 1) : n}, \overline{(n - p + 1) : n}) \end{aligned}$$

From (3.24) and in terms of $T_c(\theta)$, $T_o(\theta)$, $\Gamma_1(\theta)$, $\Gamma_2(\theta)$, $\Gamma_3(\theta)$ and $\Gamma_4(\theta)$, the desired closed-loop matrix can be parameterized as follows,

$$T_c(\theta)\bar{A}(\theta)T_o(\theta) = \left(\begin{array}{cc|c} \Gamma_1(\theta) & \Gamma_2(\theta) & \\ \hline \Gamma_3(\theta) & \Gamma_4(\theta) & \end{array} \right) - \left(\begin{array}{ccc|c} O_m & \cdots & & O_m \\ \vdots & \ddots & & \vdots \\ O_m & \cdots & & K \end{array} \right) \quad (3.25)$$

and

$$T_c(\theta)\bar{A}(\theta)T_o(\theta) = \left(\begin{array}{cc|c} \Gamma_1(\theta) & \Gamma_2(\theta) & \\ \hline \Gamma_3(\theta) & \Gamma_4(\theta) - K & \end{array} \right) \quad (3.26)$$

and

$$\bar{A}(\theta) = T_c(\theta)^{-1} \left(\begin{array}{cc|c} \Gamma_1(\theta) & \Gamma_2(\theta) & \\ \hline \Gamma_3(\theta) & \Gamma_4(\theta) - K & \end{array} \right) T_o^{-1} \quad (3.27)$$

The transformation matrices $T_c(\theta)$ and $T_o(\theta)$ are assumed to be nonsingular.

$$\Delta_{co}(\theta) = \left(\begin{array}{cc|c} O_m & \cdots & O_m \\ \vdots & \ddots & \vdots \\ O_m & \cdots & K \end{array} \right) \Rightarrow K = \Gamma_4(\theta) - A_h(\theta) \quad (3.28)$$

where K , $\Gamma_4(\theta)$ and $A_h(\theta) \in \mathbb{R}^{m \times p}$

Based on (3.27) and (3.28), we conclude that the heart block matrix $A_h(\theta)$ characterizes completely the closed-loop system. Moreover, it contains the whole set of information about the closed-loop spectrum, because is the only variable that governs the behavior of the eigenspace of the system. Figure. 3.2 shows the importance of the BT which compress the unknown desired dynamic and they determined in a small block matrix $A_h(\theta)$ in the corner of the matrix $\bar{A}(\theta)$.

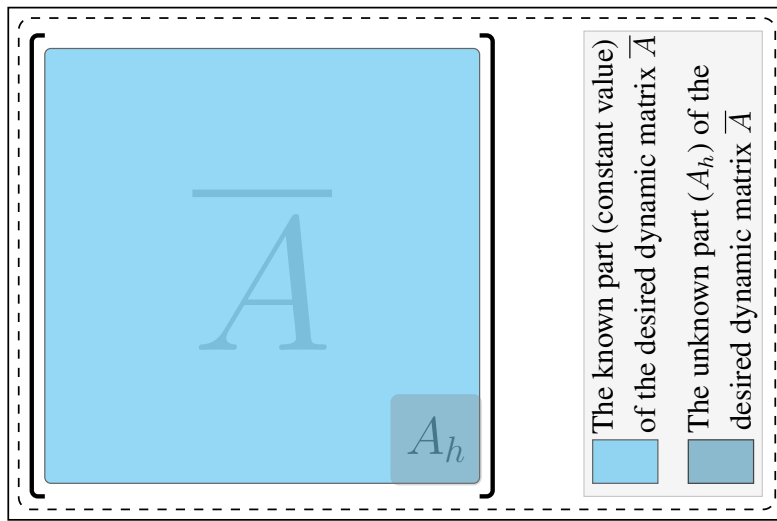


Figure 3.2: Diagram of the desired dynamic matrix \bar{A}

5.1 The selection of the heart matrix $A_h(\theta)$

The eigenvalues (poles) placement approach is very well known. However, their use in the design of the SOF matrix gain controllers is very limited for these reasons: The allowable dimension of the SOF controller space is a bit small, i.e $\dim(K) \leq \dim(A(\theta))$, consequently not all desired stable eigenvalues have image in the space of the SOF controller [4]. Thus, the selection of the desired stable eigenvalues is unavailable in this case. In general, the matrices $B(\theta)$ and $C(\theta)$ are rectangular which mean they have nontrivial kernels (null space). Consequently, the search for a K is a non-convex problem and thus only allows for local optimal solution. To avoid these problems and limitations, the choose of the best heart matrix $A_h(\theta)$ is formulated as convex optimization problem and solved by the grey wolf optimizer (GWO).

Optimization procedure The grey wolf optimizer (GWO) is a meta-heuristic algorithm proposed by **Mirjalili et al.**, [18]. It has been selected as tool in this design to solve the convex multidimensional optimization problems with constraints presented in (3.10) and (3.11), from among several meta-heuristic and evolutionary algorithms such as GA [7] and PSO [9] respectively, due to their fast convergence behavior without any complexity (just adjusting two parameters, Max-iter and number of agents) comparing with the existed algorithms [18]. The GWO imitates the social manners of grey wolves. These wolves live in a group contains 20-30 members. In this

group, the strict dominance hierarchy is practiced where the group has a leader named alpha α , supported by secondary ones named beta β , which aid α in decision-making. The rest members of the group are named δ and ω as shown in Pyramid Figure. 3.3 The procedure of hunting the prey by the grey wolves is: looking for the prey, surrounding the prey, hunting, and attacking the prey. The arithmetic model of surrounding the prey [19], is written as follows

$$\vec{D} = \left| \vec{C} \cdot \vec{X}_{pi} - \vec{X}_i \right| \quad (3.29)$$

and

$$\vec{X}_{i+1} = \vec{X}_{pi} - \vec{A} \cdot \vec{D} \quad (3.30)$$

where \vec{X}_i is the place of the grey wolf, \vec{X}_{pi} is the place of the prey, \vec{D} is the distance, \vec{A} and \vec{C} are vectors calculated as following

$$\vec{A} = 2\vec{a} \cdot \vec{r}_1 - \vec{a} \quad (3.31)$$

and

$$\vec{C} = 2 \cdot \vec{r}_2 \quad (3.32)$$

where,

$$\vec{a} = 2 \left(1 - \frac{t}{\text{Max-iter}} \right) \quad (3.33)$$

where \vec{r}_1 and \vec{r}_2 are random numbers between [0, 1]. The parameter a is a variable which is linearly reduced from 2 to 0 while the iterations increased. The process of looking for the prey position (exploration) could be attained by diverging the search entities, when $|\vec{A}| > 1$. The process of getting the prey (exploitation) could be attained by the convergence of the search entities, when $|\vec{A}| < 1$. The hunting is led by α entities with β and δ entities support as in (36), (37) and (38). Figure. 3.3 shows the flowchart of the GWO algorithm steps. Like other meta-heuristic algorithms, The GWO can be disposed to stagnate in a local minimum but the parameters \vec{A} and \vec{C} can help the GWO algorithm to avoid stagnation [18, 19].

$$\begin{aligned} \vec{D}_\alpha &= \left| \vec{C}_1 \cdot \vec{X}_{\alpha i} - \vec{X}_i \right| \\ \vec{D}_\beta &= \left| \vec{C}_2 \cdot \vec{X}_{\beta i} - \vec{X}_i \right| \\ \vec{D}_\delta &= \left| \vec{C}_3 \cdot \vec{X}_{\delta i} - \vec{X}_i \right| \end{aligned} \quad (3.34)$$

$$\begin{aligned} \vec{X}_1 &= \vec{X}_{\alpha i} - \vec{A}_1 \cdot \vec{D}_\alpha \\ \vec{X}_2 &= \vec{X}_{\beta i} - \vec{A}_2 \cdot \vec{D}_\beta \\ \vec{X}_3 &= \vec{X}_{\delta i} - \vec{A}_3 \cdot \vec{D}_\delta \end{aligned} \quad (3.35)$$

$$\vec{X}_{i+1} = \frac{\vec{X}_1 + \vec{X}_2 + \vec{X}_3}{3} \quad (3.36)$$

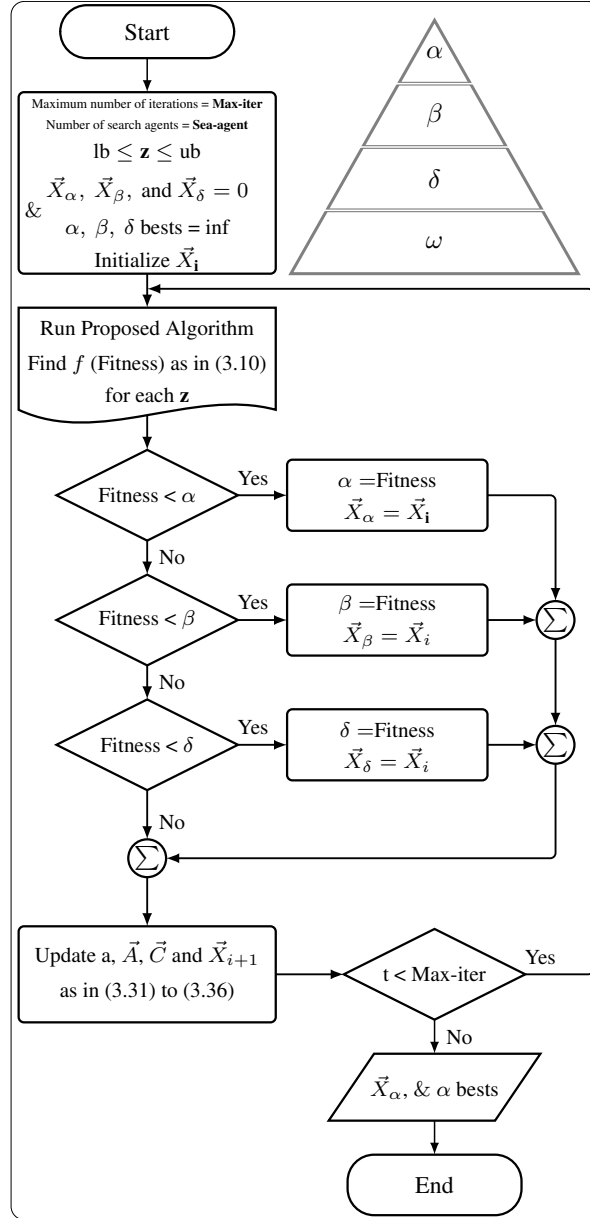


Figure 3.3: Flowchart of the Grey Wolf Optimizer

To selected the optimal heart matrix $A_h(\theta)$, an optimization problem should to be solved, the objective function $f(\mathbf{z})$ is chosen as follows:

$$f(\mathbf{z}) = \|\mathbf{K}(\mathbf{z})\|_\infty = \|\Gamma_4(\theta) - A_h(\mathbf{z})\|_\infty \quad (3.37)$$

We find \mathbf{z} which minimizes the objective function $\|\mathbf{K}(\mathbf{z})\|_\infty$ subject to certain set of constraints:

$$\left\{ \begin{array}{ll} \left| \text{eig}(\bar{A}(\theta)) \right| - \epsilon < 0, & \epsilon \in]0 \ 1[, \quad \mathbf{i} = \overline{1, \dots, \mathbf{n}} \\ (A(\theta) - B(\theta)KC(\theta)) - \bar{A}(\theta) = 0_{n \times n}, & \mathbf{j} = \overline{1, \dots, \mathbf{m}} \\ \text{rank}(\Omega_c) + \text{rank}(\Omega_o) - 2n = 0_{n \times n}, & \mathbf{j} = \overline{1, \dots, \mathbf{m}} \\ lb \leq \mathbf{z}_k \leq ub, & k = \overline{1, \dots, \mathbf{p}} \end{array} \right. \quad (3.38)$$

The inequality constraint condition has been chosen to guarantee the stability of the closed-loop system, where the eigenvalues are enforced to be placed in the region of the convergence (ROC), inside the unit circle. The

equality constraints have been chosen in order to ensure the existence of the heart matrix $A_h(\theta)$ chosen from the optimizer and check the block transformations, if are they achieved. The lower and the upper bound of the vector \mathbf{z}_k are chosen so which have produced values nearly to the values of the elements of the matrix $\Gamma_4(\theta)$.

6 The proposed algorithm steps

Summarizing all the important steps of the proposed controller

Algorithm 2 Optimal static output-feedback controller algorithm

- Step 1** Check the ratio $n/m = l$, which must be an integer.
- Step 2** Check the rank of the block controllability and block observability matrices of the nominal model Ω_c and Ω_o of (3.2) and (3.6) respectively, which must equal n (be full rank).
- Step 3** Calculate the similarity transformations T_c and T_o of the nominal model as in (3.4) and (3.8).
- Step 4** Defined the uncertainties level of the studied model.
- Step 5** Compute the matrix $A_{co}(\theta)$, see (3.24).
- Step 6** Truncate the matrix $\Gamma_4(\theta)$ from the matrix $A_{co}(\theta)$, see (3.24).
- Step 7** Compute the optimal static output feedback matrix K based on the choose of matrix $A_h(\theta)$ using the GWO, as follows:
- (a) Find the elements of the heart matrix $A_h(\theta)$ which minimize the norm of the static output feedback matrix gain K as in (3.37).
 - (b) Check the verification of the inequality condition of the stability in each iteration, see (3.38).
 - (c) Check the equality constraints of the block transformations and the validity in each iteration, as in (3.38).
 - (d) Set the values of the lower and the upper bound lb and ub respectively of the vector \mathbf{z}_k , and choose initial value to the vector \mathbf{z}_0 , see (3.38).
 - (e) All the optimization procedures steps are illustrated in the Flowchart shown in Figure. 3.3
- Step 8** When the stopping criterion is satisfied and the algorithm converge, the best heart $A_h(\theta)$ matrix was selected.
- Step 9** Finally, The SOF matrix gain K is calculated based on (3.28).
-

7 Experimental application and results

The centrifugal gas compressor system studied in this chapter is shown in Figure. 3.4, and its characteristics are presented in Table B.1, (Appendix B). This studied system is driven by a two shaft gas turbines (GE MS5002C) as shown in Figure. 3.5. It is a multivariable process with two inputs, the aspiration temperature $T1$ and the aspiration pressure $P1$ and two outputs, the discharge pressure $P2$, and the discharge temperature $T2$. The parametric model of this system has been obtained based on experimental data acquired via several tests to get the optimal data that are covering all possible dynamic behavior of this centrifugal gas compressor [8, 20].



Figure 3.4: The studied centrifugal gas compressor system BCL 505 installed in the natural gas compression station

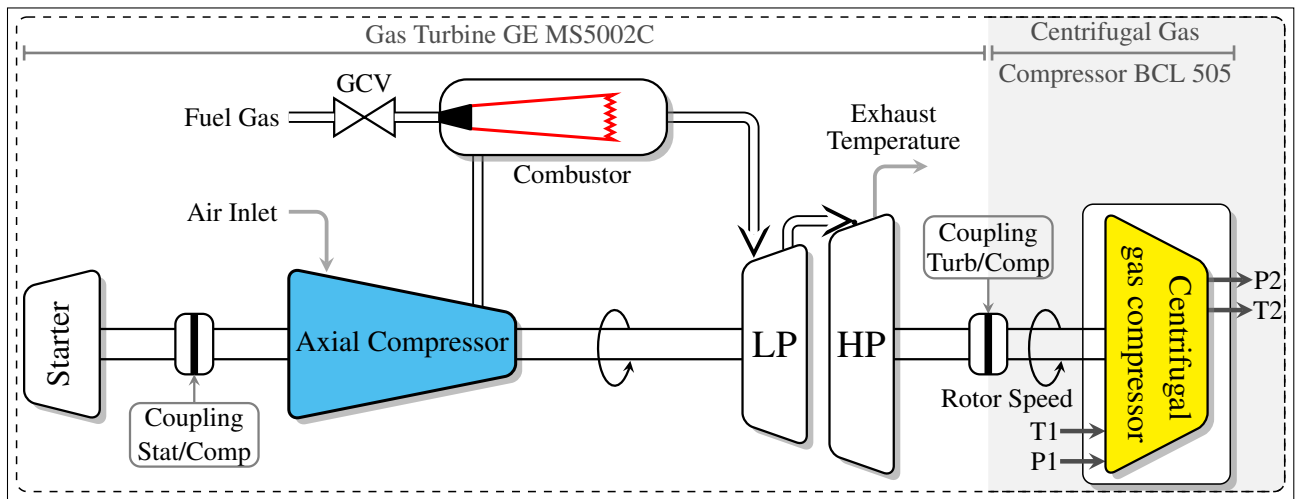


Figure 3.5: Schematic block diagram of the studied centrifugal gas compressor driven by two shaft gas turbines.

The studied system is represented by its state space model as follows [8]:

$$\begin{cases} x(k+1) = A(\theta)x(k) + B(\theta)u(k) \\ y(k) = C(\theta)x(k) \end{cases} \quad (3.39)$$

where, this discrete-time state space dynamic model of the examine system is a large scalae of order, $n = 10$, and with two inputs ($m = 2$) and two outputs ($p = 2$), and its characteristic matrices A, B, C are mentioned in (B.1), (Appendix B). where, this discrete-time state space dynamic model of the examine system is a large scalae of order, $n = 10$, and with two inputs ($m = 2$) and two outputs ($p = 2$).

7.1 Implementation of Proposed optimal SOF controller

To achieve the main purpose of this paper, the proposed algorithm is applied to the studied system, following the aforementioned steps as follows:

1. The ratio $l = n/m$ equals $10/2 = 5$ and is an integer.
2. The block controllability and observability matrices of the nominal model are satisfied, as $\text{rank}(\Omega_c) = \text{rank}(\Omega_o) = 10$ (are full rank).
3. The similarity transformations matrices $\{T_c, T_o\} \in \mathbb{R}^{10 \times 10}$ are calculated based on (3.4) and (3.8) respectively. Their values are presented in (B.2) and (B.3), (Appendix B).
4. The uncertainties level applied on the studied nominal model is $-50\% \leq \Delta\theta \leq +50\%$. Where, $-50\%A \leq \Delta A(\theta) \leq +50\%A$, $-50\%B \leq \Delta B(\theta) \leq +50\%B$ and $-50\%C \leq \Delta C(\theta) \leq +50\%C$.
5. The matrix $A_{co}(\theta)$ is calculated based on the (3.24). Their nominal value is presented in (B.4), (Appendix B).
6. Truncate the matrix $\Gamma_4(\theta) \in \mathbb{R}^{2 \times 2}$ from the matrix $A_{co}(\theta)$, based on (3.24), their nominal value is given as follows:

$$\Gamma_4 = \begin{pmatrix} -6.0654 & -3.0397 \\ 4.2343 & 3.4407 \end{pmatrix}$$

7. Compute the static output feedback matrix K based on the choose of the heart matrix $A_h \in \mathbb{R}^{2 \times 2}$ using GWO, as follows:

- Minimize the norm of $\|K\|_\infty = \|\Gamma_4(\theta) - \mathbf{z}_{ij}\|_\infty$ as in (3.37).
- Subject to: $|\text{eig}(\bar{A}(\theta))| - 0.6 < 0$, where $\epsilon = 0.6$ is the unit circle diameter.
- $(A(\theta) - B(\theta)KC(\theta)) - \bar{A}(\theta) = 10^{-14}$
- $\text{rank}(\Omega_c) + \text{rank}(\Omega_o) - 2n = 20 - 20 = 0$
- The values of the lower and the upper bound lb and ub of the vector is $\mathbf{z} \in [-10 \quad 10]$, where $\mathbf{z} \in \mathbb{R}^{1 \times 4}$. This interval presents the **search space** as shown in Figure. 3.6.

Initialisation of the vector \mathbf{z}_0 is take this value $\mathbf{z}_0 = [0, 0, 0, 0]$.

The typical parameters for GWO is given as follows: the maximum number of iterations, **Max-iter** = 400, and the number of search agents, **Sea-agent** = 20, as shown in the Figure. 3.6 and the Figure. 3.7 respectively.

8. The stopping criterion is satisfied and the algorithm converge, and the best heart matrix is chosen as follows:

$$A_h(\mathbf{z}) = \begin{pmatrix} -3.4879 & -1.6071 \\ 2.6081 & 1.4287 \end{pmatrix}$$

Finally, the optimal SOF matrix gain K is obtained based on applying all steps of the proposed algorithm and is given as follows:

$$K = \begin{pmatrix} -0.1881 & -0.2351 \\ -0.0419 & 0.6566 \end{pmatrix}$$

7.2 Comparative study and discussion results

In order to examine the proposed optimal SOF controller, and to prove its effectiveness and advantage, two comparative studies have been made. The first one with three well known optimization algorithms, GA, PSO and IPM methods [7, 9, 10], to prove the good choice of GWO as a optimizer, while the second one with recent and well known controllers. The first one is H_∞ SOF controller based on optimization considering pole constraints [12], while the second one is robust structured MIMO H_∞ design [11].

Based on the obtained results presented in Table 3.1, it is clear that the GWO provides a good optimization result compared with GA, PSO and IPM optimizers in all the two criteria ($\|.\|_\infty$ and ROC), Figure. 3.12 shows the flexibility to place the desired poles in any place in the unit circle, while in IPM method the stability of CLS is not ensured (limit of stability), and in the GA, PSO and IPM methods the infinity norm of the controller gain is too big and the constraint of the stability is violated $|\bar{A}| > \epsilon = 0.6$. So the GWO optimizer is a good choice in our proposed controller. Figure. 3.6 and Figure. 3.7 show the GWO evolution curves during the optimization process and the fitness function curve during the iterations, where it stops at **Max-iter** = 400. On the other hand, in the second comparison with the two controllers, the results show the superiority of the proposed controller in the infinity norm **0.69** of the controller where, the stability in the CLS is ensured with lowest possible energy, and differently from the two controllers [11, 12], where a great energy consumption from the controllers to ensure the stability in CLS is required.

Table 3.1: Comparison the ($\|.\|_\infty$, ROC and BTs) characteristics of each SOF matrix gain K methods

Method & Optimizer	SOF Matrix Gain K	$\ K\ _\infty$	ROC	BTs
Proposed SOF Using GWO	$\begin{pmatrix} -0.1881 & -0.2351 \\ -0.0419 & 0.6566 \end{pmatrix}$	0.69	[0.26 , 0.60]	Verified
Proposed SOF Using GA [7]	$\begin{pmatrix} 0.5761 & -0.4052 \\ -0.5179 & 1.1118 \end{pmatrix}$	1.37	[0.39 , 0.96]	Verified
Proposed SOF Using PSO [9]	$\begin{pmatrix} -1.2452 & -0.2846 \\ 0.3177 & 1.0178 \end{pmatrix}$	1.45	[0.37 , 0.99]	Verified
Proposed SOF Using IPM [10]	$\begin{pmatrix} 1.4358 & 0.1793 \\ -0.8239 & 0.6081 \end{pmatrix}$	1.66	[0.61 , ~1]	Verified
Method Based H_∞ [11]	$\begin{pmatrix} -1.8155 & -0.5717 \\ 0.6240 & 1.1656 \end{pmatrix}$	2.17	[0.37 , 0.98]	Verified
Method Based H_∞ [12]	$\begin{pmatrix} -1.0684 & -1.0548 \\ 0.4757 & 1.5049 \end{pmatrix}$	2.11	[0.48 , 0.98]	Verified

Table 5.1 presents the specifications regarding the time-response of the closed-loop system (Rise time (t_r), Settling time (t_s), Settling min (S_{Min}), Settling max (S_{Max}), Overshoot (O_{shoot}), Undershoot (U_{shoot}), Peak (**Peak**) and Peak time (t_p)) for the proposed controller and the compared methods [11, 12], Based on the assessment of the obtained results, the proposed controller reach the desired value in best time specification in all the response characteristics in comparison with the other methods, except in some undershoot and overshoot U_{shoot} and O_{shoot} characteristic, outperforms the compared methods, which allows the system to maintain its performances under the considered uncertainty.

Table 3.2: Comparison the time specifications of dynamic system response in each methods

Inputs	Outputs	Characteristics	Method Based H_∞ [12]	Method Based H_∞ [11]	SOF Using GWO
From input $T1$	To output $P2$	t_r	159	172	4
		t_s	284	306	6
		S_{Min}	-79.6770	-185.6374	0.3645
		S_{Max}	-71.7362	-167.4240	0.3821
		O_{shoot}	0	0	0.2641
		U_{shoot}	1.6783	0.4381	0
		Peak	79.6770	185.6374	0.3821
	To output $T2$	t_r	161	173	5
		t_s	275	301	11
		S_{Min}	639.7949	590.5383	0.7118
		S_{Max}	709.8274	654.5301	0.7881
		O_{shoot}	0	0	0
		U_{shoot}	0.0113	0.0122	10.1520
		Peak	709.8274	654.5301	0.7881
From input $P1$	To output $P2$	t_r	159	172	4
		t_s	285	307	7
		S_{Min}	-144.7808	-295.2633	0.6721
		S_{Max}	-130.5518	-266.2478	0.7182
		O_{shoot}	0	0	0.0838
		U_{shoot}	1.9586	0.5964	0
		Peak	144.7808	295.2633	0.7182
	To output $T2$	t_r	161	173	6
		t_s	276	302	12
		S_{Min}	$1.1661 \times 10^{+3}$	940.8059	0.7255
		S_{Max}	$1.2938 \times 10^{+3}$	$1.0428 \times 10^{+3}$	0.8008
		O_{shoot}	0	0	0
		U_{shoot}	0.0032	0.0040	5.1504
		Peak	$1.2938 \times 10^{+3}$	$1.0428 \times 10^{+3}$	0.8008
	t_p	519	479	69	

Table 3.3 presents the eigenvalues sensitivity of the uncertainty perturbed system. It is obvious that the proposed method is more robust against the changes in the internal dynamics in comparison with the other methods, and this due to the best selection of the SOF matrix gain K based on BT and GWO.

Table 3.3: Robust stability (Eigenvalues sensitivity $s(\lambda)$)

K	$s(\lambda_1)$	$s(\lambda_2)$	$s(\lambda_3)$	$s(\lambda_4)$	$s(\lambda_5)$	$s(\lambda_6)$	$s(\lambda_7)$	$s(\lambda_8)$	$s(\lambda_9)$	$s(\lambda_{10})$
SOF Using GWO	26.2867	32.8166	14.5680	3.4064	3.4064	4.6529	4.5529	4.0717	1.2853	5.2853
Method Based H_∞ [11]	35.1612	48.9137	23.5602	4.2572	4.2572	12.3833	4.5859	4.5859	2.1985	2.1985
Method Based H_∞ [12]	3.9905	3.9905	42.4162	60.9825	5.4663	5.4663	20.0368	32.7376	2.2328	2.2328

The relative change in the eigenvalues $r(\lambda)$ and the three stability measures $M_{1,2,3}$ are presented in Table 3.4 and Table 3.5 respectively. The results indicate that there is a bit of change concerning the perturbed eigenvalues of the proposed controller and a significant change in the perturbed eigenvalues of the comparison methods which may cause instability problem. On the other hand, and based on the definition of the stability measures, the proposed algorithm provides the best values in the all measures $M_{1,2,3}$. Consequently, the proposed algorithm can fulfill the requirement of the best stability quality measures.

Table 3.4: Robust performance (Relative change r in the eigenvalues λ under perturbation)

K	$r(\lambda_1)$	$r(\lambda_2)$	$r(\lambda_3)$	$r(\lambda_4)$	$r(\lambda_5)$	$r(\lambda_6)$	$r(\lambda_7)$	$r(\lambda_8)$	$r(\lambda_9)$	$r(\lambda_{10})$
SOF Using GWO	0.0341	0.0260	0.0104	0.0029	0.0029	0.0047	0.0047	0.0046	0.0046	0.0046
Method Based H_∞ [11]	0.0463	0.0407	0.0145	0.0037	0.0037	0.0072	0.0049	0.0049	0.0049	0.0049
Method Based H_∞ [12]	0.0035	0.0035	0.0518	0.0477	0.0049	0.0049	0.0123	0.0192	0.0050	0.0050

Table 3.5: Stability measures

Methods	Stability measures		
	M_1	M_2	M_3
SOF Using GWO	0.0171	0.0012	0.0276
Method Based H_∞ [11]	0.0196	0.0033	0.0192
Method Based H_∞ [12]	0.0204	0.0019	0.0147

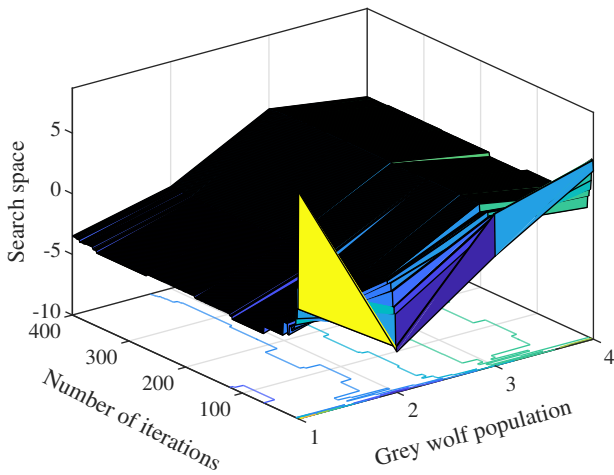


Figure 3.6: GWO evolution during the tuning optimization process

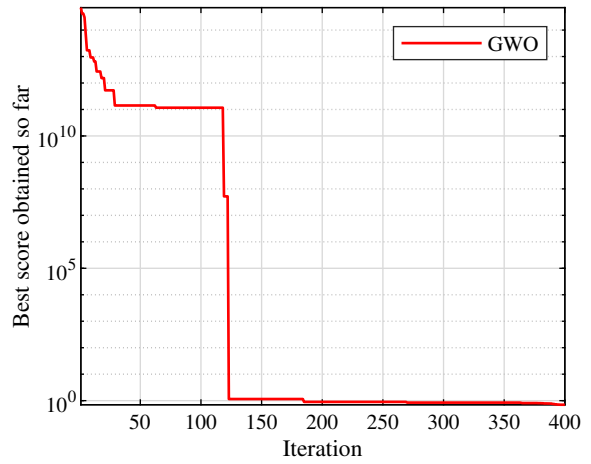


Figure 3.7: The change of objective function f in terms of GWO iteration

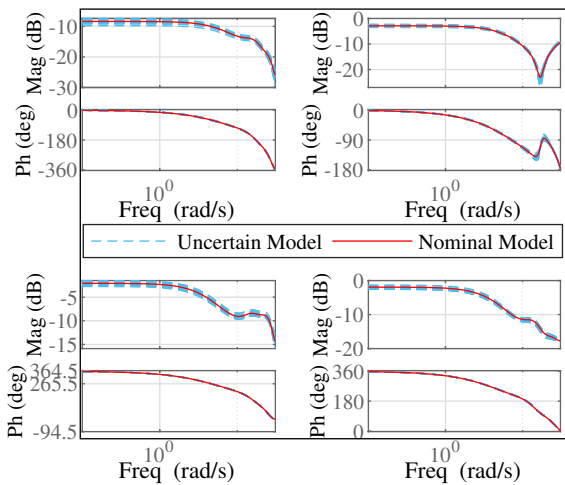


Figure 3.8: Bode diagram of the CLS

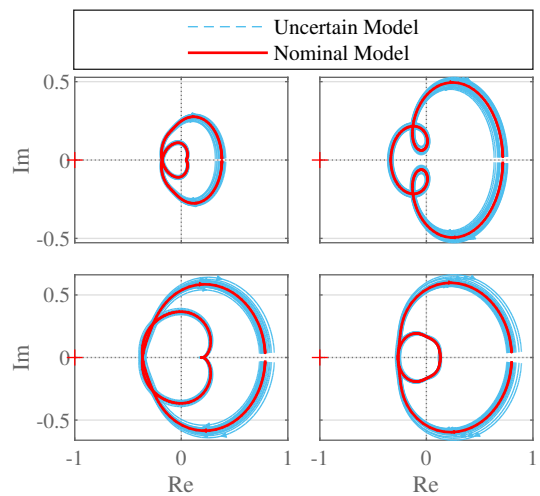


Figure 3.9: Nyquist diagram of the CLS

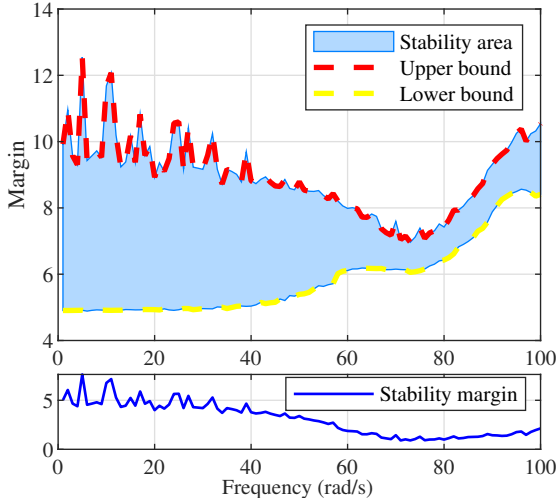


Figure 3.10: Robust stability of CLS.

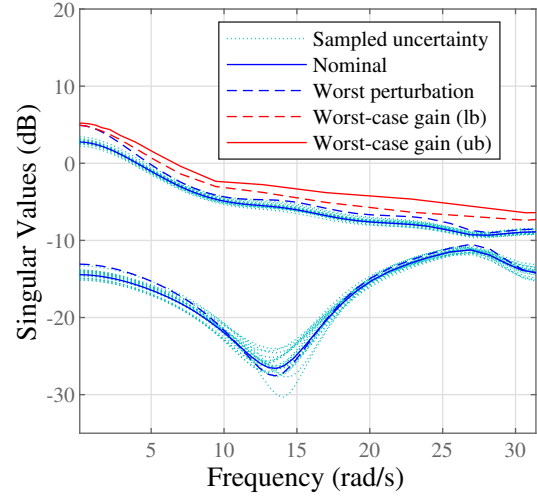


Figure 3.11: worst-case gain of uncertain CLS

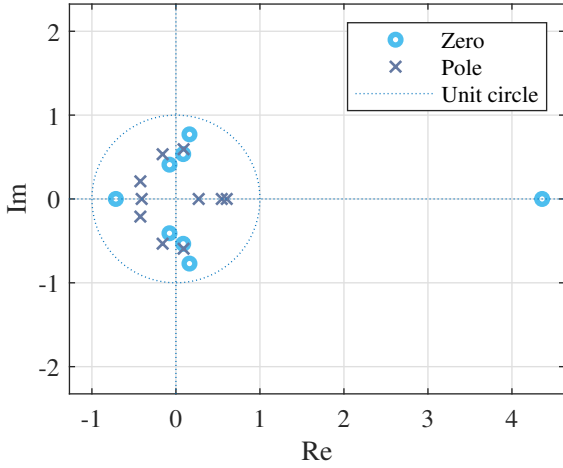


Figure 3.12: Zeros-Poles map of Uncertain CLS

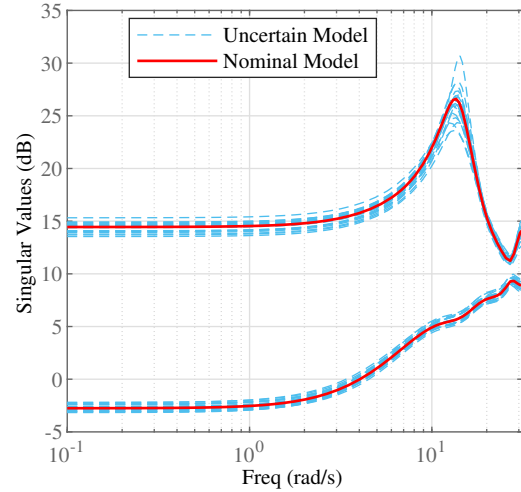


Figure 3.13: Singular values of CLS

Frequency domain, singular values, stability and robustness analysis In this subsection a stability and robustness of the uncertain centrifugal gas compressor system is studied, where Figure. 3.8 shows the bode frequency response of the CLS $\mathbf{usys}(e^{j\omega T_s})$, it's clear that the system remained stable during all time under applied uncertainties, when the phase take the angle phase $\phi = -180$ the magnitude is less then 0. Figure. ?? shows the nyquist plot, the stability is determined by analysing how Nyquist contour Γ_c is mapped by $\mathbf{usys}(e^{j\omega T_s})$, the open-loop system is stable ($\mathbf{P} = 0$), then ($\mathbf{N} = \mathbf{Z}$). The stability of the system is then ensured because the map of Γ_c does not encircle the critical point $(-1, 0)$.

The frequency response plot in Figure. 3.10 shows the robust stability margin for the uncertain model, this stability margin is relative to the uncertainty level specified by $-50\% \leq \Delta\theta \leq +50\%$. A robust stability interval is greater than 1 in all frequency range $[0 \quad 100](\text{rad/s})$, means that the system is stable for all values of its modeled uncertainty, and except to the interval less than 1 in the neighborhood of the critical point frequency $=71 \text{ (rad/s)}$, corresponding to stability margin = 0.9057, means that the system becomes unstable for some values of the uncertain elements within their specified ranges, but the global system rest and maintain its stability.

Figure. 3.11 shows the nominal and worst-case gains of the uncertain system in frequency domain, the gain refers to the largest singular value of the frequency response, accordingly after the uncertainties applied on the nominal system we can said that there is not a big change in the largest singular value $\bar{\sigma}$. Figure. 3.13 shows the singular values of the frequency response of uncertain CLS, it is frequency response extend to the Bode magnitude, is useful for robustness analysis, through the plot we note that no significant change for the largest singular value $\bar{\sigma}$, and this is due to the effective selection of the SOF matrix gain K with minimum infinity norm.

7.3 The proposed controller algorithm presents some limitations with suggested solutions

- If the ratio n/m be not an integer, there are some results available in the literature, e.g. extending the original system by adding no-dominant states to make the value of the ratio to be integer [6]. Or by our proposal of decoupling the model and decomposed into two parts, the first one is block transformable, and the second one is controlled separately [3], so this limitation can be fixed.
- If the both block controllability and observability conditions are not satisfied (not have full rank). However, in some model systems, model order reduction can solve this problem, by eliminating the uncontrollable and the unobservable states (Minimal realization).

8 Conclusion

In this experimental study, a novel design of optimal SOF controller has been introduced, based on block transformations and GWO. The proposed algorithm is very simple to implement unlike some designs their implementation are more expensive due to their computational complexity. To illustrate the main elements of the new proposed, an experimental investigation was carried on the uncertain multivariable model of a natural gas centrifugal compressor system. The obtained results show that the proposed SOF controller exhibit a good behaviour in the terms of: norms, time responses, sensitivity, robustness and stability measures. In fact, from practical point of view the proposed optimal SOF controller can be employed as backup controller, which is not active during the control operation but is used in the case of faults (fault tolerant control), for their simple design and their good performance under perturbations condition.

9 References

- [1] G. Chesi and R. H. Middleton, LMI-Based Fixed Order Output Feedback Synthesis for Two-Dimensional Mixed Continuous-Discrete-Time Systems, *IEEE Transactions on Automatic Control*, vol. 63, no. 4, pp. 960-972, Apr. 2018.
- [2] B. Nail, A. Kouzou, and A. Hafaiifa, "Robust block roots assignment in linear discrete-time sliding mode control for a class of multivariable system: gas turbine power plant application," *Transactions of the Institute of Measurement and Control*, p. 1-17, Jul. 2018.
- [3] B. Bekhiti, A. Dahimene, B. Nail, and K. Hariche, "On λ -matrices and their applications in MIMO control systems design," *International Journal of Modelling, Identification and Control*, vol. 29, no. 4, p. 281-294, 2018.

- [4] B. Nail, A. Kouzou, A. Hafaifa, and B. Bekhiti, "Parametric output feedback stabilization in MIMO systems: Application to gas turbine power plant," in 2016 8th International Conference on Modelling, Identification and Control (ICMIC), Algiers, Algeria, 2016, pp. 971-976.
- [5] M. Yaici, K. Hariche, "On eigenstructure assignment using block poles placement polynomials," *European Journal of Control*, vol. 20, no. 5, pp. 217-226, 2014,.
- [6] L. S. Shieh, Y. T. Tsay, and R. E. Yates, "Block transformations of a class of multivariable control systems to four basic block companion forms," *Computers & Mathematics with Applications*, vol. 9, no. 6, pp. 703-714, 1983.
- [7] A. Chehouri, R. Younes, J. Perron, and A. Ilinca, A Constraint-Handling Technique for Genetic Algorithms using a Violation Factor, *Journal of Computer Science*, vol. 12, no. 7, pp. 350-362, Jul. 2016.
- [8] B. Nail, A. Kouzou, A. Hafaifa, A. Chaibet, Parametric identification and stabilization of turbo-compressor plant based on matrix fraction description using experimental data, *Journal of Engineering Science and Technology*, vol. 13, no. 6, pp. 1850-1868, Jun. 2018.
- [9] I. Mazhoud, K. Hadj-Hamou, J. Bigeon, and P. Joyeux, Particle swarm optimization for solving engineering problems: A new constraint-handling mechanism, *Engineering Applications of Artificial Intelligence*, vol. 26, no. 4, pp. 1263-1273, Apr. 2013.
- [10] R. A. Waltz, J. L. Morales, J. Nocedal, and D. Orban, An interior algorithm for nonlinear optimization that combines line search and trust region steps, *Mathematical Programming*, vol. 107, no. 3, pp. 391-408, Jul. 2006.
- [11] M. Řezáč and Z. Hurák, Structured MIMO design for dual-stage inertial stabilization: Case study for HIFOO and Hinfstruct solvers, *Mechatronics*, vol. 23, no. 8, pp. 1084-1093, Dec. 2013.
- [12] I. Yaesh, U. Shaked, H_∞ Optimization With Pole Constraints of Static Output-Feedback Controllers-A Non-Smooth Optimization Approach, *IEEE Transactions on Control Systems Technology*, vol. 20, no. 4, pp. 1066-1072, Jul. 2012.
- [13] C.-C. Tsui, "A new robust stability measure for state feedback systems, *Systems & Control Letters*, vol. 23, no. 5, pp. 365-369, Nov. 1994.
- [14] C.-C. Tsui, "Robust Control System Design: Advanced State Space Techniques, (2004) Second edition, Marcel Dekker.
- [15] A. Agney, S. Singh, and G. Srinivas, "Structural and Fluid Flow Analysis of Subsonic Aircraft jet Engine Centrifugal Compressor," *Materials Today: Proceedings*, vol. 5, no. 9, pp. 19507-19516, 2018.
- [16] A. Meroni, B. Zühlsdorf, B. Elmegaard, and F. Haglind, "Design of centrifugal compressors for heat pump systems," *Applied Energy*, vol. 232, pp. 139-156, Dec. 2018.
- [17] I. Eker and T. Kara, "Operation and control of a water supply system," *ISA Transactions*, vol. 42, no. 3, pp. 461-473, Jul. 2003.
- [18] S. Mirjalili, S. M. Mirjalili, and A. Lewis, Grey Wolf Optimizer, *Advances in Engineering Software*, vol. 69, pp. 46-61, Mar. 2014.

- [19] M. H. Qais, H. M. Hasanien, and S. Alghuwainem, A Grey Wolf Optimizer for Optimum Parameters of Multiple PI Controllers of a Grid-Connected PMSG Driven by Variable Speed Wind Turbine, *IEEE Access*, vol. 6, pp. 44120-44128, 2018.
- [20] Bachir Nail, Abdellah Kouzou, Ahmed Hafaifa, Nadji Hadroug, and Vicenç Puig. A Robust fault diagnosis and forecasting approach based on Kalman filter and Interval Type-2 Fuzzy Logic for efficiency improvement of centrifugal gas compressor system. *Diagnostyka*, Vol. 20, no. 2, pp. 57-75, May. 2019.

Faults-detection approaches based on Interval Type-2 Fuzzy Logic and Interval Observer: A comparative study

1 Introduction

In the last few years, the maintenance of industrial systems during their operating modes is one of the main strategic problems facing the industry, from the design of a machine until to its exploitation. Therefore, the diagnostic system is essential for ensuring the smooth and continuous operation of dynamic systems and for increasing their performances by guaranteeing better reliability. Indeed, the diagnostic system is used to provide the control system by the required real data of the dynamic system operating status in un-faulty (healthy) mode and in faulty mode. On the other side, the diagnostic system has to fulfill the requirement of robustness to avoid the practical cases of non-detection and false alarms, which means avoiding the eventual accidental and catastrophic situations.

The proposed diagnostic approach presented in this chapter is applied on the centrifugal gas compressor system which is used in many sectors and covers a very wide range of industrial applications. Indeed, this system is at the heart of many industrial sectors, such as the petroleum industry, the thermal and the nuclear power generation, the aeronautic and the space propulsion, the automobile industry, and the transport of gases (pipelines).

First part, of this chapter focuses on the development of a robust faults diagnosis and detection approach which aims to increase the system monitoring performance during the operating mode of the studied centrifugal gas compressor plant. This proposed approach is based on the combination of the two FDI diagnosis model approaches (based on the parametric identification model and on observer system), with the intelligent expert fuzzy type-II system, and the ARIMA model for predicting the remaining time of the system under study to reach the danger and/or the failure stage, the following diagram as shown in Figure. 4.1, summarizing the main points of the proposed approach.

Second part, of this chapter proposes an interval observer framework for the design of fault detection for

multivariable linear uncertain systems. The methodology proposed in this chapter consists in using interval observer on block roots of matrix polynomials theory, and grey wolf optimizer in order to take into account the noises, disturbances, parameter uncertainties and faults. The main contribution is to determine the matrix observer gain L that ensuring the stability of observer matrix and the positivity of the estimated errors. This methodology can be considered as an interesting alternative to classical FDI approaches.

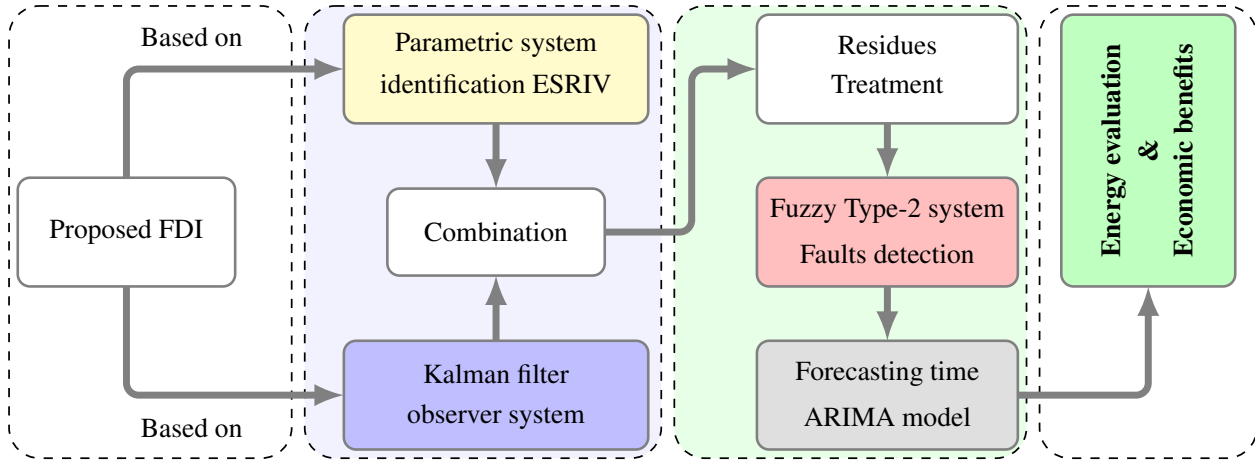


Figure 4.1: Schematic diagram of the proposed FDI approach.

2 Centrifugal gas compressor BCL 505 system

Centrifugal compressors are used in many industrial sectors, such as the oil industry, the production of thermal and nuclear energy, aerospace propulsion, automotive, water distribution, etc. Indeed, a good understanding of the operation of these devices is essential to increase their performance and reduce their operating cost. In this case, one of the limits of use of these systems is determined by its stability limits, limits beyond which stable operation of systems is no longer ensured. The centrifugal gas compressor studied in this chapter is the BCL 505 type which is shown in Figure. 4.2, its characteristics are presented in Table B.1, (Appendix B).

This compressor is constructed by Nuovo Pignone company and it is used in a gas compression heavy applications such as in gas field production and gas network transportation, it is equipped with a control room computer-based where the ACS is a part of it which allows to take directly inputs / outputs measurements from the installed sensors. The main function of the studied centrifugal gas compressor in this chapter, is to ensure the pressure rise of the continuous flow of gas passing through it based on kinetic energy. Where The increase of the gas pressure by a compressor is used to:

- ✓ Reach a level of gas pressure.
- ✓ Compensate the pressure losses related to the circulation of the gas flow in a gas network.

The compressors can be classified according to their characteristics depending on the type of gas to be compressed such as, air compressors and gas compressors, and/or depending on the movement of the moving parts such as, linear or rotary motion, and/or depending on the operating principle such as, volumetric compressors and dynamic compressors which are the application area of the present chapter.

The centrifugal gas compressor dynamic model is represented by its state space model as follows [1, 2]:

$$\begin{cases} x(k+1) = Ax(k) + Bu(k) \\ y(k) = Cx(k) \end{cases} \quad (4.1)$$

where, this discrete-time state space dynamic model of the examine system is a large scalae of order, $n = 10$, and with two inputs ($m = 2$) and two outputs ($p = 2$), and its characteristic matrices A, B, C are mentioned in (B.1), (Appendix B). where, this discrete-time state space dynamic model of the examine system is a large scalae of order, $n = 10$, and with two inputs ($m = 2$) and two outputs ($p = 2$).

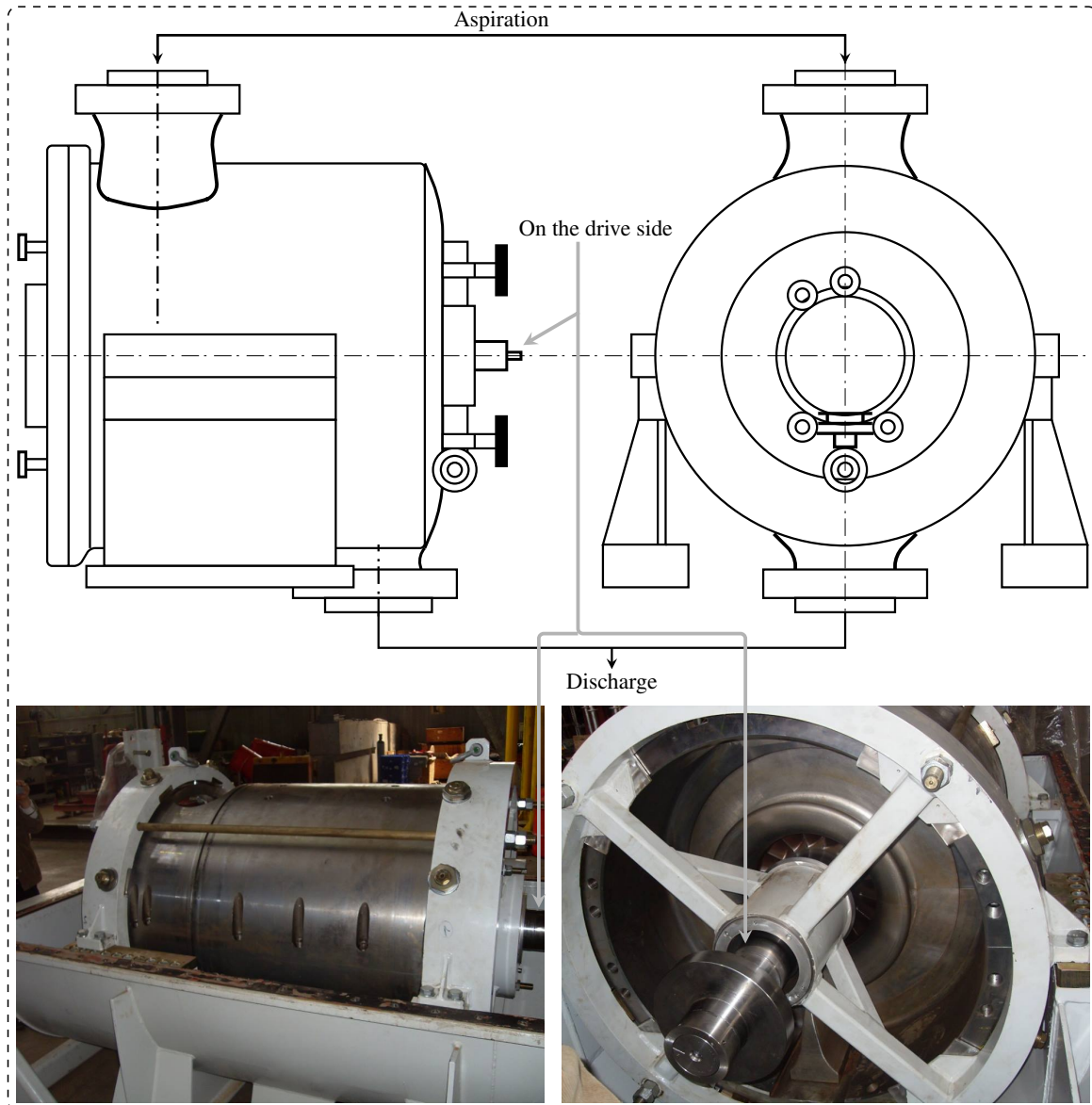


Figure 4.2: Centrifugal gas compressor BCL 505 body, with real view in vertical joint plane

Faults detection and remaining time forecasting approach Based on: Kalman filter, Interval Type-2 Fuzzy Logic and ARIMA model

3 Outputs estimation based on Kalman filter

The Kalman filter is a set of mathematical equations which provides an efficient recursive computational algorithm to ensure the estimation of dynamic systems outputs states, in a way to minimize the mean of the squared error between the estimated output values and the real or the measured outputs. This filter is very useful in several domains: robotic motion planning, signal processing and econometrics. It can achieve the estimations of the past, the present, and even the future states. the last estimation which is dedicated to the future states is the main target of the work presented in this chapter.

The Kalman Filter observer algorithm is used to estimate the unmeasured states and the two filtered outputs $\hat{Y} \in \mathbb{R}^{2 \times 1}$ of the centrifugal gas compressor model presented in (B.1), (Appendix B). The discharge pressure $\hat{P}2$ and The discharge temperature $\hat{T}2$ respectively, The algorithm steps of the Kalman filter are presented in Algorithm 5, (Appendix B).

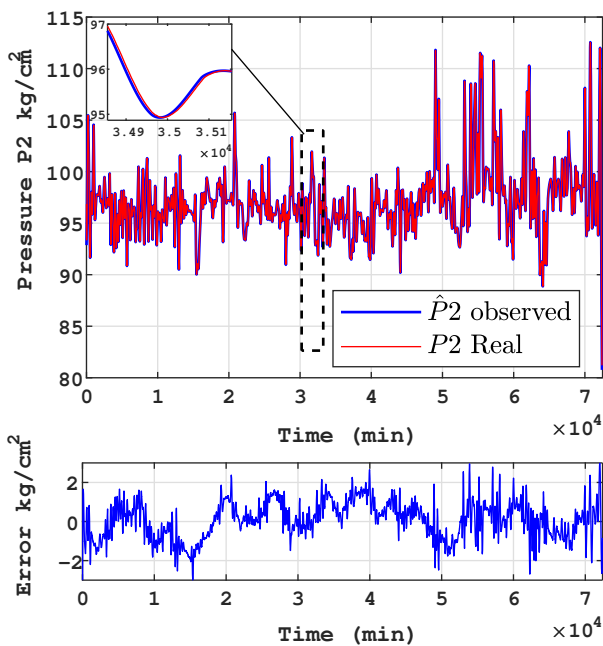


Figure 4.3: Observed and experimental discharge pressure, and the error between them

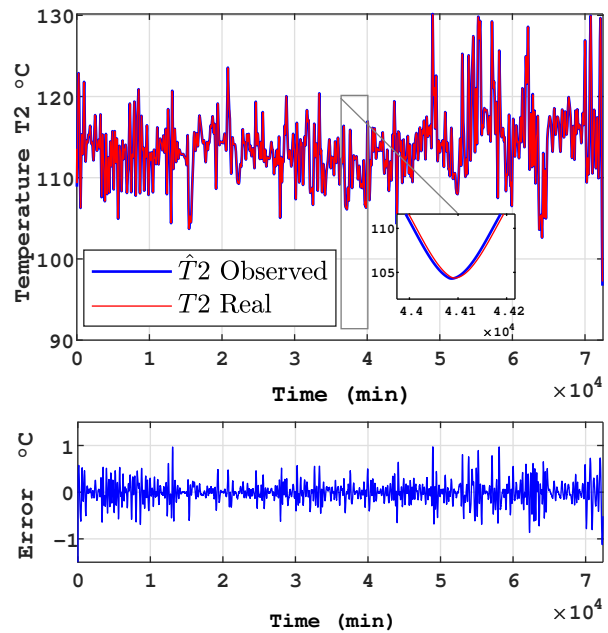


Figure 4.4: Observed and experimental discharge temperature, and the error between them

From these results, it can be concluded that the proposed Kalman filter allows to obtain an accurate estimated output \hat{Y} for the discharge pressure $P2$ and the discharge temperature $T2$ in comparison with the experimental measured outputs Y . Based on the zoom zones presented in Figure 4.4 and Figure 4.3, it can be said that the residues presenting the deviation between the two outputs respectively are neglected and the designed Kalman filter can be an adequate observer for the applications presented in this chapter. This observer is used as an essential and important part of the proposed faults diagnosis and detection approach which is applied to the centrifugal gas compressor presented in this chapter.

4 Preliminary concepts about Interval Type-2 Fuzzy Logic

Initially, the concept of the fuzzy type-2 set was introduced by the founder of the fuzzy logic Lotfi Zadeh [3, 4] as an extension of the concept of the fuzzy type-1 set. The fuzzy type-2 set is characterized by a fuzzy membership function, that is, the degree of belonging of each element of the set is itself a fuzzy set in $[0, 1]$. Such sets are advisable in the case where there is an uncertainty at the level of the value of the membership itself. The uncertainty can be either in the form of the membership function or in one of its parameters. The transition from an ordinary set to a fuzzy set is the direct consequence of the indeterminism of the value belonging to an element by 0 or 1. Similarly, when the functions of an element belonging to fuzzy numbers cannot be determined in real numbers within $[0,1]$, then the fuzzy sets type-2 is used. For this purpose, the fuzzy sets type-1 can be considered as an approximation of the first order of uncertainty and the fuzzy sets type-2 as a second-order approximation.

Depending on the form of primary membership, there are many types of fuzzy sets type-II, among them: triangular, interval, gaussian, and the gaussian 2 which is used in the fuzzy type-2 system faults detection in this chapter. The structure of a fuzzy type-2 system is represented in Figure 4.5, it is similar to fuzzy type-1, whereas the fifth block appears in the output processing is of the reduction type.

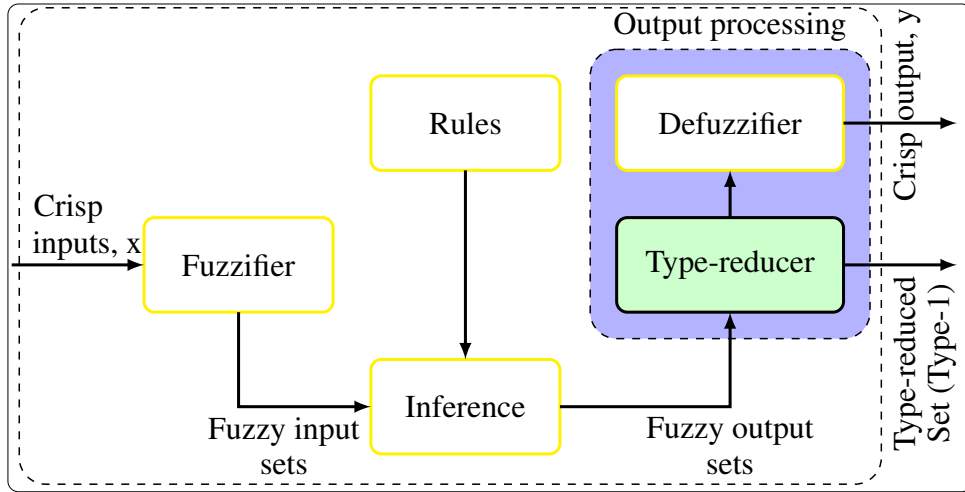


Figure 4.5: The structure of the type-2 Fuzzy Logic System.

The difference between the rules of FL and FL-2, reside only in the nature of the membership functions. Therefore, the structure of the rules in the case of FL-2 will remain exactly the same as that of FL. The only difference is that some (or all) membership functions will be of FL-2. therefore, the j^{th} rule of a FL-2 system will have the following form [3, 4]:

$$\text{If } x_1 \text{ is } \tilde{F}_1^j \text{ and } x_2 \text{ is } \tilde{F}_2^j \dots \text{ and } x_p \text{ is } \tilde{F}_p^j \text{ Then } y \text{ is } \tilde{G}^j \quad (4.2)$$

Where, $x_1 \in X_1, x_2 \in X_2, \dots, x_p \in X_p$ are the outputs, the \tilde{F}_1^j are the sets of premises such as $i = 1, 2, \dots, p, y \in Y$ is the output, and the \tilde{G}^j are the sets of consequences.

5 The proposed FDI setup for a centrifugal gas compressor plant

The faults diagnosis and detection approach proposed in this research chapter takes into consideration all the phases of the operating cycle of the centrifugal gas compressor system under study, such as the evolution of the pressure and the temperature of the gas in the centrifugal gas compressor, the evolution of mass and volume flows as function of the gas pressure and temperature.

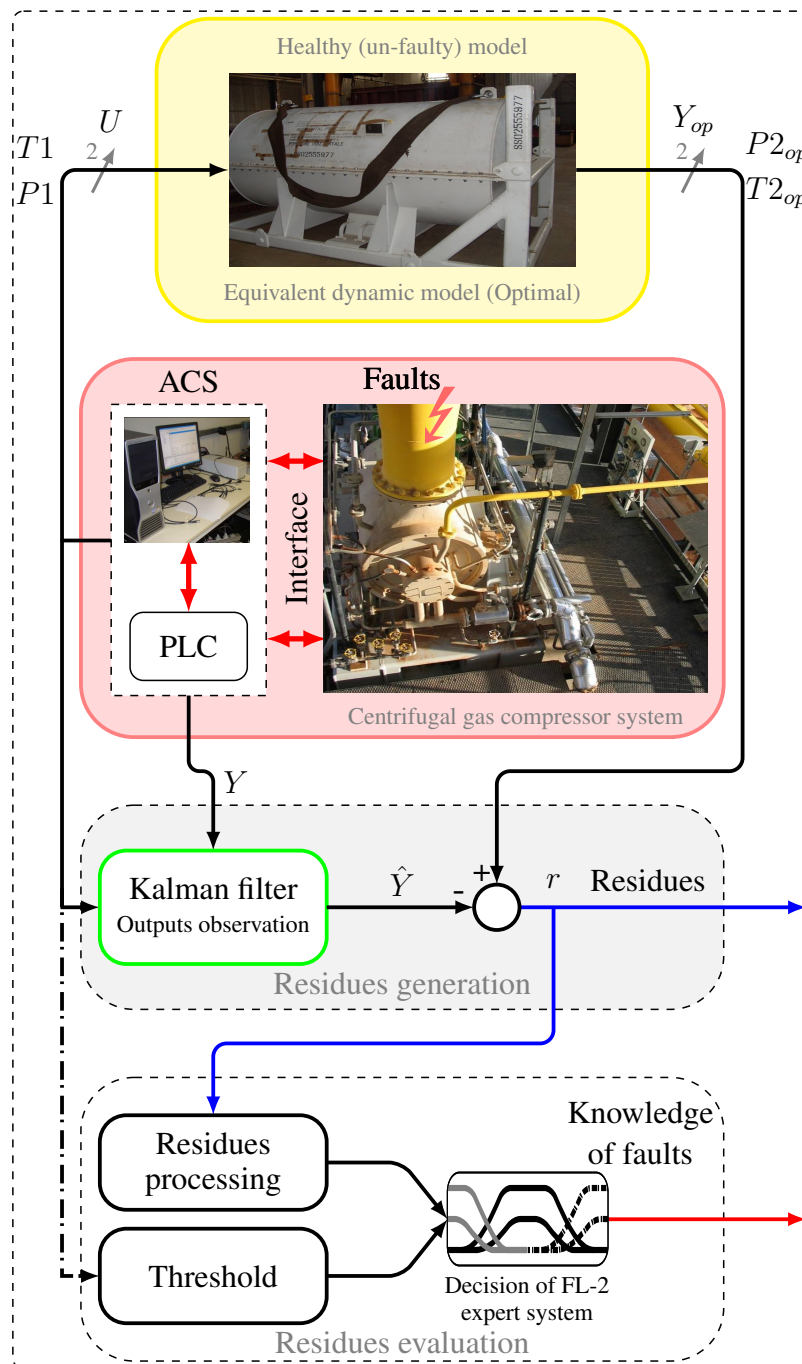


Figure 4.6: Real-time faults detection diagnosis configuration for centrifugal gas compressor.

In the same time ,it takes into account the power absorbed as a function of the gas, and other operating conditions that allow to obtain precise information about the dynamic behavior and to maximize the availability of this system. On the other side, it is well known that the industrial systems have complex behaviors, and they are characterized by uncertain variables or parameters as a function of time, this constraint complicates their control task and implies many difficulties in achieving the good performances of such systems. For this purpose, this work proposes a real-time faults diagnosis and detection approach, where the main aim is to detect and to localize the defective components in the studied centrifugal gas compressor system.

In this proposed diagnostic system a hybrid between the mathematical theory of estimation based on the stochastic kalman filter observer, and the artificial intelligence algorithms based on a type-2 fuzzy system. Figure. 4.6, shows the proposed faults diagnosis and detection approach details studied presented in this chapter.

This proposed approach is based on the calculation of the residues $r(k)$ following (4.3), which presents the errors between the optimal Y_{op} and the observed \hat{Y} outputs respectively. On the other side, the residues are the inputs for the fuzzy type-2 system, when the system is under healthy operating state, these residues have generally a null average and a determined variance.

In practice, the residues do not have exactly zero value in the absence of faults as shown in the previous figures Figure. 4.4 and Figure. 4.3, because the obtained model of the studied system in this chapter does not take into account all the internal and external parameters, which means that only the preponderant parameters are taken into account and that certain simplification has been considered. On the other side the measurements performed on the system are often affected by measurement noise.

The residues are expressed as follows:

$$r(k) = Y_{op}(k) - \hat{Y}(k) \quad (4.3)$$

Where,

$$r(k) = [r_P(k) \quad , \quad r_T(k)]^T \in \mathbb{R}^{2 \times 1}$$

In this context, an elementary detection method consists in comparing the value of the obtained residues with a predefined threshold (modeling errors function). An alarm is triggered each time this threshold is crossed:

$$\begin{cases} r(k) \leq \varepsilon \Leftrightarrow d(k) = 0 \\ r(k) > \varepsilon \Leftrightarrow d(k) \neq 0 \end{cases} \quad (4.4)$$

$d(.)$ presents the vector of the faults.

5.1 Fault detection and isolation (FDI)

The purpose of the detection procedure is to determine the instant of fault occurrence. To achieve this objective, the residues obtained by comparing the system optimal model outputs with the system estimated outputs.

In the presence of faults, the evolutions of the discharge temperature $T2$ and the discharge pressure $P2$ during the time interval of 7×10^4 minutes are registered via the ACS, where a rising vibration in the discharge temperature $T2$, and in the discharge pressure $P2$ are remarked, comparison between the outputs dynamic behavior of the centrifugal gas compressor with and without faults are shown in Figure. 4.7 and Figure. 4.8.

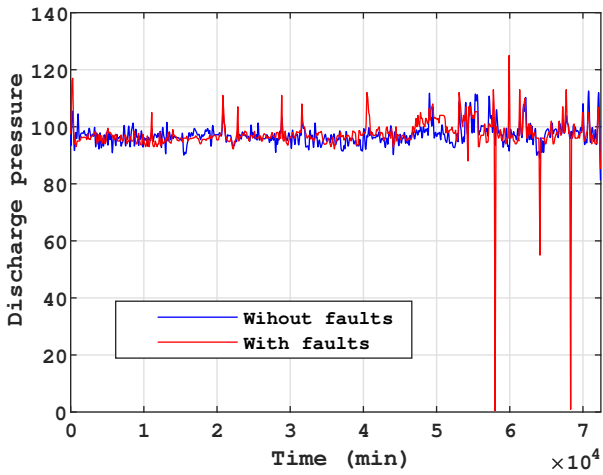


Figure 4.7: The discharge pressure $P2$ with and without faults

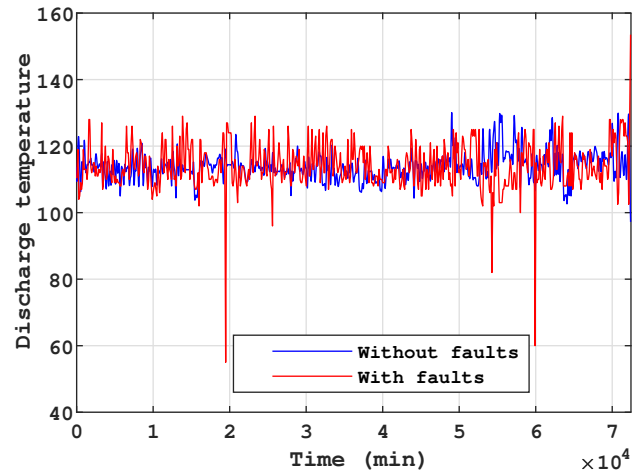


Figure 4.8: The discharge temperature $T2$ with and without faults

After the residues generation step, the next task is the detection of faults based on the obtained residues signals. In the present work, to ensure a robust faults diagnosis and defection, the statistical process control (SPC) is integrated in the monitoring of centrifugal gas compressor. This process control was introduced by Walter Shewhart [5], and it occupies a prominent place among the statistical quality control (SQC) tools. It includes a set of statistical methods to monitor and improve a production process.

The Shewhart graph is able to control the distribution of deviations instead of trying to control each individual deviation. The horizontal axis presents the time and the vertical axis presents the quality scale. It also contains three horizontal lines: The middle line presents the reference line of the normal operation mode output, the upper line is the upper specification limit (USL) of the control quality, and the lowest line is the lower specification limit (LSL) of the minimum control quality. When decisions are confined between the upper and lower limits, the deviation is acceptable and the centrifugal gas is operating in normal conditions. The following Table 4.1 presents the average value m , standard deviation s , and the (USL,LSL) of the two outputs signal that are calculated based on Shewhart algorithm [5].

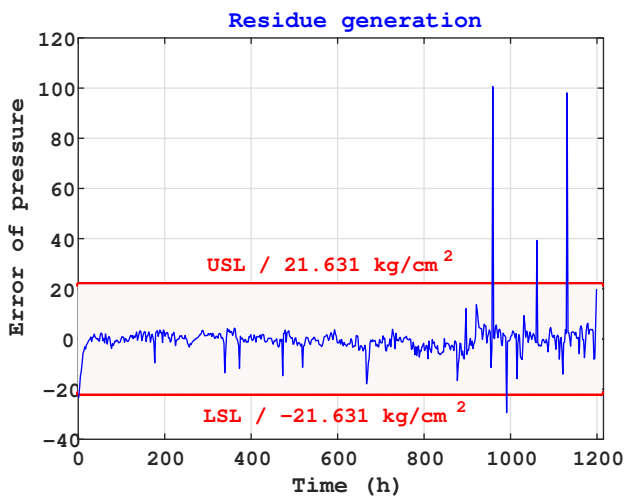


Figure 4.9: The detection faults of ($P2$) with respect to a threshold

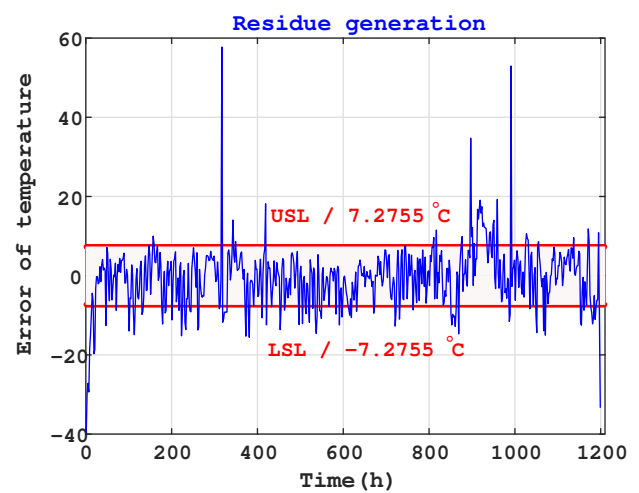


Figure 4.10: The detection faults of ($T2$) with respect to a threshold

Table 4.1: The threshold faults detection

Error	m	s	(USL,LSL)
E_{T2}	-0.0015	3.3063e-8	± 7.2755
E_{P2}	0.0014	3.7597e-9	± 21.631

Figure. 4.9 and Figure. 4.10, show the variation of the generated residues of the discharge pressure and the discharge temperature respectively, that are included within the upper and lower detection faults lines (USL,LSL) of Shewhart graph for the two outputs of the studied centrifugal gas compressor system.

When the residues exceed the upper and lower allowed limits (threshold), the system operates with faults that may not appear externally at the beginning. Therefore, the problem which needs to be solved is to find an efficient way which allows to indicate immediately the faults when they are occurred. To solve this problem a type-2 fuzzy logic system is suggested as an expert models in order to detect and identify the type of occurring faults. In this case many tests have been done to select the best fuzzy sets type-2 that gives a robust performance and good results, in this work the gaussian 2 membership function was chosen as the best one. Figure. 4.11, shows the expert model detection of the discharge pressure $P2$ which contains three membership functions of type gaussian 2, that are the small, the medium, and the large with identical intervals between the upper and lower lines faults detection presented in Table 4.1, if there are faults, the expert model indicates "1". Figure. 4.12, shows the detection expert model of the discharge temperature $T2$, it differs from the first one only by the faults detection upper and lower lines (threshold).

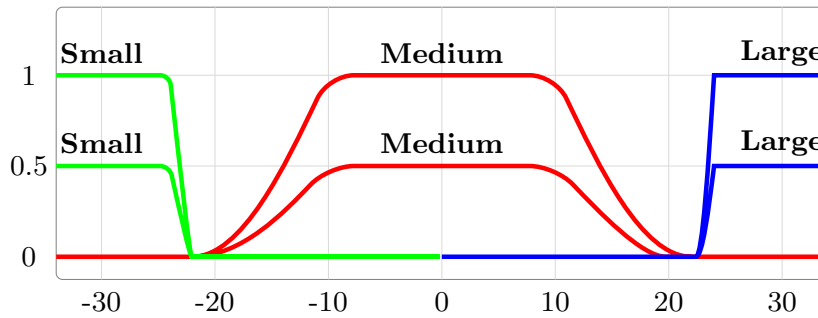


Figure 4.11: Type-2 fuzzy sets of discharge pressure $P2$ expert model faults detection

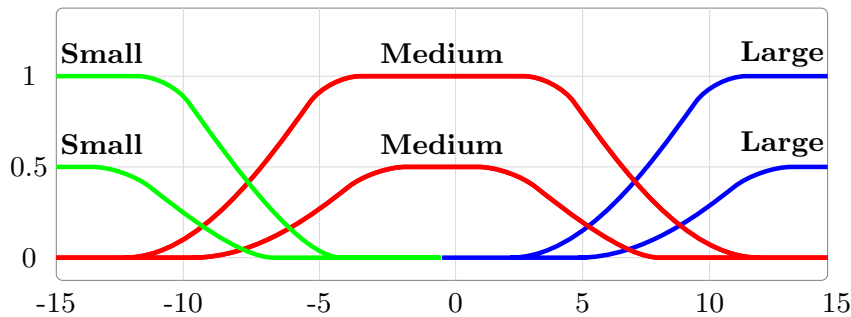


Figure 4.12: Type-2 fuzzy sets of discharge temperature $T2$ expert model faults detection

20 faults are detected related to the discharge pressure output $P2$, 12 faults were accurate during the first 12 hours and 8 faults during the time interval from 968 hours to 1142 hours, regarding the discharge temperature

output $T2$, around 400 faults are detected, these faults have been occurred during almost the operating time along the interval time from 1 hour to 1208 hours.

The detection faults of the discharge pressure and the discharge temperature respectively are shown in Figure. 4.13 and Figure. 4.14 based on 2D thermal card, where the red color symbolizes the detected fault and each fault is represented by stem.

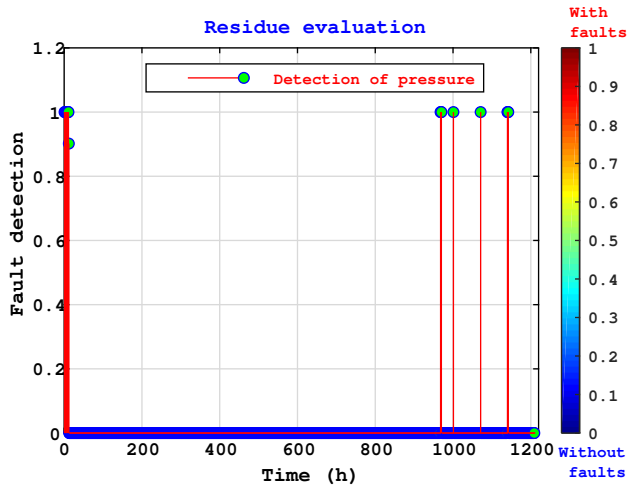


Figure 4.13: The fault evaluation of ($P2$) gas compressor system examined

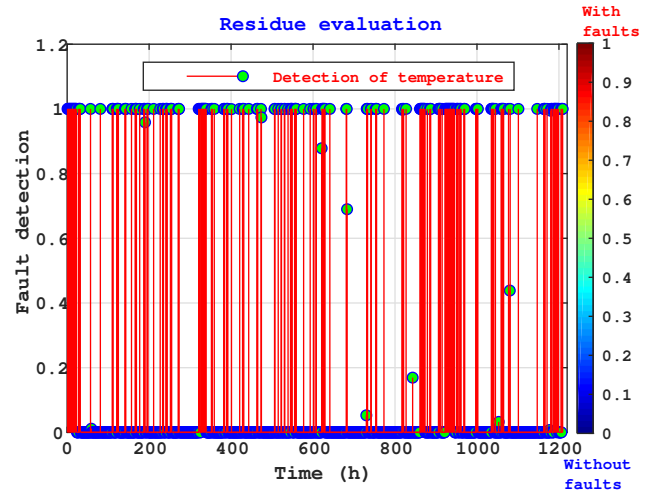


Figure 4.14: The fault evaluation of ($T2$) gas compressor system examined

After the faults detection based on the output signals of the centrifugal gas compressor $T2$ and $P2$ through the proposed faults detection setup, a maintenance schedule is required for the system to identify the nature of the faults, the resulting damages and the affected components, where the main aim is to ensure the required change and reparation in the system to restart the system operating mode again.

During the experimental study, the system was completely opened for performing the maintenance, checking the inside body of the studied system and for the validation of the proposed faults diagnosis and detection presented in this chapter and its accuracy for the determination and assessment of the fault levels. Indeed, after careful examination, the damage observed and realized in the components of the BCL 505 gas compressor are presented in the following figures:

- ✓ Scratch on the blades of the impeller1, as shown in Figure. 4.15.
- ✓ Light streaks at the spacers level, as shown in Figure. 4.16.
- ✓ O-ring joints defects, as shown in Figure. 4.17.

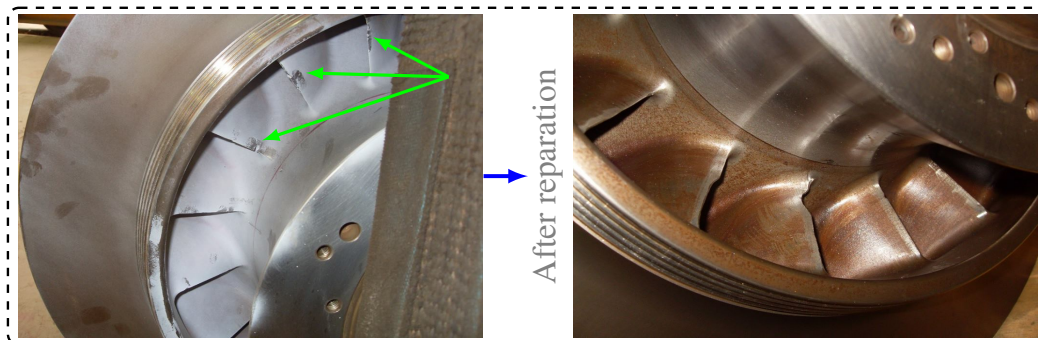


Figure 4.15: The status of scratch on the blades of the impeller1 and after reparation.

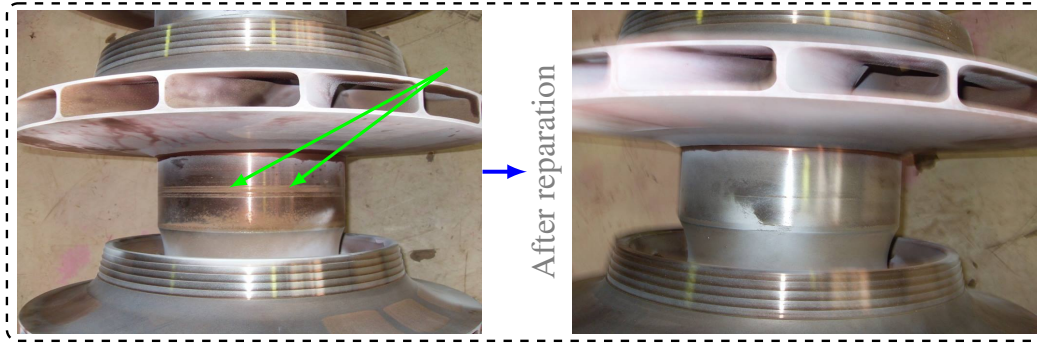


Figure 4.16: The status of light streaks at the spacers level and after reparation.

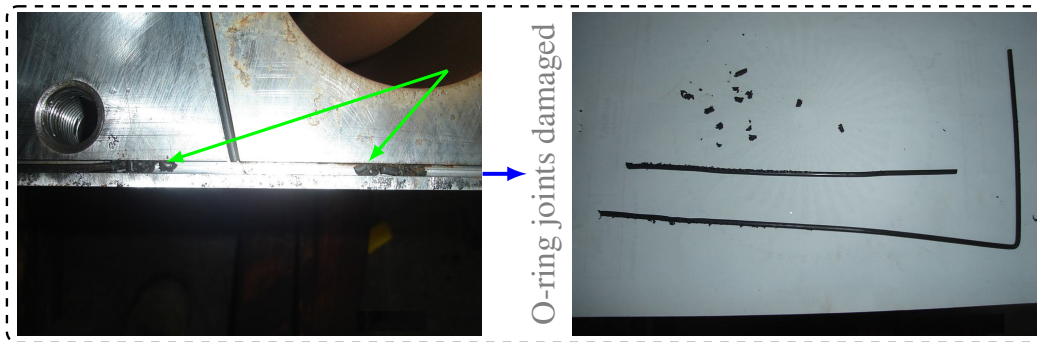


Figure 4.17: The status of O-ring joints defective.

After viewing and identifying the affected parts in the centrifugal gas compressor system, the below Table 4.2 confirm the results obtained from the proposed setup for the faults detection. In comparison with the constructor operating system documents, it can be said that the obtained results are within the norms given by the constructor.

Table 4.2: Faults identification and classification

Faults	Outputs	Signal	Faults identification
F_1	P2	↗	• Distortions and incision in the level of blades
	T2	↗	
F_2	P2	✓	• O-ring joints defective • Friction between the blades and wheel-space
	T2	↗	
F_3	P2	✓	• looseness in screws • O-ring joints defective
	T2	✓	
		↗ : Rise	↘ : Fall

5.2 Forecasting the remaining time

In this section, it is assumed that the centrifugal gas compressor is operating under faulty mode. In this case, the proposed approach of faults diagnosis and detection needs to be improved. It means that depending on the level and quality of faults, the safety time for which the studied system can continue its operation mode before it falls completely in failure and reaches the operating interruption. In order to achieve this important required task, the ARIMA model is used to know the evolution of both temperature and pressure with respect to time, to know when the centrifugal gas compressor be out of control (damage).

The ARIMA model and the interpolation algorithm techniques [6, 7] are highly used in speech signal processing and in statistics (time series), as well as in the deterministic and random case, which will be the only one considered in this work. The ARIMA model is used to predict the value of a discrete-time signal at a defined instant as a function of its past or all its future,. The main aim of implementation of this algorithm is to predict the time at which the system reaches the stage of damage or danger. From the results shown in Figures Figure. 4.18, for the discharge temperature $T2$ output, the time between the alarm warning and the time of the system to be out of control is 60 hours. For the discharge pressure $P2$ and based on Figures. Figure. 4.19, the time between the alarm warning and the time of the system to be out of control is 75 hours.

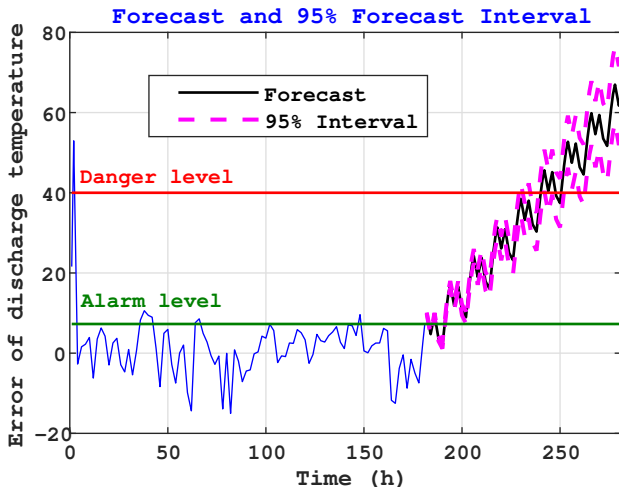


Figure 4.18: Forecasting time level danger of ($P2$)

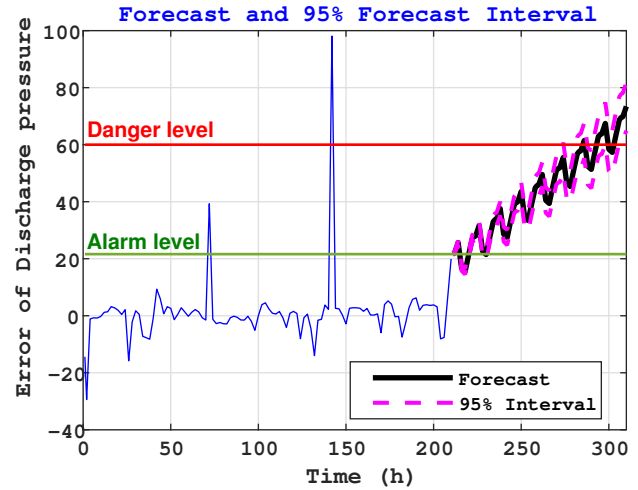


Figure 4.19: Forecasting time level danger of ($T2$)

These results mean that the safety time for the system to operate under the detected faults until falling into danger or damage is 60 hours, beyond this time the safety of the whole system is not guaranteed. Thus, through these prediction, the system damages and its maintenance time loss can be avoided, furthermore, the system can be isolated in time from critical danger. It can be said from the obtained results that the proposed and improved faults diagnosis and detection approach in this chapter can improve the operation of centrifugal gas compressor system and guarantee its production continuity within the whole installation.

6 Economic study

6.1 Reparation costs

During the first phase, within the time interval from 0 to 1000 hours, the centrifugal gas compressor operates in healthy operating mode, consequently the value of the faults detection system indicates "0" Figure. 4.20. During the second phase, along the time interval from 1000 hours to 2209 hours, the centrifugal gas compressor operates under intermittent faulty state. Hence, the faults detection system indicates "1" as the measured signal for faults detection pass the threshold aforementioned Figure. 4.20. It is important to clarify that the faults occurrence in percentage rises to 38.9776% at the end of the second phase, this percentage is calculated based on the number of zeros and ones obtained by the faults detection system during the second phase as shown in Figure. 4.20. this percentage value means that the performances of the centrifugal gas compressor are decreased, due to the increase of the temperature $T2$ and the decrease of the output pressure $P2$ as shown in Figure. 4.20. Consequently, at the end of the second phase, the machine is stopped to perform the maintenance of the whole

system, not only the studied compressor. This operation is performed during the time of 744 hours (31 days) where the main aim is to achieve all the required reparations. On the other side, the total repair cost was estimated at 357,000€(this maintenance is performed to all the equipment without the intervention of the manufacturer or an external company). It can be seen clearly that the reparation cost increases as the reparation time increase as shown in Figure. 4.20. After the reparation, the centrifugal gas compressor is restarted up and connected to the installation to work with a fully capacity again.

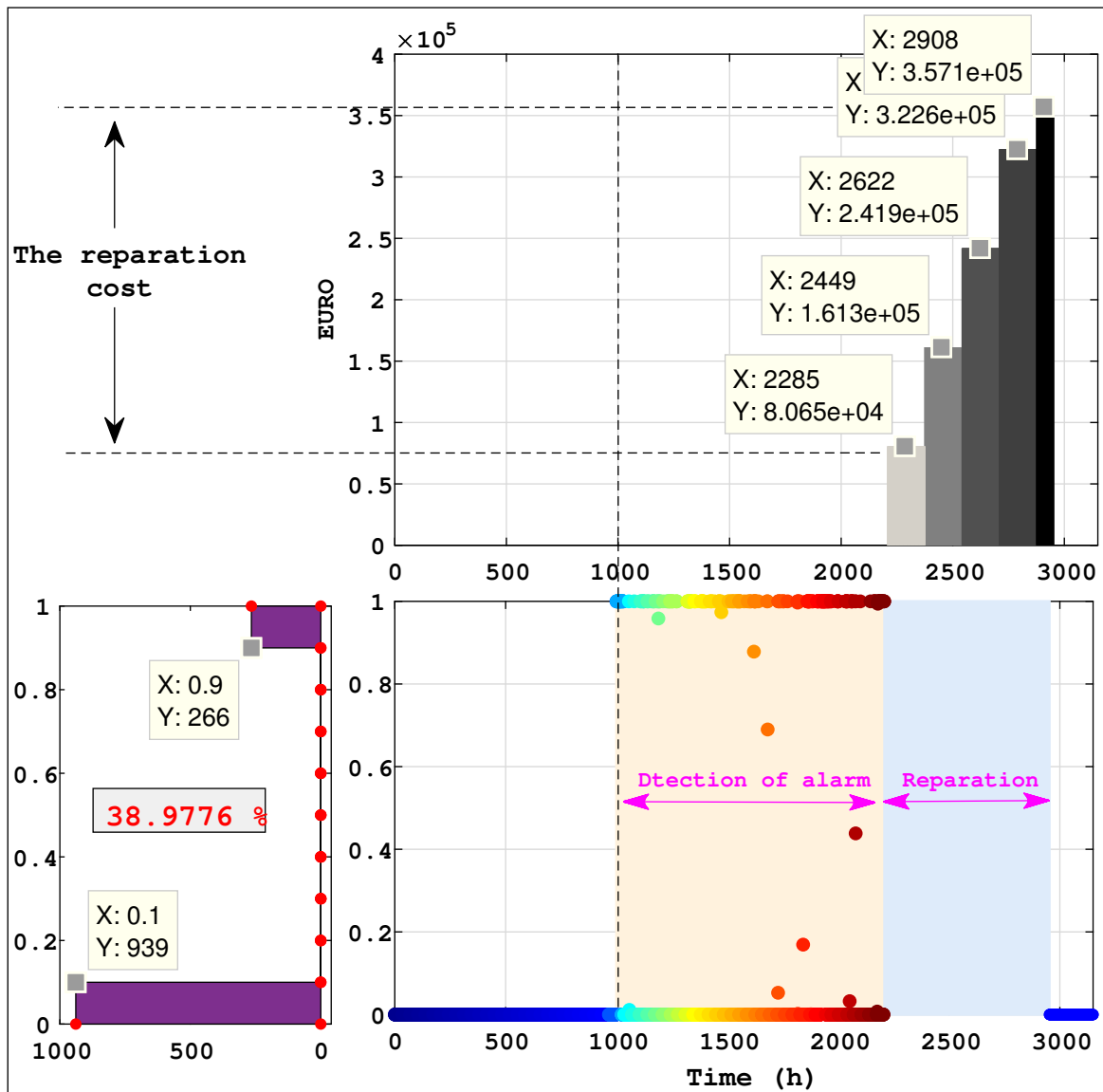


Figure 4.20: The diagnosis approach impact on the financial cost

6.2 Benefits

When the intervention of reparation is performed at the time where the percentage of the fault occurrence reaches 10% based on the proposed diagnostic and faults detection system, the cost of reparation will be approximately 96,267€, furthermore the reparation period will take approximately 204 hours (8 days and a half day). In this case it can be said that the proposed diagnostic system for early faults detection is economically efficient, where the reparation intervention of defects will be done in time, more faster and with reduced financial burdens.

Fault detection based on interval observer using block roots assignment and grey wolf optimizer

7 Preliminaries

7.1 Interval Relations

Let the two vectors $\{x_1, x_2\} \in \mathbb{R}^n$ or the two matrices $\{A_1, A_2\} \in \mathbb{R}^{n \times n}$, the relations $x_1 \leq x_2$ and $A_1 \leq A_2$ are understood elementwise. The relation $P < 0$ ($P > 0$) means that the matrix $P \in \mathbb{R}^{n \times n}$ is negative (positive) definite. Given a matrix $A \in \mathbb{R}^{m \times n}$, define $A^+ = \max\{0, A\}$, $A^- = A^+ - A$ (similarly for vectors) and denote the matrix of absolute values of all elements by $|A| = A^+ + A^-$ [9].

Lemma 4.1. [9, 10]. Let $x \in \mathbb{R}^{n \times n}$ be a vector variable, $\underline{x} \leq x \leq \bar{x}$ for some $\underline{x}, \bar{x} \in \mathbb{R}^n$.

1. If $A \in \mathbb{R}^{m \times n}$ is a constant matrix, then

$$A^+ \underline{x} - A^- \bar{x} \leq Ax \leq A^+ \bar{x} - A^- \underline{x} \quad (4.5)$$

2. If $A \in \mathbb{R}^{m \times n}$ is a matrix variable and $\underline{A} \leq A \leq \bar{A}$ for some $\underline{A}, \bar{A} \in \mathbb{R}^{m \times n}$, then

$$\underline{A}^+ \underline{x}^+ - \bar{A}^- \underline{x}^- - \underline{A}^- \bar{x}^+ + \bar{A}^- \bar{x}^- \leq Ax \leq \bar{A}^+ \bar{x}^+ - \underline{A}^+ \bar{x}^- - \bar{A}^- \bar{x}^+ + \underline{A}^- \underline{x}^-. \quad (4.6)$$

Furthermore, if $-\bar{A} = \underline{A} \leq 0 \leq \bar{A}$, then the inequality (4.6) can be simplified: $-\bar{A}(\bar{x}^+ + \underline{x}^-) \leq Ax \leq \bar{A}(\bar{x}^+ + \underline{x}^-)$.

7.2 Nonnegative Linear Invariant-Time (LTI) Systems

7.2.1 Case of LTI Continuous-time systems

A matrix $A \in \mathbb{R}^{n \times n}$ is called **Hurwitz** if all its eigenvalues have negative real parts, it is called **Metzler** if all its elements outside the main diagonal are nonnegative. Any solution of the linear system.

$$\begin{cases} \dot{x}(t) = Ax(t) + Bu(t), & u: \mathbb{R}_+ \rightarrow \mathbb{R}_+^q, \quad u \in \mathcal{L}_\infty^q \\ y(t) = Cx(t) \end{cases} \quad (4.7)$$

with $x \in \mathbb{R}^{n \times n}$, $y \in \mathbb{R}^p$ and a **Metzler** matrix $A \in \mathbb{R}^{n \times n}$, is elementwise nonnegative for all $t \geq 0$ provided that $x(0) \geq 0$ and $B \in \mathbb{R}_+^{n \times q}$ [9, 11, 12]. The output solution $y(t)$ is **nonnegative** if $C \in \mathbb{R}_+^{p \times n}$ and $D \in \mathbb{R}_+^{p \times q}$. Such dynamical systems are called **cooperative (monotone) or nonnegative** if only initial conditions in \mathbb{R}_+^n are considered [9, 11, 12].

For a **Metzler** matrix $A \in \mathbb{R}^{n \times n}$ its stability can be checked verifying a Linear Programming (LP) problem

$$A^T \lambda < 0 \quad (4.8)$$

for some $\lambda \in \mathbb{R}_+^n \setminus \{0\}$, or Lyapunov matrix equation

$$A^T P + P A < 0 \quad (4.9)$$

for a diagonal matrix $P \in \mathbb{R}^{n \times n}$, $P > 0$ (in general case the matrix P should not be diagonal). The L_1 and L_∞ gains for nonnegative systems (4.7), *i.e.* gains of transfer function from input to output in different norms, have been studied in [13, 14], for this kind of systems these gains are interrelated.

Lemma 4.2. [13, 14]. Let the system (4.7) be nonnegative (*i.e.* A is Metzler, $B \geq 0$, $C \geq 0$ and $D \geq 0$), then it is asymptotically stable if and only if there exist $\lambda \in \mathbb{R}_+^n \setminus \{0\}$ and a scalar $\gamma > 0$ such that the following LP problem is feasible:

$$\begin{pmatrix} A^T \lambda + C^T E_p \\ B^T \lambda - \gamma E_q + D E_p \end{pmatrix} < 0.$$

Moreover, in this case L_1 gain of the operator $u \rightarrow y$ is lower than γ .

Lemma 4.3. [13, 14]. Let the system (4.7) be cooperative (*i.e.* A is Metzler, $B \geq 0$, $C \geq 0$ and $D \geq 0$), then it is asymptotically stable if and only if there exist $\lambda \in \mathbb{R}_+^n \setminus \{0\}$ and a scalar $\gamma > 0$ such that the following LP problem is feasible:

$$\begin{pmatrix} A \lambda + B E_q \\ C \lambda - \gamma E_p + D E_q \end{pmatrix} < 0.$$

Moreover, in this case L_∞ gain of the transfer $u \rightarrow y$ is lower than γ .

The conventional results and definitions on L_2/L_∞ stability for linear systems can be found in [15].

7.2.2 Case of LTI Discrete-time systems

A matrix $A \in \mathbb{R}^{n \times n}$ is called **Schur stable** if all its eigenvalues have absolute value less than one, it is called **nonnegative** if all its elements are nonnegative (*i.e.* $A > 0$). Any solution of the system

$$x(k+1) = A x(k) + u(k), \quad u : \mathbb{Z}_+ \rightarrow \mathbb{R}_+^n, \quad u \in \mathcal{L}_\infty^n, \quad t \in \mathbb{Z}_+, \quad (4.10)$$

with $x(k) \in \mathbb{R}^n$ and a nonnegative matrix $A \in \mathbb{R}_+^{n \times n}$ (for the discrete-time case $\|\omega\| = \sup_{k \in \mathbb{Z}_+} |\omega_k|$ and by \mathcal{L}_∞^n we denote the set of inputs $\omega : \mathbb{Z}_+ \rightarrow \mathbb{R}^n$ with the property $\|\omega\| < +\infty$), is elementwise nonnegative for all $k \geq 0$ provided that $x(0) \geq 0$ [16]. Such a system is called cooperative (monotone) or nonnegative [16].

Lemma 4.4. [11]. A matrix $A \in \mathbb{R}_+^{n \times n}$ is Schur stable if there exists a diagonal matrix $P \in \mathbb{R}_+^{n \times n}$, $P > 0$ such that $A^T P A - P < 0$.

7.3 Survey on matrix polynomials

Here we are going to define and explore some algebraic theory of matrix polynomials, solvent, latent structure, spectral factors and the transformation between solvents and spectral factors.

Corollary 4.1. *given the set of $m \times m$ complex matrices A_0, A_1, \dots, A_l , the following matrix valued function of the complex variable s is called a matrix polynomial of degree l and order m :*

$$A(s) = A_0 s^l + A_1 s^{l-1} + \dots + A_{l-1} s + A_l \quad (4.11)$$

The matrix polynomial $A(s)$ is called:

- *Monic if is A_0 the identity matrix.*
- *Comonic if A_l is the identity matrix.*
- *Regular if $\det(A(s)) \neq 0$.*
- *Nonsingular if $\det(A(s))$ is not identically zero.*
- *Unimodular if $\det(A(s))$ is nonzero constant.*

Corollary 4.2. *The complex number s_i is called a latent root of the matrix polynomial $A(s)$ if it is a solution of the scalar polynomial equation $\det(A(s)) = 0$. The nontrivial vector p , solution of $A(s_i)p = 0_m$ is called a primary right latent vector associated with s_i . Similarly the nontrivial vector q solution of $q^T A(s_i) = 0_m$ is called a primary left latent vector associated with s_i .*

Remark 1. If $A(s)$ has a singular leading coefficient (A_l) then $A(s)$ has latent roots at infinity.

From the corollary we can see that the latent problem of a matrix polynomial is a generalization of the concept of eigenproblem for square matrices. Indeed, we can consider the classical eigenvalues/vector problem as finding the latent root/vector of a linear matrix polynomial $(sI - A)$.

We can also define the spectrum of a matrix polynomial $A(s)$ as being the set of all its latent roots (notation $\sigma(s)$). It is essentially the same definition as the one of the spectrum of a square matrix.

Corollary 4.3. *A right block root also called solvent of s -matrix $A(s)$ and is an $m \times m$ real matrix R such that:*

$$\begin{aligned} R^l + A_1 R^{l-1} + \dots + A_{l-1} R + A_l &= O_m \\ \Leftrightarrow A_R(R) = \sum_{i=0}^l A_i R^{l-i} &= O_m \end{aligned} \quad (4.12)$$

While a left solvent is an $m \times m$ real matrix L such that:

$$\begin{aligned} L^l + L^{l-1} A_1 + \dots + L A_{l-1} + A_l &= O_m \\ \Leftrightarrow A_L(L) = \sum_{i=0}^l L^{l-i} A_i &= O_m \end{aligned} \quad (4.13)$$

The following are important facts on solvents:

- *Solvents of a matrix polynomial do not always exist.*
- *Generalized right (left) eigenvectors of a right (left) solvent are the generalized latent vectors of the corresponding matrix polynomial*

Corollary 4.4. *A matrix R (respectively: L) is called a right (respectively: left) solvent of the matrix polynomial if and only if the binomial $(sI - R)$ (respectively: $(sI - L)$) divides exactly $A(s)$ on the right (respectively: left).*

Theorem 4.1. *given a matrix polynomial*

$$A(s) = A_0 s^l + A_1 s^{l-1} + \dots + A_{l-1} s + A_l \quad (4.14)$$

- *The remainder of the division of $A(s)$ on the right by the binomial $(sI - X)$ is $A_R(X)$*

- The remainder of the division of $A(s)$ on the left by the binomial $(sI - X)$ is $A_L(X)$

Means that there exist matrix polynomials $Q(s)$ and $S(s)$ such that:

$$\begin{aligned} A(s) &= Q(s)(sI - X) + A_R(X) \\ &= (sI - X)S(s) + A_L(X) \end{aligned} \quad (4.15)$$

Corollary 4.5. also gives the fundamental relation that exist between right solvent (respectively: left solvent) and right (respectively: left) linear factor:

$$\begin{aligned} A_R(X) = 0 &\text{ iff } A(s) = Q(s)(sI - X) \\ A_L(X) = 0 &\text{ iff } A(s) = (sI - X)S(s) \end{aligned} \quad (4.16)$$

7.4 The concept of Block roots

The l block roots $R_L \in \mathbb{R}^{m \times m}$ are the block solvents (solutions) of the z polynomial matrix $A(z)$, there exist two types of block roots, right block roots and left block roots, in this observer gain matrix design just focusing for assigning a set of left block roots [18–22].

7.4.1 The left Block roots

The polynomial matrix of order m and degree l is defined by:

$$D_L(z) = I_m z^l + A_1 z^{l-1} + \dots + A_l \quad (4.17)$$

A left block root defined by $R_L \in \mathbb{R}^{p \times p}$ matrices satisfying:

$$D_L(R_L) = R_L^l A_0 + R_L^{l-1} A_1 + \dots + R_L A_{l-1} + A_l = 0_p \quad (4.18)$$

7.4.2 The choice form of the desired Block roots

The set of desired left block roots $R_L \in \mathbb{R}^{p \times p}$ are to be selected from class of stable eigenvalues chosen in the dominant zone and without consuming the dynamics of the system in the same time, there are many forms will be selected (controller/observer and diagonal/general forms), the diagonally form is restricted in this observer design to their performance [18–22].

$$R_L = \left(\overbrace{\left(\begin{array}{c|c|c} \lambda_1 & 0 & 0 \\ \hline 0 & \ddots & 0 \\ \hline 0 & 0 & \lambda_m \end{array} \right)}^{R_{L1}}, \dots, \overbrace{\left(\begin{array}{c|c|c} \lambda_{n-p+1} & 0 & 0 \\ \hline 0 & \ddots & 0 \\ \hline 0 & 0 & \lambda_n \end{array} \right)}^{R_{Li}} \right) \quad (4.19)$$

Theorem 4.2. [17]. *The condition of complete set of left block roots* Consider the set of block roots $\{R_{L1}, R_{L2}, \dots, R_{Li}\}$ extracted from the eigenvalues $(\lambda_1, \lambda_2, \dots, \lambda_n)$ of a matrix A_o , where $\{R_{L1}, R_{L2}, \dots, R_{Li}\}$ is a complete set of left block roots if and only if [18–22]:

$$\begin{cases} \sigma(R_{Li}) \cup \sigma(R_{Lj}) = \sigma(A_c) \\ \sigma(R_{Li}) \cap \sigma(R_{Lj}) = \emptyset \\ \det(V_L(R_{L1}, R_{L2}, \dots, R_{Li})) \neq 0 \end{cases} \quad (4.20)$$

where, σ denotes the spectrum of the matrix and V_L is the left block vandermonde matrix corresponding to $\{R_{L1}, R_{L2}, \dots, R_{Ll}\}$ given as:

$$V_L(R_{L1}, R_{L2}, \dots, R_{Ll}) = \begin{pmatrix} I_p & R_{L1} & \cdots & R_{L1}^{l-2} & R_{L1}^{l-1} \\ I_p & R_{L2} & \cdots & R_{L2}^{l-2} & R_{L2}^{l-1} \\ \vdots & \vdots & \ddots & \vdots & \vdots \\ I_p & R_{Ll} & \cdots & R_{Ll}^{l-2} & R_{Ll}^{l-1} \end{pmatrix} \quad (4.21)$$

The conditions for the existence of the complete set of left block roots have been proved by [18–22].

Remark 2. A left block vandermonde matrix extracted from a complete set of block roots of a polynomial matrix is assumed and must to be nonsingular.

7.5 Problem statement

Consider the following Linear uncertain system

$$\begin{cases} x(k+1) = A(\theta)x(k) + B(\theta)u(k) + d(k) \\ y(k) = C(\theta)x(k) + v(k) \end{cases} \quad (4.22)$$

where, θ is the vector of the uncertain parameters with the bounded values by an compact set Θ as $\Theta = \{\theta \in \mathbb{R}^{n\theta} \mid \underline{\theta}_i \leq \theta_i \leq \bar{\theta}_i, i = 1, \dots, n\}$

$$\begin{aligned} \underline{A}(\theta) &\leq A(\theta) \leq \bar{A}(\theta) \\ \underline{B}(\theta) &\leq B(\theta) \leq \bar{B}(\theta) \\ \underline{C}(\theta) &\leq C(\theta) \leq \bar{C}(\theta) \end{aligned} \quad (4.23)$$

where $\underline{\bullet}$ and $\bar{\bullet}$ denote the lower and the upper bound of each matrix, respectively. Note that the inequalities in (4.23) should be understood as element-wise inequalities. Therefore, the uncertainties in matrices $A(\theta)$, $B(\theta)$ and $C(\theta)$ can be decomposed as $A(\theta) = A_n + \Delta A(\theta)$, $B(\theta) = B_n + \Delta B(\theta)$ and $C(\theta) = C_n + \Delta C(\theta)$, where A_n , B_n and C_n are the matrices of the system (4.22), and the nominal part of the system matrices $A(\theta)$, $B(\theta)$ and $C(\theta)$, respectively.

where $x(k) \in \mathbb{R}^n$, $u(k) \in \mathbb{R}^m$ and $y(k) \in \mathbb{R}^p$ are the state, the input and the output vectors. $d(k) \in \mathbb{R}^n$ is the disturbance, $d \in \mathcal{L}_\infty^n$, $v(k) \in \mathbb{R}^p$ is the measurement noise, $v \in \mathcal{L}_\infty^p$. This model has also three sources of uncertainty: initial conditions for $x(0)$, instant values of $d(k)$ and $v(k)$, all of them belonging to known intervals.

Assumption 4.1. Let $x(0) \in [\underline{X}_0, \bar{X}_0]$ for some known $\underline{X}_0, \bar{X}_0 \in \mathbb{R}^n$, let also two functions $\underline{d}, \bar{d} \in \mathcal{L}_\infty^n$ and a constant $V > 0$ are given such that

$$\underline{d}(k) \leq d(k) \leq \bar{d}(k), \quad |v(k)| \leq V \quad \forall k \in \mathbb{Z}_+. \quad (4.24)$$

It is required to calculate two estimates $\underline{x}, \bar{x} \in \mathcal{L}_\infty^n$ using the available information on these intervals and $y(k)$, such that

$$\underline{x}(k) \leq x(k) \leq \bar{x}(k), \quad \forall k \in \mathbb{Z}_+. \quad (4.25)$$

The following simplest interval observer is a solution to this problem:

$$\begin{cases} \underline{x}(k+1) = A(\theta)\underline{x}(k) + L|y(k) - C(\theta)\underline{x}(k)| - |L|E_p V + B(\theta)u(k) + \underline{d}(k) \\ \bar{x}(k+1) = A(\theta)\bar{x}(k) + L|y(k) - C(\theta)\bar{x}(k)| + |L|E_p V + B(\theta)u(k) + \bar{d}(k) \end{cases} \quad (4.26)$$

$$\underline{x}_0 = \underline{X}_0, \bar{x}_0 = \bar{X}_0$$

where $L \in \mathbb{R}^{n \times p}$ is the observer gain to be designed as it is required below.

Theorem 4.3. [17]. *Let Assumption 4.1 hold and $x \in \mathcal{L}_\infty^n$, then in the system (4.22) with the interval observer (4.26) the relations (4.25) are satisfied provided that the matrix $A - LC$ is nonnegative. In addition, $\underline{X}, \bar{x} \in \mathcal{L}_\infty^n$ if $A - LC$ is Schur stable.*

Proof. The system (4.22) can be equivalently rewritten as follows:

$$x(k+1) = (A(\theta) - LC(\theta))x(k) + Ly(k) - Lv(k) + B(\theta)u(k) + d(k). \quad (4.27)$$

Let us again consider behavior of two estimation errors $\underline{e}(k) = x(k) - \underline{x}(k)$ and $\bar{e}(k) = \bar{x}(k) - x(k)$:

$$\begin{cases} \underline{e}(k+1) = (A(\theta) - LC(\theta))\underline{e}(k) + \underline{d}(k) - \underline{d}(k) + |L|E_p V - Lv(k). \\ \bar{e}(k+1) = (A(\theta) - LC(\theta))\bar{e}(k) + \bar{d}(k) - d(k) + |L|E_p V + Lv(k). \end{cases}$$

By The **Assumption 4.1**, $d(k) - \underline{d}(k) + |L|E_p V - Lv(k) \geq 0$ and $\bar{d}(k) - d(k) + |L|E_p V + Lv(k) \geq 0$ for all $k \in \mathbb{Z}_+$, then since $A(\theta) - LC(\theta) \geq 0$ and $\underline{e}_0 \geq 0, \bar{e}_0 \geq 0$ we conclude that $\underline{e}(k) \geq 0, \bar{e}(k) \geq 0$ for all $k \in \mathbb{Z}_+$. Therefore, the interval inclusion (4.15) is satisfied. For a Schur stable matrix $A(\theta) - LC(\theta)$ and bounded inputs $Ly(k) - |L|E_p V + \underline{d}(k), Ly(k) + |L|E_p V + \bar{d}(k)$ the boundedness of $\underline{x}(k)$ and $\bar{x}(k)$ immediately follows by standard arguments. ■

Design of observer matrix gain L The matrix observer gain L can be found as a solution of the following Linear Matrix Inequalities LMIs problem [17]:

$$\begin{pmatrix} P & PA - WC \\ A^T P - C^T W^T & P \end{pmatrix} > 0, \quad P > 0 \quad (4.28)$$

$$PA - WC \geq 0$$

where $P \in \mathbb{R}^{n \times n}$ is diagonal and $W \in \mathbb{R}^{n \times p}$ are two matrix variables to determine, then $L = P^{-1}W$. A gain optimization problem can also be formulated to find L providing a minimal interval width $\bar{x}(k) - \underline{x}(k)$ in some sense for given in The **Assumption 4.1** uncertainty.

The solution of LMIs problem presented in (4.28) is not all time is possible, the interval observer gain L can be constructed by a new design based on block roots of matrix polynomial and grey wolf optimizer.

8 Main results

The system presented in (4.22) is transformed into block observer form (3.7), after using the block observer form transformation T_o presented in (3.8) and (3.9), the new observer matrix take the following form:

$$A_{obs}(\theta) = (A_o(\theta) - LC_o(\theta)) = A_o(\theta) - \begin{pmatrix} L_1 \\ L_2 \\ \vdots \\ L_{l-1} \\ L_l \end{pmatrix} \begin{pmatrix} O_p & O_p & \cdots & O_p & I_p \end{pmatrix} \quad (4.29)$$

and,

$$(A_o(\theta) - LC_o(\theta)) = \begin{pmatrix} O_p & \cdots & O_p & -A_l(\theta) - L_1 \\ I_p & \cdots & O_p & -A_{l-1}(\theta) - L_2 \\ \vdots & \vdots & \vdots & \vdots \\ O_p & \cdots & O_p & -A_2(\theta) - L_{l-1} \\ O_p & \cdots & I_p & -A_1(\theta) - L_l \end{pmatrix} \quad (4.30)$$

Based on (4.30), the characteristic matrix polynomial of the designed system is:

$$P_d(z, \theta) = I_p z^l + (A_1(\theta) + L_l)z^{l-1} + \cdots + (A_{l-1}(\theta) + L_2)z + (A_l(\theta) + L_1) \quad (4.31)$$

Suppose that a set of l left block roots constructed from on a set of n constraints desired eigenvalues, are the solvents of the following desired matrix polynomial $D_d(z)$:

$$D_d(z) = I_p z^l + (Ad_1)z^{l-1} + \cdots + (Ad_{l-1})z + (Ad_l) \quad (4.32)$$

The design of the block roots is chosen diagonally as follows:

$$R_L(\mathbf{x}) = \left(\overbrace{\begin{pmatrix} \mathbf{x}_1 & 0 & 0 \\ 0 & \ddots & 0 \\ 0 & 0 & \mathbf{x}_p \end{pmatrix}}^{R_{L1}(\mathbf{x})}, \dots, \overbrace{\begin{pmatrix} \mathbf{x}_{n-p+1} & 0 & 0 \\ 0 & \ddots & 0 \\ 0 & 0 & \mathbf{x}_n \end{pmatrix}}^{R_{Ll}(\mathbf{x})} \right) \quad (4.33)$$

The left block vandermonde matrix corresponding to $\{R_{L1}(\mathbf{x}), R_{L2}(\mathbf{x}), \dots, R_{Ll}(\mathbf{x})\}$ is given as:

$$V_L(\mathbf{x})(R_{L1}(\mathbf{x}), R_{L2}(\mathbf{x}), \dots, R_{Ll}(\mathbf{x})) = \begin{pmatrix} I_p & R_{L1}(\mathbf{x}) & \cdots & R_{L1}(\mathbf{x})^{l-2} & R_{L1}(\mathbf{x})^{l-1} \\ I_p & R_{L2}(\mathbf{x}) & \cdots & R_{L2}(\mathbf{x})^{l-2} & R_{L2}(\mathbf{x})^{l-1} \\ \vdots & \vdots & \ddots & \vdots & \vdots \\ I_p & R_{Ll}(\mathbf{x}) & \cdots & R_{Ll}(\mathbf{x})^{l-2} & R_{Ll}(\mathbf{x})^{l-1} \end{pmatrix} \quad (4.34)$$

The matrix coefficients of the desired characteristic matrix polynomial $D_d(z)$ is expressed as:

$$D_d(\mathbf{x}) = V_L(\mathbf{x})^{-1} \begin{pmatrix} R_{L1}(\mathbf{x}) \\ R_{L2}(\mathbf{x}) \\ \vdots \\ R_{Ll}(\mathbf{x}) \end{pmatrix} \quad (4.35)$$

by put this equating, (4.31) = (4.35) $\Rightarrow P_d(z, \theta) = D_d(\mathbf{x})$, we get the observer matrix gain L :

$$L_o(\mathbf{x}, \theta) = \left[A_o(\theta)(: , \overline{(n-p+1):n}) - D_d(\mathbf{x}) \right] \quad (4.36)$$

9 Constrained nonlinear optimization

The grey wolf optimizer is a metaheuristics algorithm that solve a convex multidimensional optimization problems with constraints [25]. To finds the minimum of a problem specified by

$$\min_{\mathbf{x}} f(\mathbf{x}) \text{ such that } \begin{cases} \mathbf{c}(\mathbf{x}) \leq 0 \\ \mathbf{ceq}(\mathbf{x}) = 0 \\ \mathbf{A} \cdot \mathbf{x} \leq \mathbf{b} \\ \mathbf{Aeq} \cdot \mathbf{x} = \mathbf{beq} \\ lb \leq \mathbf{x} \leq ub \end{cases} \quad (4.37)$$

\mathbf{b} and \mathbf{beq} are vectors, \mathbf{A} and \mathbf{Aeq} are matrices, $\mathbf{c}(\mathbf{x})$ and $\mathbf{ceq}(\mathbf{x})$ are functions that return vectors, and $f(\mathbf{x})$ is a function that returns a scalar. $f(\mathbf{x})$, $\mathbf{c}(\mathbf{x})$, and $\mathbf{ceq}(\mathbf{x})$ can be nonlinear functions.

The obtained observer matrix gain $L_o(\mathbf{x}, \theta)$ is a nonlinear function, in order to find the observer matrix gain L which can solve the problem of the proposed interval observer presented in (4.26), therefore satisfying the conditions of the Theorem 4.1. In this regard, the observer gain function (4.36) is formulated as a convex minimization problem with constraints which can be solved by the well-known metaheuristics optimization algorithm Grey Wolf Optimizer [23], where the objective function $f(\mathbf{x})$ is chosen as follows:

$$f(\mathbf{x}, \theta) = \|L_o(\mathbf{x}, \theta)\|_\infty = \left\| \left[A_o(\theta) (:, \overline{(n-p+1):n}) - D_d(\mathbf{x}) \right] \right\|_\infty \quad (4.38)$$

Find \mathbf{x} which minimize the objective function $\min_{\mathbf{x}} \left\| \left[A_o(\theta) (:, \overline{(n-p+1):n}) - D_d(\mathbf{x}) \right] \right\|_\infty$ subject to certain set of constraints:

$$\begin{cases} |\lambda(A_o(\theta) - L_o(\mathbf{x}, \theta)C_o(\theta))| - \epsilon < 0, & \epsilon \in]0, 1[\\ (A_o(\theta) - L_o(\mathbf{x}, \theta)C_o(\theta)) \geq 0 \\ V_L V_L^{-1} - I_n = O_n \\ \underline{e} > 0 \ \& \ \bar{e} > 0 \\ lb \leq \mathbf{x} \leq ub, & \{lb, ub\} \in]-1, 1[-\{0\} \end{cases} \quad (4.39)$$

The inequality constraint condition has been chosen to adjust the bounded stability of the observer matrix $A_{obs}(\theta)$ (Schur stable), to ensure the conditions of the interval observer, the the positivity of the lower and the upper estimate errors signals, the positivity of the observer matrix $A_{obs}(\theta)$. The equality constraints have been chosen in order to ensure the validity of the block vandermonde matrix V_L , because the inverse of this block matrix cause problems occasionally (ill-conditioned matrix). The lower and the upper bound of the elements of vector $\mathbf{x} \in \mathbb{R}^n$ are chosen in which their values are kept within the unit circle.

10 The proposed algorithm steps

Summarizing all the important steps of the proposed interval observer

Algorithm 3 Robust interval observer algorithm

Step 1 Check the ratio $n/p = l$, which must be an integer.

Step 2 Check the rank of the block observability matrix of the nominal model Ω_o of (3.6), which must equal n (be full rank).

Step 3 Transforming the system (4.22) into block observable form, see (3.9).

Step 4 Define the uncertainties parameters level $\Delta\theta$ of the studied model (4.22).

Step 5 Define the bounded disturbance and measurement noise signals.

Step 6 Computing the observer matrix gain L as follows:

(a) Find the elements of the optimization vector which minimize the norm of the observer matrix gain L as in (4.38).

(b) Check the verification of the inequality condition of the nonnegativity in each iteration, see (3.39).

- (c) Check the equality constraints of the left block vandermonde matrix in each iteration, as in (3.39).
- (d) Set the values of the lower and the upper bound lb and ub respectively of the vector \mathbf{z}_k , and choose initial value to the vector \mathbf{z}_0 , see (3.39).

Step 7 When the stopping criterion is satisfied and the algorithm converge, the best optimization vector was selected.

Step 8 Finally, The observer matrix gain L is obtained based on (3.28).

11 Experimental application and results

The reduced dynamical model of the centrifugal gas compressor BCL 505 is chosen as good case of study, due to their hard pairing and interactions between their inputs-outputs. The studied model has two inputs $T1$: is aspiration temperature, $P1$: is aspiration pressure and two outputs $T2$: is discharge temperature and $P2$: is discharge pressure. The studied system (4.22) is represented by its reduced state space model. Where, the order of the model, $n = 4$, with two inputs $m = 2$ and two outputs $p = 2$, and its characteristic matrices A , B , and C , the model is transformed to block observer form based on (4.15) and (4.16), given as follows:

$$A_o = \begin{pmatrix} 0 & 0 & -0.0110 & 0.0274 \\ 0 & 0 & 0.0397 & 0.0555 \\ 1 & 0 & 0.0882 & 0.0946 \\ 0 & 1 & 0.1210 & 0.1447 \end{pmatrix}, B_o = \begin{pmatrix} 0.0488 & 0.0357 \\ 0.1353 & 0.0678 \\ 0.1213 & 0.1659 \\ 0.1665 & 0.2486 \end{pmatrix}, C_o = \begin{pmatrix} 0 & 0 & 1 & 0 \\ 0 & 0 & 0 & 1 \end{pmatrix}$$

The time-invariant uncertain parameters are bounded $[-100,+100]\%$ from the nominal values, by the following intervals:

$$\begin{aligned} -100\%A(\theta) &\leq \Delta A(\theta) \leq +100\%A(\theta) \\ -100\%B(\theta) &\leq \Delta B(\theta) \leq +100\%B(\theta) \\ -100\%C(\theta) &\leq \Delta C(\theta) \leq +100\%C(\theta) \end{aligned} \quad (4.40)$$

The measurement noise signal given as follow $v(k) = V \sin(k)$, is bounded where $\|v(k)\| \leq V = 0.1$.

The disturbance signal is a bounded nonlinear function coupled with system state is given as:

$$d(k) = [\sin(0.1k) \cos(0.2k) \sin(0.1k) \cos(0.2k)]^T + \delta [\sin(0.5k \cdot x(2)) \sin(0.3k) \sin(0.5kx(2)) \sin(0.3k)]^T$$

The lower disturbance signal

$$\underline{d}(k) = [\sin(0.1k) \cos(0.2k) \sin(0.1k) \cos(0.2k)]^T - \delta$$

The upper disturbance signal

$$\bar{d}(k) = [\sin(0.1k) \cos(0.2k) \sin(0.1k) \cos(0.2k)]^T + \delta$$

where, $\delta = 0.8$

After solving the optimization problem using the GWO optimizer, the following parameters of the optimizer are setting as :

The optimization vector $\mathbf{x} \in \mathbb{R}^{12}$, where the lower bound and the upper bound vectors are given as: $lb =$

$[-0.99\text{ones}(1,4) - 300\text{ones}(1,8)]$ and $ub = [0.99\text{ones}(1,4) 300\text{ones}(1,8)]$ respectively, the number of search agents is $SA_n = 20$, and after maximum number of iterations $Max = 500$ as shown in Figure. 4.21 and Figure. 4.22, respectively. all the constraints are not violated and the conditions mentioned in the Theorem 4.1 are satisfied.

The set of the desired left block roots $R_L = \{R_{L1}, R_{L2}\}$ are the solvents of the left matrix polynomial presented in (4.32), and they were constructed in the observer form from the optimal eigenvalues λ , given as:

$$R_{L1} = \begin{pmatrix} 0.0939 & 0.0472 \\ 0.2312 & 0.3409 \end{pmatrix}, \quad R_{L2} = \begin{pmatrix} -0.0332 & -0.0019 \\ -0.0610 & -0.1583 \end{pmatrix}$$

The left block vandermonde V_L given as:

$$V_L = \begin{pmatrix} 1 & 0 & 0.0939 & 0.0472 \\ 0 & 1 & 0.2312 & 0.3409 \\ 1 & 0 & -0.0332 & -0.0019 \\ 0 & 1 & -0.0610 & -0.1583 \end{pmatrix}$$

Finally, the matrix observer gain L is given as:

$$L = \begin{pmatrix} -0.0157 & 0.0233 \\ 0.0030 & 0.0013 \\ -0.0109 & -0.0082 \\ 0.0018 & 0.0017 \end{pmatrix} \quad (4.41)$$

The nominal observer matrix $A_{obs}(\theta)$ is given as:

$$A_{obs}(\theta) = \begin{pmatrix} 0 & 0 & 0.0047 & 0.0041 \\ 0 & 0 & 0.0367 & 0.0542 \\ 1 & 0 & 0.0991 & 0.1028 \\ 0 & 1 & 0.1192 & 0.1430 \end{pmatrix} \quad (4.42)$$

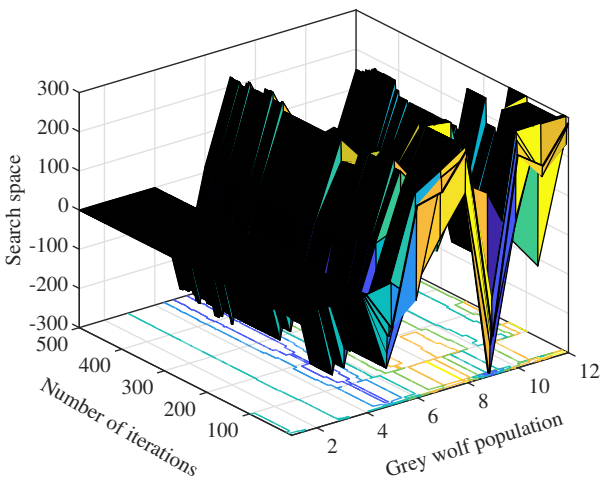


Figure 4.21: The evolution of the grey wolf population values during the tuning optimization process

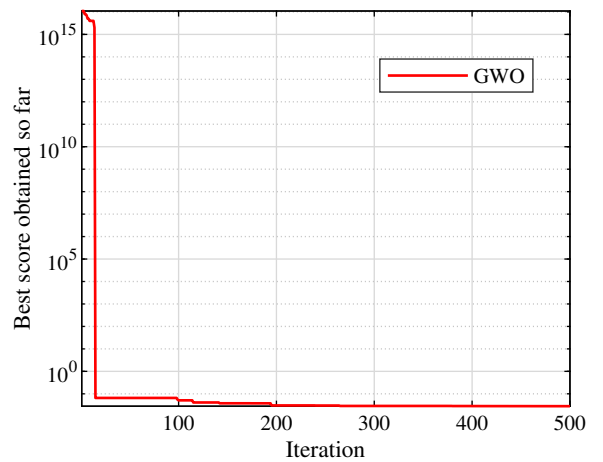


Figure 4.22: The change of objective function f in terms of GWO iteration

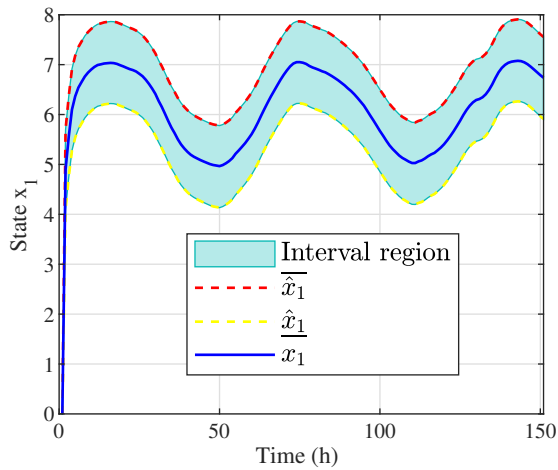


Figure 4.23: Interval estimation of state x_1

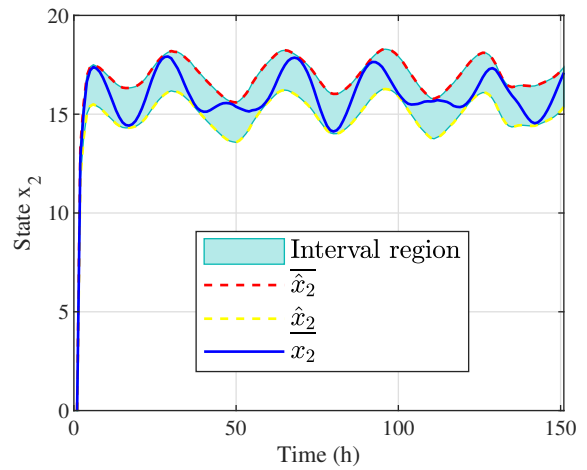


Figure 4.24: Interval estimation of state x_2

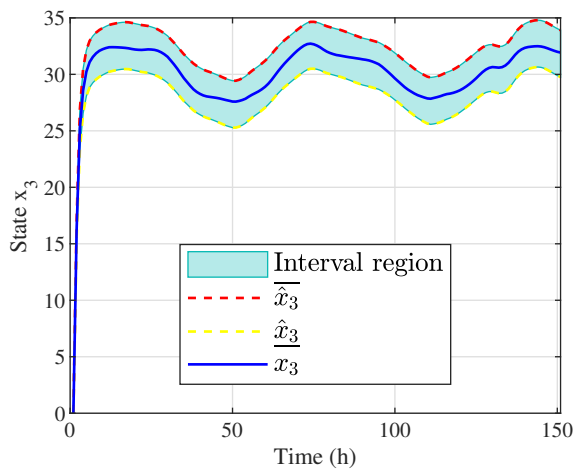


Figure 4.25: Interval estimation of state x_3

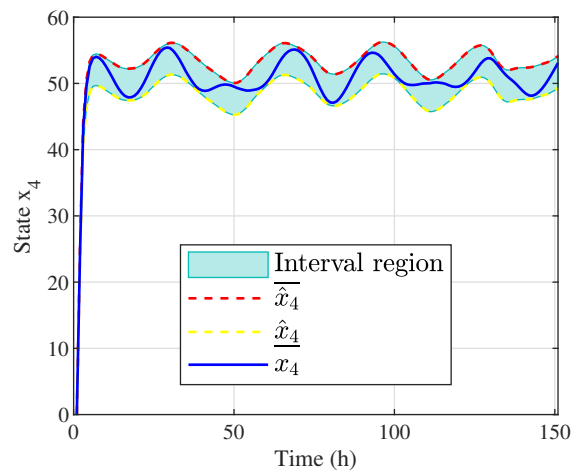


Figure 4.26: Interval estimation of state x_4

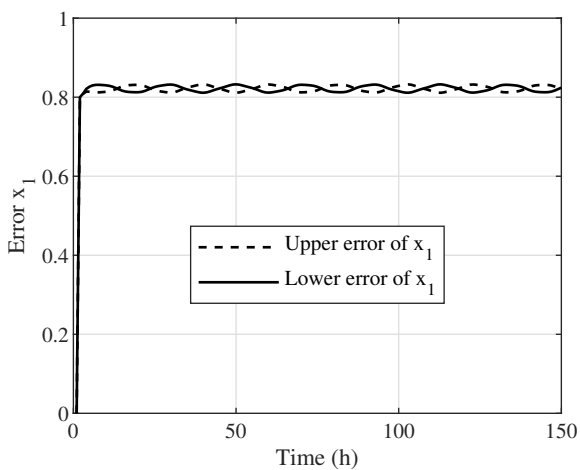


Figure 4.27: Interval error estimation of state x_1

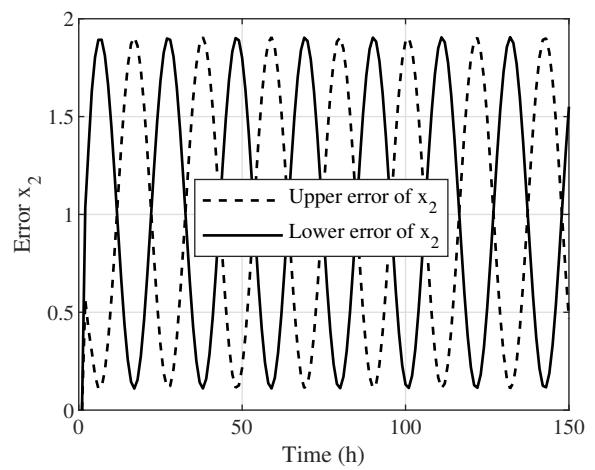


Figure 4.28: Interval error estimation of state x_2

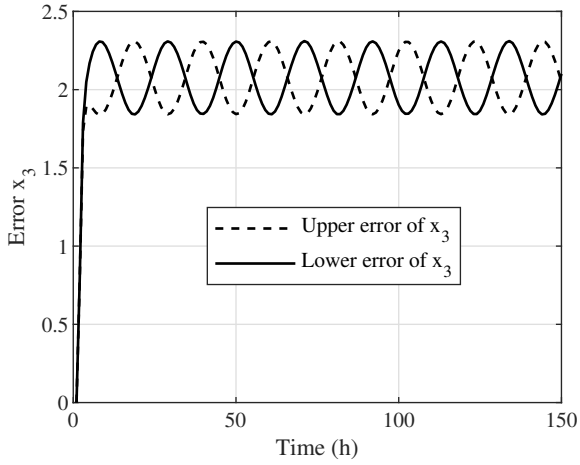


Figure 4.29: Interval error estimation of state x_3

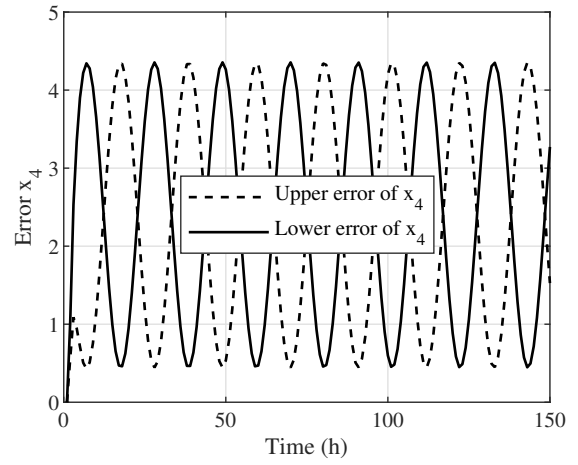


Figure 4.30: Interval error estimation of state x_4

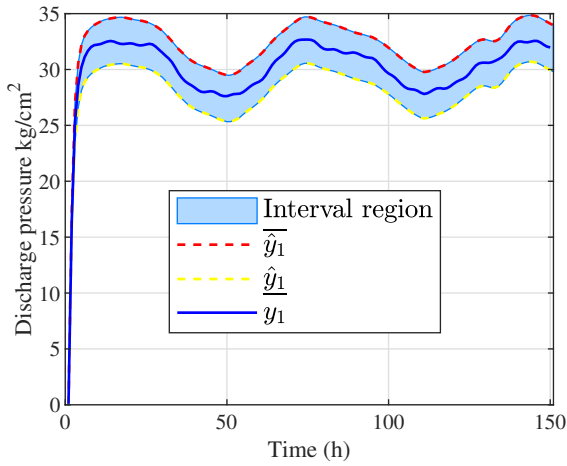


Figure 4.31: Forecasting time level danger of P_2

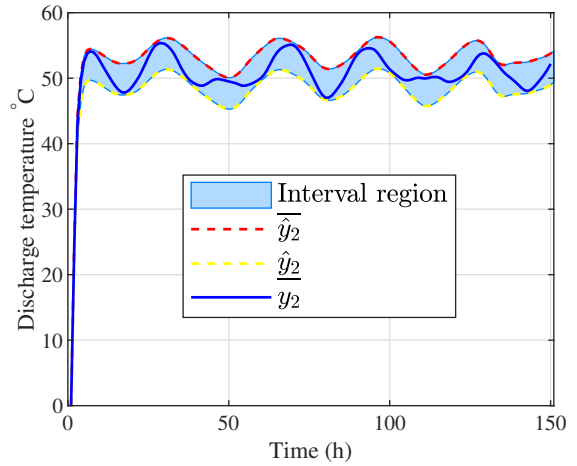


Figure 4.32: Interval estimation of output P_2

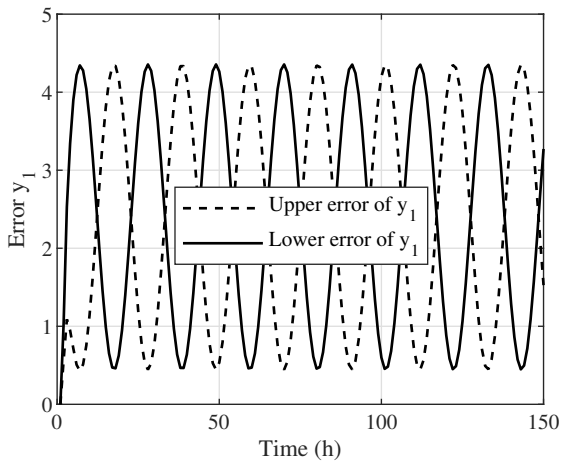


Figure 4.33: Interval error estimation of output P_2

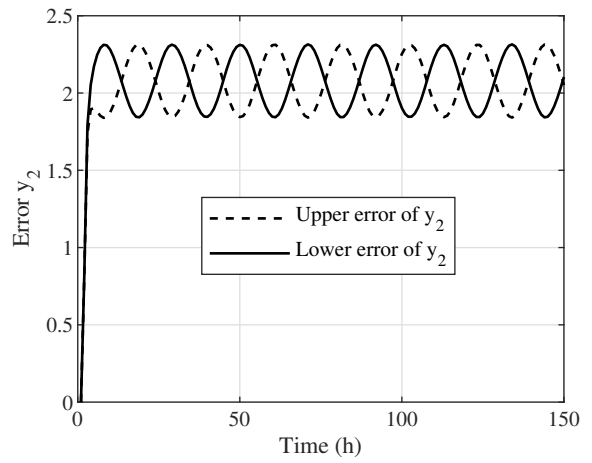


Figure 4.34: Interval error estimation of output T_2

Based on the obtained results, the effect of the proposed designed observer gain L is shown in the interval estimated states of the systems, where the estimated interval states upper and lower, respectively, making the systems states remaining and maintaining inside the estimated interval as shown in Figure. 4.23, Figure. 4.24, Figure. 4.25 and Figure. 4.26, in the presence of uncertainty, noise and disturbance signals, the positivity of the estimated states errors prove the effect of this observer gain, as shown in Figure. 4.27, Figure. 4.28, Figure. 4.29 and Figure. 4.30.

On the other hand, the estimated upper and lower outputs signals make the outputs signals maintain inside the estimated interval, as shown in Figure. 4.31 and Figure. 4.32, the estimated outputs errors prove the effect of this observer gain, as shown in Figure. 4.33 and Figure. 4.34.

Remark 3. In general to providing minimal interval width $\left(\underline{x}(k) \quad \bar{x}(k) \right)$ and $\left(\underline{y}(k) \quad \bar{y}(k) \right)$ a gain optimization problem can also be formulated to find a new L . In our example you can minimize the interval width by reducing the value of the constant δ until you reach an interval width is nearly to zero.

12 Interval observer-based fault detection

One of the most important applications of the interval observer is fault detection. The advantage of interval observer based fault detection is that it can generate an adaptive threshold used in residual evaluation [24]. Based on the design results of the proposed interval observer summarized in section 10, in this section a fault detection method based on interval observer is presented.

Consider the following Linear uncertain system

$$\begin{cases} x(k+1) = A(\theta)x(k) + B(\theta)u(k) + d(k) \\ y(k) = C(\theta)x(k) + v(k) + I_p f(k) \end{cases} \quad (4.43)$$

where $f(k) \in \mathbb{R}^p$ denotes the fault vector and $I_p \in \mathbb{R}^p$ is identity matrix.

we can only use the measurable output $y(k)$ for fault detection. Based on the proposed interval observer, we construct the following fault detection system:

$$\underline{\hat{y}}(k) \leq y(k) \leq \bar{\hat{y}}(k) \quad (4.44)$$

Obviously, $\underline{\hat{y}}(k)$ and $\bar{\hat{y}}(k)$ are the estimates of upper and lower boundaries of output signal $y(k)$ for system (4.40) in the fault-free case. Thus, we can set $\underline{\hat{y}}(k)$ and $\bar{\hat{y}}(k)$ as the dynamic thresholds for fault detection and present the following fault detection scheme:

$$\begin{cases} \underline{\hat{y}}(k) \leq y(k) \leq \bar{\hat{y}}(k) & \text{Fault-free} \\ y(k) < \underline{\hat{y}}(k) \text{ or } y(k) > \bar{\hat{y}}(k) & \text{Faulty} \end{cases} \quad (4.45)$$

After adding a real faults to the outputs signals, considered as a virtual faults sensors, where the following sensor fault is simulated:

$$f(k) = \begin{pmatrix} f_1(k) \\ f_2(k) \end{pmatrix} \quad (4.46)$$

where

$$f(k) = \begin{cases} 0 & 0h \leq k \leq 150 * \text{rand}(1)h \\ \text{Random} & 0h \leq k \leq 150h \end{cases} \quad (4.47)$$

The obtained results shown in Figure. 4.35 and Figure. 4.36, the detection of the faults represented by red stems is activated in case of occurrence fault, i.e if the outputs signals exceed to its estimated threshold generated by interval observer.

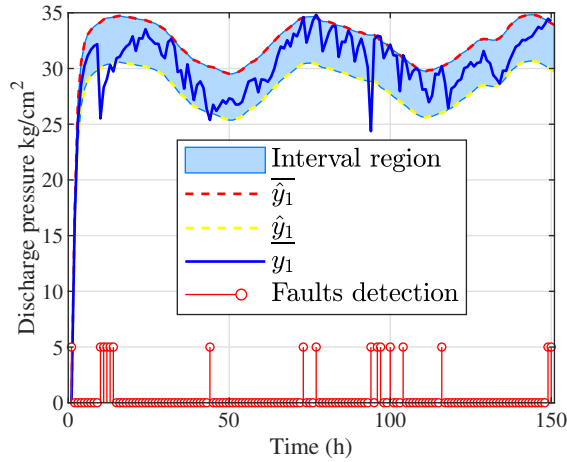


Figure 4.35: The adaptive interval threshold generated by interval observer of output $P2$ in presence of faults

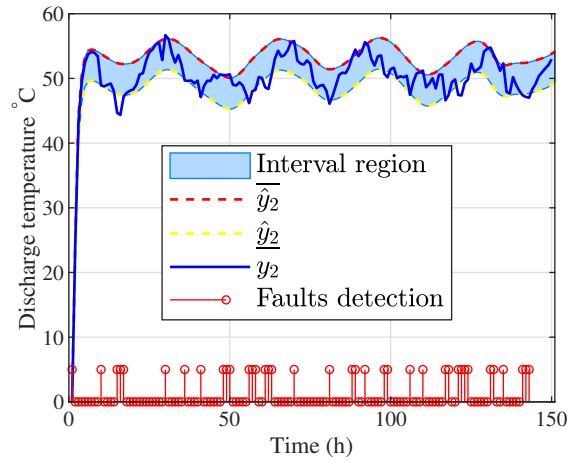


Figure 4.36: The adaptive interval threshold generated by interval observer of output $T2$ in presence of faults

interval observer gives reliable interval estimation in the fault-free case. After the fault occurrence, the interval observer-based fault detection method can timely detect the fault. The below Table 4.3 shows A comparative study performance between the two proposed Fault Detection (FD) approaches, Fuzzy approach and Interval observer approach. Concerning the time of the fault detection the interval observer is more faster due to its simple design compared with the fuzzy approach which its design contains many tasks (Filtering, Comparing with healthy model, and detecting based on expert system of Fuzzy-logic 2), the interval observer generate an flexible and adaptive threshold which make the detection more precise comparing with the fuzzy approach, the design of the interval observer take in consideration three sources of uncertainties: disturbance and noise signals and parameters model uncertainties which becomes more robust compared with the fuzzy approach.

Table 4.3: Comparative study and performance analysis

FD Approaches	Time of fault detection	Complexity design	Threshold	Robustness
Fuzzy-logic 2	Suitable	Complex	Constant	Sensitive
Interval observer	Excellent (Faster)	Simple	Adaptive	Robust

13 Conclusion

A robust faults diagnosis and detection approaches are proposed in this chapter and applied on the centrifugal gas compressor BCL 505 based on experimental data obtained on site from the measurement of the real time acquisition control system (ACS). The main purpose of the proposed approach is to improve the energy efficiency by improving the operating mode and the monitoring performance of the BCL 505 centrifugal gas compressor used in gas transportation station and studied in this chapter.

First part, the proposed faults diagnosis and detection approach is a combination of the two faults detection and isolation (FDI) approaches that are mainly based on the optimal identified healthy parametric equivalent

model, the Kalman observation system, and the intelligent expert fuzzy type-2 system. Whereas the Kalman filter is used to obtain the estimation of the output signals and to ensure the robustness against the eventual disturbances and noise contained in the measured output signals from the ACS. The output of the optimal identified parametric model and the estimated output based on real time inputs are used to generate the current residues on real time. In this chapter these residues are used through the expert system which was designed based on the type-2 fuzzy logic to ensure the faults diagnosis and detection in real time, this expert system achieves this main task with the help of the calculated and defined limits of the threshold defining the degree of the faults and its level of damage and risk on the studied centrifugal gas compressor BCL 505 system. Furthermore, the prediction of the remaining time before the failure of the studied machine is investigated based on the autoregressive integrated moving average (ARIMA) model, where the main aim is to avoid the an expected failure and to provide an accurate maintenance schedule. It can be concluded that the proposed approach of faults diagnosis and detection which has been applied on the centrifugal gas compressor BCL 505 possesses several advantages such as the decrease of the reparation time, avoiding the system from an expected operating risks and reducing the maintenance costs. These advantages affect positively the energy efficiency of the whole studied system and therefore increase the stability of the production, on the operation mode of the studied system and improves the overall studied system reliability and its robustness against the eventual faults.

Second part, the proposed interval observer is designed based on block roots of matrix polynomial and grey wolf optimizer, this observer is well used in fault detection and diagnosis approaches to their efficiency and simplicity design, the obtained results shown that the proposed observer play the same role of the design approach of the first part without need to more tasks, the interval observer makes us dispense with the use more tasks that is used in the approach presented in the first part, with a high efficiency in the presence of three sources of obstacles such as, noise, disturbance and parameters uncertainties.

Finally, it can be said that the proposed faults diagnosis and detection approaches investigated in this chapter is a promising approach which can be applied for different heavy industrial systems to improve their efficiency, especially in the area of petrol and oil industrial applications such as the gas turbine, the turbo-alternator, the turbo gas compressor...etc, where the main aim is to improve their dynamic behaviors, their operation mode, their reliability, their economics and their efficiency.

14 References

- [1] B. Nail, A. Kouzou, A. Hafaifa, A. Chaibet, Parametric identification and stabilization of turbo-compressor plant based on matrix fraction description using experimental data, *Journal of Engineering Science and Technology*, vol. 13, no. 6, pp. 1850-1868, Jun. 2018.
- [2] Bachir Nail, Abdellah Kouzou, Ahmed Hafaifa, Nadji Hadroug, and Vicenç Puig. A Robust fault diagnosis and forecasting approach based on Kalman filter and Interval Type-2 Fuzzy Logic for efficiency improvement of centrifugal gas compressor system. *Diagnostyka*, Vol. 20, no. 2, pp. 57-75, May. 2019.
- [3] M. B. Ozek and Z. H. Akpolat, A software tool: Type-2 fuzzy logic toolbox, *Computer Applications in Engineering Education*, vol. 16, no. 2, pp. 137-146, 2008.
- [4] M. Manceur, N. Essounbouli, and A. Hamzaoui, Second-Order Sliding Fuzzy Interval Type-2 Control for an Uncertain System With Real Application, *IEEE Transactions on Fuzzy Systems*, vol. 20, no. 2, pp. 262-275, Apr. 2012.

-
- [5] N. Hadroug, A. Hafaifa, A. Kouzou, Ahmed Chaibet, Faults detection in gas turbine using hybrid adaptive network based fuzzy inference systems, *DIAGNOSTYKA*, vol. 17, no. 4, pp. 3-17, 2016.
- [6] G. E. P. Box, G. M. Jenkins, G. C. Reinsel, G. M. Ljung, *Time Series Analysis: Forecasting and Control*, 5th Edition, Wiley Series in Probability and Statistics, Wiley, 2015.
- [7] T. Zhu, L. Luo, X. Zhang, Y. Shi, and W. Shen, Time-Series Approaches for Forecasting the Number of Hospital Daily Discharged Inpatients, *IEEE Journal of Biomedical and Health Informatics*, vol. 21, no. 2, pp. 515-526, Mar. 2017.
- [8] Bachir Nail, Abdellah Kouzou, Ahmed Hafaifa, Nadji Hadroug, and Vicenç Puig. A Robust fault diagnosis and forecasting approach based on Kalman filter and Interval Type-2 Fuzzy Logic for efficiency improvement of centrifugal gas compressor system. *Diagnostyka Journal*, Online first, April 2019.
- [9] D. Efimov and T. Raïssi, Design of interval observers for uncertain dynamical systems, *Automation and Remote Control*, vol. 77, no. 2, pp. 191-225, Feb. 2016.
- [10] D. Efimov, L. Fridman, T. Raïssi, A. Zolghadri, and R. Seydou, Interval estimation for LPV systems applying high order sliding mode techniques, *Automatica*, vol. 48, no. 9, pp. 2365-2371, Sep. 2012.
- [11] Farina, L. and Rinaldi, S., *Positive Linear Systems. Theory and Applications*, New York: Wiley, 2000.
- [12] Smith, H., *Monotone Dynamical Systems. An Introduction to the Theory of Competitive and Cooperative Systems*, in *Surveys and Monographs*, vol. 41, Providence: AMS, 1995.
- [13] Briat, C., Robust Stability Analysis of Uncertain Linear Positive Systems via Integral Linear Constraints: l_1 and l_∞ -gain Characterizations, *Proc. 50th IEEE CDC and ECC*, Orlando, 2011, pp. 6337-6342.
- [14] Ebihara, Y., Peaucelle, D., and Arzelier, D., L1 Gain Analysis of Linear Positive Systems and Its Application, *Proc. 50th IEEE CDC and ECC*, Orlando, 2011, pp. 4029-4035.
- [15] Khalil, H.K., *Nonlinear Systems*, Upper Saddle River: Prentice Hall, 2002, 3rd ed.
- [16] Hirsch, M.W. and Smith, H.L., Monotone Maps. A Review, *J. Differ. Equat. Appl.*, 2005, vol. 11, nos. 4-5, pp. 379-398.
- [17] D. Efimov, W. Perruquetti, T. Raïssi, and A. Zolghadri, "On interval observer design for time-invariant discrete-time systems," in *2013 European Control Conference (ECC)*, Zurich, 2013, pp. 2651-2656.
- [18] B. Nail, A. Kouzou, and A. Hafaifa, Robust block roots assignment in linear discrete-time sliding mode control for a class of multivariable system: gas turbine power plant application, *Transactions of the Institute of Measurement and Control*, p. 1-17, Jul. 2018.
- [19] B. Bekhiti, A. Dahimene, B. Nail, and K. Hariche, On λ -matrices and their applications in MIMO control systems design, *International Journal of Modelling, Identification and Control*, vol. 29, no. 4, p. 281-294, 2018.
- [20] B. Nail, A. Kouzou, A. Hafaifa, and B. Bekhiti, Parametric output feedback stabilization in MIMO systems: Application to gas turbine power plant, in *2016 8th International Conference on Modelling, Identification and Control (ICMIC)*, Algiers, Algeria, 2016, pp. 971-976.

- [21] M. Yaici, , K. Hariche, On eigenstructure assignment using block poles placement polynomials, *European Journal of Control*, vol. 20, no. 5, pp. 217-226, 2014,.
- [22] L. S. Shieh, Y. T. Tsay, and R. E. Yates, Block transformations of a class of multivariable control systems to four basic block companion forms, *Computers & Mathematics with Applications*, vol. 9, no. 6, pp. 703-714, 1983.
- [23] S. Mirjalili, S. M. Mirjalili, and A. Lewis, Grey Wolf Optimizer, *Advances in Engineering Software*, vol. 69, pp. 46-61, Mar. 2014.
- [24] L. Li, Z. Shao, R. Niu, G. Liu, and Z. Wang, A New Interval Observer Design Method with Application to Fault Detection, in *Positive Systems*, vol. 480, J. Lam, Y. Chen, X. Liu, X. Zhao, and J. Zhang, Eds. Cham: Springer International Publishing, 2019, pp. 233-243.
- [25] B. Nail, A. Kouzou, A. Hafaifa, and V. Puig, Optimal Static State-Feedback Controller Design for MIMO LTI Systems Based on Constraints Block Roots and Interior-Point Algorithm: Application to Gas Compressor System, in *2018 International Conference on Applied Smart Systems (ICASS)*, Medea, Algeria, 2018, pp. 1-6.

A robust fractional-order $PI^\lambda D^\mu$ controller design based on pseudo block-roots assignment

1 Introduction

Due to its simple structure and design, its simplicity of implementation and satisfactory control performance, the classical PID controller remains until now the most widely used regulator in the industrial systems and processes. However, with the complexity of the new industrial installations, the classical PID regulators become powerless and often give less effective results in some times. Therefore, it was incumbent on researchers find improvements more sophisticated and effective designs for the existed PID controllers, the use for example the optimization algorithms and the artificial intelligent techniques...etc, to select the optimal parameters which can improve the quality of the existed classical controllers, but this improvement remained insufficient because the classical design does not match its capabilities with the complexities of existing industrial systems, therefore. In this chapter, a robust multivariable fractional-order $PI^\lambda D^\mu$ controller is proposed, where its algebraic design is based on assignment of a set of optimal pseudo-block-roots of quasi matrix polynomial, where the proposed design is formulated as a convex optimization problem and has been solved using a grey wolf optimizer (GWO). A centrifugal gas compressor system is also considered in this chapter as case of application where the reduced model of this system is controlled under high level of parameters uncertainty conditions, the robustness of the proposed controller is also proved in passive fault-tolerant control (PFTC) configuration in presence of faults, under additive and multiplicative disturbances, respectively.

2 Preliminaries

2.1 Canonical Block Controller Form Transformation

In this subsection, we attempt to introduce the necessary fundamental of a matrix polynomials theory, that are used in the design of the proposed multivariable fractional-order $PI^\lambda D^\mu$ controller .

Let us consider the following multivariable LTI system described by a state space representation:

$$\begin{cases} \dot{x}(t) = Ax(t) + Bu(t) \\ y(t) = Cx(t) + Du(t) \end{cases} \quad (5.1)$$

where, $x \in \mathbb{R}^n$ is the state vector, $y \in \mathbb{R}^p$ and $u \in \mathbb{R}^m$ denote the output and the input vectors, respectively. $A \in \mathbb{R}^{n \times n}$, $B \in \mathbb{R}^{n \times m}$, $C \in \mathbb{R}^{p \times n}$ and $D \in \mathbb{R}^{p \times m}$ are the matrices of the system.

Corollary 5.1. *System (5.1) can be transformed to block controllable canonical form of index l if two conditions are satisfied [1–9]:*

1. *The ratio $l = n/m$ is integer.*

2. *The rank of block controllability matrix $\Omega_{bc} \triangleq \begin{pmatrix} B & AB & \cdots & A^{l-2}B & A^{l-1}B \end{pmatrix}$ is full, $\text{rank}(\Omega_{bc}) = n$.*

If the both conditions are satisfied, then the change of coordinates $x_c(t) = T_c x(t)$ transforms the system into the following Block controller form:

$$\begin{cases} \dot{x}_c(t) = A_c x_c(t) + B_c u(t) \\ y(t) = C_c x_c(t) + D_c u(t) \end{cases} \quad (5.2)$$

and,

$$A_c \triangleq T_c A T_c^{-1} = \begin{pmatrix} O_m & I_m & \cdots & O_m & O_m \\ O_m & O_m & \cdots & O_m & O_m \\ \vdots & \vdots & \cdots & \vdots & \vdots \\ O_m & O_m & \cdots & O_m & I_m \\ -A_l & -A_{l-1} & \cdots & -A_2 & -A_1 \end{pmatrix}, \quad B_c \triangleq T_c B = \begin{pmatrix} O_m & O_m & \cdots & O_m & I_m \end{pmatrix}^T \quad (5.3)$$

$$C_c \triangleq C T_c^{-1} = \begin{pmatrix} C_l & C_{l-1} & \cdots & C_2 & C_1 \end{pmatrix}, \quad D_c \triangleq D \quad (5.4)$$

where,

$$T_c \triangleq \begin{pmatrix} T_{c1} \\ T_{c1}A \\ \vdots \\ T_{c1}A^{l-2} \\ T_{c1}A^{l-1} \end{pmatrix}, \quad T_{c1} = \begin{pmatrix} O_m & O_m & \cdots & O_m & I_m \end{pmatrix} \begin{pmatrix} B & AB & \cdots & A^{l-2}B & A^{l-1}B \end{pmatrix}^{-1}$$

O_m stands for $m \times m$ zero matrix and I_m stands for $m \times m$ identity matrix.

2.2 Matrix Fraction Descriptions (MFDs)

The MFDs representations of linear multivariable systems are not unique. The system (5.1) can be presented into the left or the right MFD if the conditions presented in Corollary 5.1 are satisfied.

The right and the Left MFD of the system (5.1) is given as follows:

$$H(s) = N_R(s)D_R(s)^{-1} = D_L(s)^{-1}N_L(s) \quad (5.5)$$

The right numerator matrix polynomial $N_p(s)$ of system $H(s)$ is given as follow:

$$N_p(s) = N_{rl}s^l + N_{r(l-1)}s^{l-1} + \dots + N_{r(1)}s + N_{r0} = \sum_{i=l}^0 N_{ri}s^i, \quad N_{ri} \in \mathbb{R}^{p \times m}, \quad N_{rl} = D_c \quad (5.6)$$

The right denominator matrix polynomial $D_p(s)$ of system $H(s)$ is given as follow:

$$D_R(s) = D_{rl}s^l + D_{r(l-1)}s^{l-1} + \dots + D_{r(1)}s + D_{r0} = \sum_{i=l}^0 D_{ri}s^i, \quad D_{ri} \in \mathbb{R}^{m \times m}, \quad D_{rl} = I_{m \times m} \quad (5.7)$$

The matrices coefficients of matrices polynomials $N_R(s)$ and $D_R(s)$ are calculated based on block controllability matrices (5.3) and (5.4) as follows:

$$\begin{cases} D_{r0} = -A_l & N_{r0} = C_l + D_c D_{r0} \\ D_{r1} = -A_{l-1} & N_{r1} = C_{l-1} + D_c D_{r1} \\ \vdots & \vdots \\ D_{r(l-1)} = -A_1 & N_{r(l-1)} = C_{l-1} + D_c D_{r(l-1)} \\ D_{rl} = I & N_{rl} = D_c \end{cases} \quad (5.8)$$

2.3 Characteristics of matrix polynomials with integer order

Definition 5.1. Let we consider the following polynomial of complex variable s and matrix coefficients $\{A_0, A_1, \dots, A_l\}$:

$$A(s) = A_0s^l + A_1s^{l-1} + \dots + A_{l-2}s^2 + A_{l-1}s + A_l \quad (5.9)$$

(5.9) is called matrix polynomial of degree l and order m if their coefficients $coif = \{A_0, A_1, \dots, A_l\}$ are matrices of dimension $\in \mathbb{R}^{m \times m}$.

Definition 5.2. A real matrix $R \in \mathbb{R}^{m \times m}$ is called a right block root or right block solvent of matrix polynomial (5.9) such that:

$$\begin{aligned} R_r^l + A_1R_r^{l-1} + \dots + A_{l-1}R_r + A_l &= O_m \\ \Leftrightarrow A(R_r) &= \sum_{i=0}^l A_i R_r^{l-i} = O_m \end{aligned} \quad (5.10)$$

While a real matrix R is a left block root or left solvent such that:

$$\begin{aligned} L^l + L^{l-1}A_1 + \dots + LA_{l-1} + A_l &= O_m \\ \Leftrightarrow A_L(L) &= \sum_{i=0}^l L^{l-i}A_i = O_m \end{aligned} \quad (5.11)$$

2.4 Fundamentals of fractional-order calculus

Fractional order calculus of differentiation and integration is a more general to non-integer order calculus operator ${}_a \mathcal{D}_t^\alpha$, where α denotes the fractional order and belongs to \mathfrak{R} (any rational number), t and a denote the limits of the operation such that the differ-integral operator is represented as follow:

$${}_a \mathcal{D}_t^\alpha \triangleq \begin{cases} \frac{d^\alpha}{dt} & \mathfrak{R}(\alpha) > 0, \\ 1 & \mathfrak{R}(\alpha) = 0, \\ \int_a^t (d\tau)^{-\alpha} & \mathfrak{R}(\alpha) < 0, \end{cases} \quad (5.12)$$

Among the different definitions of fractional order derivative that exist in literatures, there are three most popular and usefull definitions are: Riemann-Liouville, Grunwald-Letnikov, and Caputo's definitions. In practical applications in engineering, the Caputo's definition is widely used [12, 13]. The Caputo's formulation of the fractional order derivative of order ν is given by:

$${}^C \mathcal{D}_t^\nu f(t) = \frac{1}{\Gamma(n-\nu)} \int_a^t \frac{f^{(n)}(\tau)}{(t-\tau)^{1-(n-\nu)}} d\tau \quad (5.13)$$

where ν ($n-1 < \nu < n \in \mathbb{N}$) is a positive non-integer number. $\Gamma(\nu)$ is the Euler's Gamma function. Also, a and t are respectively the lower and the upper terminals of the integral [12, 13].

The Laplace transform of the Caputo's fractional order derivative is given by

$$L \left\{ {}^C \mathcal{D}_t^\nu f(t) \right\} = s^\nu L \{ f(t) \} - \sum_{j=0}^{n-1} s^{\nu-1-j} f^{(j)}(0), \quad (5.14)$$

which for zero initial conditions is simplified to

$$L \left\{ {}^C \mathcal{D}_t^\nu f(t) \right\} = s^\nu L \{ f(t) \}. \quad (5.15)$$

3 Problem statement

The general fractional order $PI^\lambda D^\mu$ ($FO - PI^\lambda D^\mu$) controller is given by its left $C_l(s)$ and right $C_r(s)$ matrix fraction description formula as follows:

$$C_l(s) = (s^\lambda I_{m \times p})^{-1} (K_i + K_p s^\lambda I_{m \times p} + K_d s^{\lambda+\mu} I_{m \times p}) \quad (5.16)$$

and,

$$C_r(s) = (K_i + K_p s^\lambda I_{m \times p} + K_d s^{\lambda+\mu} I_{m \times p}) (s^\lambda I_{m \times p})^{-1} \quad (5.17)$$

The controller numerator $N_c(s)$ given as follow

$$N_c(s) = K_i + K_p s^\lambda I_{m \times p} + K_d s^{\lambda+\mu} I_{m \times p} \quad (5.18)$$

The controller denominator $D_c(s)$ given as follow

$$D_c(s) = s^\lambda I_{m \times p} \quad (5.19)$$

where, K_p is the proportional matrix gain $K_p \in \mathbb{R}^{m \times p}$, K_i is the integral matrix gain $K_i \in \mathbb{R}^{m \times p}$, K_d is the derivative matrix gain $K_d \in \mathbb{R}^{m \times p}$, λ is the integration fractional order $\lambda > 0$, and μ is the differentiation fractional order $\mu > 0$.

$$C(s) = \begin{pmatrix} \frac{\mathbf{K}_{d(1,1)} s^{\lambda+\mu} + \mathbf{K}_{p(1,1)} s^\lambda + \mathbf{K}_{i(1,1)}}{s^\lambda} & \frac{\mathbf{K}_{d(1,2)} s^{\lambda+\mu} + \mathbf{K}_{p(1,2)} s^\lambda + \mathbf{K}_{i(1,2)}}{s^\lambda} & \dots & \frac{\mathbf{K}_{d(1,p)} s^{\lambda+\mu} + \mathbf{K}_{p(1,p)} s^\lambda + \mathbf{K}_{i(1,p)}}{s^\lambda} \\ \frac{\mathbf{K}_{d(2,1)} s^{\lambda+\mu} + \mathbf{K}_{p(2,1)} s^\lambda + \mathbf{K}_{i(2,1)}}{s^\lambda} & \ddots & \ddots & \frac{\mathbf{K}_{d(2,p)} s^{\lambda+\mu} + \mathbf{K}_{p(2,p)} s^\lambda + \mathbf{K}_{i(2,p)}}{s^\lambda} \\ \vdots & \ddots & \ddots & \vdots \\ \frac{\mathbf{K}_{d(m,1)} s^{\lambda+\mu} + \mathbf{K}_{p(m,1)} s^\lambda + \mathbf{K}_{i(m,1)}}{s^\lambda} & \frac{\mathbf{K}_{d(m,2)} s^{\lambda+\mu} + \mathbf{K}_{p(m,2)} s^\lambda + \mathbf{K}_{i(m,2)}}{s^\lambda} & \dots & \frac{\mathbf{K}_{d(m,p)} s^{\lambda+\mu} + \mathbf{K}_{p(m,p)} s^\lambda + \mathbf{K}_{i(m,p)}}{s^\lambda} \end{pmatrix} \quad (5.20)$$

Remark 1. The system model have been transformed to the right matrix fraction description form RMFD instead the left form, because the right form is more appropriate in the controllers designs. The opposite of, the left matrix fraction description LMFD is more appropriate in the observers and estimators designs [8–10].

The control signal $u(s)$ is given as follow:

$$u(s) = C(s)e(s) \tag{5.21}$$

The error signal $e(t)$ is given as follow:

$$e(t) = r(t) - y(t) \tag{5.22}$$

where, $r(t)$ is the set-point signal, $e(t)$ and $r(t) \in \mathbb{R}^p$.

The closed loop control system shown in the Figure. 5.1 is described by a multivariable fractional-order transfer function and is given as follow:

$$H(s) = (C(s)G(s))(I + C(s)G(s))^{-1} \tag{5.23}$$

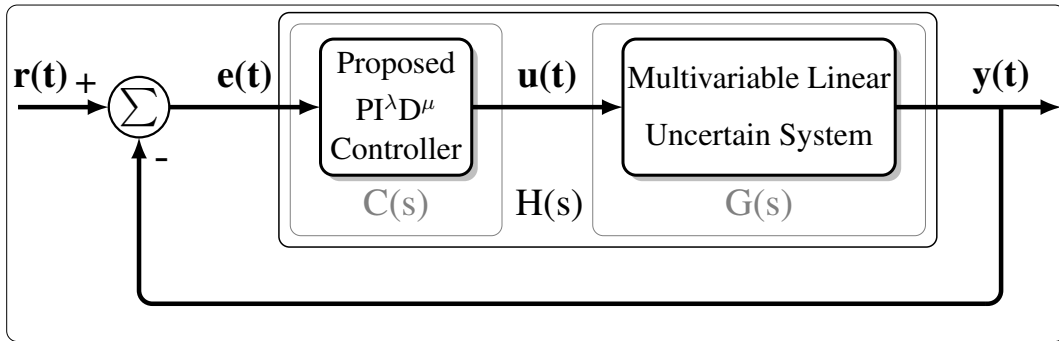


Figure 5.1: Closed loop system of the system $G(s)$ and the controller $C(s)$.

The objective is to determine the matrices gains of the fractional-order controller K_p , K_i and K_d respectively and its fractional parameters λ and μ . Such that, the proposed design algorithm should guaranteed the following specifications in the CLS:

- Ensured the closed-loop stability
- Best disturbance rejection (without need a excessive control action)
- Fast and good set-point tracking (without need a excessive control action)
- A satisfactory degree of robustness to system parameters variations, uncertainty and unmodeled dynamics
- Low sensitivity to the noise
- Minimum gain of control signal energy

To achieve all of the above requirements, the required is to exploit the specifications and the advantage of the block roots of matrix polynomial and extend their application to the matrix polynomial of the fractional order powers.

By convention and from the existed knowledge in literatures, new terminologies are extended from the monovaryable fractional-order to the multivariable fractional-order and suggested to use in this chapter

Multivariable Integer Order	Monovaryable Fractional Order	Multivariable Fractional Order
Block Roots	Pseudo Roots	Pseudo Block Roots
Matrix Polynomial	Quasi Polynomial	Quasi Matrix Polynomial
Block Vandermonde Matrix	–	Pseudo Block Vandermonde Matrix
Diophantine Matrix Equation	Quasi Diophantine Equation	Quasi Diophantine Matrix Equation
Generalized Sylvester Matrix Equation	–	Quasi Generalized Sylvester Matrix Equation

4 Main results

The system $G(s)$ is given in the right matrix fraction description representation as follows:

$$G(s) = N_R(s)D_R(s)^{-1} \quad (5.24)$$

The controller $C(s)$ is given in the left matrix fraction description representation as follows:

$$C_l(s) = D_c(s)^{-1}N_c(s) \quad (5.25)$$

Remark 2. When we choose the right fraction description for the plant it is advisable to choose the left fraction description for the controller design, Thomas Kailath [10].

The closed loop system $H_{cls}(s)$ is obtained based on equation (5.24) and (5.25) as follows:

$$H_{cls}(s) = (N_R(s)D_R(s)^{-1}D_c(s)^{-1}N_c(s))(N_R(s)D_R(s)^{-1}D_c(s)^{-1}N_c(s) + I)^{-1} \quad (5.26)$$

Multiplying the left and the right sides of (5.26) by $N_R(s)^{-1}$ and $N_c(s)^{-1}$ respectively, we obtain

$$H_{cls}(s) = (D_R(s)^{-1}D_c(s)^{-1})(D_R(s)^{-1}D_c(s)^{-1} + N_R(s)^{-1}N_c(s)^{-1})^{-1} \quad (5.27)$$

Multiplying the left and the right sides of (5.27) by $D_R(s)D_c(s)$ and $N_R(s)N_c(s)$ respectively, we obtain

$$H_{cls}(s) = N_R(s)N_c(s)(D_R(s)D_c(s) + N_R(s)N_c(s))^{-1} \quad (5.28)$$

Multiplying the left and the right sides of (5.28) by $N_R(s)^{-1}$ and $N_c(s)^{-1}$ respectively, we obtain

$$H_{cls}(s) = (N_R(s)^{-1}(D_R(s)D_c(s) + N_R(s)N_c(s))N_c(s)^{-1})^{-1} \quad (5.29)$$

Hence, the close loop controller-system take this form

$$H_{cls}(s) = N_R(s) \left(\underbrace{D_R(s)D_c(s) + N_R(s)N_c(s)}_{D_{cls}(s)} \right)^{-1} N_c(s) \quad (5.30)$$

The closed loop controller-system $H_{cls}(s)$ is a multivariable fractional-order transfer function, where it contains the specific information about the controller-system. The objective now is to determine the matrices gain of the proposed $FO - PI^\lambda D^\mu$ controller K_p , K_i , K_d and the fractional-order parameters λ and μ respectively, such away that the CLS stability is guaranteed and the tracking signal error is approaches to zero with minimum gain control signal energy.

The denominator $D_{cls}(s)$ of the closed-loop control-system $H_{cls}(s)$ is a quasi **Diophantine** matrix equation form, let us transform it from the matrix transfer function to the block matrix form, by the expansion of the matrices elements of $D_{cls}(s)$ and aggregate all the matrices which have the same fractional-orders, after the mathematical manipulations a quasi generalized **Sylvester** matrix equation \mathcal{S} is obtained where it contains the matrices coefficients of the numerator $N_p(s)$ and the free matrix \mathcal{D} contains the matrices coefficients of the denominator $D_p(s)$, in order to determine the block **Sylvester** \mathcal{S} and \mathcal{D} matrices respectively, a problem of fractional orders values of integration λ and derivation μ respectively is posed, for which one is greater then the other?.

The outputs of the $FO - PI^\lambda D^\mu$ controller severely fluctuates when the sampling time T_s is very small, and this can reduce the life-time of some actuators like the valves, due to hight sensitivity of the derivative action

to the noise. Therefore, it is not recommended to use the derivative action in the slow processes, if the process is sufficiently damped (i.e., large time-constant), because it can amplify the large frequency noise. For these objective reasons we have assumed in this design that the order value λ of the integral action I^λ is always greater than to the order value μ of the derivative action D^μ , meaning that the proposed $FO-PI^\lambda D^\mu$ is closer to the $FO-PI^\lambda$ controller from than to the $FO-PD^\mu$ controller.

The quasi **Diophantine** matrix equation $D_{cls}(s)$ can transformed to the block matrix form as follows:

$$D_{cls}(s) \equiv SK + D \quad (5.31)$$

The denominator $D_{cls}(s)$ presented in equation (5.31) of the closed loop controller-system is enforced to match the desired proposed quasi matrix polynomial $\mathcal{X}(s)$, where this quasi matrix polynomial is achieves some important specifications such as the stability in the sense of the fractional order dynamics i.e theirs pseudo-eigenvalues are stable and it has the same fractional order than the $D_{cls}(s)$, (i.e: order = $l + \lambda + \mu$).

(5.31) can takes three distinguished forms and their desired $\mathcal{X}(s)$ quasi matrix polynomial, and this according to the intervals of which the fractional-orders λ and μ belongs to:

4.1 Case 1

If $\lambda \in]0 \ 1[$ and $\mu \in]0 \ 1[$ with $(\lambda + \mu) < 1$, the equation (5.31) take the following form:

$$\begin{array}{c} \overbrace{\left(\begin{array}{c} D^{l+\lambda+\mu} \\ \hline D^{l+\lambda} \\ \hline D^l \\ \hline D^{l+\lambda+\mu-1} \\ \hline D^{l+\lambda-1} \\ \hline D^{l-1} \\ \hline \vdots \\ \hline D^{\lambda+\mu+1} \\ \hline D^{\lambda+1} \\ \hline D^1 \\ \hline D^{\lambda+\mu} \\ \hline D^\lambda \\ \hline D^0 \end{array} \right)}^{D_{cls}} = \begin{array}{c} \overbrace{\left(\begin{array}{c} s^{l+\lambda+\mu} \\ \hline s^{l+\lambda} \\ \hline s^l \\ \hline s^{l+\lambda+\mu-1} \\ \hline s^{l+\lambda-1} \\ \hline s^{l-1} \\ \hline \vdots \\ \hline s^{\lambda+\mu+1} \\ \hline s^{\lambda+1} \\ \hline s^1 \\ \hline s^{\lambda+\mu} \\ \hline s^\lambda \\ \hline s^0 \end{array} \right)}^S \begin{array}{c} \left(\begin{array}{ccc} N_{rl} & O_m & O_m \\ O_m & N_{rl} & O_m \\ O_m & O_m & N_{rl} \\ \hline N_{r(l-1)} & O_m & O_m \\ O_m & N_{r(l-1)} & O_m \\ O_m & O_m & N_{r(l-1)} \\ \hline \vdots & \vdots & \vdots \\ \hline N_{r1} & O_m & O_m \\ O_m & N_{r1} & O_m \\ O_m & O_m & N_{r1} \\ \hline N_{r0} & O_m & O_m \\ O_m & N_{r0} & O_m \\ O_m & O_m & N_{r0} \end{array} \right) \end{array} \begin{array}{c} \left(\begin{array}{c} K_d \\ K_p \\ K_i \end{array} \right) \end{array} + \begin{array}{c} \overbrace{\left(\begin{array}{c} s^{l+\lambda+\mu} \\ \hline s^{l+\lambda} \\ \hline s^l \\ \hline s^{l+\lambda+\mu-1} \\ \hline s^{l+\lambda-1} \\ \hline s^{l-1} \\ \hline \vdots \\ \hline s^{\lambda+\mu+1} \\ \hline s^{\lambda+1} \\ \hline s^1 \\ \hline s^{\lambda+\mu} \\ \hline s^\lambda \\ \hline s^0 \end{array} \right)}^D \begin{array}{c} \left(\begin{array}{c} O_m \\ D_{rl} \\ O_m \\ \hline O_m \\ D_{r(l-1)} \\ O_m \\ \hline \vdots \\ \hline O_m \\ D_{r1} \\ O_m \\ \hline O_m \\ D_{r0} \\ O_m \end{array} \right) \end{array} \end{array} \quad (5.32)$$

4.2 Case 2

If $\lambda \in]0, 1[$ and $\mu \in]0, 1[$ with $(\lambda + \mu) \in]1, 2[$, the equation (1.31) take the following form:

$$D_{cls}(s) = \begin{array}{c} \overline{\overline{\begin{array}{c} s^{l+\lambda+\mu} \\ \hline s^{l+\lambda} \\ \hline s^{l+\lambda+\mu-1} \\ \hline s^l \\ \hline s^{l+\lambda-1} \\ \hline s^{l+\lambda+\mu-2} \\ \hline s^{l-1} \\ \hline s^{l+\lambda-2} \\ \hline \vdots \\ \hline s^{\lambda+\mu} \\ \hline s^1 \\ \hline s^\lambda \\ \hline s^{\lambda+\mu-1} \\ \hline s^0 \end{array}}} \\ \vdots \\ \overline{\overline{\begin{array}{c} s^{\lambda+\mu} \\ \hline s^1 \\ \hline s^\lambda \\ \hline s^{\lambda+\mu-1} \\ \hline s^0 \end{array}}} \end{array} \begin{array}{c} \overbrace{\begin{array}{ccc} O_m & O_m & N_{rl} \\ N_{rl} & O_m & O_m \\ O_m & O_m & N_{r(l-1)} \\ O_m & N_{r(l)} & O_m \\ N_{r(l-1)} & O_m & O_m \\ O_m & O_m & N_{r(l-2)} \\ O_m & N_{r(l-1)} & O_m \\ N_{r(l-2)} & O_m & O_m \\ \vdots & \vdots & \vdots \\ O_m & O_m & N_{r0} \\ O_m & N_{r1} & O_m \\ N_{r0} & O_m & O_m \\ O_m & O_m & O_m \\ O_m & N_{r0} & O_m \end{array}}^S \\ \vdots \\ \overbrace{\begin{array}{ccc} O_m & O_m & N_{r0} \\ O_m & N_{r1} & O_m \\ N_{r0} & O_m & O_m \\ O_m & O_m & O_m \\ O_m & N_{r0} & O_m \end{array}}^S \end{array} \begin{array}{c} \overbrace{\begin{array}{c} O_m \\ D_{rl} \\ O_m \\ O_m \\ D_{r(l-1)} \\ O_m \\ O_m \\ D_{r(l-2)} \\ \vdots \\ O_m \\ O_m \\ D_{r(l-2)} \\ \vdots \\ O_m \\ O_m \\ D_{r0} \\ O_m \\ O_m \end{array}}^D \\ \vdots \\ \overbrace{\begin{array}{c} O_m \\ D_{rl} \\ O_m \\ O_m \\ D_{r(l-1)} \\ O_m \\ O_m \\ D_{r(l-2)} \\ \vdots \\ O_m \\ O_m \\ D_{r0} \\ O_m \\ O_m \end{array}}^D \end{array} \begin{array}{c} \overbrace{\begin{array}{c} K_p \\ K_i \\ K_d \end{array}}^{\mathcal{K}} \\ + \end{array} \quad (5.37)$$

The corresponding desired Quasi matrix polynomial of fractional order $\mathcal{X}(s)$ take this form:

$$\mathcal{X}(s) = I_m s^{l+\lambda+\mu} + \mathcal{X}_{3l+1} s^{l+\lambda} + \mathcal{X}_{3l} s^{l+\lambda+\mu-1} + \mathcal{X}_{3l-1} s^l + \mathcal{X}_{3l-2} s^{l+\lambda-1} + \dots + \mathcal{X}_1 s^{\lambda+\mu-1} + \mathcal{X}_0 \quad (5.38)$$

where, $\mathcal{X}_{3l+2} = I_m$

If we consider that the set of the desired pseudo-block-roots $\{R_1, R_2, \dots, R_{3l+2}, R_{3l+2}\}$ are the solvents of the quasi matrix polynomial $\mathcal{X}(s)$ presented in (5.38), and which can be satisfy this equalities as follows:

$$\left\{ \begin{array}{l} R_{3l+2}^{l+\lambda+\mu} + \mathcal{X}_{3l+1} R_{3l+2}^{l+\lambda} + \mathcal{X}_{3l} R_{3l+2}^{l+\lambda+\mu-1} + \mathcal{X}_{3l-1} R_{3l+2}^l + \mathcal{X}_{3l-2} R_{3l+2}^{l+\lambda-1} + \dots + \mathcal{X}_1 R_{3l+2}^{\lambda+\mu-1} + \mathcal{X}_0 = O_m \\ R_{3l+1}^{l+\lambda+\mu} + \mathcal{X}_{3l+1} R_{3l+1}^{l+\lambda} + \mathcal{X}_{3l} R_{3l+1}^{l+\lambda+\mu-1} + \mathcal{X}_{3l-1} R_{3l+1}^l + \mathcal{X}_{3l-2} R_{3l+1}^{l+\lambda-1} + \dots + \mathcal{X}_1 R_{3l+1}^{\lambda+\mu-1} + \mathcal{X}_0 = O_m \\ \vdots \\ R_2^{l+\lambda+\mu} + \mathcal{X}_{3l+1} R_2^{l+\lambda} + \mathcal{X}_{3l} R_2^{l+\lambda+\mu-1} + \mathcal{X}_{3l-1} R_2^l + \mathcal{X}_{3l-2} R_2^{l+\lambda-1} + \dots + \mathcal{X}_1 R_2^{\lambda+\mu-1} + \mathcal{X}_0 = O_m \\ R_1^{l+\lambda+\mu} + \mathcal{X}_{3l+1} R_1^{l+\lambda} + \mathcal{X}_{3l} R_1^{l+\lambda+\mu-1} + \mathcal{X}_{3l-1} R_1^l + \mathcal{X}_{3l-2} R_1^{l+\lambda-1} + \dots + \mathcal{X}_1 R_1^{\lambda+\mu-1} + \mathcal{X}_0 = O_m \end{array} \right. \quad (5.39)$$

After some mathematical manipulations we get:

$$\mathcal{X} = \overbrace{\begin{pmatrix} I & I & \dots & I & I \\ R_1^{\lambda+\mu-1} & R_2^{\lambda+\mu-1} & \dots & R_{3l+1}^{\lambda+\mu-1} & R_{3l+2}^{\lambda+\mu-1} \\ R_1^\lambda & R_2^\lambda & \dots & R_{3l+1}^\lambda & R_{3l+2}^\lambda \\ \vdots & \vdots & \ddots & \vdots & \vdots \\ R_1^{l+\lambda+\mu-1} & R_2^{l+\lambda+\mu-1} & \dots & R_{3l+1}^{l+\lambda+\mu-1} & R_{3l+2}^{l+\lambda+\mu-1} \\ R_1^{l+\lambda} & R_2^{l+\lambda} & \dots & R_{3l+1}^{l+\lambda} & R_{3l+2}^{l+\lambda} \end{pmatrix}}^{V_r} = - \begin{pmatrix} R_1^{l+\lambda+\mu} & R_2^{l+\lambda+\mu} & \dots & R_{3l+1}^{l+\lambda+\mu} & R_{3l+2}^{l+\lambda+\mu} \end{pmatrix} \quad (5.40)$$

where, V_r is the right Pseudo Block Vandermonde matrix

Hence, the matrices coefficients of the desired Quasi matrix polynomial $\mathcal{X}(s)$ are obtained as follows:

$$\mathcal{X} = - \left[\begin{pmatrix} R_1^{l+\lambda+\mu} & R_2^{l+\lambda+\mu} & \dots & R_{3l+1}^{l+\lambda+\mu} & R_{3l+2}^{l+\lambda+\mu} \end{pmatrix} V_r^{-1} \right]^T \quad (5.41)$$

4.3 Case 3

If $1 < \lambda < 2$ and $0 < \mu < 1$ with $(\lambda + \mu) < 2$ If $\lambda \in]1 \ 2[$ and $\mu \in]0 \ 1[$ with $(\lambda + \mu) \in]1 \ 2[$, the equation (1.31) take the following form:

$$D_{cls}(s) = \overbrace{\begin{pmatrix} N_{rl} & O_m & O_m \\ O_m & N_{rl} & O_m \\ N_{r(l-1)} & O_m & O_m \\ O_m & N_{r(l-1)} & O_m \\ O_m & O_m & N_{rl} \\ N_{r(l-2)} & O_m & O_m \\ O_m & N_{r(l-2)} & O_m \\ O_m & O_m & N_{r(l-1)} \\ \vdots & \vdots & \vdots \\ N_{r0} & O_m & O_m \\ O_m & N_{r0} & O_m \\ O_m & O_m & N_{rl} \\ O_m & O_m & O_m \\ O_m & O_m & O_m \\ O_m & O_m & N_{r0} \end{pmatrix}}^S + \begin{pmatrix} K_d \\ K_p \\ K_i \end{pmatrix} + \overbrace{\begin{pmatrix} O_m \\ D_{rl} \\ O_m \\ D_{r(l-1)} \\ O_m \\ O_m \\ D_{r(l-2)} \\ O_m \\ \vdots \\ O_m \\ D_{r0} \\ O_m \\ O_m \\ O_m \\ O_m \end{pmatrix}}^D \quad (5.42)$$

The corresponding desired Quasi matrix polynomial of fractional order $\mathcal{X}(s)$ take this form:

$$\mathcal{X}(s) = I_m s^{l+\lambda+\mu} + \mathcal{X}_{3l+3} s^{l+\lambda} + \mathcal{X}_{3l+2} s^{l+\lambda+\mu-1} + \mathcal{X}_{3l+1} s^{l+\lambda-1} + \mathcal{X}_{3l} s^l + \dots + \mathcal{X}_2 s^{\lambda+\mu-1} + \mathcal{X}_1 s^{\lambda-1} + \mathcal{X}_0 \quad (5.43)$$

where, $\mathcal{X}_{3l+4} = I_m$

If we consider that the set of the desired pseudo-block-roots $\{R_1, R_2, \dots, R_{3l+3}, R_{3l+4}\}$ are the solvents of the quasi matrix polynomial $\mathcal{X}(s)$ presented in (5.43), and which can be satisfy this equalities as follows:

$$\begin{cases} R_{3l+4}^{l+\lambda+\mu} + \mathcal{X}_{3l+3}R_{3l+4}^{l+\lambda} + \mathcal{X}_{3l+2}R_{3l+4}^{l+\lambda+\mu-1} + \mathcal{X}_{3l+1}R_{3l+4}^{l+\lambda-1} + \mathcal{X}_{3l}R_{3l+4}^l + \dots + \mathcal{X}_2R_{3l+4}^{\lambda+\mu-1} + \mathcal{X}_1R_{3l+4}^{\lambda-1} + \mathcal{X}_0 = O_m \\ R_{3l+3}^{l+\lambda+\mu} + \mathcal{X}_{3l+3}R_{3l+3}^{l+\lambda} + \mathcal{X}_{3l+2}R_{3l+3}^{l+\lambda+\mu-1} + \mathcal{X}_{3l+1}R_{3l+3}^{l+\lambda-1} + \mathcal{X}_{3l}R_{3l+3}^l + \dots + \mathcal{X}_2R_{3l+3}^{\lambda+\mu-1} + \mathcal{X}_1R_{3l+3}^{\lambda-1} + \mathcal{X}_0 = O_m \\ \vdots \\ R_2^{l+\lambda+\mu} + \mathcal{X}_{3l+3}R_2^{l+\lambda} + \mathcal{X}_{3l+2}R_2^{l+\lambda+\mu-1} + \mathcal{X}_{3l+1}R_2^{l+\lambda-1} + \mathcal{X}_{3l}R_2^l + \dots + \mathcal{X}_2R_2^{\lambda+\mu-1} + \mathcal{X}_1R_2^{\lambda-1} + \mathcal{X}_0 = O_m \\ R_1^{l+\lambda+\mu} + \mathcal{X}_{3l+3}R_1^{l+\lambda} + \mathcal{X}_{3l+2}R_1^{l+\lambda+\mu-1} + \mathcal{X}_{3l+1}R_1^{l+\lambda-1} + \mathcal{X}_{3l}R_1^l + \dots + \mathcal{X}_2R_1^{\lambda+\mu-1} + \mathcal{X}_1R_1^{\lambda-1} + \mathcal{X}_0 = O_m \end{cases} \quad (5.44)$$

After some mathematical manipulations we get:

$$\mathcal{X} \begin{pmatrix} \overbrace{I \quad I \quad \dots \quad I \quad I}^{V_r} \\ R_1^{\lambda-1} \quad R_2^{\lambda-1} \quad \dots \quad R_{3l+3}^{\lambda-1} \quad R_{3l+4}^{\lambda-1} \\ R_1^{\lambda+\mu-1} \quad R_2^{\lambda+\mu-1} \quad \dots \quad R_{3l+3}^{\lambda+\mu-1} \quad R_{3l+4}^{\lambda+\mu-1} \\ \vdots \quad \vdots \quad \ddots \quad \vdots \quad \vdots \\ R_1^{l+\lambda+\mu-1} \quad R_2^{l+\lambda+\mu-1} \quad \dots \quad R_{3l+3}^{l+\lambda+\mu-1} \quad R_{3l+4}^{l+\lambda+\mu-1} \\ R_1^{l+\lambda} \quad R_2^{l+\lambda} \quad \dots \quad R_{3l+3}^{l+\lambda} \quad R_{3l+4}^{l+\lambda} \end{pmatrix} = - \begin{pmatrix} R_1^{l+\lambda+\mu} & R_2^{l+\lambda+\mu} & \dots & R_{3l+3}^{l+\lambda+\mu} & R_{3l+4}^{l+\lambda+\mu} \end{pmatrix} \quad (5.45)$$

where, V_r is the right Pseudo Block Vandermonde matrix

Hence, the matrices coefficients of the desired Quasi matrix polynomial $\mathcal{X}(s)$ are obtained as follows:

$$\mathcal{X} = - \left[\begin{pmatrix} R_1^{l+\lambda+\mu} & R_2^{l+\lambda+\mu} & \dots & R_{3l+3}^{l+\lambda+\mu} & R_{3l+4}^{l+\lambda+\mu} \end{pmatrix} V_r^{-1} \right]^T \quad (5.46)$$

Remark 3. A right pseudo block Vandermonde matrix extracted from a complete set of pseudo-block-roots of Quasi matrix polynomial is assumed and must be nonsingular.

Remark 4. From theoretical point of view it is possible to make $\lambda > 2$ or $\mu > 2$ or to make $\mu > \lambda$, but this cases practically is not realizable or without any physical interpretation.

Make (5.31) = {(5.33), (5.38), or (5.43)} i.e. Matching the block matrix form $D_{cls}(s)$ with the matrices coefficients of the desired Quasi matrix polynomial $\mathcal{X}(s)$ of equations (5.36), (5.41), or (5.46) according the cases 1, 2 or 3 respectively, we get this system of linear equation:

$$SK = \mathcal{X} - D \quad (5.47)$$

The matrix \mathcal{K} which contains the matrices gains of the $(FO - PI^\lambda D^\mu)$ controller is obtained after solving linear system of equation (5.47):

$$\mathcal{K} = \text{linsolve}(S, (\mathcal{X} - D)) \quad (5.48)$$

Finally, the below Table 5.1 gives the matrices gains K_d , K_p and K_i of the $FO - PI^\lambda D^\mu$ controller.

Table 5.1: The matrices gains of the proposed controller according to each cases

	Case 1	Case 2	Case 3
K_d	$\mathcal{K}(\overline{1:m}, :)$	$\mathcal{K}(\overline{(2m+1):3m}, :)$	$\mathcal{K}(\overline{1:m}, :)$
K_p	$\mathcal{K}(\overline{(m+1):2m}, :)$	$\mathcal{K}(\overline{1:m}, :)$	$\mathcal{K}(\overline{(m+1):2m}, :)$
K_i	$\mathcal{K}(\overline{(2m+1):3m}, :)$	$\mathcal{K}(\overline{(m+1):2m}, :)$	$\mathcal{K}(\overline{(2m+1):3m}, :)$

4.4 The choice of the desired Pseudo-Block-Roots

The selection of the desired pseudo-block-roots $R \in \mathbb{R}^{m \times m}$ is subjected to several criteria, for example according the design, the left fraction description is more suitable with the observer form and the right fraction description is more suitable with controller and the diagonal forms...etc, also the vandermonde matrix V_r inverse, some times the diagonal form it causes a ill-conditioned matrix problem. In the no-integer order design we remark that the pseudo-block-roots R of the pseudo vandermonde matrix V_r have a fractional power, which mean if the eigenvalues of the pseudo-block-root matrix have negative real part, in this case the fractional power of R gives a matrix that have elements of complex values, this is a constraint, the second constraint about the diagonal form is no suitable in this design because it can not accept conjugate eigenvalues. So, we are limited to differentiating between the observer form and the controller form, due to the design of the controller $C(s)$, has been chosen in the left fraction description LMFD $C_l(s)$ see (5.16), the observer form is more suitable in this case [5, 6, 8], the allowable eigenvalues locus are determined by the conditions of the stability of the FO-LTI systems, which is introduced in the following Matignon's stability theorem [15, 16].

Theorem 5.1. *The CLS multivariable fractional transfer function $H_{cls}(s)$ is stable if and only if the following condition is satisfied in σ -plane:*

$|\arg(\lambda)| > q\frac{\pi}{2}$, with λ being the set pseudo-roots of the pseudo-polynomial $D_{cls}(\sigma) = 0$, $\sigma = s^q$, $\forall \sigma \in \mathbb{C}$ and $0 < q < 1$

Remark 5. Theorem 1.1 is valid just for a commensurate order fractional-order transfer functions. For the incommensurate case, there exist many theorems in literatures addressed to study the stability of this kind of systems, among them the concept of bounded input-bounded output (BIBO) stability or external stability using the Müntz-Szász theory, see [17, 18].

A set of desired pseudo-block-roots R are to be selected from class of stable pseudo-eigenvalues chosen in the right half plane to ensure the positivity of the real part of the pseudo-eigenvalues and thus avoiding generating a pseudo-vandermonde V_r matrix with complex values, the absolute values of the imaginary part should to be greater then zero, to guarantee the eigenvalues locating are in stability region, Figure. 5.2 shows the allowable region that can be choose from them the suitable eigenvalues, and also shows the stable and the unstable regions of the LTI commensurate fractional-order system.

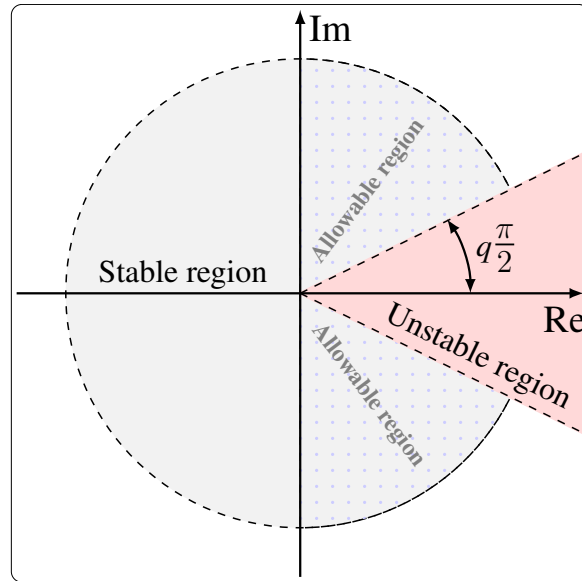


Figure 5.2: Stability region for the fractional-order LTI systems with allowable region

The desired pseudo-block-roots R are take the observer form as shown in the equation (5.50), where the observer form is extracted based on the characteristic polynomial of each pseudo-eigenvalues, and the pseudo-eigenvalues are chosen from the allowable region shown in Figure. 5.2.

$$R = \left(\begin{array}{c} \overbrace{\left(\begin{array}{cccc} 0 & \cdots & 0 & -r1_m \\ 1 & \cdots & 0 & -r1_{(m-1)} \\ \vdots & \ddots & \vdots & \vdots \\ 0 & \cdots & 1 & -r1_1 \end{array} \right)}^{R_f = \{R_{(3l+3)}, R_{(3l+2)}, R_{(3l+4)}\}} \cdots \left(\begin{array}{cccc} 0 & \cdots & 0 & -rf_m \\ 1 & \cdots & 0 & -rf_{(m-1)} \\ \vdots & \ddots & \vdots & \vdots \\ 0 & \cdots & 1 & -rf_1 \end{array} \right) \\ \underbrace{\hspace{10em}}_{R_1} \hspace{10em} \underbrace{\hspace{10em}}_{R_f} \end{array} \right) \quad (5.49)$$

Remark 6. The fractional power of the pseudo-block-roots R in the pseudo-vandermonde-matrix V_r is calculated based on A Schur-Padé Algorithm [14], because is more suitable and gives a precise values, than the tool existed in Matlab, where it is unreliable.

The selection of the pseudo block roots and the fractional orders which can achieve the set-point tracking and the CLS stability conditions is not difficult, just enough choose the set of the pseudo block roots in the allowable region and try to tuning manually the fractional orders λ in the neighborhood of "1" and μ tuning to less then 1. Thus it is effortlessly to be obtained a configuration that ensure the stability and the tracking of the closed loop in the same time , and this flexibility in choices, may proof that existed a several local optimum configurations. To select the best or among the best local optimum configuration that archives another subjected constraints, similar to the stability and the tracking that are guaranteed intuitively in all the possible solutions. A grey wolf optimizer (GWO) is proposed in this design to solve this optimization problem.

4.5 Controller parameters tuning under model uncertainty using grey wolf optimizer

In this subsection the uncertainty in the model parameters are considered in the design of the proposed controller, where the system (5.1) is represented in the uncertain state space form as follows:

$$\begin{cases} x(t) = A(\theta)x(t) + B(\theta)u(t) \\ y(t) = C(\theta)x(t) + D(\theta)u(t) \end{cases} \quad (5.50)$$

where, θ is the vector of the uncertain parameters with the bounded values by an compact set Θ as $\Theta = \{\theta \in \mathbb{R}^{n\theta} \mid \underline{\theta}_i \leq \theta_i \leq \bar{\theta}_i, i = 1, \dots, n\}$

$$\begin{aligned} \underline{A}(\theta) &\leq A(\theta) \leq \bar{A}(\theta) \\ \underline{B}(\theta) &\leq B(\theta) \leq \bar{B}(\theta) \\ \underline{C}(\theta) &\leq C(\theta) \leq \bar{C}(\theta) \\ \underline{D}(\theta) &\leq D(\theta) \leq \bar{D}(\theta) \end{aligned} \quad (5.51)$$

where $\underline{\bullet}$ and $\bar{\bullet}$ denote the lower and the upper bound of each matrix, respectively. Note that the inequalities in (5.51) should be understood as element-wise inequalities. Therefore, the uncertainties in matrices $A(\theta)$, $B(\theta)$, $C(\theta)$ and $D(\theta)$ can be decomposed as $A(\theta) = A_n + \Delta A(\theta)$, $B(\theta) = B_n + \Delta B(\theta)$, $C(\theta) = C_n + \Delta C(\theta)$ and $D(\theta) = D_n + \Delta D(\theta)$, where A_n , B_n , C_n and D_n are the matrices of the system (5.1), and the nominal part of the system matrices $A(\theta)$, $B(\theta)$, $C(\theta)$ and $D(\theta)$, respectively [23].

To obtained the parameters of the proposed controller $FO - PI^\lambda D^\mu$ which can achieved the best control specifications of the uncertain parameters model (5.50), the proposed controller is formulated as a convex multidimensional optimization problems with constraints specified by

$$\min_{\mathbf{x}} J(\mathbf{x}) \text{ such that } \begin{cases} \mathbf{c}(\mathbf{x}) \leq 0 \\ \mathbf{ceq}(\mathbf{x}) = 0 \\ \mathbf{A} \cdot \mathbf{x} \leq \mathbf{b} \\ \mathbf{Aeq} \cdot \mathbf{x} = \mathbf{beq} \\ lb \leq \mathbf{x} \leq ub \end{cases} \quad (5.52)$$

where, \mathbf{b} and \mathbf{beq} are vectors, \mathbf{A} and \mathbf{Aeq} are matrices, $\mathbf{c}(\mathbf{x})$ and $\mathbf{ceq}(\mathbf{x})$ are functions that return vectors, and $J(\mathbf{x})$ is a objective function that returns a scalar. $J(\mathbf{x})$, $\mathbf{c}(\mathbf{x})$, and $\mathbf{ceq}(\mathbf{x})$ can be nonlinear functions [21].

The objective function $J(\mathbf{x})$ has been chosen as

$$J = \int \left(e(t)^T Q_u e(t) + u(t)^T R_u u(t) \right) dt \quad (5.53)$$

where the minimization of the quadratic forms of the error and the control signals respectively is to guaranteed optimal tracking with minimum energy possible,

To select the optimal pseudo block roots that guaranteed the best performances of the controller under model parameters uncertainty (5.50), the following set of constraints have been introduced:

$$\text{Constraint 1: } |\text{Arg}(\lambda(H_{cls}(\sigma)))| > q \frac{\pi}{2} \quad (5.54)$$

This constraint guaranteed the stability in the closed loop controller-system.

$$\text{Constraint 2: } V_r V_r^{-1} - I = 0 \quad (5.55)$$

This constraint check the existing of set of pseudo block-roots R .

$$\text{Constraint 3: } \mathcal{J}_{\{\theta, \bar{\theta}\}} \leq \nu \mathcal{J}_n \quad (5.56)$$

This constraint ensure the selection of a set pseudo block-roots which may achieve a best performance of the controller in the presence of model parameters uncertainty.

Optimization procedure The grey wolf optimizer (GWO) is a meta-heuristic algorithm proposed by **Mirjalili et al.**, [11]. It has been selected as tool in this design to solve the convex multidimensional optimization problems with constraints presented in (5.52), from among several meta-heuristic and evolutionary algorithms such as GA and PSO respectively, due to their fast convergence behavior without any complexity (just adjusting two parameters, Max-iter and number of agents) comparing with the existed algorithms [11]. The GWO imitates the social manners of grey wolves. These wolves live in a group contains 20-30 members. In this group, the strict dominance hierarchy is practiced where the group has a leader named alpha α , supported by secondary ones named beta β , which aid α in decision-making. The rest members of the group are named δ and ω as shown in Pyramid Figure. 5.3 The procedure of hunting the prey by the grey wolves is: looking for the prey, surrounding the prey, hunting, and attacking the prey. The arithmetic model of surrounding the prey [22], is written as follows

$$\vec{D} = \left| \vec{C} \cdot \vec{X}_{pi} - \vec{X}_i \right| \quad (5.57)$$

and

$$\vec{X}_{i+1} = \vec{X}_{pi} - \vec{A} \cdot \vec{D} \quad (5.58)$$

where X_i is the place of the grey wolf, X_{pi} is the place of the prey, D is the distance, A and C are vectors calculated as following

$$\vec{A} = 2\vec{a} \cdot \vec{r}_1 - \vec{a} \quad (5.59)$$

and

$$\vec{C} = 2 \cdot \vec{r}_2 \quad (5.60)$$

where,

$$\vec{a} = 2 \left(1 - \frac{t}{\text{Max-iter}} \right) \quad (5.61)$$

where r_1 and r_2 are random numbers between [0, 1]. The parameter a is a variable which is linearly reduced from 2 to 0 while the iterations increased. The process of looking for the prey position (exploration) could be attained by diverging the search entities, when $|A| > 1$. The process of getting the prey (exploitation) could be attained by the convergence of the search entities, when $|A| < 1$. The hunting is led by α entities with β and δ entities support as in (5.62)-(5.64). Figure. 5.3 shows the flowchart of the GWO algorithm steps. Like other meta-heuristic algorithms, The GWO can be disposed to stagnate in a local minimum but the parameters A and C can help the GWO algorithm to avoid stagnation [22, 22].

$$\begin{aligned} \vec{D}_\alpha &= \left| \vec{C}_1 \cdot \vec{X}_{\alpha i} - \vec{X}_i \right| \\ \vec{D}_\beta &= \left| \vec{C}_2 \cdot \vec{X}_{\beta i} - \vec{X}_i \right| \\ \vec{D}_\delta &= \left| \vec{C}_3 \cdot \vec{X}_{\delta i} - \vec{X}_i \right| \end{aligned} \quad (5.62)$$

$$\begin{aligned}\vec{X}_1 &= \vec{X}_{\alpha i} - \vec{A}_1 \cdot \vec{D}_\alpha \\ \vec{X}_2 &= \vec{X}_{\beta i} - \vec{A}_2 \cdot \vec{D}_\beta\end{aligned}\tag{5.63}$$

$$\begin{aligned}\vec{X}_3 &= \vec{X}_{\delta i} - \vec{A}_3 \cdot \vec{D}_\delta \\ \vec{X}_{i+1} &= \frac{\vec{X}_1 + \vec{X}_2 + \vec{X}_3}{3}\end{aligned}\tag{5.64}$$

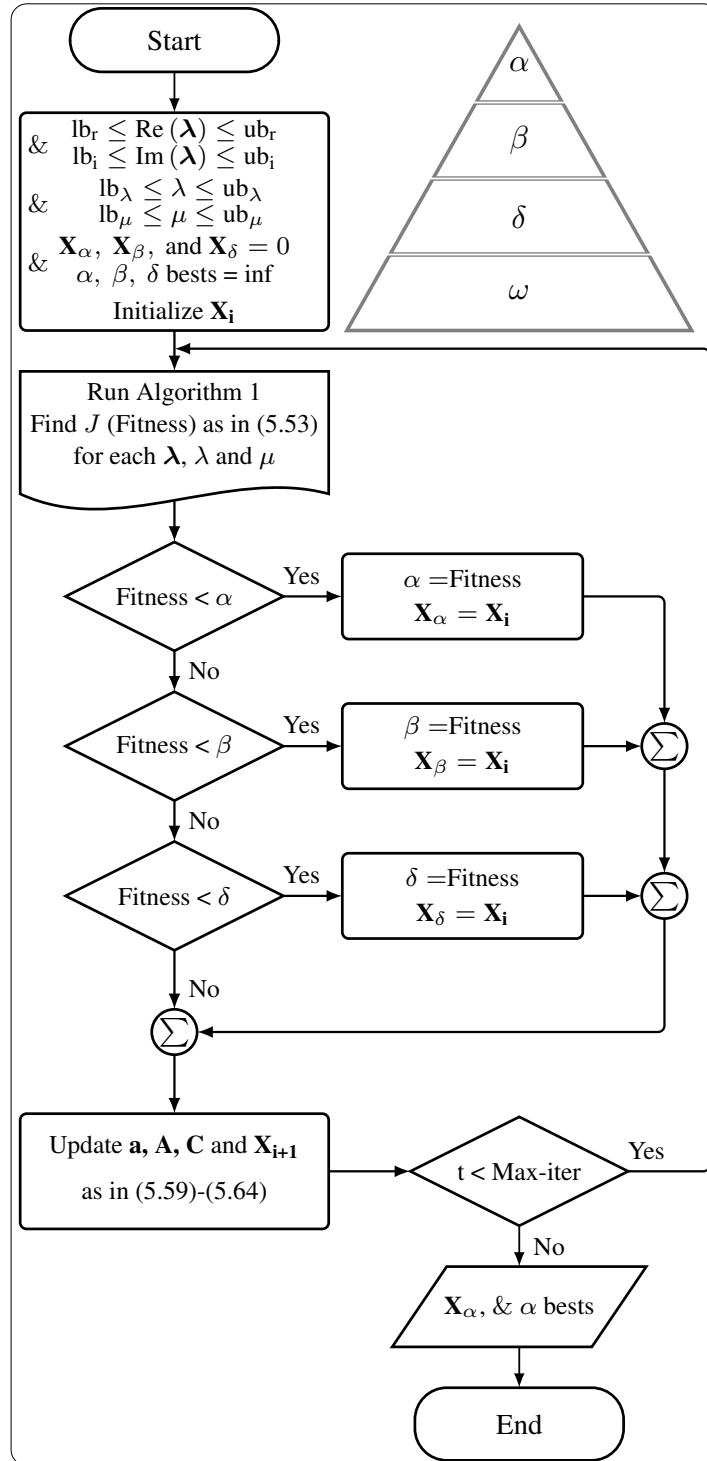


Figure 5.3: Flowchart of the Grey Wolf Optimizer.

5 The proposed algorithm steps

Summarizing all the important steps of the proposed controller

Algorithm 4 Robust fractional-order $PI^\lambda D^\mu$ controller algorithm

Case 1: Without model uncertainty

- a Step 1** Checking the conditions mentioned in Corollary 5.1 and transform the system (5.1) to the canonical block controllable form, based on (5.2), (5.3) and (5.4).
- Step 2** Transform the system (5.2) to the right matrix fraction descriptions (RMFD), based on equations (5.5), (5.6), (5.7) and (5.8).
- Step 3** Constructing the multivariable fractional-order transfer function $H_{cls}(s)$ of the closed-loop control-system based on equation (5.30).
- Step 4** Transform the quasi diophantine matrix equation $D_{cls}(s)$ to the block matrix form, see equation (5.31).
- Step 5** Choosing one from the three cases that is appropriate to your problem design.
- Step 6** The chosen desired pseudo block-roots take the observer form as, see (5.49) are calculated based on selected pseudo-roots in the allowable region see Figure. 5.2.
- Step 7** Calculating the corresponding desired right quasi matrix polynomial $\mathcal{X}(s)$ based on a set of desired stable pseudo block-roots and the right pseudo-vandermonde matrix V_r .
- Step 8** Solving the obtained linear system of equation, see (5.48).
- Step 9** The matrices gains K_d , K_p and K_i of the $FO - PI^\lambda D^\mu$ controller is obtained from Table 5.1.
- Step 10** The selection of the pseudo block roots must be designed based on pseudo-roots allocated in the allowable region Figure. 5.2, and try to tuning manually the fractional orders λ in the neighborhood of "1" and μ tuning to less than 1.
- b Case 2: With model uncertainty**
- Step 11** Selecting the nominal objective function $J(\mathbf{x})$ as, see equation (5.53).
- Step 12** Defining the set of the constraints based on equations, (5.54), (5.55) and (5.56).
- Step 13** Go to the label **a**.
- Step 14** Solving the previous optimization problem using GWO algorithm shown in the flowchart Figure. 5.3.
- Step 15** Finally, when the stopping criterion is satisfied and the constraints conditions are not violated, then best local optimal solution was obtained.
-

6 Experimental application and results

The reduced dynamical model of the centrifugal gas compressor BCL 505 is chosen as good case of study, due to their hard pairing and interactions between their inputs-outputs and the existing of the coupling matrix D which is make the model not proper and this increases the difficulty of controlling the system which makes the controller in a good examination. The studied model has two inputs $T1$: is aspiration temperature, $P1$: is aspiration pressure and two outputs $T2$: is discharge temperature and $P2$: is discharge pressure. Their schematic diagram is shown in Figure. 5.4.

$$S = \begin{pmatrix} N_{r2} & O_m & O_m \\ O_m & N_{r2} & O_m \\ N_{r1} & O_m & O_m \\ O_m & N_{r1} & O_m \\ O_m & O_m & N_{r2} \\ N_{r0} & O_m & O_m \\ O_m & N_{r0} & O_m \\ O_m & O_m & N_{r1} \\ O_m & O_m & O_m \\ O_m & O_m & O_m \\ O_m & O_m & N_{r0} \end{pmatrix}, \quad D = \begin{pmatrix} O_m \\ D_{r2} \\ O_m \\ D_{r1} \\ O_m \\ O_m \\ D_{r0} \\ O_m \\ O_m \\ O_m \\ O_m \end{pmatrix}$$

✓ Based on grey wolf optimizer (GWO) and as shown in Figure. 5.5 and Figure. 5.6, the number of max iteration is Max-iter = 600, the variable ranges $0.01 \leq \text{Re}(\lambda) \leq 4$ and $-4 \leq \text{Im}(\lambda) \leq 4$ of the real and the imaginary part of the pseudo-roots λ , respectively. And the variable ranges $1.1 \leq \lambda \leq 1.5$ and $0.01 \leq \mu \leq 0.5$ of the integration and derivation FO-Power, respectively. The optimal values of FO-Power of the integration and the derivation of the proposed $PI^\lambda D^\mu$ controller are given as, $\lambda = 1.02$ and $\mu = 0.45$ respectively, with the following optimal pseudo-roots:

$$\lambda = \begin{pmatrix} \lambda & \lambda^* \\ 1.5896 + 0.0178i & 1.5896 - 0.0178i \\ 0.0779 + 0.1351i & 0.0779 - 0.1351i \\ 0.0207 + 0.0104i & 0.0207 - 0.0104i \\ 0.1075 + 0.2600i & 0.1075 - 0.2600i \\ 0.0602 + 0.0142i & 0.0602 - 0.0142i \\ 0.0322 + 0.3331i & 0.0322 - 0.3331i \\ 0.1978 + 0.0346i & 0.1978 - 0.0346i \\ 0.0129 + 0.0364i & 0.0129 - 0.0364i \\ 0.0116 + 0.0142i & 0.0116 - 0.0142i \\ 0.3599 + 0.7913i & 0.3599 - 0.7913i \end{pmatrix}$$

Based on (5.43), the corresponding desired right quasi matrix polynomial of fractional-order $\mathcal{X}(s)$ takes this form:

$$\mathcal{X}(s) = I s^{3.47} + \mathcal{X}_9 s^{3.02} + \mathcal{X}_8 s^{2.47} + \mathcal{X}_7 s^{2.02} + \mathcal{X}_6 s^2 + \mathcal{X}_5 s^{1.47} + \mathcal{X}_4 s^{1.02} + \mathcal{X}_3 s^1 + \mathcal{X}_2 s^{0.47} + \mathcal{X}_1 s^{0.02} + \mathcal{X}_0 s^0 \quad (5.65)$$

The set of the desired right pseudo-block-roots $R = \{R_1, R_2, \dots, R_9, R_{10}\}$ are the solvents of the right quasi matrix polynomial $\mathcal{X}(s)$ presented in (5.57), and they were constructed in the observer form from the optimal pseudo-roots λ , are given as:

$$R_1 = \begin{pmatrix} 0 & -2.5271 \\ 1 & 3.1792 \end{pmatrix}, \quad R_2 = \begin{pmatrix} 0 & -0.0243 \\ 1 & 0.1558 \end{pmatrix}, \quad R_3 = \begin{pmatrix} 0 & -0.0005 \\ 1 & 0.0414 \end{pmatrix}, \quad R_4 = \begin{pmatrix} 0 & -0.0792 \\ 1 & 0.2150 \end{pmatrix}$$

$$R_5 = \begin{pmatrix} 0 & -0.0038 \\ 1 & 0.1204 \end{pmatrix}, \quad R_6 = \begin{pmatrix} 0 & -0.1120 \\ 1 & 0.0644 \end{pmatrix}, \quad R_7 = \begin{pmatrix} 0 & -0.0403 \\ 1 & 0.3957 \end{pmatrix}, \quad R_8 = \begin{pmatrix} 0 & -0.0015 \\ 1 & 0.0258 \end{pmatrix}$$

$$R_9 = \begin{pmatrix} 0 & -0.0003 \\ 1 & 0.0233 \end{pmatrix}, \quad R_{10} = \begin{pmatrix} 0 & -0.7556 \\ 1 & 0.7197 \end{pmatrix}$$

Based on the optimal set of the desired right pseudo-block-roots R , the right pseudo block vandermonde matrix V_r is calculated and extracted according (1.45).

Remark 7. The numerical application of $V_r \in \mathbb{R}^{20 \times 20}$, $S \in \mathbb{R}^{22 \times 6}$, and $D \in \mathbb{R}^{22 \times 2}$ are mentioned in the Appendix D.

The matrices coefficients of the desired quasi matrix polynomial $\mathcal{X}(s)$ are computed based on (5.46) as:

$$\mathcal{X} = - \left[\left(R_1^{\lambda+\mu+l} \quad R_2^{\lambda+\mu+l} \quad R_3^{\lambda+\mu+l} \quad \dots \quad R_8^{\lambda+\mu+l} \quad R_9^{\lambda+\mu+l} \quad R_{10}^{\lambda+\mu+l} \right) V_r^{-1} \right]^T \quad (5.66)$$

where,

$$\mathcal{X} = - \left[\left(R_1^{3.47} \quad R_2^{3.47} \quad R_3^{3.47} \quad \dots \quad R_8^{3.47} \quad R_9^{3.47} \quad R_{10}^{3.47} \right) V_r^{-1} \right]^T \quad (5.67)$$

Hence,

$$\mathcal{X}_{10} = I = \begin{pmatrix} 1 & 0 \\ 0 & 1 \end{pmatrix}, \quad \mathcal{X}_9 = \begin{pmatrix} 1.3980 & -0.2616 \\ -4.2133 & -0.4814 \end{pmatrix}, \quad \mathcal{X}_8 = \begin{pmatrix} -2.8209 & 0.3157 \\ 4.9518 & -0.6258 \end{pmatrix}, \quad \mathcal{X}_7 = \begin{pmatrix} -1.6375 & -0.7800 \\ -4.6559 & -3.1583 \end{pmatrix}$$

$$\mathcal{X}_6 = \begin{pmatrix} -199.0756 & 117.1666 \\ 287.8061 & -236.1483 \end{pmatrix}, \quad \mathcal{X}_5 = \begin{pmatrix} 206.3722 & -127.3976 \\ -294.2801 & 256.9186 \end{pmatrix}, \quad \mathcal{X}_4 = \begin{pmatrix} -14.5882 & 28.8612 \\ -4.4142 & -64.6461 \end{pmatrix}$$

$$\mathcal{X}_3 = \begin{pmatrix} -3.0419 & -7.818 \\ 1.2194 & 1.6635 \end{pmatrix}, \quad \mathcal{X}_2 = \begin{pmatrix} 3.1633 & 7.8522 \\ -1.2502 & -1.6738 \end{pmatrix}, \quad \mathcal{X}_1 = \begin{pmatrix} -13.4167 & -25.8564 \\ 53.0694 & 58.5975 \end{pmatrix}$$

$$\mathcal{X}_0 = \begin{pmatrix} 0.0639 & 3.8106 \\ -8.0366 & -10.6621 \end{pmatrix}$$

✓ The matrices gains K_d , K_p and K_i of the fractional order PID controller are calculated based on solving the linear system of equation, $\mathcal{K} = \text{linsolve}(S, (\mathcal{X} - D))$.

where,

$$\mathcal{K} = \begin{pmatrix} -28.8126 & 64.5293 \\ -64.3704 & 89.4609 \\ 7.4282 & -23.1703 \\ 4.5681 & 5.2452 \\ -513.8190 & 1.1958 \\ 183.3391 & -558.8740 \end{pmatrix}$$

Based on Table 5.1 the matrices gains K_d , K_p and K_i of the $(FO - PI^\lambda D^\mu)$ controller are given as follows:

$$K_d = \mathcal{K}(\overline{1:2}, :) = \begin{pmatrix} -28.8126 & 64.5293 \\ -64.3704 & 89.4609 \end{pmatrix}$$

$$K_p = \mathcal{K}(\overline{3:4}, :) = \begin{pmatrix} 7.4282 & -23.1703 \\ 4.5681 & 5.2452 \end{pmatrix}$$

$$K_i = \mathcal{K}(\overline{5:6}, :) = \begin{pmatrix} -513.8190 & 1.1958 \\ 183.3391 & -558.8740 \end{pmatrix}$$

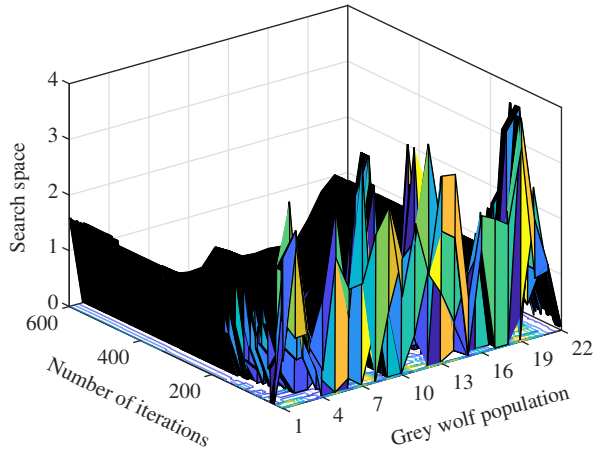


Figure 5.5: The evolution of the grey wolf population values during the tuning optimization process

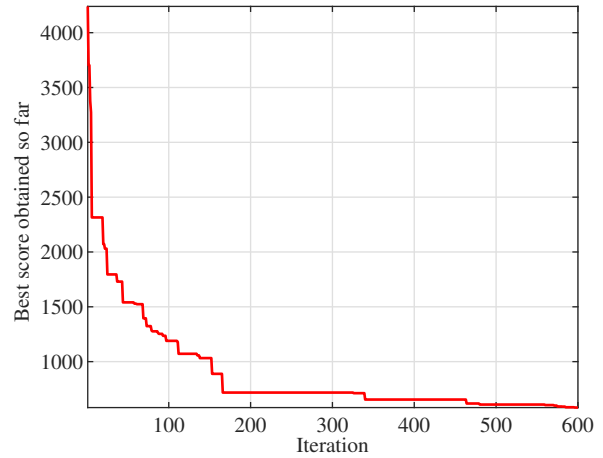


Figure 5.6: The change of objective function J in terms of GWO iteration

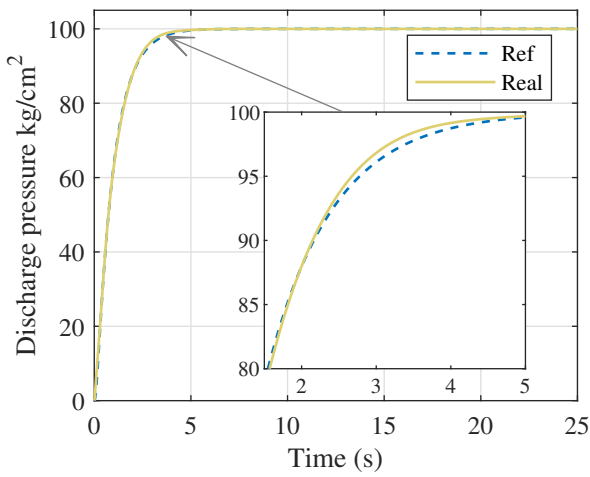


Figure 5.7: Output signal of reference and real discharge pressure

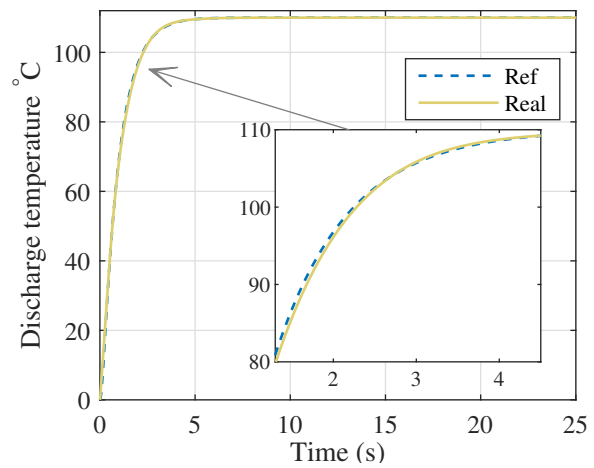


Figure 5.8: Output signal of reference and real discharge temperature

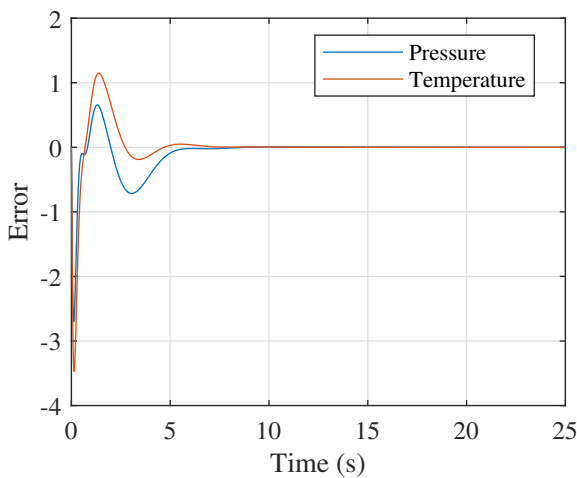


Figure 5.9: The error between the reference and real outputs signals

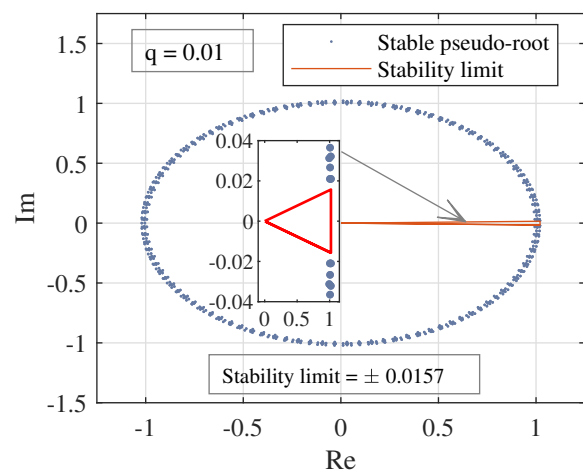


Figure 5.10: CLS pseudo-roots position in complex σ -plane

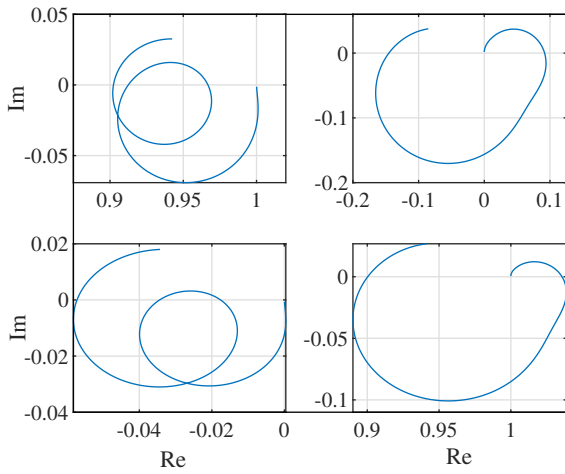


Figure 5.11: Nyquist diagram of the CLS

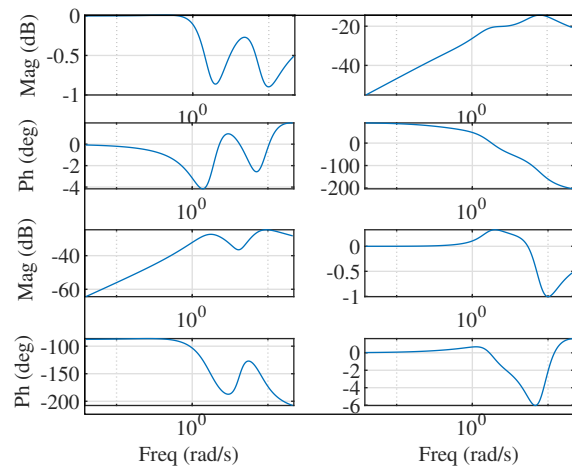


Figure 5.12: Bode diagram of the CLS

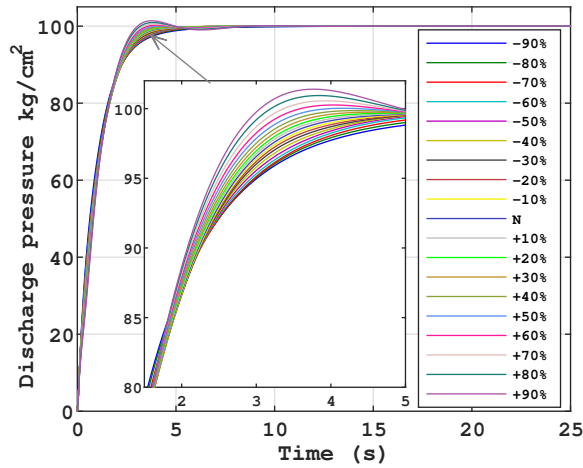


Figure 5.13: Output signal of reference and real discharge pressure under $-90\% \leq \Delta\theta \leq +90\%$ of nominal system uncertainty

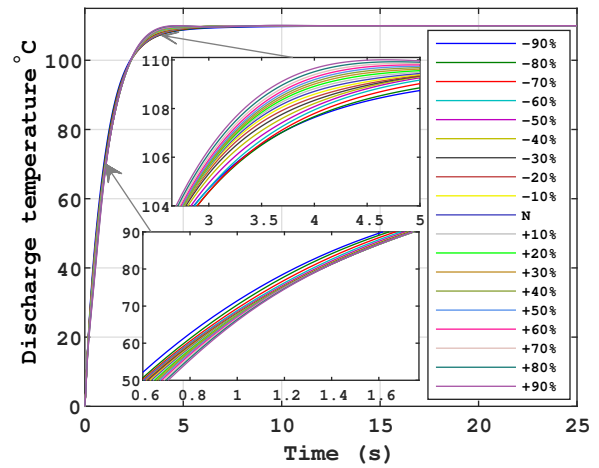


Figure 5.14: Output signal of reference and real discharge temperature under $-90\% \leq \Delta\theta \leq +90\%$ of nominal system uncertainty

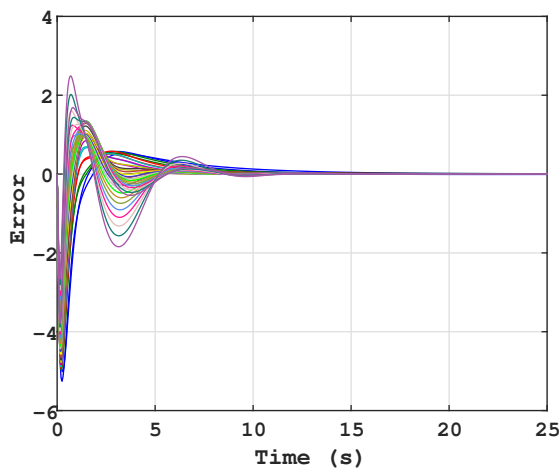


Figure 5.15: The error between the reference and real outputs signals under $-90\% \leq \Delta\theta \leq +90\%$ of nominal system uncertainty

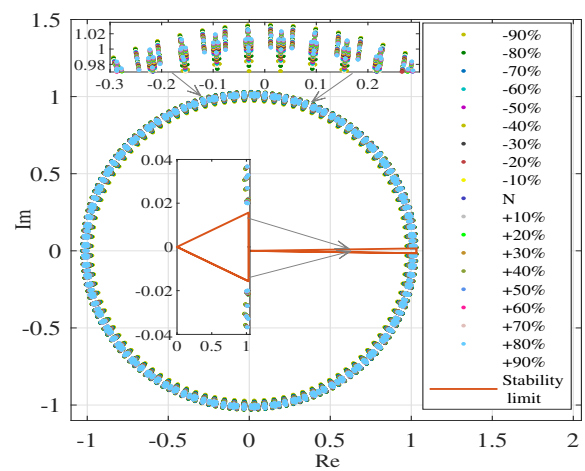


Figure 5.16: CLS pseudo-roots position in complex σ -plane under $-90\% \leq \Delta\theta \leq +90\%$ of nominal system uncertainty

The obtained results of Figure. 5.7 and Figure. 5.8 show that the outputs signals of the discharge pressure and temperature respectively, meet the desired dynamical behavior specified by the references, with very small static error see Figure. 5.9, and no overshooting peak. The pseudo-roots of the CLS FO-TF presented in (5.30) and the stability boundary $\pm q \frac{\pi}{2}$ are depicted in Figure. 5.10 of the nominal system and in Figure. 5.16 of the nominal system under uncertainties, it can be concluded from [19, 20] that the CLS FO-TF (5.30) is **Lyapunov globally asymptotically stable** since all the pseudo-roots of the nominal and the uncertain systems satisfy the condition of the Matignon's stability mentioned in Theorem 5.1, (i.e. $|\arg(\lambda)| > q \frac{\pi}{2}$, in which $q = 0.01$). Under interval $\pm 90\%$ of uncertainty, the closed loop rest maintain their key specifications of stability and good set-point tracking as shown in Figure. 5.13 and Figure. 5.14, the output static error under the presence of the parameters uncertainty as shown in Figure. 5.15 is very small and this give us opportunity to talk about the robustness of the proposed controller. Also the CLS stability is checked using the frequency analysis, where the CLS Nyquist and Bode diagrams shown in Figure. 5.11 and Figure. 5.12, where no encirclement on the critical point $(-1,0)$ and when the phase $\text{Ph}=-180^\circ$ the magnitude $\text{mag}<0$ (dB).

7 Passive FTC Investigation

In this section the passive FTC approach is investigated on the proposed $FO - PI^\lambda D^\mu$ controller, where this approach is used so that the CLS remains insensitive to a certain set of faults, where the fault tolerance is ensured without the use of online information relating to faults affecting the system and without changing the structure of the nominal controllers. The faults considered in this passive FTC approach are a source of external additive and multiplicative disturbances as shown in Figure. 5.22 and Figure. 5.23 , and internal disturbances represented in the parameter uncertainties of studied system of $-90\% \leq \Delta\theta \leq +90\%$, also a real system faults where the faults presented in the previous chapter 4 of the centrifugal gas compressor system are taken into account on this FTC approach see Figure. 5.17.

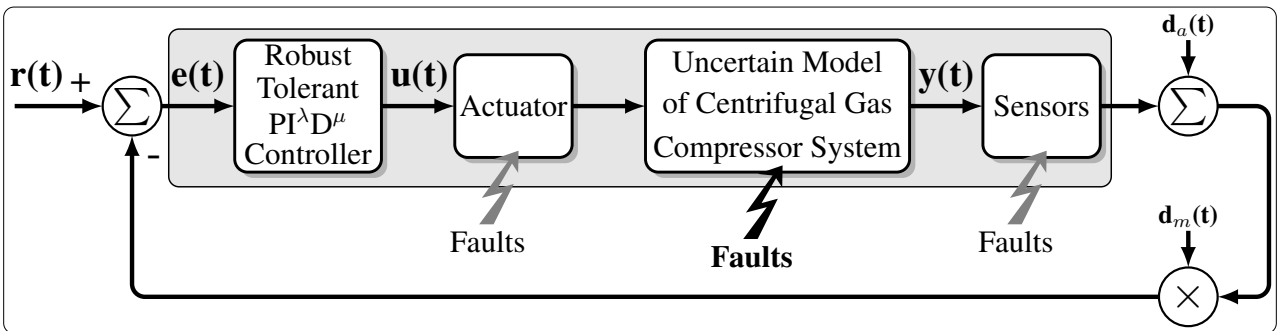


Figure 5.17: Schematic design of Robust $FO-PI^\lambda D^\mu$ Passive FTC system.

Figure. 5.18 and Figure. 5.20 illustrate the comparison between the PFTC control based on $FO - PI^\lambda D^\mu$ design in presence of system faults and the embeded PID controller of constructor (maker) in faulty and healthy systems of the outputs (discharge pressure and temperature), we can notice in the presence of the system faults, the PFTC manages to ensure acceptable performances comparing with the performances of the embeded PID controller, and the response time of the proposed controller is shown in the curves of the errors (residues) Figure. 5.19 and Figure. 5.21, where the the obtained error signals is in the allowaible thershold of the temperature and the pressure, respectively.

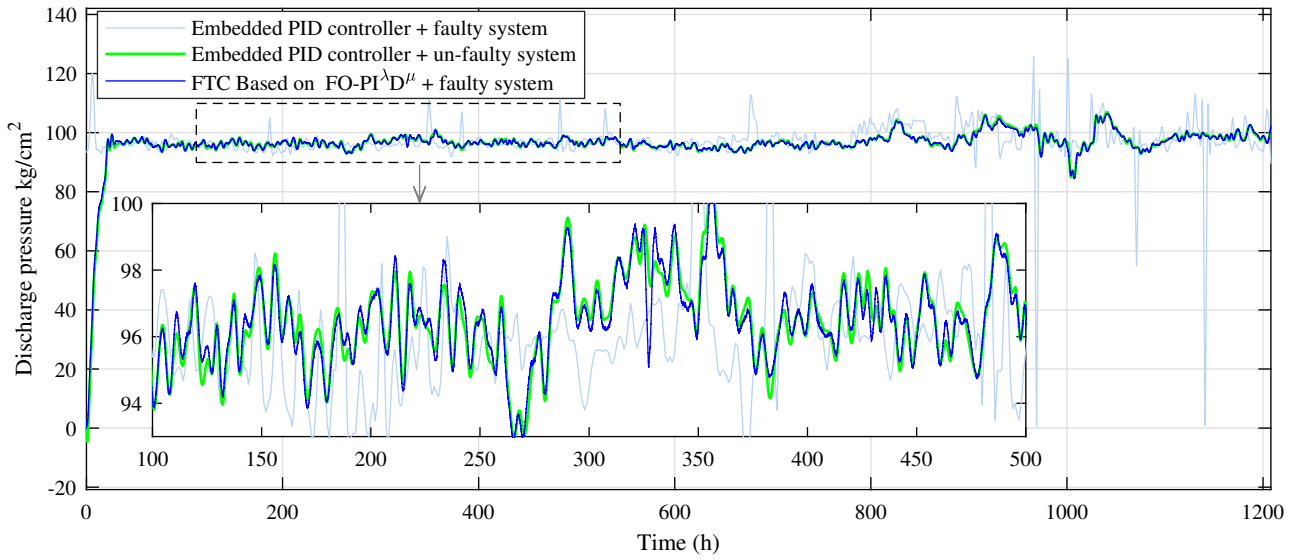


Figure 5.18: Output discharge pressure signals of no faulty (reference) and faulty system under embedded PID controller and with PFTC approach

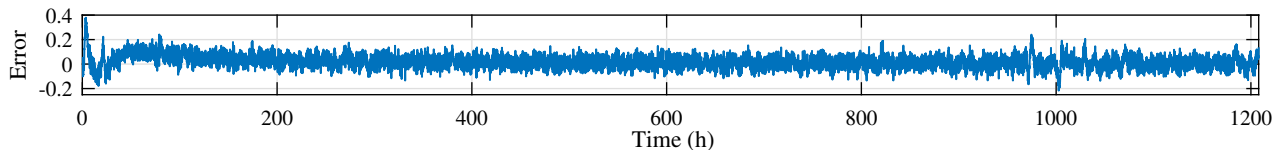


Figure 5.19: Error between faulty system under embedded PID controller and under proposed PFTC approach

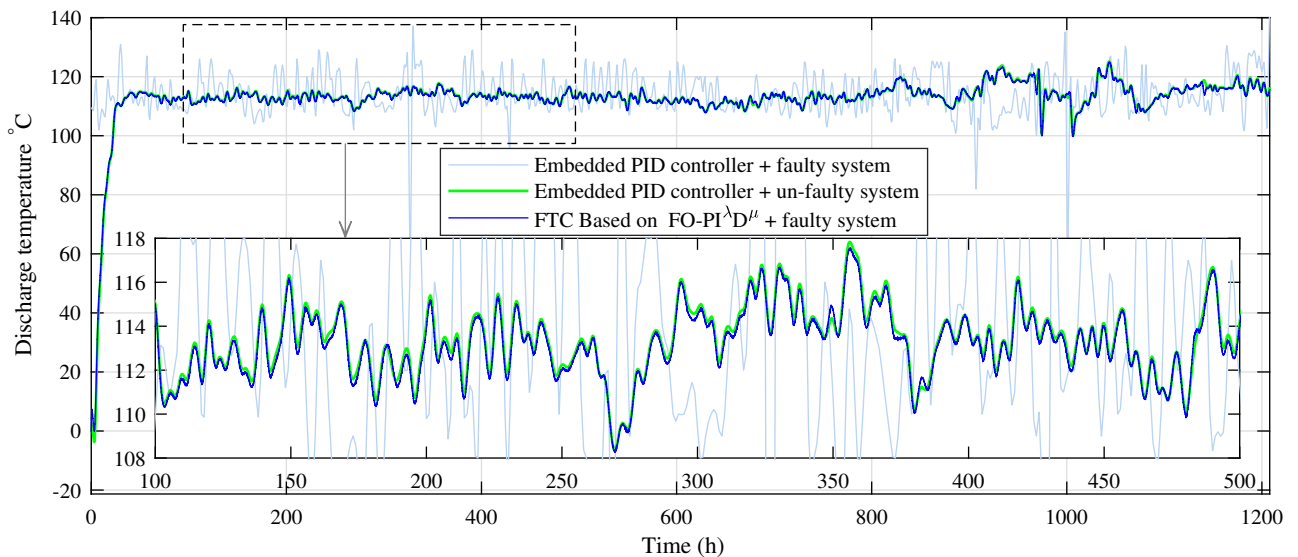


Figure 5.20: Output temperature pressure signals of no faulty (reference) and faulty system under embedded PID controller and with passive FTC approach

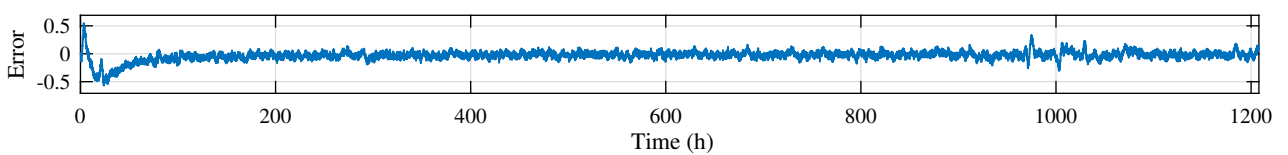


Figure 5.21: Error between faulty system under embedded PID controller and under proposed PFTC approach

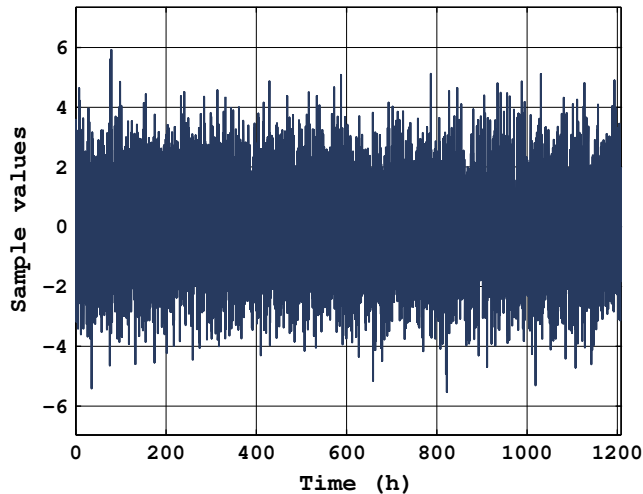


Figure 5.22: External additive disturbance

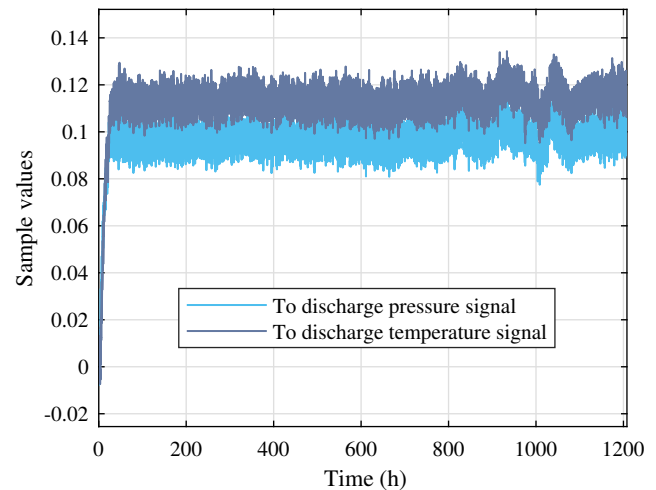


Figure 5.23: External multiplicative disturbance

8 Conclusion

In this chapter a robust $FO-PI^\lambda D^\mu$ controller is designed and introduced based on pseudo block roots placements oriented to the multivariable uncertain linear system. Where, in our steps to design this controller, a many contributions have been presented in this chapter, first one is the extension of the concept of the matrix polynomial to the fractional order (quasi) matrix polynomial, second one is the solvents of this quasi matrix polynomial is the pseudo block roots which are the keystone of this design, the third one is the pseudo block vandermonde matrix is introduced in this design with fractional power matrix elements, and the fourth one is the quasi diophantine matrix equation. Based on the previous contributions the selection of the optimal pseudo block roots that achieve the robustness of the proposed controller using GWO algorithm, the capability of the proposed controller is studied and illustrated on PFTC approach on uncertain centrifugal gas compressor dynamical model under real experimental conditions, with comparison study with industrial embedded PID controller,

9 References

- [1] Malika Yaici, Kamel Hariche, On eigenstructure assignment using Block poles placement, European Journal of Control, May 2014.
- [2] L. S. Shieh and Y. T. Tsay, Block modal matrices and their applications to multivariable control systems, IEE Proc. D Control Theory Appl. 2:41-48(1982).
- [3] L. S. Shieh and Y. T. Tsay, Transformation of a class of multivariable control systems to Block companion forms, IEEE Trans. Automat. Control 27: 199-203 (1982).
- [4] J. E. Dennis, J. F. Traub, and R. P. Weber, The algebraic theory of matrix polynomials, SZAIZI J. Numer. Anal. 13:831-845 (1976).
- [5] B. Nail, A. Kouzou, and A. Hafaiifa, Robust block roots assignment in linear discrete-time sliding mode control for a class of multivariable system: gas turbine power plant application, Transactions of the Institute of Measurement and Control, pp. 1-17, Jul. 2018.

- [6] B. Nail, A. Kouzou, A. Hafaifa, A. Chaibet, Parametric identification and stabilization of turbo-compressor plant based on matrix fraction description using experimental data, *Journal of Engineering Science and Technology*, vol. 13, no. 6, pp. 1850-1868, Jun. 2018.
- [7] B. Nail, A. Kouzou, A. Hafaifa, and B. Bekhiti, Parametric output feedback stabilization in MIMO systems: Application to gas turbine power plant, in *2016 8th International Conference on Modelling, Identification and Control (ICMIC)*, Algiers, Algeria, 2016, pp. 971-976.
- [8] B. Bekhiti, A. Dahimene, B. Nail, and K. Hariche, On λ -matrices and their applications in MIMO control systems design, *International Journal of Modelling, Identification and Control*, vol. 29, no. 4, pp. 281-294, 2018.
- [9] B. Nail, A. Kouzou, and A. Hafaifa, Digital Stabilizing and Control for Two-Wheeled Robot. In: Derbel N., Ghommam J., Zhu Q. (eds) *New Developments and Advances in Robot Control. Studies in Systems, Decision and Control*, vol 175. Springer, Singapore, 2019, pp. 237-253.
- [10] T. Kailath, W. Li, *Linear Systems*, Prentice Hall, 1980.
- [11] S. Mirjalili, S. M. Mirjalili, and A. Lewis, Grey Wolf Optimizer, *Advances in Engineering Software*, vol. 69, pp. 46-61, Mar. 2014.
- [12] R. Azarmi, M. Tavakoli-Kakhki, A. Fatehi, and A. K. Sedigh, Robustness analysis and design of fractional order $I^\lambda D^\mu$ controllers using the small gain theorem, *International Journal of Control*, pp. 1-13, Jul. 2018.
- [13] I. Podlubny, *Fractional Differential Equations: An Introduction to Fractional Derivatives, Fractional Differential Equations to Methods of Their Solution and Some of Their Applications (Vol. 198)*. Academic Press, San Diego, 1998.
- [14] N. J. Higham and L. Lin, An Improved Schur-Padé Algorithm for Fractional Powers of a Matrix and Their Fréchet Derivatives, *SIAM Journal on Matrix Analysis and Applications*, vol. 34, no. 3, pp. 1341-1360, Jan. 2013.
- [15] D. Matignon, Stability result on fractional differential equations with applications to control processing, in *Proceedings of the International Meeting on Automated Compliance Systems and the International Conference on Systems, Man, and Cybernetics (IMACS-SMC '96)*, pp. 963-968, Lille, France, 1996.
- [16] D. Matignon, Stability properties for generalized fractional differential systems, in *Proceedings of the Fractional Differential Systems: Models, Methods and Applications*, pp. 145-158, 1998.
- [17] H. Akçay and R. Malti, On the Completeness Problem for Fractional Rationals with Incommensurable Differentiation Orders, *IFAC Proceedings Volumes*, vol. 41, no. 2, pp. 15367-15371, 2008.
- [18] M. Rivero, S. V. Rogosin, J. A. Tenreiro Machado, and J. J. Trujillo, Stability of Fractional Order Systems, *Mathematical Problems in Engineering*, vol. 2013, pp. 1-14, 2013.
- [19] W. Deng, C. Li, and J. Lü, Stability analysis of linear fractional differential system with multiple time delays, *Nonlinear Dynamics*, vol. 48, no. 4, pp. 409-416, Mar. 2007.

- [20] P. Badri and M. Sojoodi, Stability and Stabilization of Fractional-Order Systems with Different Derivative Orders: An LMI Approach: LMI Stability and Stabilization of FO Systems with Different Orders, *Asian Journal of Control*, Jul. 2018.
- [21] B. Nail, A. Kouzou, A. Hafaifa, and V. Puig, Optimal Static State-Feedback Controller Design for MIMO LTI Systems Based on Constraints Block Roots and Interior-Point Algorithm: Application to Gas Compressor System , *International Conference on Applied Smart Systems (ICASS)*, 24-25 Nov. 2018 Medea, Algeria, pp. 1-6.
- [22] M. H. Qais, H. M. Hasanien, and S. Alghuwainem, A Grey Wolf Optimizer for Optimum Parameters of Multiple PI Controllers of a Grid-Connected PMSG Driven by Variable Speed Wind Turbine, *IEEE Access*, vol. 6, pp. 44120-44128, 2018.
- [23] M. Pourasghar, V. Puig, C. Ocampo-Martinez, and Q. Zhang, Reduced-order Interval-observer Design for Dynamic Systems with Time-invariant Uncertainty, *IFAC-PapersOnLine*, vol. 50, no. 1, pp. 6271-6276, Jul. 2017.

General Conclusion

The block roots of matrix polynomials theory are the fundamental tool used in the design of the contributions presented in this thesis, the exploiting of the characteristics of this theory and functioning them correctly to design robust controllers approaches which can be subjected to the FTC systems. The metaheuristics optimization algorithms used in these designs are used as tools, it has been made the process of selecting the set of block-roots more easier than the classical methods that exist in literatures.

X Introduction

The works done in this thesis concerns the development of three controller's algorithms laws, maybe can be used in Fault-tolerant Control systems, also a fault detection approach is introduced in this thesis.

First , a discrete robust static state feedback controller is designed based on sliding mode control theory and robust block-roots assignments, this design is addressed for the class of multivariable systems described by SSD, the investigation of the validity of this proposed algorithm, has been verified on GE MS500P gas turbine system. This proposed algorithm is applied to the best-chosen real model of the gas turbine studied system, which is obtained from experimental data obtained on-site, using parametric identification based on the Left MFD and MIMO Least Square method.

The terms of the applicability of this algorithm:

- Linear multivariable systems.
- The ratio between the dimension of the system and the number of the inputs n/m is integer.
- The system is block controllable.

The robustness stability of this algorithm is demonstrate based on the extended stability measures. Furthermore, a comparison study with classical and recent algorithms is proved the effectiveness and the high performances of this proposed.

Second Discrete optimal static output-feedback controller is designed based on block transformations matrices and Grey Wolf Optimizer, this design is addressed for the class of multivariable systems described by SSD, the validity of this proposed approach, has been investigated on centrifugal gas compressor system BCL 505. Where, the dynamic model of the studied system is obtained based on system parametric identification using experimental data acquired on-site.

The terms of the applicability of this algorithm:

- Linear multivariable systems.

- The ratio between the dimension of the system and the number of the inputs n/m and the number of the outputs n/p , respectively, are integers.
- The system is block minimal, i.e. block controllable and block observable.

The proposed controller exhibits a good behavior in the terms of, norms, time responses, sensitivity, robustness and stability measures. In fact, from practical point of view the proposed optimal SOF controller can be employed as backup controller, which is not active during the control operation but is used in the case of FTC, a comparison study with a recent H_∞ algorithms they proved the superiority of this proposed.

Third

Part one Intelligent Fault detection approach is designed using Kalman filter, where its role is denoising the outputs of the process and gives the real measures, and an expert system is designed based on the interval fuzzy logic type 2. Where, an experimental examination is carried out on the centrifugal gas compressor system in presence of real faults, also a forecasting remaining time is calculated using ARIMA predictor model. Economic study has been done based on the faulty state of the studied system before and after reparation, taking in consideration the loss of the production of this system during the reparation times.

Part two Fault detection approach based on interval observer, the design of this observer is based on the left block roots of matrix polynomial and grey wolf optimizer, a set of left block roots and left block vandermonde matrix are constructing the matrix observer gain L , after investigating this observer on the studied system with subjected to real faults, the detection of the faults is made by a high performance.

The terms of the applicability of this algorithm:

- Linear or nonlinear multivariable systems.
- LPV or Uncertain parameters systems.
- The ratio between the dimension of the system and the number of the outputs n/p , should be integer.
- The system is block observable.

Fifth , Robust fractional order proportional integrator and derivation controller $FO-PI^\mu D^\lambda$ is designed, based on the new introduced pseudo block-roots of the quasi matrix polynomials, and Grey Wolf Optimizer which play a role of selecting the optimal pseudo block-roots that check the solution of the quasi polynomial Diophantine matrix equation, a passive FTC applied on uncertain system is investigated in presence of real faults and additive/multiplicative disturbances, where the results show that FTC system preserve the nominal keys specification of the studied system without need to the new reconfiguration of the proposed controller. The terms of the applicability of this algorithm:

- Linear multivariable systems.
- The ratio between the dimension of the system and the number of the inputs n/m is integer.
- The system is block controllable.

XI Contributions

To the best of the author's knowledge, the list below describes the novel contributions presented in the thesis:

1. Exploiting the block-roots of the matrix polynomial theory in the design of FTC and FDI approaches is considered as challenge and in our knowledge, is a new proposal.
2. The implementation of the Meta-heuristics Algorithms (GWO,GA,...etc) tools to select the optimal set block-roots to solve the formulated constraints problem is also a new proposal.
3. Design an interval observer based on the block-roots assignments.
4. The combination between the fractional-order dynamics and the matrix polynomial theory also considered as challenge and it's can open new horizons and further studies.
5. Quasi matrix polynomial is introduced and defined in this thesis, is an extended to the matrix polynomial .
6. Pseudo block roots of quasi matrix polynomial is introduced, is an extended to the block-roots.
7. Pseudo Block Vandermonde Matrix is introduced and used in the design of $FO-PI^\mu D^\lambda$ controller, is an extended to Block Vandermonde Matrix.
8. Quasi polynomial diophantine matrix equation is introduced and solved in this thesis, is an extended to polynomial diophantine matrix equation.
9. Pseudo Sylvester block matrix is introduced and generated from the quasi polynomial Diophantine matrix equation in this thesis.
10. Intelligent expert system designed using Fuzzy Logic Type 2.

XII Further studies

1. Using linear matrix inequalities (LMI) to select and assign the block-roots of matrix polynomial.
2. If the pseudo block-root R_i with multiplicity m_i exists (repeated pseudo block-roots) then the corresponding pseudo general block Vandermonde matrix will be checked and extended.
3. Design an interval observer for fractional-order system based on the pseudo block-roots assignments.
4. Design fractional state-feedback controller based on the pseudo block-roots assignments.
5. Design fractional output-feedback controller based on the pseudo block-roots assignments.
6. Block observability and Block controllability Study of linear multivariable fractional-order system.
7. Stability study of linear multivariable fractional-order system.
8. Model order reduction of linear multivariable fractional-order system.



GE MS5001P Gas Turbine System and Robustness-Sensitivity Theories

I GE MS5001P Gas Turbine dynamical model

The studied gas turbine which is used in electric power generation plants, located at M, $\hat{\text{S}}\text{ILA}$ in Algeria is presented in this chapter. Indeed, the choice of this application model is due to the availability of the data measurement which is presumably generated by collecting it in real time around the power generators operating point. It is important to clarify that the gas turbine system used in power generation plant, works for a long period without stop and start-up that can be occurred very rarely due to the nature of the power generation plants and its operating constraints. This turbine stop and start-up are generally imposed by the maintenance schedule given by the constructor and they are performed for a relatively long periods. Therefore, these transition stages are not taken into account while the application of the proposed control.

This electrical power plant contains 22 gas turbine units of type GE MS5001P that are used for driving the main electric power generators tied to the main power system network. This kind of gas turbine is an external combustion engine with a single shaft, it is composed of three principal parts, the first part is the axial compressor, the second part is the combustion chamber in which a liquid or gaseous fuel burns partially with the air supplied by the compressor, resulting in an increase of the combustion gas-air mixture temperature, and accordingly an increase in its volume, the third is a turbine, where the combustion gases are expanded in several stages and then are utilized to drive the main shaft which is connected to an electric alternator, a part of the turbine energy is used to drive the compressor too, the general characteristics of the studied gas turbine (GE MS5001P) are illustrated in Table A.1.

Many parameters can influence the turbine dynamics at varying degrees depending on their importance in the gas turbine sections (compressor, combustion and turbine), The study presented in this paper focuses only on the modelling of the two main outputs parameters in the GEMS5001P gas turbine within the normal mode operation rang: the rotor speed and the exhaust temperature that are affected and interacted directly by three main inputs parameters: the gas control valve (GCV), the axial temperature compressor discharge (TCD), and the axial pressure compressor discharge (PCD). Figure. A.1 shows the axial compressor of GE Gas turbine 5001P

studied in the chapter 2, Figure. A.1 shows the turbine of GE Gas turbine 5001P studied in the chapter 2.

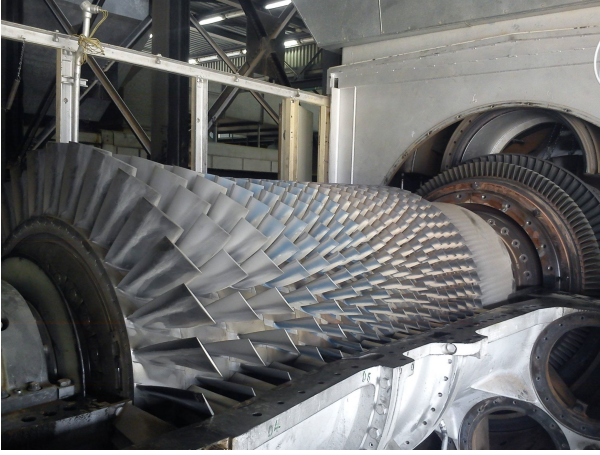


Figure A.1: Axial compressor of GE Gas turbine 5001P

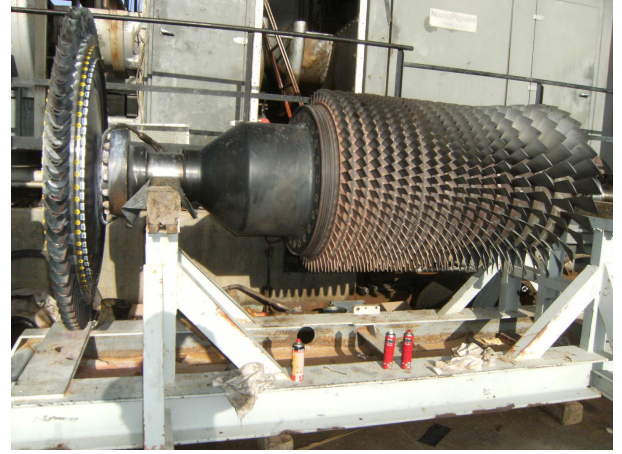


Figure A.2: Turbine of GE Gas turbine 5001P

The real time data for the parametric identification of the studied gas turbine contains $M=10,000$ samples for a duration of time =10000 second, it is important to clarify that this experimental data is obtained via several tests during the normal mode operation to get the optimal data that is covering all possible frequencies of this gas turbine.

$$A = \begin{pmatrix} 0 & 0 & 0 & 0 & 0 & 0 & 0 & 0 & 0 & 0 & 0 & 0.0741 & 0.4262 \\ 0 & 0 & 0 & 0 & 0 & 0 & 0 & 0 & 0 & 0 & 0 & -0.1206 & -0.7895 \\ 1 & 0 & 0 & 0 & 0 & 0 & 0 & 0 & 0 & 0 & 0 & -1.2322 & -2.0671 \\ 0 & 1 & 0 & 0 & 0 & 0 & 0 & 0 & 0 & 0 & 0 & 2.2830 & 4.0358 \\ 0 & 0 & 1 & 0 & 0 & 0 & 0 & 0 & 0 & 0 & 0 & 1.7584 & 2.7118 \\ 0 & 0 & 0 & 1 & 0 & 0 & 0 & 0 & 0 & 0 & 0 & -3.8440 & -6.1277 \\ 0 & 0 & 0 & 0 & 1 & 0 & 0 & 0 & 0 & 0 & 0 & -2.3713 & -2.0011 \\ 0 & 0 & 0 & 0 & 0 & 1 & 0 & 0 & 0 & 0 & 0 & 5.4853 & 5.4656 \\ 0 & 0 & 0 & 0 & 0 & 0 & 1 & 0 & 0 & 0 & 0 & 4.7297 & 2.4885 \\ 0 & 0 & 0 & 0 & 0 & 0 & 0 & 1 & 0 & 0 & 0 & -10.3708 & -6.2941 \\ 0 & 0 & 0 & 0 & 0 & 0 & 0 & 0 & 1 & 0 & 0 & -2.0817 & -1.5865 \\ 0 & 0 & 0 & 0 & 0 & 0 & 0 & 0 & 0 & 1 & 0 & 6.7356 & 4.7397 \end{pmatrix}, B = \begin{pmatrix} 1.1962 & -0.3205 & 3.6002 \\ -2.1029 & 0.6207 & -6.8734 \\ -6.9574 & 0.0203 & -4.5627 \\ 13.0303 & -0.2144 & 10.4620 \\ -1.2037 & -0.1013 & 4.8988 \\ -1.3873 & 0.2559 & -11.9031 \\ -6.4595 & 0.1898 & -5.5900 \\ 11.9648 & -0.4166 & 13.6894 \\ 15.7037 & 0.2908 & 0.7169 \\ -32.2800 & -0.3830 & -6.0437 \\ 2.1116 & 0.0877 & 0.4259 \\ 5.6209 & -0.0849 & 1.4357 \end{pmatrix}, C^T = \begin{pmatrix} 0 & 0 \\ 0 & 0 \\ 0 & 0 \\ 0 & 0 \\ 0 & 0 \\ 0 & 0 \\ 0 & 0 \\ 0 & 0 \\ 0 & 0 \\ 0 & 0 \\ 1 & 0 \\ 0 & 1 \end{pmatrix} \quad (A.1)$$

II The robustness stability and sensitivity performance analysis

II.1 The sensitivity of eigenvalues (robust performance)

Theorem A.1. [1, 3] Let λ_1 and λ_2 the eigenvalues of the matrices A and $(A + \Delta A)$ respectively, and let V be the right eigenvectors matrix of A , the derived the variation in eigenvalues as follows:

$$\min_i (\lambda_{1i} - \lambda_{2i}) \triangleq \min_i (\Delta(\lambda_{1i})) \leq k(V) \cdot \|\Delta A\| \quad (A.2)$$

$\|\cdot\|$ matrix norm and $k(\cdot)$ Is the condition number.

Theorem A.2. [1, 3] Let λ_j , v_j and t_i be the i^{th} eigenvalue, right and left eigenvectors of a matrix A respectively $k(i = 1, \dots, n)$ and let $(\lambda_j + \Delta\lambda_j, \dots, n)$ be the i^{th} eigenvalue of the matrix $(A + \Delta)$. Then, for small enough $\|\Delta A\|$:

$$\Delta\lambda_j \leq \|v_j\| \|t_j\| \|\Delta A\| \triangleq s(\lambda_j) \|\Delta A\| \quad (A.3)$$

such that, $s(\lambda_j) = \|v_i\| \|t_i\|$

The sensitivity of an eigenvalue is calculated by determined the corresponding right and left eigenvectors and after adding a small perturbations ΔA in the system matrix A .

II.1.1 The relative change

Let λ_1 and λ_2 the eigenvalues of the matrices A and $(A + \Delta A)$ respectively.

The relative change r_i of the eigenvalue λ_i is defined [1, 3] as follows:

$$r_i = \frac{|\lambda_{1i} - \lambda_{2i}|}{|\lambda_i|} = \frac{|\Delta \lambda_i|}{|\lambda_i|} \quad i = 1, \dots, n \quad (\text{A.4})$$

II.1.2 The robust stability

Let $\{\lambda_1, \lambda_2, \dots, \lambda_n\}$ be the set of eigenvalues of an $n \times n$ matrix denoted by A and assuming that all the eigenvalues are stable (*i. e.* $|\lambda_j| < 1 \forall j$) and all the eigenvalues are already arbitrary assigned for guaranteed performance, the three robust stability measures are defined by [1–3]:

1. $M_1 = \min_{0 < \omega < \infty} \left\{ \sigma(A - e^{T_s j \omega} I_n) \right\}$, σ denotes the smallest singular value and T_s the sampling time.
2. $M_2 = (k(V))^{-1} |(\lambda_j)|$ such that: $|\lambda_n| \leq \dots \leq |\lambda_1|$ and V is the right eigenvector of matrix A .
3. $M_3 = \min_{0 < j < n} \left\{ (s(\lambda_j))^{-1} |(\lambda_j)| \right\}$

- M_1 is the smallest possible matrix variation norm for the matrix A to have an eigenvalue outside circle unit .
- M_2 is the $|(\lambda_j)|$ term that represent the shortest distance between the unstable region (outside circle unit) and eigenvalues λ_j .
- M_3 is more precise than M_1 and M_2 and reflects the instability likelihood of all eigenvalues.
- The three measures M_3 , M_1 and M_2 cited depending on the degree of their importance and quality, respectively [1–3].

Table A.1: General performance of gas turbine GE MS5001P

Quantity	Value
Compressor stages	16
Firing temperature	1,730 (°F)
Exhaust temperature	898 (°F)
Air flow	928.5 (10 ³ Lb/hr)
Output	24,700 (kW)
Heat rate	12,950 (kJ/kW-h)
Rotor Speed	5355 (rpm) (105%)
Efficiency	27.8%

III References

- [1] B. Nail, A. Kouzou, and A. Hafaifa, Robust block roots assignment in linear discrete-time sliding mode control for a class of multivariable system: gas turbine power plant application, Transactions of the Institute of Measurement and Control, vol. 41, no. 5, pp. 1216-1232, Mar. 2019.
- [2] C.-C. Tsui, A new robust stability measure for state feedback systems, Systems & Control Letters, vol. 23, no. 5, pp. 365-369, Nov. 1994.
- [3] C.-C. Tsui , Robust Control System Design: Advanced State Space Techniques, (2004) Second edition, *Marcel Dekker*.

BCL 505 Centrifugal Gas Compressor System with Supplementary Data

I BCL 505 Centrifugal Gas Compressor dynamical model and Hassi R'Mel gas field

Figure. B.1 shows the combustion chambers of GE Gas turbine 5002C which is drive the studied BCL 505 centrifugal gas compressor, and Figure. B.2 shows the high and the low pressure centrifugal gas compressors.



Figure B.1: Combustion chambers of GE Gas turbine 5002C



Figure B.2: HP and LP of centrifugal gas compressor

Hassi R'Mel gas field is located approximately 550 km south of Algiers (Algeria), at an altitude of 760 m. This gas field covers an area of 3500 km², 70 km in the north-south direction and 50 km in the east-west direction. The landscape is composed of a vast rocky plateau, the climate is characterized by an average humidity of 19% in summer and 34% in winter. The temperature has a large range variation between 0°C in winter to 45°C in summer. The production of the Hassi R'Mel gas field can reach the capacity of 100 billion cubic meters of natural dry gas, 12 million tons of condensate gas and 3.5 million tons of liquefied natural gas (LNG). The main

exploitation zone of oil stations and gas compression stations contains the centrifugal gas compressor. The main role of the gas compression stations is to constantly pressurize the dry gas to maintain its required pressure level. to regulate the gas pressure at the national level and the international market level. Each station contains 18 turbo gas compressor (Centrifugal gas compressor driven by a gas turbine (GE-MS5002C)) as shown in Figure. B.5 and Figure. B.6, the Stator and the rotor of GE Gas turbine 5002C respectively , each pair of turbo-compressor forms a compression line. The compression process is carried out through two stages, the low pressure stage and the high pressure stage as shown in Figure. B.3 and Figure. B.2, a speed rotor multiplier is connected between the LP and HP centrifugal gas compressor systems as shown in Figure. B.4, where a cooling system based on air coolers is used to regulate the temperature at the intermediary of the two stages [1].

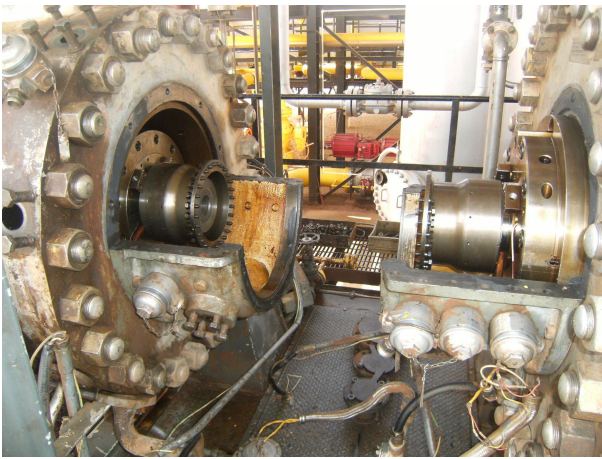


Figure B.3: HP and LP rotor

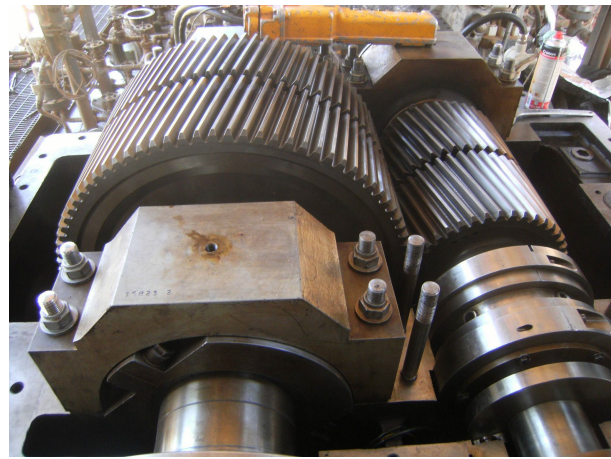


Figure B.4: Multiplier of rotor speed

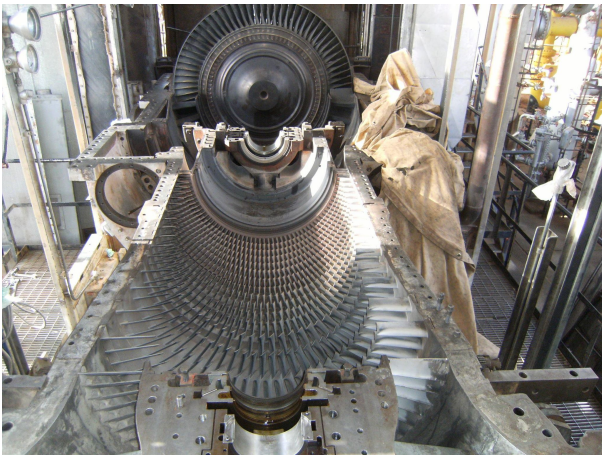


Figure B.5: Stator of GE Gas turbine 5002C



Figure B.6: Rotor of of GE Gas turbine 5002C

The BCL 505 centrifugal gas studied in the chapter 3, chapter 4, and chapter 5 is a mimo system with two inputs, the aspiration temperature T_1 and the aspiration pressure P_1 and two outputs, the discharge pressure P_2 , and the discharge temperature T_2 . The data used in this modeling is obtained experimentally on site, it contains $N=1208$ samples along a duration of 1208 hours, it is important to clarify that this experimental data is obtained via several tests to get the optimal data that are covering all possible dynamic behavior of this centrifugal gas compressor, the centrifugal gas compressor dynamical model obtained using the ESRIV algorithm, its main steps are summarized in [1, 2].

The general characteristics performance of centrifugal gas compressor BCL 505 is presented in Table B.1.

Table B.1: General performance of centrifugal gas compressor BCL 505

Quantity	Value
Stages	1-5
Maximum discharge pressure	123 kg/cm^2
Maximum discharge temperature	121 $^{\circ}C$
Efficiently -%	73%
Speed	3000 to 20000 rpm
Compressed gas	LNG

The state space model of the studied centrifugal gas compressor BCL 505 is give, as follows [1, 2]:

$$A = \begin{pmatrix} 0 & 0 & 0 & 0 & 0 & 0 & 0 & 0 & 0 & -0.0152 & 0.0185 \\ 0 & 0 & 0 & 0 & 0 & 0 & 0 & 0 & 0 & 0.0389 & 0.0436 \\ 1 & 0 & 0 & 0 & 0 & 0 & 0 & 0 & 0 & 0.0666 & 0.0696 \\ 0 & 1 & 0 & 0 & 0 & 0 & 0 & 0 & 0 & 0.0881 & 0.1080 \\ 0 & 0 & 1 & 0 & 0 & 0 & 0 & 0 & 0 & 0.0959 & 0.0784 \\ 0 & 0 & 0 & 1 & 0 & 0 & 0 & 0 & 0 & 0.0508 & 0.0701 \\ 0 & 0 & 0 & 0 & 1 & 0 & 0 & 0 & -0.0171 & 0.0319 \\ 0 & 0 & 0 & 0 & 0 & 1 & 0 & 0 & 0.1294 & 0.0158 \\ 0 & 0 & 0 & 0 & 0 & 0 & 1 & 0 & -0.0052 & 0.0145 \\ 0 & 0 & 0 & 0 & 0 & 0 & 0 & 1 & 0.0699 & 0.0038 \end{pmatrix} B = \begin{pmatrix} 0.0245 & 0.0262 \\ 0.0686 & 0.0045 \\ 0.0219 & 0.0425 \\ 0.0199 & 0.0710 \\ 0.0820 & 0.2317 \\ 0.1615 & 0.1233 \\ 0.1762 & 0.0941 \\ 0.3274 & 0.1871 \\ 0.0857 & 0.2576 \\ -0.0801 & -0.0413 \end{pmatrix} C^T = \begin{pmatrix} 0 & 0 \\ 0 & 0 \\ 0 & 0 \\ 0 & 0 \\ 0 & 0 \\ 0 & 0 \\ 0 & 0 \\ 0 & 0 \\ 1 & 0 \\ 0 & 1 \end{pmatrix} \quad (B.1)$$

$$T_c = \begin{bmatrix} -91.6745 & -27.4695 & 54.7681 & -23.3698 & -12.3091 & 16.4484 & -15.8289 & 10.4330 & 7.6684 & -5.8166 \\ 200.8850 & 7.0315 & -65.8920 & 46.1545 & -7.7039 & -10.3132 & 28.9183 & -20.9065 & -5.0933 & 4.9881 \\ 90.3674 & -38.5601 & -20.3100 & 27.1399 & -26.1178 & 17.2145 & 12.6528 & -9.5975 & 4.5194 & -2.7466 \\ -108.7218 & 76.1549 & -12.7114 & -17.0168 & 47.7152 & -34.4957 & -8.4040 & 8.2304 & -11.8508 & 5.9773 \\ -33.5114 & 44.7809 & -43.0943 & 28.4039 & 20.8771 & -15.8358 & 7.4569 & -4.5318 & -8.4768 & 1.5990 \\ -20.9738 & -28.0777 & 78.7302 & -56.9179 & -13.8666 & 13.5802 & -19.5538 & 9.8626 & 11.1854 & -0.6127 \\ -71.1056 & 46.8664 & 34.4472 & -26.1291 & 12.3040 & -7.4776 & -13.9866 & 2.6384 & 4.1607 & 3.2666 \\ 129.9047 & -93.9146 & -22.8799 & 22.4073 & -32.2637 & 16.2733 & 18.4559 & -1.0110 & 0.5376 & -4.4921 \\ 56.8379 & -43.1130 & 20.3015 & -12.3380 & -23.0780 & 4.3534 & 6.8652 & 5.3898 & 7.3954 & 0.6895 \\ -37.7518 & 36.9720 & -53.2351 & 26.8509 & 30.4522 & -1.6681 & 0.8871 & -7.4119 & -13.5382 & -2.8038 \end{bmatrix} \quad (B.2)$$

$$T_o = \begin{bmatrix} 0.1349 & 0 & 0 & 0 & 0 & 0 & 0 & 0 & 0 & 0 & 0 \\ 0 & 0.1349 & 0 & 0 & 0 & 0 & 0 & 0 & 0 & 0 & 0 \\ 0 & 0 & 0.2226 & 0 & 0 & 0 & 0 & 0 & 0 & 0 & 0 \\ 0 & 0 & 0 & 0.2226 & 0 & 0 & 0 & 0 & 0 & 0 & 0 \\ 0 & 0 & 0 & 0 & 0.3673 & 0 & 0 & 0 & 0 & 0 & 0 \\ 0 & 0 & 0 & 0 & 0 & 0.3673 & 0 & 0 & 0 & 0 & 0 \\ 0 & 0 & 0 & 0 & 0 & 0 & 0.6061 & 0 & 0 & 0 & 0 \\ 0 & 0 & 0 & 0 & 0 & 0 & 0 & 0.6061 & 0 & 0 & 0 \\ 0 & 0 & 0 & 0 & 0 & 0 & 0 & 0 & 0 & 1.0000 & 0 \\ 0 & 0 & 0 & 0 & 0 & 0 & 0 & 0 & 0 & 0 & 1.0000 \end{bmatrix} \quad (B.3)$$

$$A_{co} = \begin{bmatrix} 12.1920 & -5.2024 & -4.5212 & 6.0417 & -9.5933 & 6.3230 & 7.6684 & -5.8166 & 4.5194 & -2.7466 \\ -14.6683 & 10.2745 & -2.8297 & -3.7881 & 17.5263 & -12.6706 & -5.0933 & 4.9881 & -11.8508 & 5.9773 \\ -4.5212 & 6.0417 & -9.5933 & 6.3230 & 7.6684 & -5.8166 & 4.5194 & -2.7466 & -8.4768 & 1.5990 \\ -2.8297 & -3.7881 & 17.5263 & -12.6706 & -5.0933 & 4.9881 & -11.8508 & 5.9773 & 11.1854 & -0.6127 \\ -9.5933 & 6.3230 & 7.6684 & -5.8166 & 4.5194 & -2.7466 & -8.4768 & 1.5990 & 4.1607 & 3.2666 \\ 17.5263 & -12.6706 & -5.0933 & 4.9881 & -11.8508 & 5.9773 & 11.1854 & -0.6127 & 0.5376 & -4.4921 \\ 7.6684 & -5.8166 & 4.5194 & -2.7466 & -8.4768 & 1.5990 & 4.1607 & 3.2666 & 7.3954 & 0.6895 \\ -5.0933 & 4.9881 & -11.8508 & 5.9773 & 11.1854 & -0.6127 & 0.5376 & -4.4921 & -13.5382 & -2.8038 \\ 4.5194 & -2.7466 & -8.4768 & 1.5990 & 4.1607 & 3.2666 & 7.3954 & 0.6895 & -6.0654 & -3.0397 \\ -11.8508 & 5.9773 & 11.1854 & -0.6127 & 0.5376 & -4.4921 & -13.5382 & -2.8038 & 4.2343 & 3.4407 \end{bmatrix} \quad (B.4)$$

The algorithm steps of the Kalman filter are presented as follows [1]:

Algorithm 5 Kalman observer algorithm

Step 1 The predicted estimated state $\hat{X}_{k|k-1}$ is expressed as follows:

$$\hat{X}_{k|k-1} = A\hat{X}_{k-1|k-1} + Bu_k \quad (B.5)$$

Step 2 The predicted estimated covariance $P_{k|k-1}$ is expressed as follows:

$$P_{k|k-1} = AP_{k-1|k-1}A^T + Q_k \quad (B.6)$$

Step 3 The measurement residues \tilde{Y}_k is given as follows

$$\tilde{Y}_k = Z_k - C\hat{X}_{k|k-1} \quad (B.7)$$

Step 4 The innovation covariance S_k is given as follows

$$S_k = CP_{k|k-1}C^T + R_k \quad (B.8)$$

Step 5 The optimal Kalman gain K_k is then

$$K_k = P_{k|k-1}C^TS_k^{-1} \quad (B.9)$$

Step 6 A posteriori state estimate $\hat{X}_{k|k}$ can be evaluated as follows

$$\hat{X}_{k|k} = \hat{X}_{k|k-1} + K_k\tilde{Y}_k \quad (B.10)$$

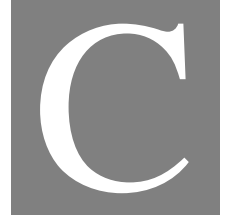
Step 7 Finally the updated estimated covariance $P_{k|k}$ is obtained

$$P_{k|k} = (1 - K_kC)P_{k|k-1} \quad (B.11)$$

II References

- [1] B. Nail, A. Kouzou, A. Hafaifa, N. Hadroug, and P. Vicenç, A Robust fault diagnosis and forecasting approach based on Kalman filter and Interval Type-2 Fuzzy Logic for efficiency improvement of centrifugal gas compressor system, *Diagnostyka*, vol. 20, no. 2, pp. 57-75, May 2019.
- [2] B. Nail, A. Kouzou, A. Hafaifa, A. Chaibet, Parametric identification and stabilization of turbo-compressor

plant based on matrix fraction description using experimental data, *Journal of Engineering Science and Technology*, vol. 13, no. 6, pp. 1850-1868, Jun. 2018.



**Supplementary Data of fractional-order $PI^\lambda D^\mu$
controller application results**

Begins an appendix

$$\begin{aligned}
& \left(\begin{aligned}
& 117s^{6.94} - 70.74s^{6.49} + 9.085s^{6.04} + 1225s^{5.94} - 800.8s^{5.49} + 2619s^{5.47} + 99.75s^{5.04} - 668.4s^{5.02} + 3853s^{4.94} - 2493s^{4.49} + 2.743 \times 10^4 s^{4.47} + \\
& 310.5s^{4.04} - 6867s^{4.02} + 5041s^4 + 4964s^{3.94} - 3042s^{3.49} + 8.626 \times 10^4 s^{3.47} + 383s^{3.04} - 2.151 \times 10^4 s^{3.02} + 5.279 \times 10^4 s^3 + 1778s^{2.94} - \\
& 833.7s^{2.49} + 1.111 \times 10^5 s^{2.47} + 114.8s^{2.04} - 2.765 \times 10^4 s^{2.02} + 1.66 \times 10^5 s^2 + 3.981 \times 10^4 s^{1.47} - 1.016 \times 10^4 s^{1.02} + 2.139 \times 10^5 s + 7.661 \times 10^5
\end{aligned} \right) \\
& \left(\begin{aligned}
& 117s^{6.94} - 44.39s^{6.49} + 6.273s^{6.04} + 1225s^{5.94} - 569.3s^{5.49} + 2619s^{5.47} + 64.04s^{5.04} - 515.2s^{5.02} + 3853s^{4.94} - 1801s^{4.49} + 2.743 \times 10^4 s^{4.47} + \\
& 187.4s^{4.04} - 4887s^{4.02} + 5041s^4 + 4964s^{3.94} - 2244s^{3.49} + 8.626 \times 10^4 s^{3.47} + 243.1s^{3.04} - 1.451 \times 10^4 s^{3.02} + 5.279 \times 10^4 s^3 + 1778s^{2.94} - \\
& 519.2s^{2.49} + 1.111 \times 10^5 s^{2.47} + 75.83s^{2.04} - 1.92 \times 10^4 s^{2.02} + 1.66 \times 10^5 s^2 + 3.981 \times 10^5 s^{1.47} - 7434s^{1.02} + 2.139 \times 10^5 s + 7.661 \times 10^4
\end{aligned} \right) \\
& \left(\begin{aligned}
& -2.842 \times 10^{-14} s^{6.94} - 15.46s^{6.49} + 2.167s^{6.04} - 2.274 \times 10^{-13} s^{5.94} - 128.8s^{5.49} + 4.547 \times 10^{-13} s^{5.47} + 20.68s^{5.04} - 74.4s^{5.02} \\
& - 373.1s^{4.49} + 64.61s^{4.04} - 909.7s^{4.02} - 1.819 \times 10^{-12} s^4 - 9.095 \times 10^{-13} s^{3.94} - 425.8s^{3.49} - 2.91 \times 10^{-11} s^{3.47} + 75.45s^{3.04} - \\
& 3158s^{3.02} - 174.6s^{2.49} + 1.455 \times 10^{-11} s^{2.47} + 28.19s^{2.04} - 3795s^{2.02} + 5.821 \times 10^{-11} s^2 - 1251s^{1.02} - 1.164 \times 10^{-10} s
\end{aligned} \right) \\
& \left(\begin{aligned}
& 117s^{6.94} - 44.39s^{6.49} + 6.273s^{6.04} + 1225s^{5.94} - 569.3s^{5.49} + 2619s^{5.47} + 64.04s^{5.04} - 515.2s^{5.02} + 3853s^{4.94} - 1801s^{4.49} + 2.743 \times 10^4 s^{4.47} + \\
& 187.4s^{4.04} - 4887s^{4.02} + 5041s^4 + 4964s^{3.94} - 2244s^{3.49} + 8.626 \times 10^4 s^{3.47} + 243.1s^{3.04} - 1.451 \times 10^4 s^{3.02} + 5.279 \times 10^4 s^3 + 1778s^{2.94} - \\
& 519.2s^{2.49} + 1.111 \times 10^5 s^{2.47} + 75.83s^{2.04} - 1.92 \times 10^4 s^{2.02} + 1.66 \times 10^5 s^2 + 3.981 \times 10^4 s^{1.47} - 7434s^{1.02} + 2.139 \times 10^5 s + 7.661 \times 10^4
\end{aligned} \right) \\
& \left(\begin{aligned}
& -5.684 \times 10^{-14} s^{6.94} - 32.92s^{6.49} - 2.031s^{6.04} - 259.5s^{5.49} - 18.08s^{5.04} + 211.6s^{5.02} - 1.819 \times 10^{-12} s^{4.94} - 858.6s^{4.49} + 7.276 \times 10^{-12} s^{4.47} \\
& - 52.3s^{4.04} + 1791s^{4.02} + 1.455 \times 10^{-11} s^4 - 1364s^{3.49} - 57.89s^{3.04} + 5480s^{3.02} + 1.164 \times 10^{-10} s^3 + 1.819 \times 10^{-12} s^{2.94} - 863.7s^{2.49} + \\
& 2.91 \times 10^{-11} s^{2.47} - 21.29s^{2.04} + 7211s^{2.02} + 6.985 \times 10^{-10} s^2 + 3655s^{1.02} + 1.164 \times 10^{-10}
\end{aligned} \right) \\
& \left(\begin{aligned}
& 117s^{6.94} - 44.39s^{6.49} + 6.273s^{6.04} + 1225s^{5.94} - 569.3s^{5.49} + 2619s^{5.47} + 64.04s^{5.04} - 515.2s^{5.02} + 3853s^{4.94} - 1801s^{4.49} + 2.743 \times 10^4 s^{4.47} + \\
& 187.4s^{4.04} - 4887s^{4.02} + 5041s^4 + 4964s^{3.94} - 2244s^{3.49} + 8.626 \times 10^4 s^{3.47} + 243.1s^{3.04} - 1.451 \times 10^4 s^{3.02} + 5.279 \times 10^4 s^3 + 1778s^{2.94} - \\
& 519.2s^{2.49} + 1.111 \times 10^5 s^{2.47} + 75.83s^{2.04} - 1.92 \times 10^4 s^{2.02} + 1.66 \times 10^5 s^2 + 3.981 \times 10^4 s^{1.47} - 7434s^{1.02} + 2.139 \times 10^5 s + 7.661 \times 10^4
\end{aligned} \right) \\
& \left(\begin{aligned}
& 117s^6.94 - 68.14s^6.49 + 6.938s^6.04 + 1225s^5.94 - 757.9s^5.49 + 2619s^5.47 + 68.39s^5.04 - 445.3s^5.02 + 3853s^4.94 - 2420s^4.49 + 2.743 \times 10^4 s^4.47 \\
& + 203.7s^4.04 - 4287s^4.02 + 5041s^4 + 4964s^3.94 - 3211s^3.49 + 8.626 \times 10^4 s^3.47 + 276.3s^3.04 - 1.27 \times 10^4 s^3.02 + 5.279 \times 10^4 s^3 + 1778s^2.94 - \\
& 1121s^2.49 + 1.111 \times 10^5 s^2.47 + 102.7s^2.04 - 1.693 \times 10^4 s^2.02 + 1.66 \times 10^5 s^2 + 3.981 \times 10^4 s^{1.47} - 6367s^{1.02} + 2.139 \times 10^5 s + 7.661 \times 10^4
\end{aligned} \right) \\
& \left(\begin{aligned}
& 117s^6.94 - 44.39s^6.49 + 6.273s^6.04 + 1225s^5.94 - 569.3s^5.49 + 2619s^5.47 + 64.04s^5.04 - 515.2s^5.02 + 3853s^4.94 - 1801s^4.49 + 2.743 \times 10^4 s^4.47 \\
& + 187.4s^4.04 - 4887s^4.02 + 5041s^4 + 4964s^3.94 - 2244s^3.49 + 8.626 \times 10^4 s^3.47 + 243.1s^3.04 - 1.451 \times 10^4 s^3.02 + 5.279 \times 10^4 s^3 + 1778s^2.94 \\
& - 519.2s^2.49 + 1.111 \times 10^5 s^2.47 + 75.83s^2.04 - 1.92 \times 10^4 s^2.02 + 1.66 \times 10^5 s^2 + 3.981 \times 10^4 s^{1.47} - 7434s^{1.02} + 2.139 \times 10^5 s + 7.661 \times 10^4
\end{aligned} \right)
\end{aligned}
\tag{C.1}$$

$H_{cls}(s) =$

$$A_c = \begin{pmatrix} 0.0000 & 0.0000 & 1.0000 & 0.0000 \\ 0.0000 & -0.0000 & -0.0000 & 1.0000 \\ -5.3708 & -0.6555 & -4.2152 & -0.2307 \\ -0.3026 & -4.0809 & -0.2892 & -4.2529 \end{pmatrix}, B_c = \begin{pmatrix} 0 & 0 \\ 0 & 0 \\ 1 & 0 \\ -0 & 1 \end{pmatrix} \quad (C.5)$$

$$C_c = \begin{pmatrix} -0.3008 & -0.1891 & 0.0747 & 0.1614 \\ -0.3681 & -0.3958 & 0.4595 & -0.2378 \end{pmatrix}, D_c = \begin{pmatrix} 0.0038 & -0.3707 \\ 0.1987 & 0.1512 \end{pmatrix} \quad (C.6)$$

$$S = \begin{pmatrix} 0.0038 & -0.3707 & 0 & 0 & 0 & 0 \\ 0.1987 & 0.1512 & 0 & 0 & 0 & 0 \\ 0 & 0 & 0.0038 & -0.3707 & 0 & 0 \\ 0 & 0 & 0.1987 & 0.1512 & 0 & 0 \\ -0.0167 & -1.4142 & 0 & 0 & 0 & 0 \\ 1.3409 & 0.4511 & 0 & 0 & 0 & 0 \\ 0 & 0 & -0.0167 & -1.4142 & 0 & 0 \\ 0 & 0 & 1.3409 & 0.4511 & 0 & 0 \\ 0 & 0 & 0 & 0 & 0.0038 & -0.3707 \\ 0 & 0 & 0 & 0 & 0.1987 & 0.1512 \\ -0.3929 & -1.6993 & 0 & 0 & 0 & 0 \\ 0.7451 & 0.3514 & 0 & 0 & 0 & 0 \\ 0 & 0 & -0.3929 & -1.6993 & 0 & 0 \\ 0 & 0 & 0.7451 & 0.3514 & 0 & 0 \\ 0 & 0 & 0 & 0 & -0.0167 & -1.4142 \\ 0 & 0 & 0 & 0 & 1.3409 & 0.4511 \\ 0 & 0 & 0 & 0 & 0 & 0 \\ 0 & 0 & 0 & 0 & 0 & 0 \\ 0 & 0 & 0 & 0 & 0 & 0 \\ 0 & 0 & 0 & 0 & 0 & 0 \\ 0 & 0 & 0 & 0 & 0 & 0 \\ 0 & 0 & 0 & 0 & -0.3929 & -1.6993 \\ 0 & 0 & 0 & 0 & 0.7451 & 0.3514 \end{pmatrix} \quad (C.7)$$



Processor Intel(R) Xeon(R) E5-2630 v2 @ 2.60 GHz

Infos essentielles et performances

Vertical Segment	Server
Number of Cores	12
Number of CPUs	24
Memory	16 GB
Memory CPU Cache	15 MB
Lithography	22 nm
Max Memory Size	768 GB
Memory Types	DDR3
Bus Speed	7.2 GT/s QPI

Fundamental parallel computing functions

- parpool :** Create the parallel pool
- parfor :** Parallel for loop
- spmatrix :** Execute code in parallel on workers
- distributed :** Create distributed array from data

Figure C.1: High performance Xenon PC used for optimization computing

Abstracts: Arabic / English / French

المخلص

هذه الأطروحة تُعنى بتطوير واقتراح:

- 1- متحكمات خطية متينة متعددة المتغيرات متسامحة مع الأخطاء لغرض استعمالها في التحكم في الأنظمة الديناميكية الغير يقينية في ظل وجود اضطرابات وضوضاء.
- 2- مقاربات خطية متينة متعددة المتغيرات لغرض استعمالها في الكشف عن الأخطاء و التشخيص، يتم التحقق من فاعليتها بتطبيقها على نفس الأنظمة الديناميكية السابقة الغير يقينية وفي نفس الظروف.

تستند تصاميم هذه المتحكمات والمقاربات الى نظريتين: النظرية الأولى، على الوصف المصفوفي الكسري نميز هنا صيغتان، الوصف المصفوفي الكسري اليساري و الوصف المصفوفي الكسري اليميني. النظرية الثانية، على الجذور المصفوفية حيث تعتبر حلول لـ كثيرات الحدود المصفوفية ذوات الأس الصحيح، وعلى أشباه الجذور المصفوفية حيث تعتبر حلول لـ أشباه كثيرات الحدود المصفوفية ذوات الأس الكسري.

في هذه الأطروحة تم اقتراح متحكم الحالة الكاملة (Full states) بكسب رجوعي ثابت (Feedback static gains) يستند في تصميمه على نظرية وضع الانزلاق بالإضافة الى تعيين جذور الكتلة المتينة، تم التحقق من فاعلية التصميم المقترح بتطبيقه على نموذج ديناميكي لنظام توربينات الغاز والذي تم الحصول عليه من خلال استغلال بيانات تجريبية حقيقية. أيضا.

تم اقتراح متحكم بكسب رجوعي ثابت أمثل يعتمد فقط على مخارج النظم الديناميكية حيث يستند في تصميمه على تحويلات المصفوفتين الممددتين للرصد والمراقبة، والى خوارزمية التحسين المسماة بـ محسن الذئاب الرمادية.

أيضا، تم اقتراح تصميم مقارنة ذكية للتشخيص و الكشف عن الأخطاء والتكهن، تم تجريبيها على نموذج نظام ضاغط الغاز بالطرد المركزي، حيث يتم استعمال مرشح كالمان في هذه المقاربة لغرض ضمان خالية من الضجيج والضوضاء، واستعمال نظام خبير مصمم من خلال نظرية المنطق الضبابي نوع 2 لغرض ضمان كشف وتشخيص للأخطاء متين، واستعمال نموذج أريما (ARIMA) لغرض التوقع بالوقت المتبقي لوقوع النظام الديناميكي المعيب في التلف.

أيضا، تم اقتراح راصد فاصل (Interval observer) متين أعتمد في تصميمه الى تعيين جذور الكتلة المتينة و محسن الذئاب الرمادية حيث أثبت النتائج فعاليته في الكشف عن الأخطاء بالمقارنة مع المقاربة الضبابية الذكية.

أخيرا، تم اقتراح تصميم جديد لمراقب PI^2D^m ذو أسس كسرية، حيث يستند في تصميمه على تعيين أشباه الجذور المصفوفية وذلك باستغلال: أشباه كثيرات الحدود المصفوفية، المعادلة المصفوفية الديقونتينية الشبيهة، مصفوفة فانديرموند الممددة الشبيهة، ومصفوفة سيلفستر الشبيهة، ومحس الذئاب الرمادية، تبين النتائج المتحصل عليها بعد التحقق والتجربة على نموذج خطي متعدد المخارج والمداخل غير يقيني و في ظل وجود أخطاء، وبيئة مضطربة، نجاعة المتحكم المقترح، وكفائته والذي يمكن اعتباره كمتحكم متسامح متين.

الكلمات المفتاحية: متحكمات متسامحة مع الأخطاء، كشف وتشخيص الاخطاء، تحكم في النظم الخطية، الجذور المصفوفية، أشباه الجذور المصفوفية، متحكم PI^2D^m ذو أس كسري، كثيرات الحدود المصفوفية، متحكم انزلاقي، متحكم رجوعي، راصد فاصل، المنطق الضبابي نوع 2، محسن الذئاب الرمادية، نظام توربينات الغاز، نظام ضاغط الغاز بالطرد المركزي.

Abstract

This thesis is concerned with development and proposal of robust fault-tolerant controllers (FTCs) and robust fault-detection and diagnosis (FDD) approaches, its designs are based on the advanced control theories, the proposed FTCs and FDD approaches are examined on uncertain multivariable linear systems in the presence of disturbances and noises, for the purpose of validate its effectiveness and performances.

The design of the proposed controllers and approaches in this thesis are mainly based on using two theories: The first theory, on the **Matrix Fraction Description** (MFD), left and right forms are investigated. The second theory, on the **Block-Roots**, which are the solvents of the **Matrix Polynomials** with integer-order exponent, and the **Pseudo Block-Roots** which are the solvents of the **Quasi Matrix Polynomials** with fractional-order exponent.

In this thesis, the full static state-feedback **Sliding Mode** controller was proposed and designed based on robust block-roots assignments, the proposed design efficiency is investigated on the dynamic model of the gas turbine system which is obtained using experimental data.

Also, a static output-feedback controller design has been proposed, its design is based on block transformations matrices of the block observability and the block controllability respectively, and the **Gray Wolf Optimizer** (GWO) algorithm, the proposed controller is applied on uncertain multivariable model of **Centrifugal Gas Compressor System** and compared with recent controllers, the proposal proved its superiority and robustness.

Also, a design of faults detection, diagnosis and forecasting approach, which is applied on the model of the centrifugal gas compressor system. Where, **Kalman Filter** is used in this approach for denoising and filtering the outputs, the use of an expert system designed by **Type-2 Fuzzy Logic** theory, for the purpose of ensuring the robust faults detection and diagnosis. and the use of the **ARIMA** model for the purpose of predicting the remaining time for the defective dynamic system to be in damaged.

Also, an **Interval Observer** has been proposed for uncertain multivariable systems, its design is based on block-roots assignments and grey wolf optimizer, the obtained results proved the domination of this proposed observer comparing with the first approach of the fuzzy expert system.

Finally, a new fractional-order $PI^{\lambda}D^{\mu}$ controller design was proposed. Its design is based on the assignments of pseudo block-roots by exploiting: quasi matrix polynomials, **Quasi Diophantine Matrix Equation**, **Pseudo Block Vandermonde Matrix**, **Pseudo Sylvester Matrix**, and the gray wolf optimizer. After implementing the proposed controller on multivariable uncertain model, and under the disturbances injection with the presence of faults, the obtained results show the robustness and the efficiency of this proposed, which can be considered as robust FTC controller.

Key words: Fault tolerant control, Fault detection and diagnosis, linear control systems, block-roots, pseudo block-roots, sliding mode controller, state-feedback, output-feedback, interval observer, fractional-order $PI^{\lambda}D^{\mu}$ controller, matrix polynomials, Type-2 fuzzy logic, gray wolf optimizer (GWO), gas turbine system, centrifugal gas compressor system.

Résumé

Cette thèse concerne le développement et la proposition de contrôleurs robustes tolérants aux défauts (FTC) et de méthodes robustes de détection et de diagnostic des défauts (FDD), ses conceptions sont basées sur les théories de contrôle avancées, les approches FTC et FDD proposées dans cette thèse sont examinées sur des systèmes linéaires multivariable incertains en présence de perturbations et de bruits, dans le but de valider ses efficacités et performances.

La conception des contrôleurs et approches proposés dans cette thèse sont principalement basées sur l'utilisation de deux théories : la première théorie, la **Description Matricielle Fractionnelle**, deux types de description matricielle fractionnelle (gauche et droite) sont étudiés. La seconde théorie concerne les **Blocs-Racines**, qui sont les solvants des **Polynômes Matriciels** à exposant d'ordre entier, et les **Pseudo Blocs-Racines**, qui sont les solvants des **Quasi Polynômes Matriciels** à exposant d'ordre fractionnaire.

Dans cette thèse, le contrôleur de **Mode Glissant** à retour d'état statique complet a été proposé et conçu sur la base d'affectations robustes de blocs-racines, l'efficacité de conception proposée est étudiée sur le modèle dynamique du système de turbine à gaz obtenu à l'aide de données expérimentales.

Également, une conception de contrôleur de retour de sortie statique basée sur les matrices de bloc transformations de bloc d'observabilité et de la contrôlabilité, respectivement, et l'algorithme d'optimisation de l'**Optimiseur de Loups Gris**, le contrôleur proposé est appliqué sur un modèle multivariable incertain du **Système de Compresseur de Gaz Centrifuge** et comparé aux contrôleurs récents, la proposition a prouvé sa supériorité et sa robustesse.

En outre, conception d'une approche de détection, diagnostic et prévision des défauts, qui est appliquée sur le modèle du système de compresseur de gaz centrifuge. Lorsque le **Filtre de Kalman** est utilisé dans cette approche pour réduire le bruit et filtrer les sorties, il utilise un système expert conçu par la théorie de la **Logique Floue de Type-2**, afin de garantir la détection et le diagnostic des défauts robustes. Et l'utilisation du modèle **ARIMA** afin de prédire le temps restant avant que le système dynamique défectueux soit endommagé.

En outre, un **Observateur d'Intervalle** a été proposé pour les systèmes multivariables incertains, sa conception est basée sur des affectations de blocs-racines et l'optimiseur loup gris, les résultats obtenus ont prouvé la domination de cet observateur proposé par rapport à la première approche du système expert flou.

Finalement, une nouvelle conception de contrôleur $PI^{\lambda}D^{\mu}$ d'ordre fractionnel a été proposée. Sa conception est basée sur les assignations de pseudo blocs-racines en exploitant : quasi polynômes matriciels, **quasi diophantienne matricielle équation**, **pseudo bloc matrice de Vandermonde**, **pseudo matrice de Sylvestre** et l'optimiseur loup gris. Après avoir mis en œuvre le contrôleur proposé sur un modèle multivariable incertain et sous l'injection de perturbations avec la présence de défauts, les résultats obtenus montrent la robustesse et l'efficacité de ce proposé, que l'on peut considérer comme un contrôleur FTC robuste.

Mots clés : Commande à tolérance de défauts, Détection et diagnostic de défauts, systèmes de contrôle linéaires, blocs-racines, pseudo blocs-racines, contrôleur de mode glissant, retour d'état, retour de sortie, observateur d'intervalle, contrôleur $PI^{\lambda}D^{\mu}$ d'ordre fractionnel, polynômes matriciels, logique floue de type-2, optimiseur de loup gris, système de turbine à gaz, système de compresseur de gaz centrifuge.

